Novel 3C Concepts in Isoparametric and Anisoparametric Finite Elements

THESIS

Submitted in partial fulfilment of the requirements for the degree of

DOCTOR OF PHILOSOPHY

by

R. MURALIKRISHNA

Under the Supervision of

Dr. Gangan Prathap

BIRLA INSTITUTE OF TECHNOLOGY AND SCIENCE
PILANI (RAJASTHAN) INDIA
2010

BIRLA INSTITUTE OF TECHNOLOGY AND SCIENCE
PILANI (RAJASTHAN)

CERTIFICATE

This is to certify that the thesis entitled "**Novel 3C Concepts in Isoparametric and Anisoparametric Finite Elements**" and submitted by R. Muralikrishna, ID. No. 2001PHXF031 for award of Ph. D. Degree of the Institute embodies original work done by him under my supervision.

Dr. GANGAN PRATHAP
Director, NISCAIR, New Delhi

Date: April 30, 2010

Acknowledgements

The journey of my Ph.D has been pretty long. I would like to acknowledge the support of people who had been with me all along this journey.

My first person to whom I am forever grateful to is my father late N. Rangharajhan, who has not lived to see the day that I complete my thesis. His moral support had always been tacit, and I am beyond words to express my feelings for his constant encouragement of my pursuits.

I am deeply indebted to my supervisor, Dr. Gangan Prathap, for accepting me as his student and bearing with me all along, despite my inconsistencies in completing tasks, quirkiness in going off-track and inordinate delays in writing this thesis itself. Seldom have I met such a person in my life who is down-to-earth in his interactions with students, and solid in his engineering principles. With a rare blend of technical expertise and humane values, there has not been a single occasion where I have not learnt any thing from him. He has helped me understand and appreciate the beauty of field-consistency in the subtle way that he alone can, and I consider it an honour to be his student.

My alma mater, BITS, Pilani has always been a source of inspiration for me. With the flexibility of its academic programs, it has instilled maturity, discipline and values to all those who have used it appropriately. Thanks to its continued flexibility, I have now reached this stage of completing my journey. I am immensely thankful to Prof. L. K. Maheshwari, Vice-Chancellor, BITS, Pilani for providing me the opportunity to continue my off-campus Ph.D of the Institute. I express my gratitude to Prof. Ravi Prakash, Dean, Research and Consultancy Division (RCD), BITS, Pilani for his official support and encouragement. I would like to thank the nucleus members of RCD, Shri Sharad Srivastava and Shri Dinesh Kumar without whose cooperation it would not have been possible to pursue such goal oriented research during each of the past few semesters. I

thank my Doctoral Advisory Committee (DAC) members, Dr.T.V.V.L.N.Rao and Dr. Manoj Kumar who spared their valuable time to go through my draft thesis and were audience to my pre-submission seminar in order to provide several valuable suggestions that immensely helped in improving the quality of my Ph.D thesis report. My teacher Prof. Rajiv Gupta has been of great moral support to me for the past two decades and I am grateful to him forever.

My organization, GE India Technology Centre, Bangalore, has supported my career ambitions all along, and the open work culture here has enabled me to work towards my Ph.D without compromising on my work. I am sure, it would have been very difficult for me to complete my Ph.D, had I been in any other organization. Several of my colleagues at GE have helped me in various forms. I am thankful to Dr. Sudhakar Marur for the professional discussions that we regularly had in the recent past which gave me a new insight to the world of anisoparametric elements. His critical thinking at a higher level has left a deep influence on me. Dr. Jafar Ali, has gone though the draft versions of the chapters of this thesis, and I am thankful to him for his comments. I would like to express my thanks to my colleagues, Jaswinder Walia, Randy Ketterer and Bob Maffeo for their support in getting the necessary approvals for submission of this thesis.

My family has been fully supportive all along, and has been generous enough to spare their week-ends to work on my thesis. My wife Srividya often ensured to prick my conscience of not doing enough towards my thesis, and has graciously ignored my early-morning vanishing acts from home. My kids, Sanjay and Sai Sanjeeth, have been patiently waiting for me to get the prefix Dr. for whatever excitement it may give them. My special thanks to my wife and kids for their wonderful moral encouragement. My mother, Lakshmi, has admonished me at times to accelerate my thesis and I would like to express my gratitude to her.

R. Muralikrishna

Bangalore, April 30, 2010

Abstract

Finite element formulations have historically relied on key principles of continuity and completeness. Three relatively new concepts of correspondence, consistency and correctness are yet to form an inherent part of element formulation. This thesis attempts to lay a framework for element formulation that is based on these novel 3C concepts of correspondence, consistency and correctness. The concept of isoparametric element formulations can be thought of as a good reason for the widespread use of finite element analysis across different engineering domains. Through the two decades of 1970s and 1980s, the early pitfalls of this formulation like shear locking were studied in detail. The solutions offered by the researchers can be classified into two broad categories. The tactical ones like use of selective integration is one solution. The other solution, more strategic in nature was through judicious use of strain fields, which could be field-consistent, or a substitute strain field. Great amount of work done on the strain fields have resulted in a reasonably clear understanding of the phenomena of shear locking, though the new and emerging concepts of correspondence were not a part of these formulations. Later formulations like anisoparametric elements that did not require selective integration were not formulated keeping the concepts of correspondence, consistency and correctness in mind.

In this thesis, the 3C concepts are first explained from fundamental principles for both statics and dynamics applications. Since isoparametric elements have been so versatile in their applications, these elements are first examined from the perspective of 3C concepts, more as a prelude to the detailed study of anisoparametric formulations from the same 3C concepts. In the process, some of the historical elements that were introduced in the 1960's are studied and shown that they are totally oblivious to the 3C concepts. A significant portion of this thesis is on ansioparametric elements - which have been extensively used for the study of curved shear-flexible shells and quadrilateral plate bending

elements. Current applications of anisoparametric elements are mostly on linear elastostatics, and this thesis investigates the applications of anisoparametric elements for nonlinear elastostatics and linear elastodynamics as well. For both cases of isoparametric and anisoparametric elements, beam, axisymmetric shell and plate problems are considered for their applications in linear elastostatics, nonlinear elastostatics and linear elastodynamics. A total of 67 element formulations are studied in detail, that include 22 anisoparametric elements. For the nonlinear elastostatics applications, the incremental matrices for 4 element formulations are derived explicitly and the results from these formulations are compared with those from a commercial finite element software. Through detailed investigations on both isoparametric and anisoparametric elements, this thesis brings to light several aspects of these element formulations that have not been fully known to researchers in the field of element technology.

Contents

List of Tables

List of Figures

List of Abbreviation and Symbols

$a_0, a_1, a_2, ,, a_n$ = *Generalised parameters used in interpolation functions*

$b_0, b_1, b_2, ,, b_n$ = *Generalised parameters used in interpolation functions*

$a(u,u)$ = *Inner product of the function u*

B = *Strain displacement matrix*

B_b = *Strain displacement matrix for bending strain*

B_s = *Strain displacement matrix for shear strain*

B^N = *Nonlinear strain displacement relation matrix*

A = *Area of cross - section of a beam*

d = *Displacement matrix*

C_{ij} = *Terms of the material matrix*

D = *Rigidity/Material matrix, relation between stress and strain*

D_b = *Material matrix - relation between bending stress and bending strain*

D_s = *Material matrix - relation between shear stress and shear strain*

eqn. = *Equation*

E = *Modulus of Elasticity*

E^+ = *Error in the deflections*

Fig. = *Figure*

G = *Shear Modulus*

h = *Element length*

I = *Moment of Inertia of a beam*

K = *Stiffness matrix*

K^{N1} = *Incremental matrix for nonlinear solution*

K^{N2} = *Incremental matrix for nonlinear solution*

K_s = *Stiffness matrix due to shear terms*

K_b = *Stiffness matrix due to bending terms*

K_s = *Secant stiffness matrix*

K_t = *Tangent stiffness matrix*

l = Length of beam

m = mass per unit length/area

M = Mass matrix

M_r = Radial bending moment

M_θ = Hoop bending moment

M_x = Bending moment in a beam

n, p = Mode numbers for a plate vibration

$N_1, N_2, N_3, , , N_n$ = Interpolation functions

N_s = Radial membrane force

N_θ = Hoop membrane force

N^1 = Matrix used in formulation of incremental matrix

N^2 = Matrix used in formulation of incremental matrix

P = Applied load

$P_0, P_1, P_2, ...P_n$ = Legendre polynomial terms

q = Generalized displacement matrix

r = Radial distance from plane of symmetry

t = Thickness of beam/plate

u = Inplane displacement in a beam/plate, in x direction

u^h = Approximate solution

U_b = Flexural strain energy

U_b = Membrane strain energy

U_s = Shear strain energy

v = Inplane displacement in a beam/plate, in y direction

V_x = Shear force in a beam

w = Translational displacement in a beam/plate

z = Distance from neutral axis

β = Rotation of neutral axis of beam

χ_x = Curvature, Flexural Strain in x direction

χ_y = Flexural Strain in y direction

χ_r = Radial curvature

χ_θ = Hoop curvature

χ_{xy} = Twist of the neutral axis of the plate

δ = Variation of the quantity

$\bar{\varepsilon}$ = Strain computed from the approximate method

ε = Exact strain

ε_r = Radial membrane strain

ε_θ = Hoop membrane strain

γ_{xy} = Shear Strain

κ = Shear correction factor

θ_x = Slope of the neutral axis of beam/plate about x axis

θ_y = Slope of the neutral axis of beam/plate about y axis

π = Potential

ρ = Density of the material

$\bar{\sigma}$ = Stress computed from $\bar{\varepsilon}$

$\bar{\bar{\sigma}}$ = Lagrangian Multiplier

τ = Shear stress

ν = Poisson's Ratio

ω = Natural frequency of beam/plate

ω^h = Natural frequency of beam/plate from finite element solution

ξ = Non - dimensional parameter used in interpolation functions

Chapter-1

Introduction

The finite element method has been in vogue for close to 50 years now, and has evolved over these years as a versatile and powerful numerical technique for solving the mathematical formulations of engineering problems. The technological advancements in the field of computational mechanics in terms of sophisticated computers and efficient numerical algorithms have made the finite element method a potent weapon in the arsenal of a mechanical/structural design engineer. Unlike in the 1950's and 1960's, when the finite element codes were written by engineers to solve specific problems, today commercial finite element programs are readily available for solving most of the engineering problems. The finite element method can now be considered to have matured enough to be used as an indispensable tool in engineering design.

In parallel, the mathematical understanding of the finite element method has progressed equally rapidly. This has looked at the accuracy, errors and convergence of the method using tools such as functional analyses and variational calculus.

In this thesis an attempt is made to classify the canonical concepts that form the logical formulation of the displacement type approach and obtain an understanding of how errors, accuracy and convergence of solutions can be predicted *a priori* where possible, or reconciled *a posteriori* in the rest of the cases, using mathematical tools that include variational calculus.

One of the goals of the work reported in the thesis is to progress towards an entropic paradigm for computational modeling. Recent work, Prathap and Mukherjee (2003a), on error analyses of the finite element method has shown that the canonical concepts (C-concepts) such as Completeness, Continuity,

Consistency, Correspondence, and Correctness lead to computational solutions governed by energy error theorems. It was also seen that optimal solutions were those where the energy errors were distributed in an equi-distribution way leading to the possibility that these were entropy optimal solutions. In other words, computational algorithms do imitate the laws of nature and have energy and entropy sensibilities.

Prigogine (1997) had observed of entropy in thermodynamics, "…..systems considered in thermodynamics are so complex that we are obliged to introduced approximations. The Second Law of Thermodynamics would have its roots in these approximations!.....entropy is only the expression of our ignorance." Computations are based on approximations of very complex situations. It is not surprising that entropic rules should govern how computations produce solutions.

1.1 The Canonical C-Concepts Introduced

The pioneering work of Turner *et al.* (1956) can be considered to be the basis for finite element method. In this work, they presented for the first time, the stiffness matrix for a triangular and rectangular plate bending element. As the finite element approach gives an approximate solution, a question that arises immediately is how errors, accuracy and convergence are linked to the choice of the admissible functions. As more terms are added to the trial functions, or as more nodes are added in to the mesh that replaces the original structure, the sequence of approximate solutions is expected to approach the exact solution. Melosh (1963) systematically presented a case for monotonic convergence of the results of the finite element solution to the exact solution.

During the initial stages of the development of the finite element method, it became obvious that the rudimentary requirements of ***continuity*** and ***completeness*** played a crucial role in determining the accuracy and rate of

convergence of the solution. However these two were necessary but not sufficient conditions in all the cases. It was in the early 80s' that the additional concept of field-consistency was brought out by Prathap (1984). Through the ***consistency*** concepts, phenomena like shear locking began to be understood with more clarity. Prathap (1996a) continued further, and brought out the concept of stress ***correspondence*** and gave a new interpretation to the way the results of the finite element solution were related. For example, the fact that the stresses and strains obtained from the finite element solution were very accurate at certain points (the so-called Barlow points) within an element was taken for granted for a long time. Prathap (1993,1996b) showed through the stress correspondence concepts the reasons behind the accuracy of the results at these points, and proved that these points are not always the Barlow points. The canonical concept that has been around for a while and which is highly relevant in the context of adaptive mesh refinement is the variational ***correctness*** of the finite element formulations. Strang and Fix (1973) had addressed this many years back, and a detailed discussion on the relevance of this concept is provided in the literature survey of this chapter.

The relevance of C-concepts can be envisioned from the recent report prepared by the US National Committee on Theoretical and Applied Mechanics, Oden *et al.* (2003), an extract of which runs as follows "….model error estimation, and model adaptivity are exciting areas of CM (Computational Mechanics) and promise to provide an active area of research for the next decade and beyond. It is predicted that *a posteriori* error estimation and adaptivity will become a common ingredient in all significant computer simulations in CM during the next decade. An important advance in this area has been the recent discovery of methods to determine upper and lower bounds of local approximation error, so that in any given simulation, once a particular model is selected, computable bounds giving upper and lower limits to computed quantities of interest could be a natural by-product in every simulation. This is a fertile area of research, one in which significant work will be done during the next decade." Error estimation

requires a deep understanding of the C-concepts, and in a later section of this chapter the link between error estimation and C-concepts is explained in detail.

In this section the canonical concepts of ***continuity, conformity, completeness, consistency, correspondence*** and ***correctness*** are explained. Later, in the thesis it is shown how these concepts translate into performance in terms of energy-error norms and observable entities like errors, convergence and accuracy by first formulating the elements which are strictly in accordance with these concepts, and later relaxing or enforcing them to assess their impact.

1.1.1 Continuity and Completeness

The concepts of continuity and completeness have been in existence right from the genesis of the finite element method. The significance of the concept of continuity can be traced back to Courant (1943), who used piecewise polynomials over different regions of a domain. Even before Courant, trigonometric functions, or special functions like Legendre or Bessel functions were used to approximate the variable within the whole domain. What marked the difference in Courant's idea was the use of the piecewise polynomials over each sub-domain. This formed the basis of the finite element method, which evolved many years later.

The use of polynomials for the shape functions ensured the continuity of the displacements within an element (intra-element continuity). This still did not ensure that displacements are continuous across element edges (*i.e.* no gaps or overlaps develop as elements are assembled, and deform after loading). The compatibility or conformity condition ensured that the inter-element continuity was maintained before, during and after deformation of the elements. The compatibility requirement also ensured that "neighbourhoods remain as neighbourhoods", Fung (1968). Based on the order of the derivatives of the displacements that appear in the strain energy functional, the finite element compatibility requirements could be established. For example, for a plane stress

problem, the strain energy has the terms of the first derivative of displacement only (C^0 continuity). The finite element formulation thus required inter-element compatibility of just the displacement alone. The strain energy for a beam/plate has terms involving the second derivative of the displacement, which required the inter-element compatibility of both the displacement and its first derivative (C^1 continuity).

Completeness is more difficult to understand especially as a physical basis for it is not obvious. It is usually expressed from a mathematical basis in terms of the order of the polynomial which must be represented exactly. The best physical rationalization offered for completeness is that the functions must be able to represent strain free rigid body motions and constant strain states. The completeness requirement calls for the careful choice of the terms that are used in the interpolation functions in the finite element model in order to capture certain specific states of deformation – like the rigid body displacements of the whole element, or the state of a constant strain in an element. The approximation used for the element shape functions is called complete of order ***n***, if it represents exactly all monomial terms up to order ***n*** in Cartesian coordinates. The introduction of parametric elements based on natural coordinates complicated this understanding somewhat.

In the finite element method, an unknown function *u(x)*, which is the exact solution to a boundary value problem over a domain enclosed by a boundary is replaced by an approximate function $u^h(x)$ which is constituted from a set of trial, shape or basis functions. It is desired to have a trial function set that will ensure that the approximation approaches the exact solution as the number of trial functions is increased. It can be argued that the convergence of the trial function set to the exact solution will take place if $u^h(x)$ will be sufficient to represent any well behaved function such as *u(x)* as closely as possible as the number of functions used becomes indefinitely large. This is called the completeness requirement. In the finite element context, where the total domain is sub-divided

into smaller sub-regions, completeness must be assured for the shape functions used within each domain. The continuity requirements then provide the compatibility of the functions across element edges.

It is also seen that a best-fit arrangement in some sense between $u(x)$ and $u^h(x)$ takes place, and that this best-fit can be gainfully interpreted as taking place between strain or stress quantities (*i.e.* the correspondence requirement). This has important implications in further narrowing the focus of the completeness requirement for finite element applications in particular. By bringing in the new perspective of best-fit strain or stress paradigm, the completeness requirements can be looked at entirely from this physical point of view.

The use of C^0 elements in certain structural mechanics applications created problems like shear locking. When this threatened to derail the otherwise versatile nature of C^0 elements, formulations like the Mixed Interpolation of Tensorial Components, Bathe and Dvorkin (1985), Enhanced Natural Strain, Simo and Rifai (1990) were introduced to overcome the locking problems. In these formulations, alternate or substitute fields are used to represent some of the fields, *e.g*. strain field. These approaches indirectly met the completeness requirements. On the other side of the completeness, few additional terms have been added to the interpolation functions to satisfy specific requirements (zero shear under pure bending). These terms have been named as bubble functions, Bathe (2002). Recently, Rajendran and Liew (2003b) revisited the completeness requirements in view of the sensitivity of the results of the finite elements due to mesh distortion. The scope of the current work does not address the continuity and completeness aspects specifically.

1.1.2 Conformance

The requirement of C^1 continuity for plate bending problems was explained in section 1.1.1. This condition was difficult to achieve for the plate bending problem (for some elements) and this led to the formulation of elements which did not meet the conformity requirements in totality. Soon, these “non-conforming” elements became popular and were very widely used for their apparent good results, despite the fact that these non-conforming elements did not guarantee the boundedness of the strain energy, Desai and Abel (1987).

The concepts of conformance and non-conformance in element formulations and their impact on the element performance were not given due attention initially, as the first-cut results were promising. Zienkiewicz & Cheung (1964) established a general procedure for deriving the stiffness matrices for quadrilateral plate bending elements, though this element is a non-conforming element. The use of these elements continued as the results surprisingly were very good and no serious second thoughts were given. At the conferences on matrix methods in structural mechanics (1965, 1968), researchers deliberated on these aspects, and advocated continued use of these formulations. In a review and catalogue of plate bending elements, Hrabok and Hrudey (1984) listed out 88 element formulations, several of which are non-conforming elements. To this day, the occasional use of non-conforming C^1 elements in plate bending problems is seen. Wanji and Cheung (1997) satisfied the inter-element compatibility continuity conditions in an average sense and derived the interpolation functions. Zhang and Cheung (2003) used a refined non-conforming displacement function that has additional interpolation functions with coefficients that are chosen specifically to ensure the continuity condition. This can be thought of as a pseudo-conforming element, and the element has been found to give good results for many applications including vibration and stability. Mao and Chen (2006) studied the discretisation error for anisotropic meshes and focused their investigation on a non-conforming plate bending element.

In this thesis, the behaviour of non-conforming elements is studied in detail and the performance assessed using the best-fit rule, strain energy boundedness, rate of convergence for linear and nonlinear elastostatics and linear elastodynamics problems.

1.1.3 Consistency

While researching on the phenomena of shear locking, Prathap (1984) observed that there existed many constrained strain-fields. A constrained strain-field can be thought of as a requirement in which the strain-field would vanish in certain constraining limits. The constrained strain-fields could lead to spurious results, if adequate care is not exercised during the element formulation. Examples of such constrained strain-fields include strain field of a thick plate (in the limit where the thickness tends towards the thin plate shear locking occurs), the dilational strain-field of a nearly incompressible material (in the constraining limit volumetric locking occurs) and membrane strain-field during inextensional bending of a curved beam (membrane locking occurs). To overcome this spurious behavior, Prathap (1984) proposed the use of strain-fields that are field-consistent. The consistency in the strain-field definition was required so that only true constraints emerged in the penalty regimes of constraining of the concerned strain-field. The construction of these field-consistent strain-fields was based on meeting the same variational principles that governed the original formulation, so that there is no deviation from them.

The requirement in a general purpose finite element package for 2-D formulations of plane stress/plane strain and 3-D formulations to be field-consistent was brought out by Ramesh Babu *et al.* (1985). This reference has a representative list of commonly encountered constrained strain-field problems. A comprehensive bibliography on the finite element formulations of different classes of constrained media elasticity problems was captured by Prathap and Nirmala (1990). The consequence of the use of the finite element formulation not

in line with a field-consistent or a formulation that is analogous to field-consistent is poor performance, delayed convergence, stress oscillations, locking *etc*.

Locking is a phenomena which is caused due to certain deficiencies in the element formulation (deficiency of consistency), the outcome of which is spurious/suspicious results. For example, the displacement in a thin plate, when computed using a finite element formulation based on thick-plate (Mindlin theory) can be totally erroneous, due to shear locking. Though mathematical explanations of why locking occurs (due to rank deficiency of the stiffness matrix) were offered, the remedial measures that were used historically (like reduced integration) could not bring out the rationale behind their use. However, locking is a phenomenon not restricted to shear alone, and is observed in other derived quantities of the finite element solution, like membrane strain (leading to membrane locking), dilational srains (leading to volumetric locking).

Olesen (1983) recognized that the shear strain is composed of two “incompatible” quantities, with one term of higher order than the second, and proceeds to redistribute the terms so that they are of the same order. For the simple case of a 2-noded shear flexible beam element the redistribution and reduced integration method were found to give the same stiffness matrix.

Prathap (1984) expounded on the concept of field-consistency and used it on many problems. Prathap and Ramesh Babu (1986), Ramesh Babu and Prathap (1986) showed the use of 2-noded and 3-noded shell elements to solve varied problems on circular plate, hemispherical shell and cylindrical shell subjected to different loads. Prathap and Somashekar (1988) combined the concepts of edge-consistency and field-consistency to show the efficacy of this element through a series of tests. This element has been later chosen by Mukherjee and Krishnamurthy (1996) for adaptive mesh refinement of plate problems.

Prathap and Ramesh Babu (1987a) used the field-consistency concept to explain the stress oscillations in a curved beam element. The *a priori* prediction of stress oscillations, and their removal through appropriate field-consistent reconstitution of the strain field is brought out very elegantly. A similar explanation for the stress oscillations in the case of Mindlin plates is found in Prathap and Ramesh Babu (1987b). In an interesting example of the axial force in a tapered bar, Prathap and Naganarayana (1992) showed the ability of the field-consistent formulation to explain and remove the extraneous stress oscillations. This example is not a case of a constrained-strain field, where consistency was required in the strain-terms in the constraints. Here it was the requirement of a consistent stress-field that satisfies the equilibrium. Despite the maturity of the field-consistency concept since its advent in 1984, researchers are still oblivious to its efficacy in explaining pathological phenomena like shear locking and continue to search for accurate prediction of stresses, Wang *et al.* (2002).

It would be interesting to briefly look at the various other methodologies (other than field-consistency) that have been used for overcoming locking. The reduced integration approach advocated by Zienkiewicz *et al.* (1971), Zienkiewicz and Hinton (1976) in the 70s overcame the locking problem associated with the shear deformations in the plate/beam bending elements. Though it was realized by the authors of this publication that the bounded nature of the solutions was no longer available, the reduced integration technique became quite popular.

Alternate methods that do not use the selective/reduced integration but could still overcome shear locking were researched. Along this time, it was found that a different representation of the shear strain component gave good results. The works of Bathe and Dvorkin (1985) on the mixed interpolation of tensorial components, Donea and Lamain (1987), and field/edge consistency-approach of Prathap and Somashekar (1988) are all in similar lines.

In the enhanced strain approach, Simo and Rifai (1990) laid out the conditions (orthogonality and constant stress conditions) for constructing the enhanced strain interpolation, derived the strain fields for plane elasticity and axisymmetric problems, and showed their applications to Mindlin-Reissner plate theory. It is interesting to see the close resemblance of the orthogonality condition to the correspondence concept, though Simo and Rifai (1990) do not realize it explicitly as both are based on Hu-Washizu's principle. In fact, it is much easier to see the analogy of the enhanced strain with the consistency concept. This was brought out by Perego (2000) where the enhanced strain gets embedded in the upfront formulation of the matrices from the Hu-Washizu principle.

Other approaches on isoparametric element formulations to overcome shear locking would be described at a later point in this thesis.

Tessler (1981), Tessler and Spiridigliozzi (1988) used anisoparametric elements to address shear locking. In these formulations, the interpolation functions used for the translational displacement w is of higher order than the one that is used for the rotation θ. Marur and Prathap (2000) used the field-consistency argument to show why the anisoparametric element does not produce shear locking for the case of shear-flexible beam problems.

The problem of locking is not restricted to shear alone. Membrane locking also occurs in certain problems, which again calls for special approaches to resolve. Prathap and Ramesh Babu (1986) and Ramesh Babu and Prathap (1986) examined the shear and membrane locking in axisymmetric shells, and used the field-consistent formulation to explain locking and how to overcome the same. Yunhua (1998), Yunhua and Eriksson (1999) used the field-consistency approach for overcoming shear and membrane locking by using different interpolation functions to represent the displacement and rotation. For avoiding membrane locking, the order of the interpolation function that is used here is of 5^{th} degree. When the large deformation effects are considered, the membrane

locking problem continues and reduced integration works successfully here also, with the concomitant violations on the variational aspects.

The consistency concept has now gained wide acceptance and many researchers use it for varied applications. Miranda and Ubertini (2003) used it effectively in a coupled electroelasticity problem. Ganapathi *et al.* (1999), extended the concept of field-consistency to solve laminated composite beam problems by using the B-Spline functions, and redistributing the shear and membrane strains in a field-consistent manner

The elegance of the concept of field-consistency in predicting *a priori* if the element is likely to give spurious results or not is shown in this thesis through several examples.

1.1.4 Correspondence

In the context of adaptive mesh refinement, there has been a lot of research interest on superconvergent points – points within an element that have the least error when compared with the exact solution (in other words, the convergence to the exact solution at these points is very high), Zienkiewicz and Zhu (1992). Long before the widespread use of the phrase “Superconvergent Points”, researchers knew the fact that at certain points called “Barlow Points”, Barlow (1976), the finite element solutions for stresses were more accurate. Hinton and Campbell (1974) used a smoothing technique based on least squares method to remove the stress oscillations. Herrmann’s (1972) argument of interpreting the finite element solution of displacements as a consequence of the minimization of the stress errors, and Moan’s (1973) study on distribution of errors can be termed as two studies that heuristically had the correspondence concept embedded in them, albeit unknown to them at that point of time.

The issues of stress oscillations and points of accurate stresses were treated as two separate entities, until Prathap (1984, 1996a) saw the common

thread of correspondence and consistency running through them. Prathap (1993, 1996a) laid the variational bases for the existence of these points, and through the stress-correspondence paradigm showed that the super-convergent points are not always the "Barlow Points". The "best-fit" rule explains in simple terms the location of the optimal stress points. In fact, the stress correspondence paradigm, Prathap (1996b) derived this best-fit rule, through imposing the equilibrium and orthogonality conditions on three fields (displacement, stress and strain) through the ingenious use of Hu-Washizu theorem. Prathap (1993, 1996a) has used the Legendre Polynomials extensively to reconstitute the strain/stress fields and has shown that the accurate stress recovery points are not always the Barlow points. The use of Legendre Polynomials (in the reconstituted force field) in the above work has been explored recently by Hiller and Bathe (2001). Kasper and Taylor (2000a, 2000b) followed a similar variational formulation from Hu-Washizu theorem.

Prathap (1996b) laid out a conceptual framework for the displacement correspondence and stress correspondence paradigms, and explained through both the processes, how the finite element method computed the displacements, strains and stresses. The displacement correspondence paradigm results in a process where the displacements at nodes are matched, and the stresses are computed as derivatives of displacements due to which they are less accurate than the displacements. The stress correspondence paradigm results in a process where the stresses at optimal points are matched, and the displacements are integrated from the strains due to which they are more accurate than the stresses.

The concept of correspondence was explained by Prathap (1996b) through an ingenious interpretation of the Hu-Washizu theorem. Prathap (1993, 1996a) gave proof to the existence of points in the finite element domain where stresses are more accurate. Though the existence of such points were known right in the 70's, *e.g.* Barlow (1976), Prathap laid a variational basis for it and generalized it

through correspondence concept. The recent publication by Zhang (2008) on the reasons why Barlow points do not coincide with the Gaussian Quadrature Points for higher-order elements, reinforces the correspondence concept of Prathap (1996b). The correspondence concept further lays out the framework for the "Best-fit" rule, which predicts the manner in which the finite element computed strains/stresses vary with respect to the exact strain/stress. This point has great relevance to the super-convergent patch recovery process, where the knowledge of the super-convergent points is critical to the recovery process. Super-convergence means the existence of points in the finite element domain that give the most accurate results for the derived quantities, viz., strains, stresses. Barlow (1976) had shown the existence of points within an element where the stresses were more accurate than other points. In a sequel, Barlow (1989) extended the optimal stress sampling points to the case of distorted elements.

A lot of research has gone into the understanding of the basis for the existence of these points, MacNeal (1993), Prathap (1993, 1996a). Yong-woo and Oak-key (1996) extended the concept of consistency to find the optimal stress points in 4-noded, 8-noded and 9-noded elements, using all the while an indirect form of correspondence concept. Oh and Batra (1999) computed the locations of optimal stress points for bar and quadrilateral elements of various orders and summarized them for the Lagrange and serendipity families of elements till 5^{th} order. Felippa's (2002) fitting of strains by minimizing dislocation energy is conceptually similar to Prathap's correspondence concept, with fitting displacements carried out additionally. Rajendran and Liew (2003) revisited the optimal stress sampling points for plane triangular elements using the concept of stress correspondence and showed that Barlow points do not exist for all stress/strain components. Recently, Zhang (2008) revisited the case of the superconvergent points and strengthened the argument of Prathap (1993, 1996a) that in general, the Barlow points are not the same as the superconvergent points. Rajendran (2008) computed the Barlow points for higher order bar elements (up to order 10), and compared them with Prathap points.

This comparison shows clearly that from third order onwards Barlow points and Prathap points are very different. Mukherjee and Jafarali (2008) reinforced the existence of Prathap points for statically indeterminate structures as well. Pinto (2008) used elements till fifth order to identify superconvergence (where convergence is $O(h^{k+1})$, k is the order of the interpolation), ultraconvergence (where convergence is $O(h^{k+2})$)and hyperconvergence (where convergence is $O(h^{k+3})$).

The importance of the correspondence concept in assessing the performance of an element is shown in this thesis through various examples.

1.1.5 Correctness

Correctness refers to the adherence of the finite element formulation to the canonical concepts that were outlined above. A variationally correct formulation will always give bounded results, like strain energy, natural frequencies, *etc.* Some of these aspects have been addressed in parts by de Veubeke (1965), Strang and Fix (1973). A classic example of an element formulation that is not variationally correct is the use of reduced integration in the case of shear-flexible beams and plates. Another example is the use of lumped mass matrix to compute the natural frequencies.

Incorrect element formulation could produce erroneous results, which could mislead the finite element analyst. In the context of error estimation, the recent compendium by Gratsch and Bathe (2005) listed out the characteristics of an effective error estimator, and one of them is that the error estimator should yield guaranteed and sharp upper and lower bounds on the actual error. If the element formulation is not variationally correct, it is very likely that the above requirement is violated. In the adaptive finite element analysis of plates by shear-flexible quadrilateral elements, Mukherjee and Krishnamoorthy (1996) narrowed down their choice of the elements to two formulations – both of which are variationally

correct. Prathap and Mukherjee (2003a) introduced a fresh flavor to the concepts of correctness through simple, yet elegant use of the virtual work principle and demonstrated the interpretation of the correctness of the finite element results for both elastostatics and elastodynamics problems.

The concept of variational correctness has been in place right from 70's. Strang and Fix (1973) in their treatise on the mathematic basis for the finite element method discussed in detail the concept of correctness. Strang (1973) referred to the use of elements that are not formulated in a variationally correct manner as variational crimes. Militello and Felippa (1990a,1990b) used the Hu-Washizu principle to justify the use of assumed natural strain. Kasper and Taylor (2000a, 2000b) also used the Hu-Washizu principle for consistent variational stress recovery. Prathap and Mukherjee (2003a) recently reinterpreted the error theorem of Strang and Fix (1973) and showed the results for simple elastostatics problems. Marur and Prathap (2000) investigated the variational correctness by using a simple two-noded beam element and solved the shear-flexible beam problem. Mukherjee *et al.* (2005), Jafarali *et al.* (2007), Muralikrishna and Prathap (2003) and Prathap *et al.* (2003b) assessed the correctness of the elastodynamic response of beams and plates.

1.2 Boundedness, Errors and Adaptivity

The aspect on boundedness of the recovered stresses, and more so of the energy norm, is critical to the success of the adaptive mesh refinement. One of the earliest discussions on the bounds of the finite element solution is by de Veubeke (1965). This can be seen as a forerunner for Prathap and Mukherjee's (2003a) re-derivation of the same from virtual work method. In the recent context of goal-oriented error estimation (Prathap and Mukherjee (2004)), where the interest is in specific local quantities, the bounds on the error measure has received more attention.

The correctness concept is closely related to adaptive mesh refinement. In fact, the use of a variationally incorrect element formulation in the adaptive mesh refinement in fact may lead to erroneous results. The boundedenss of strain energy is one key attribute of testing the variational correctness of the formulation. Strang and Fix (1973), Prathap and Mukherjee (2003a) showed that, the energy inner product of the approximate (Ritz or finite element) solution will always be a lower bound of the exact energy.

Error estimation can be broadly divided into two major systems, *viz*., *a priori* and *a posteriori*. *A priori* error estimation covers the process of arriving at errors even before the availability of the results from the solution of the finite element. In general, the formulation of closed-form *a priori* errors estimates are difficult and are very problem-specific. For *a posteriori* error estimation, the results of the finite element solution are used to estimate the errors. Here again, there are 2 sub-sytems, *viz*., residual based error estimate and recovery based error estimate.

One of the earliest works on the errors in the finite element method was by Walz *et al.* (1968). The finite element equilibrium equations are expanded through Taylor Series and the discretisation error for bar, beam, plane stress and plate element is provided. In the current context of error estimation, the work by Walz *et al.* (1968) can be considered to belong to *a priori* category. Prathap (1999) laid a framework based on the principles of field-consistency, for estimating *a priori* the errors in the finite element solution.

The vast amount of work done on the error estimates and adaptive mesh refinement has been captured in review articles by Iyer and Appa Rao (1992a, 1992b), Li and Bettess 1997), Mackerle (2001). The fact that most of the *a posteriori* error estimators depend on stress recovery ties up closely with the necessity of predicting stresses accurately. Though some techniques have been developed that do not require knowledge of these points for stress recovery (*e.g.*

stress recovery through equilibrium of patch by Boroomand and Zienkiewicz (1997), displacement recovery through minimization of functional by Mukherjee *et al.* (2001), lot of research continues on recovery of stresses especially with a variational aspect attached to it, Tessler *et al.* (1994,1998a,1998b), Riggs *et al.* (1997). Lo and Lee (1998) used three different techniques for the recovery of stresses in Mindlin plates. In all of the above recovery techniques, the correspondence concept is rarely discussed. Mohite and Updadhyay (2002) used a combination of strain and displacement recovery to smoothen out the stresses and apply it to the study of *a posteriori* errors for composite plates. The recovery process here has close resemblance to the correspondence concept. Miranda and Ubertini (2002) used the correspondence concepts to recover the stresses, and brought to light the consistent reconstitution of stresses.

Zienwkiewicz (2006) traced the history of error estimation in the engineering analysis, and presented the state-of-the-art in error estimation and adaptivity. The current state of the art in the field of *a posteriori* error estimation has been recently reviewed by Gratsch and Bathe (2005). From the work done so far, in the context of adaptive mesh refinement, the recovery based error estimators require accurate knowledge of the stresses at superconvergent points. Due to this, research continued on for finding these superconvergent points, Hiller and Bathe (2001), Rajendran and Liew (2003a), Liew and Rajendran (2002). A good understanding of the best-fit rule (which comes from the correspondence concept outlined in (1.1.5) gives the researcher more clarity on the superconvergent points, as shown by Rajendran (2008).

.

Prathap and Mukherjee (2003a) explained the energy error concepts in a very elegant way through the use of virtual work principle and show that for linear problems, the energy of the errors is equal to the error of the energies. This statement has many important corollaries on the boundedness of the strain energy and natural frequencies.

Leckie and Lindberg (1963) quantified the error in the natural frequencies of beams and concluded that they are of $O(h^4)$. Error analysis of natural frequencies was done in the 70's by Lindberg and Olson (1970), Fried (1971), and Fried and Malkus (1975). Lindberg and Olson (1970) studied the dynamic response of two plate bending elements from a convergence perspective and concluded that the conforming element is superior to the non-conforming element.

Rajendran and Prathap (1999) discussed the errors in potential energy and kinetic energy separately and studied the convergence of natural frequencies of a cantilever beam. They developed an *a priori* error model for the torsional frequencies, and studied in detail the consequences of using lumped mass matrices. Prathap and Pavan Kumar (2001) used a 2-node and 3-node element to study the convergence of the natural frequencies of a Timoshenko beam. Jafarali *et al.* (2004) used a combination of different formulations for the stiffness and mass matrices and studied the errors in the frequencies. Muralikrishna and Prathap (2003) studied in detail the effect of variational correctness on the natural frequencies of plates. The field-consistent way of formulating the stiffness matrix for use in elastodynamics was done by Ganapathi *et al.* (2003). In all of these cases where the element formulations were variationally correct, boundedness was ensured.

1.3 Objectives and Scope

This thesis attempts to lay a framework for element formulation that is based on novel 3C concepts of correspondence, consistence, correctness and applies this framework to several practical element formulations. Such element formulations are expected to be robust and applicable for all classes of problems. To firmly establish the core requirements of such an element formulation, a detailed review of finite element formulations for the case of beams, axisymmetric shells and plate problems over the past 40 years has been undertaken and the pathological problems faced by these elements have been identified. In this thesis, the

problems faced by finite element formulations that deviate from the canonical concepts are studied in detail.

1.3.1 Gaps in Element Formulation

A comprehensive review of the current literature in the area of finite element formulations indicates the continued use of the formulations that are not strictly adhering to the canonical concepts. Some of these element formulations have been from the very early stages of the development of the finite element method (*e.g.* use of non-conforming elements, use of lumped mass matrices), and some of them are recent (*e.g*. use of selective integration, use of anisoparametric elements). For the increased generic reliability of these finite elements, many of which are a part of the commercially available finite element software, a thorough understanding of the element technology is needed. The best-fit rule, though known in various forms, has not been investigated for a large class of problems (*e.g*. a simple plate bending problem, axisymmetric shells). The use of anisoparametric elements has not been explored in detail beyond the simple case of linear deformations for beams and to a limited case of plates (axisymmetric shells using anisoparametric elements have not been studied in detail). The field-consistency concept for large deformation problems which are prone to membrane locking has also not been investigated fully. Thus there is a case for more work on the critical examination of element formulation that is based on the concepts of consistency, correspondence and correctness, which is attempted in this thesis.

The scope of this thesis includes examining the 3C concepts on a wide variety of commonly used finite elements for beam, plate and shell problems. It is observed from the literature survey that anisoparametric elements have not been explored in detail for their applications to large deformation problems and hence a significant effort is devoted towards this. The isoparametric and field-consistent elements have so far not been analysed from the perspective of all of the 3C

concepts and hence requires a detailed study. In this thesis, the application of the above element formulations to problems in statics and dynamics is examined in detail. For the case of statics problem both linear and nonlinear elastostatics are considered. Under nonlinear elastostatics, the formulations arising due to the large deformation are discussed. For the case of dynamics, linear elastodynamics problems are considered. Material nonlinear elastostatics and nonlinear elastodynamics are beyond the scope of this thesis.

1.4 Thesis Organization

This thesis is organized in ten chapters. The description of the chapters is as follows.

Chapter-1

This introductory chapter gives an overall perspective of the canonical concepts of ***completeness, conformance, consistency, correspondence*** and ***correctness*** in finite element stress analysis, and the performance measures that are employed to evaluate these C concepts. A thorough survey of the literature for the existing research work on the canonical concepts in the finite element method is reported out, and the appropriate gaps are identified. The link between error estimation and C concepts is established. The relevance of the canonical concepts to the context of adaptive mesh refinement, boundedness and error estimation is brought out and a case is made for the requirement of a finite element formulation that adheres to all of the C concepts. The literature survey in this chapter focuses on the C concepts, and detailed literature on element technology is described in the respective chapters. The gaps that exist in the literature in the areas of C concepts and their applications to isoparametric and anisoparametric elements are identified, through which the objective and scope of the thesis are derived. The methodology that is followed in the thesis, and the various element formulations that are developed in the course of the thesis are also outlined in this chapter.

Chapter-2

In this chapter, the 3C concepts that are used in this thesis are explained. The correspondence concept is explained through Hu-Wazhisu principle. The concept of field-consistency is explained from the strain displacement relations. The process of *a priori* prediction of the conditions under which the constraints can become spurious is laid out. These constraints are worked out explicitly for both isoparametric and anisoparametric formulations for small and large deformation cases. The virtual work principle is used to establish the boundedness of strain energy. The best-fit argument is also explained through the virtual work principle. The projection theorem for elastodynamics problems is laid out. The subsequent chapters make use of the concepts that are outlined here.

Chapter-3

Chapter-3 deals with linear elastostatics problems for classical beams, axisymmetric shells and plates. The finite element formulations for simple beam shell and plate problems are derived from the fundamental principles, adhering to all of the C-concepts. For each of these formulations, the current practices that do not conform to the canonical concepts are discussed in detail. The impact of conforming and non-conforming elements for plate bending problems is shown through the concepts of best-fit rule, strain-energy boundedness and order of convergence. The conforming element that is chosen is the 4-noded plate bending elements with 4 degrees of freedom at each node (translational displacement w, rotation θ_x, θ_y , and twist θ_{xy}. The non-conforming element is a 4-noded plate bending element with 3 degrees of freedom (translational displacement w, rotation θ_x, θ_y). For a beam problem, exact closed-form solutions exist for all loadings/boundary conditions, and hence it is very straightforward to show the best-fit rule. The axisymmetric shell element that is developed here shows the best-fit for problems where the exact closed-form solution is available – a circular plate with uniform load. For a plate bending problem, the exact closed-form solution (without any series expansions) is

available for select loading/boundary conditions, and for these cases the best-fit rule is shown. For all problems, the rate of convergence and strain-energy boundedness are discussed in detail.

Chapter-4

This chapter discusses the finite element analysis of linear elastostatics problems for shear-flexible beams, axisymmetric shells and plates based on Timoshenko beam and Reissner-Mindlin plate theories. The phenomena of shear locking for the C^0 formulation is studied in detail for both isoparametric and anisoparametric element formulations. The impact of full integration and selective/reduced integration is assessed. For a beam problem, it is shown that the use of reduced integration in isoparametric element leads to violation of best-fit rule, whereas the anisoparametric element clearly satisfies the best-fit rule. The fact that anisoparametric formulation is not a panacea for overcoming shear locking is brought out clearly with the example of open hemispherical dome subjected to a tip moment. It is demonstrated that for curved shells, due to the coupling of shear and membrane terms, anisoparametric formulation also requires reduced integration to overcome both shear and membrane locking. A novel 4-noded anisoparameteric element that uses cubic Hermite polynomials for the translational displacement w, and bilinear polynomials for the independent rotations θ_x, θ_y has been formulated for plate bending problems. It is shown that this formulation does not require use of selective integration.

Chapter-5

The large deformation behaviour of classical beams, axisymmetric shells and plates are discussed in chapter-5. This chapter leads to fresh insights, with a new discussion on the errors that are specific to large deformation problems. The concept of membrane locking in the context of large deformations is examined in detail. A simple problem of a beam with different boundary conditions (hinged-hinged, pinned-pinned, clamped-clamped) is taken to examine the canonical concepts. This chapter discusses the concept of field-consistent formulation of

large deformation problems in detail. The use of reduced integration and partial field-consistency in overcoming membrane locking is discussed. The incremental matrices for axisymmetric shell elements are derived explicitly. It is demonstrated that membrane locking can occur in beam problems, if adequate care is not taken during the element formulation. For the elements considered, it is shown that membrane locking does not occur in plate and axisymmetric shells, and hence there is no requirement of using reduced integration. The results of the field-consistent formulation are robust, and do not produce any spurious membrane locking. An innovative concept of a sweep-test has been used for explaining the strain energy boundedness.

Chapter-6

This chapter discusses the large deformation of shear-flexible beams, axisymmetric shells and plates. The interesting case of coupling of membrane locking and shear locking is examined in detail. The examples that were taken in chapter-5 are used here. The anisoparametric elements that were developed in chapter-4 for the beam, shell and plate elements are now extended to large deformation analysis. Though the anisoparametric formulation does not cause shear locking, it shows membrane locking and requires selective integration. A detailed study of selective integrations of shear and membrane terms is carried out. The field consistent anisoparametric formulation for large deflection problems is a novelty of this thesis, and its applications to beam, axisymmetric shell and a plate are reported for the first time. The element matrices for the field-consistent 4-noded Mindlin plate element are derived explicitly.

Chapter-7

Chapter-7 expands on the element formulations developed in chapter-3 and chapter-4 to linear elastodynamic problems. The boundedness concept for vibration problems is studied through elegant use of virtual work principle. The extra-variational aspects of different formulations of mass matrix, and stiffness matrix are examined. The impact of different lumping procedures on the natural

frequencies is examined carefully. The effect of conformance and non-conformance, selective and full integration, and their consequences are discussed in detail for beam and plate bending vibration problems.

Chapter-8

This chapter summarizes the findings of the study undertaken, and conclusions of these investigations are discussed in detail.

Chapter-9

The specific contributions of this thesis are brought out in this chapter. All the element formulations that were studied in this thesis are summarized and the new elements that were formulated in the thesis are highlighted.

Chapter-10

This chapter outlines the further scope of work on use of 3C concepts in other domains of computational mechanics.

1.5 Research Methodology

From the research gaps identified in section 1.3, existing element formulations are studied in detail and new elements are formulated where required. Adequate care was taken to keep abreast of the current trends in element technology through dynamic literature surveys on this subject.

The approach that has been taken in this thesis is to formulate elements afresh for beam, axisymmetric shell and plate bending problems. The 3C concepts are addressed in the course of the formulation of these elements. For example while formulating a 4-noded shear flexible plate element, the concepts of selective/full integration, field-consistency, isoparametric and anisoparametric formulations are

considered. The results are first benchmarked against known solutions and after gaining confidence on the element behaviour detailed studies on best-fit rule, strain energy boundedness and rate of convergence are carried out. The element formulations are applied to linear elastostatics, nonlinear elastostatics and linear elastodynamics problems. Wherever closed form solutions are not available for analyzing the results, recourse is taken to solutions given by commercial finite element software and in this thesis ANSYS® (ANSYS is a registered trademark of ANSYS, Inc. in the USA) has been used for comparing the results of the current element formulations.

Chapter-2

3C Concepts Revisited

2.1 Introduction

In this chapter, a brief mathematical foundation of 3C concepts of correspondence, consistency, correctness and energy error is laid out. The concepts of correspondence and boundedness of strain energy are derived from first principles. The requirement of field-consistency in constrained media problems is explained through various problems for both small and large deformation cases. Virtual work principle is used to show the boundedness of strain energy for elastostatics problems and the boundedness of natural frequencies for elastodynamics problems.

2.2. Correspondence Concept

The total potential of the system can be represented in terms of the stresses, strains and the applied external loads as follows:

$$\pi = \int \left\{ \frac{1}{2} \bar{\sigma}^T \bar{\varepsilon} + P \right\} dV \qquad \ldots(2.1)$$

where

$\bar{\varepsilon}$ = *Strain computed from the approximate method*

$\bar{\sigma}$ = *Stress computed from* $\bar{\varepsilon}$

P = *Applied load*

In addition to the terms associated with the internal energy and external work in the total potential of the system, de Veubeke (1965) introduced another term called the dislocation potential. This dislocation potential can be considered as the Lagrangian multiplier, which minimizes the error between the finite element strain and the actual strain.

$$\pi = \int \left\{ \frac{1}{2} \bar{\bar{\sigma}}^T \bar{\varepsilon} + \bar{\bar{\sigma}}^T (\varepsilon - \bar{\varepsilon}) + P \right\} dV \qquad \ldots(2.2)$$

where

ε = *Exact/Actual strain*

$\bar{\varepsilon}$ = *Strain computed from the approximate method*

$\bar{\sigma}$ = *Stress computed from* $\bar{\varepsilon}$

$\bar{\bar{\sigma}}$ = *Lagrangian Multiplier*

P = *Applied load*

It can be seen that the first and the third terms in eqn. (2.2) are the same as in eqn. (2.1). The middle term represents the dislocation potential. Now this becomes a mixed variational problem and the variation of π can be taken with respect to 3 quantities. The equilibrium equations are obtained by taking the variation on u (the nodal displacements), which gives.

$$\nabla \bar{\sigma} + \text{terms from } P = 0 \qquad \ldots(2.3)$$

Variation on the additional term, the Lagrangian Multiplier (σ with double bar) gives the compatibility condition

$$\int \delta \bar{\bar{\sigma}}^T (\bar{\varepsilon} - \varepsilon)\, dV = 0 \qquad \ldots(2.4)$$

Variation on the quantity ε with single bar gives

$$\int \delta \bar{\varepsilon}^{T} (\bar{\bar{\sigma}} - \bar{\sigma}) \, dV = 0 \qquad \ldots(2.5)$$

Equations (2.4) and (2.5) form the basis of the correspondence concept. For linear elastic problems, these equations are identical. The concept of the "Best-fit" rule or that the stresses from the "finite element" solution are a least-squares fit to the "exact" solution is easily understood from these equations. These concepts are used in the assessment of all the element formulations in this chapter. Though Kasper and Taylor (2000a) followed a similar variational formulation that has been described above, what makes the present treatment unique is the interpretation from a "best-fit" rule. This is examined in more detail in the next sections, where virtual work principle is used to establish the same result.

2.3 Consistency concept

The strain displacement relations for a shear-flexible beam are given by

$$\chi_x = \frac{d\theta_x}{dx} \qquad \ldots(2.6)$$
$$\gamma_{xy} = \frac{dw}{dx} - \theta_x$$

where χ_x is the flexural strain, and γ_{xy} is the shear strain and w is the translational displacement and θ_x is the rotation of plane normal to the neutral axis.

It can be seen that the shear strain terms involve multiple "fields", with the shear strain comprising of the transverse deflection w and the slope θ_x. Field-consistent formulation requires that the interaction between these multiple fields should be

in a consistent manner, the violation of which can lead to constraints which manifests in forms like locking, spurious stresses, delayed convergence etc.

2.3.1 Field-consistency for Isoparametric Element

From the strain displacement relation in eqn. (2.6), for a 2-noded element (C^0 formulation), the shear strain would comprise of a constant term and a first degree polynomial term. This would make the shear stain "inconsistent" and would produce spurious strains in certain limits (as the beam becomes more slender, or as *l/d* ratio increases). Field-consistent formulation realizes this and the shear strain is reconstituted upfront in such a manner that the spurious strains do not exist even in the extreme conditions.

If the displacement w and rotation θ_x are represented by the following interpolation functions

$$w = a_0 + a_1 \frac{x}{l} \qquad \text{…(2.7)}$$
$$\theta_x = b_0 + b_1 \frac{x}{l}$$

Then, the flexural and shear strains are given by

$$\chi_x = \frac{b_1}{l} \qquad \text{…(2.8)}$$
$$\gamma_{xy} = (b_0 - \frac{a_1}{l}) + b_1(\frac{x}{l})$$

The flexural and shear strain energies can be expressed as

$$U_b = \frac{1}{2} EI(2l)\left(\frac{b_1}{l}\right)^2 \qquad \text{…(2.9)}$$
$$U_s = \frac{1}{2} kGA(2l)\left[\left(b_0 - \frac{a_1}{l}\right)^2 + \frac{1}{3}(b_1)^2\right]$$

where U_b is the flexural strain energy and U_s is the shear strain energy, EI is the flexural rigidity of the beam, GA is the shear rigidity and κ is the shear correction factor.

In the constraining limit of a very slender beam (as l/d tends to zero) , the shear strain energy would tend to zero. This in turn means that each of the individual terms inside the shear strain energy becomes zero

$$b_0 - \frac{a_1}{l} \Rightarrow 0 \qquad \ldots(2.10)$$
$$b_1 \Rightarrow 0$$

The first limiting condition in the above equation is field consistent, as it has terms from both of the interpolation functions w and θ_x. The second limiting condition introduces a spurious constraint, and it specifies the way in which the interpolation function for θ needs to be. This artificial constraint manifests itself as locking and generates spurious results, if the shear strain is used as it is. The field-consistent formulation reconstitutes the shear strain so to eliminate the inconsistent constraints. Thus for the present case, the shear strain would be just the constant term alone. For other interpolation functions, similar arguments hold good, and the shear strain can be reconstituted, Prathap (1984).

2.3.2. Field Consistency for Anisoparametric Element – Small Deformations

Consider a 2-noded anisoparametric element, with 4 degrees of freedom at each of the nodes (axial displacement u, transverse deflection w, derivative of the transverse deflection β, and independent slope θ_x. The reason for choosing an additional degree of freedom derivative of the transverse deflection β, is to have a higher order interpolation function for the transverse deflection w which now has cubic interpolation functions, and hence the anisoparametric formulation results (the other two variables, u and θ_x will have linear interpolation functions).

Contrast this with the element which has 3 degrees of freedom at each node (axial displacement *u*, transverse deflection *w*, and independent slope θ_x), which would result in a isoparametric formulation with linear interpolation functions for all the three variables.

For the aniosparametric formulation, the two strain terms that have the multiple field are studied carefully. The following notation is used for representing the displacements and rotations.

$$\theta = c_0 + c_1\xi$$
$$\frac{dw}{dx} = b_0 + b_1\xi + b_2\xi^2 \qquad \ldots(2.11)$$

The shear strain is obtained as

$$\gamma_{xy} = [b_0 + b_1\xi + b_2\xi^2] - [c_0 + c_1\xi] \qquad \ldots(2.12)$$

When Legendre Polynomials are used, and the above expression can be rewritten as

$$\gamma_{xy} = \left[b_0 + b_1P_1 + b_2\left(\frac{P_0 + 2P_2}{3}\right)\right] - [c_0 + c_1P_1] \qquad \ldots(2.13)$$

where

$$\xi = P_1$$
$$\xi^2 = \frac{1}{3}(P_0 + 2P_2)$$

Rearrangement of the terms gives

$$\gamma_{xy} = \left(b_0 + \frac{b_2}{3} - c_0\right)P_0 + (b_1 - c_1)P_1 + \frac{2}{3}b_2P_2 \qquad \ldots(2.14)$$

From field-consistency arguments, for a fully field-consistent element, each of the above terms should independently vanish.

$$\begin{aligned} &b_0 + \frac{b_2}{3} - c_0 \Rightarrow 0 \\ &b_1 - c_1 \Rightarrow 0 \\ &b_2 \Rightarrow 0 \end{aligned} \qquad \ldots(2.15)$$

The first of these 2 equations are field-consistent, while the third equation that has the contribution of only the transverse deflection *w* is inconsistent. The contribution of this term in the field-consistent formulation is dropped, and thus the following expression for the shear strain is used

$$\gamma_{xy} = [b_0 + \frac{b_2}{3} - c_0]P_0 + [b_1 - c_1]P_1 \qquad \ldots(2.16)$$

The strain energy arising from the 2 strain components, shear strain energy U_s, and bending strain energy U_b, are as follows

$$U_s = kGAl\left[\left(b_0 + \frac{b_2}{3} - c_0\right)^2 + \frac{1}{3}(b_1 - c_1)^2\right] \qquad \ldots(2.17)$$

$$U_b = EI\frac{c_1^{\,2}}{l}$$

Similar concepts of consistency can be worked out for several other structural problems, like a curved beam (where membrane locking can occur), incompressible hollow sphere (where volumetric locking can occur). Prathap (1984) has clearly explained the reasoning for each of the above cases. Membrane locking in curved beams/arches has been studied in detail by Stolarski and Belytschko (1983), Prathap (1985), Tessler and Spiridigliozzi (1986), Raveendranath *et al* (1999a).

2.3.3 Field-consistency for Anisoparametric Element - Large Deformations

The field-consistent concept of element formulation of Prathap (1984) is extended to the case of membrane strain energy. For the case of the large deformation, the process of the field-consistent representation of the membrane strain is similar. The strain term that will now be focused is the membrane strain ε_x, which has the multiple "fields". The membrane strain for the case of a large deflection problem is

$$\varepsilon_x = \frac{du}{dx} + \frac{1}{2}\left(\frac{dw}{dx}\right)^2 \qquad \ldots(2.18)$$

Using a similar approach that was outlined in section 2.3.2, the strain field can be represented using the following relations

$$\begin{aligned} u &= a_0 + a_1\xi \\ \theta &= c_0 + c_1\xi \\ \frac{dw}{dx} &= b_0 + b_1\xi + b_2\xi^2 \end{aligned} \qquad \ldots(2.19)$$

where

$$b_0 = \frac{3}{4l}(w_2 - w_1) - (\theta_2 + \theta_1)$$
$$b_1 = \frac{1}{2}(\theta_2 - \theta_1)$$
$$b_2 = \frac{3}{4l}(w_1 - w_2) + \frac{3}{4}(\theta_2 + \theta_1)$$

Using the process followed earlier, the membrane strain is expressed as

$$\varepsilon_x = a_1 + \frac{1}{2}b_0^{\,2} + b_0 b_1 \xi + \left(\frac{1}{2}b_1^{\,2} + b_0 b_2\right)\xi^2 + b_1 b_2 \xi^3 + \frac{1}{2}b_2^{\,2}\xi^4 \qquad \ldots(2.20)$$

In this expression u_1, u_2, w_1, w_2, θ_1, θ_2 are the nodal displacements and rotations. The above relations are used to obtain the secant stiffness and tangent stiffness matrices as explained below.

Rearranging the terms after using Legendre polynomials, the following conditions are required to be met, in the constraining limit

$$\begin{aligned}
&a_1 + \left[\frac{1}{2}b_0^{\,2} + \frac{1}{6}b_1^{\,2} + \frac{1}{10}b_2^{\,2} + \frac{1}{3}b_0 b_2\right] \Rightarrow 0 \\
&b_0 b_1 + \frac{3}{5}b_1 b_2 \Rightarrow 0 \\
&\frac{1}{6}b_1^{\,2} + \frac{1}{7}b_2^{\,2} + \frac{1}{3}b_0 b_2 \Rightarrow 0 \\
&b_1 b_2 \Rightarrow 0 \\
&b_2^{\,2} \Rightarrow 0
\end{aligned} \qquad \ldots(2.21)$$

For a fully field-consistent element, the membrane strain energy is given by the first of the constraints shown in eqn. (2.21), with the other constraints being spurious. Thus the reconstituted field-consistent membrane strain is

$$\varepsilon_x = a_1 + \left[\frac{1}{2}b_0^{\,2} + \frac{1}{6}b_1^{\,2} + \frac{1}{10}b_2^{\,2} + \frac{1}{3}b_0 b_2\right] \qquad \ldots(2.22)$$

2.4 Virtual Work Principle - Elastostatics

The boundedness of the strain energy can be established though virtual work principle. Following the nomenclature used in Strang and Fix (1973), the weak form in terms of the energy inner product for the exact solution *u* to the problem can be written as.

$$a(u,u) = (f,u) \qquad \ldots(2.23)$$

$$a(u,u^h) = (f,u^h) \qquad \ldots(2.24)$$

where
a(u,u) is the bilinear symmetric functional
(f,u) is the integral $\int ufdV$ *over the system domain V.*

The first two virtual work statements refer to the exact solution of the elastostatics problem. In eqn. (2.23), the trial function and test function are taken as *u* and the virtual work argument establishes that eqn. (2.23) is truly satisfied only when *u* is the exact solution at the point of equilibrium. In eqn. (2.24) , use is made of the fact that the test function u^h (the Ritz or finite element solution) need not be the exact displacement function for the virtual work principle to be true. For convenience, this is taken to be the discrete finite element displacement field, as long as it is admissible (that is, satisfies all the geometric boundary conditions).

2.4.1 Best-fit rule

By using u^h for both the trial and test function, the actual finite element equations are obtained, with the right hand side leading to the consistent load vector and the left hand side representing the stiffness matrix.

$$a(u^h,u^h) = (f,u^h) \qquad \ldots(2.25)$$

This equation will now reflect the error due to the finite element discretisation. Now it is easy to see how the error $e = u - u^h$ can be assessed.

Comparing (2.24) and (2.25) and noting that the energy inner product is bi-linear, Reddy (1986), results in

$$a(u,u^h) = a(u^h,u^h) \qquad \ldots(2.26)$$

From this the projection theorem can be expressed as

$$a(u - u^h,u^h) = 0 \qquad \ldots(2.27)$$

The finite element solution is therefore seen to be a best-fit or best approximation solution. In most simple linear elastostatics cases, this would imply that the strains or stresses are obtained in a best-fit sense and that there would be points in the element domain where these stresses or strains are very accurately computed (superconvergence). If eqn. (2.4) or (2.5) is compared with eqn. (2.27) it can be seen that both converge to the same fact – which is the best-fit rule.

2.4.2 Strain energy boundedness

From the fact that the energy inner product is bi-linear, it can be shown that

$$\begin{aligned} a(u - u^h,u-u^h) &= a(u,u) + a(u^h,u^h) - 2\,a(u,u^h) \\ &= a(u,u) - a(u^h,u^h) - 2[\,a(u,u^h) - a(u^h,u^h)\,] \end{aligned}$$

$$= a(u,u) - a(u^h,u^h) - 2[a(u - u^h,u^h)] \qquad \ldots(2.28)$$

Introducing the result from (2.27), the energy error theorem is obtained, which can be expressed as

$$a(u-u^h,u-u^h)=a(u,u)-a(u^h,u^h) \qquad \ldots(2.29)$$

i.e., Energy of the error = Error of the energy

This leads to a useful statement that as the left hand side of (2.29) is always positive definite,

$$a(u^h,u^h) < a(u,u) \qquad \ldots(2.30)$$

Thus, in a variationally correct approach, the energy inner product of the approximate (Ritz or finite element) solution will always be a lower bound of the exact energy.

2.5 Virtual Work - Elastodynamics

The variational aspects of elastodynamics can be understood from the Lagrangian or Hamiltonian statements, where both potential energy and kinetic energy enter into the functional.

Unlike Strang and Fix (1973), where the development of the argument is based on the Rayleigh quotient, the weak form is written in terms of the energy inner product for the exact solution u to the problem and the loading term f is replaced with the inertial force term $\omega^2\rho u$. The earlier equations yield

$$a(u,u) = \omega^2.(\rho\, u,u) \qquad \ldots (2.31)$$

$$a(u,u^h) = \omega^2.(\rho u,u^h) \qquad \ldots(2.32)$$

where ρ is the inertia density of the domain. Again, the first two virtual work statements refer to the exact solution of the elastodynamics problem. In (2.31), the trial function and test function are taken as u and the virtual work argument establishes that (2.31) is truly satisfied only when u is the exact eigenfunction and ω^2 is the exact eigenvalue. In (2.32), the fact is noted that the test function u^h (the Ritz or finite element solution) need not be the exact displacement function for the virtual work principle to be true, while ω^2 remains the exact eigenvalue. u^h is taken to be the discrete finite element displacement field, as long as it is admissible (that is, satisfies all the geometric boundary conditions).

By using u^h for both the trial and test function, the actual finite element equations are obtained, with the right hand side leading to the consistent mass matrix and the left hand side leading to the stiffness matrix.

$$a(u^h, u^h) = (\omega^h)^2.(\rho u^h, u^h) \qquad \ldots(2.33)$$

This equation will now reflect the error due to the finite element discretisation, appearing both in the eigenfunction, and in the eigenvalue. This makes the assessment of the errors a trifle more complicated than in the elastostatics case earlier, as there is the error in the eigenfunction, $u - u^h$ as well as the error in the eigenvalue, $(\omega^h)^2 - \omega^2$ to be assessed. Comparing (2.32) and (2.33) and also noting that the energy inner product is bi-linear, the following equation is obtained

$$[a(u,u^h) - [a(u^h,u^h)] - [\omega^2.(\rho u, u^h) - (\omega^h)^2.(\rho u^h, u^h)] = 0 \qquad \ldots(2.34)$$

or

$$a(u-u^h,u^h) - (\omega^2\rho u - (\omega^h)^2\rho u^h, u^h) = 0 \qquad \ldots(2.35)$$

becomes the projection theorem for elastodynamics.

The finite element solution is still seen to be a best-fit or best approximation solution. However, unlike the simple linear elastostatics cases, this would imply that the strains or stresses are only nearly obtained in a best-fit sense. It is no longer possible now to relate the error of the energy to the energy of the error, as was possible for the elastostatics case as in equation (2.29) earlier. The error of the energies is considered first. From equation (2.31) and (2.33), this becomes

$$[a(u,u)-a(u^h,u^h)]-[\omega^2.(\rho u,u)-(\omega^h)^2.(\rho u^h, u^h)] = 0 \qquad \ldots(2.36)$$

The energy of the errors is considered next. This is given by

$$\begin{aligned} a(u - u^h,u-u^h) &= a(u, \rho u) + a(u^h, u^h) - 2\, a(u, u^h) \\ &= \omega^2.(\rho u, u) - 2\omega^2.(\rho u, u^h) + (\omega^h)^2.(\rho u^h, u^h) \\ &= \omega^2.(\rho u,u)-2\omega^2.(\rho u, u^h)+ (\omega)^2(\rho u^h, u^h) + [(\omega^h)^2 - \omega^2] (\rho u^h, u^h) \\ &= \omega^2.(\rho u - \rho\, u^h,\ u - u^h) + [(\omega^h)^2 - \omega^2] .(\rho u^h, u^h) \end{aligned} \qquad \ldots(2.37)$$

This is indeed Lemma 6.3 of Strang and Fix (1973). The three virtual work equations (equations (2.31) to (2.33)) have led very easily to a projection theorem (equation (2.35)), and a separate energy-error theorem (equation (2.36)) and error-energy theorem (equation (2.37)). Unlike the case for elastostatics, a simple relationship between the energy of the error and the error of the energy cannot be derived. Also, it is not easy to show that for a conforming and variationally correct formulation, the discretised eigenvalue would

always be higher than the exact eigenvalue, whereas for the elastostatics problem, there existed an elegant lower bound result (equation (2.30)). This is because an eigenvalue problem does not give a unique displacement field u or u^h . One can side-step this issue by introducing into equation (2.37), the idea of a normalized generalized mass, where $(\rho u, u) = (\rho u^h, u^h) = 1.$ This gives the following relation

$$(\omega^h)^2 - \omega^2 = - [a(u,u) - a(u^h,u^h)] \qquad \ldots(2.38)$$

2.6 Closure

In this chapter, the broad basis for the 3C concepts was laid out. The concept of best-fit rule (the correspondence concept) was explained using both variational principle and virtual work principle. The consistency concept was brought out through various examples for both small and large deformations, and the conditions under which the violation of the consistency requirements would produce spurious constraints were explained. The requirement of strain energy boundedness for a variationally correct formulation was shown using virtual work principle. For elastodynamics problems, the equivalence of the best-fit rule of elastostatics has been shown. All subsequent chapters of this thesis would use these concepts for assessing the performance of the different element formulations.

Chapter-3

Linear Elastostatics for Classical Beams, Shells and Plates

3.1 Introduction

In this chapter, the applications of 3C concepts to linear elastostatics problems for classical beams, shells and plates are studied in detail. Two one-dimensional problems (beam and axisymmetric shell) and a two-dimensional problem (plate) are solved using different element formulations. The performance of element formulations for an Euler-Bernoulli beam with respect to the 3C concepts, is studied in detail using C^1 element. Similar study for an axisymmetric shell formulation is carried out. Subsequently, the classical thin plate bending elements using C^1 formulation are investigated. The best-fit rule, boundedness of strain energy and convergence behaviour are discussed in detail for all the above problems. The results of the findings are summarized in the closure section of this chapter.

3.2 Euler-Bernoulli Beam

The strain displacement relations for this beam are as follows:

$$\chi_x = z\frac{d^2w}{dx^2} \qquad \ldots(3.1)$$

where

χ_x is the curvature

z is the distance from the neutral axis

w is the deflection (translational displacement)

3.2.1 Element Formulation

A 2-noded C^1 element with two degrees of freedom at each node (one translational and one rotational) is considered for the study of an Euler-Bernoulli beam. Since 4 degrees of freedom are available in each element, cubic interpolation functions can be used. The shape functions for this element are

$$\begin{aligned} N_1(\xi) &= 1 - 3\xi^2 + 2\xi^3 \\ N_2(\xi) &= 3\xi^2 - 2\xi^3 \\ N_3(\xi) &= \xi - 2\xi^2 + \xi^3 \\ N_4(\xi) &= \xi^3 - \xi^2 \end{aligned} \qquad \ldots(3.2)$$

Where ξ is the non-dimensional parameter ($=x/l$, l the length of the beam, and x is the distance from the first node)

The details of the formulation of the element stiffness matrix and the force matrix are not elaborated here as they can be found in any standard textbook *e.g.* Cook *et al.* (1989).

3.2.2 Numerical Experiments and Discussion

The exact closed form solution for a beam bending problem is available for all types of loading and boundary conditions. This would facilitate easy interpretation of the best-fit rule that was outlined in chapter-2. For simplicity, the bending moments from the finite element solution obtained for a cantilever subjected to uniform load, and a linear varying load are reported here.

The fact that the finite element solution for the bending moment coincides with the exact solution at certain points within the element has been known for many years now, and these points have been referred as Barlow points (1976), and Prathap points (Rajendaran(2008)). That the finite element solution is a least-

squares best fit of the exact solution is not very well known. This fact was proved from a variational perspective by Prathap (1996b). The cantilever beam example was chosen to demonstrate that the current formulation follow a least-squares best fit stress recovery. The dimensions of the beam and loading are shown in Fig. 3.1 and Fig. 3.2.

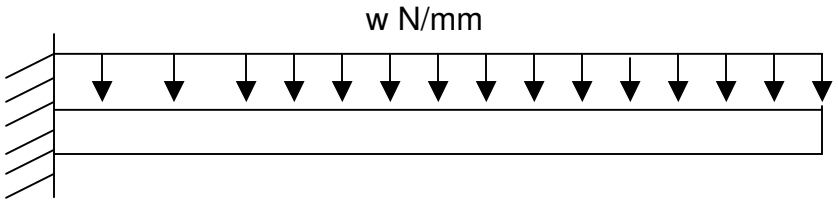

Fig. 3.1 A cantilever subjected to a uniform varying load

(Length = 10 mm, Depth = 1 mm, Width = 1 mm, E = 200000 N/mm^2, *w* = 1 N/mm)

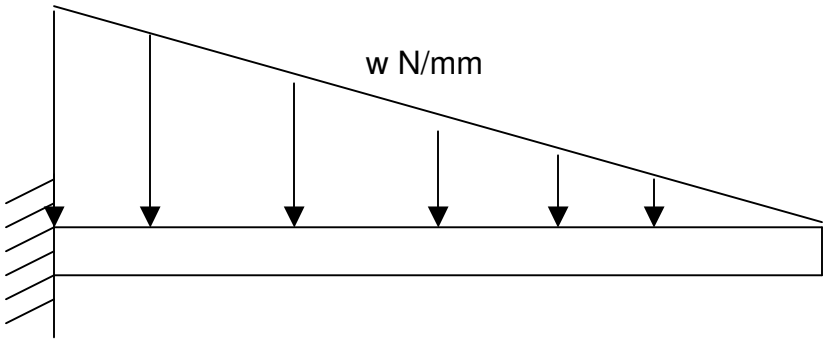

Fig. 3.2 A cantilever subjected to a linear varying load

(Length = 10 mm, Depth = 1 mm, Width = 1 mm, E = 200000 N/mm^2, *w* = 1 N/mm)

The variation of the bending moment and shear force, with length as computed from the finite element solution is compared with the theoretical solution as shown in Figs. 3.3– 3.4, for the case of uniform load. For a linear varying load the corresponding figures are Figs. 3.5 – 3.6.

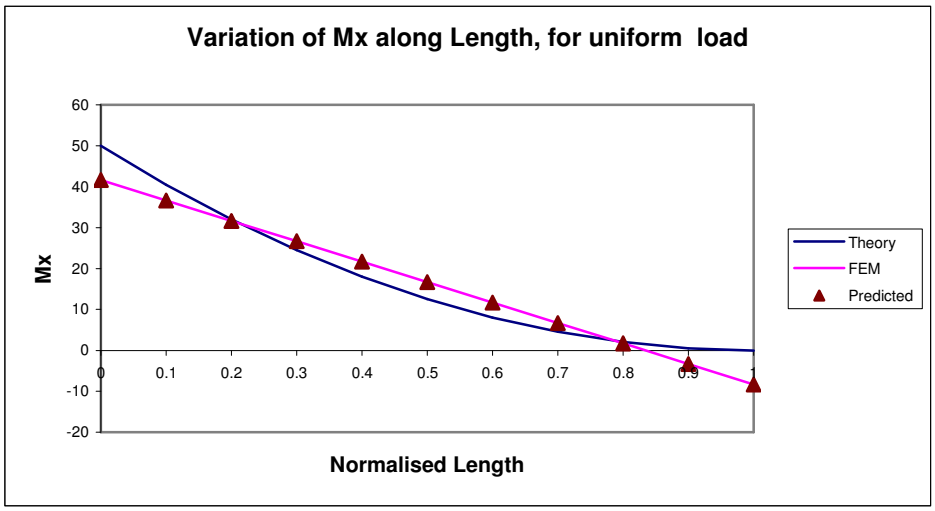

Fig. 3.3 Variation of bending moment with length (uniform load)

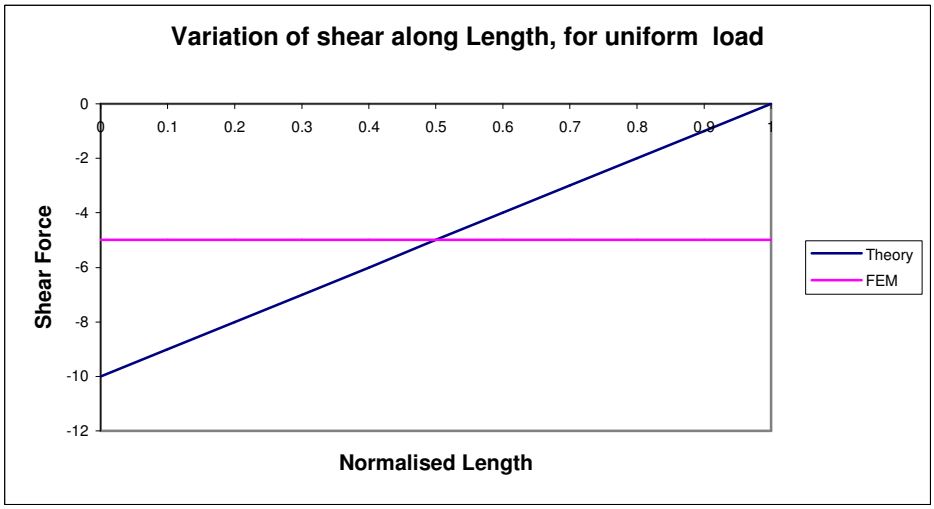

Fig. 3.4 Variation of shear force with length (uniform load)

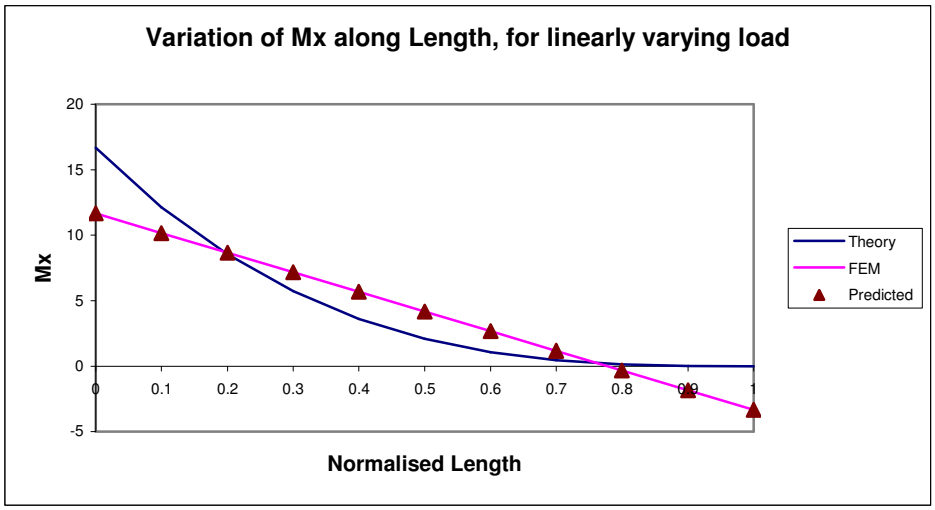

Fig. 3.5 Variation of bending moment with length (linear varying load)

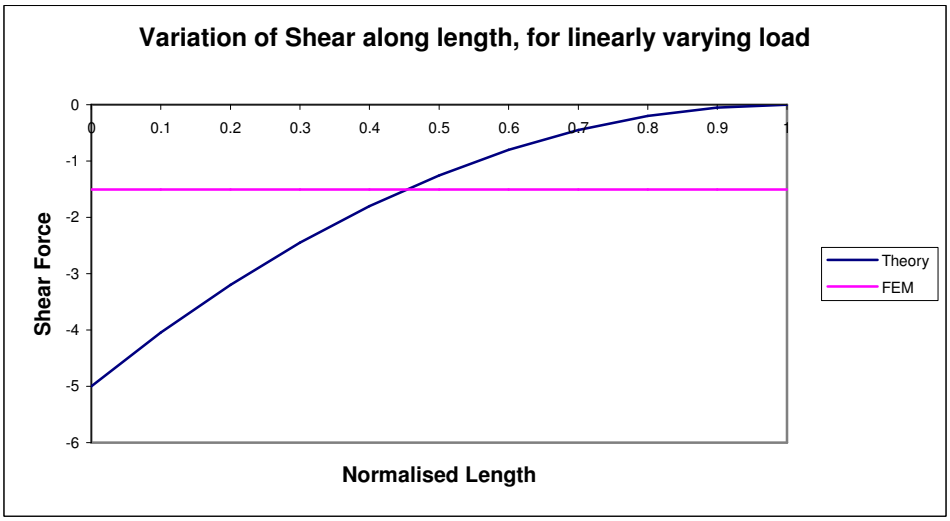

Fig. 3.6 Variation of Shear Force with Length (linear varying load)

The bending moment predicted by the finite element solution closes on to the exact solution as the mesh is progressively refined. Since M_x and V_x depend on the second and third order derivatives of w, the element can recover linearly varying bending moments and constant shear forces. What is also true is that these recovered stresses follow the best-fit rule accurately, as explained below.

To show mathematically that the bending moment given by the finite element solution is the least squares best-fit of the exact solution, assume that the best fit curve be represented by the equation $Ax + B$. Then, for the case of the uniformly distributed load on the cantilever, the bending moment at any distance x from the free end is $-wx^2/2$. Thus the error in the bending moment is $-wx^2/2 - (Ax+B)$. The constants A and B are found from the least-squares of this error which is given by

$$E = \int [- wx^2/2 - (Ax+B)]^2 \, dx \qquad \ldots(3.3)$$

The constants A and B can be found by solving $\partial E/\partial A = 0$, and $\partial E/\partial B = 0$

The above equations give the values of A and B as, $A = -1/2$, and $B = 1/12$. Note that the length of the beam in this case has been taken to be of 1 unit, and hence the bending moment as predicted by our equation $Ax + B$, at $x=0$ (Free end of the beam) is 1/12, and at the fixed end is –5/12, which match exactly with the finite element of the solution for the case of 1X1 mesh, as shown in Fig. 3.3.

Similarly, for the case of a linear varying load, a solution of the form $Cx + D$ can be assumed, and the constants, C and D can be determined, in the least squares way as was done earlier for the case of uniformly distributed load. In this case

$$E = \int [- wx^3/6 - (Cx+D)]^2 \, dx \qquad \ldots(3.4)$$

The constants C and D are found from the equations $\partial E/\partial C = 0$, and $\partial E/\partial D = 0$

The above equations give the values of C and D as, C= -3/20, and D = 1/30. Here too, the bending moment at the free end and the fixed end from the finite

element solution match exactly with the values given by the above best-fit curve (Fig. 3.5), suggesting that the bending moment from the finite element solution is nothing but the best-fit of the exact solution.

Prathap (1999) has shown from the correspondence concept that if the displacement fields are chosen so that the finite element strains are complete to the order x^{n-1}, then the finite element solution produces strains that are accurate to $O(h^n)$, energies that are accurate to $O(h^{2n})$ and the errors (in displacements) are removed at the rate of $O(h^{2n})$. Thus for an Euler-Bernoulli beam bending problem that is analysed with a finite element that has cubic interpolation functions, it can be predicted *a priori* that the displacements would converge at the rate of $O(h^4)$.

The convergence of the strain energy for the case of a simply supported beam subjected to a uniform load is tabulated in Table 3.1. The length of the beam is taken as 1000 mm, with the width and depth both as 10 mm. The Young's Modulus used is 200000 N/mm^2. The beam is subjected to a uniformly distributed load of 1 unit. It can be seen clearly that the strain energy is bounded as per eqn. (2.30)

Simply Supported Beam - UDL		
# of Elements	C^1 Formulation	
	Deflection	Strain Energy
2	0.520833	8.327908
4	0.520833	8.332994
8	0.520833	8.333312
16	0.520833	8.333332
32	0.520833	8.333333
64	0.520833	8.333333

Table 3.1 Strain energy boundedness in a simply supported beam (uniform load)

It can be seen from the Table 3.1 that the displacement at the centre of the beam is the same under all cases and is in fact the exact displacement. The reason why in this particular example, the finite element solution matches with the exact

solution at the nodes is due to the loading and the interpolation function that has been used in the element formulation. The exact solution is a 4^{th} order polynomial, and with a cubic interpolation functions the displacements at the nodes would always match. It can also be seen that the strain energy converges at $O(h^4)$.

It would be of interest to see the convergence of the displacement. For this case, an exact solution for the central deflection is known. Fig. 3.7 shows the $O(h^4)$ rate of convergence predicted theoretically. Here, in this example, the results for the nodal displacements are reported at the centre of the beam. This formulation gives the exact solution for the displacement, even with one element representing the total length of the beam. The beam has been discretised into 1, 3, 5, 7, 9 and so on. Discretisation in this fashion ensures that no node comes at the centre of the beam, and the displacement at the centre of the beam was re-computed from the finite element displacements of the element on which the centre of the beam falls. This strategy enables computation of the errors in the displacement at the centre of the beam.

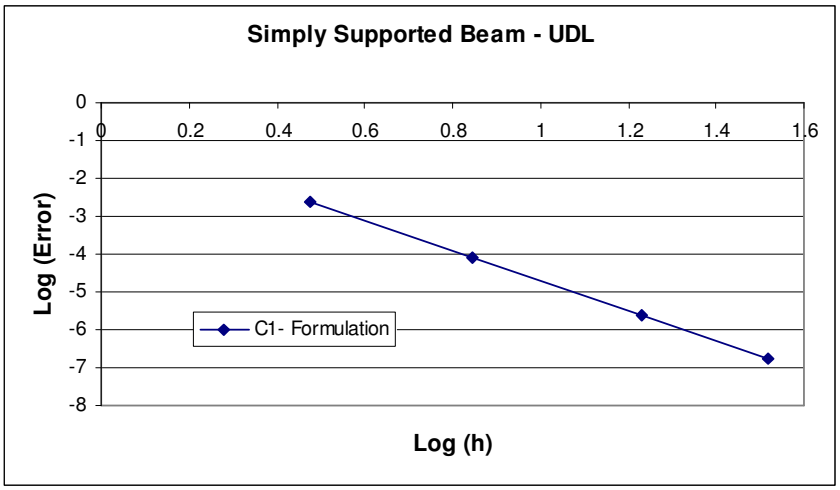

Fig. 3.7 Rate of convergence of deflection in a simply supported beam (uniform load)

The concepts explained above with the help of a cantilever beam are true for other cases boundary conditions/loading conditions also.

3.3 Axisymmetric Shell

The applications of the finite element method to the analyses of axisymmetric shells started in the early 60's, Grafton and Strome (1963) and work on this subject has since been continuously performed. Jones and Strome (1965) presented detailed reviews of the conical shell elements used for the axisymmetric analysis. The conical shell element can now be found in any standard text book on finite element analysis, say, Cook *et al.* (1989). In this section, the formulation of the 2-noded axisymmetric element is discussed. The finite element formulation for the classical 2-noded C^1 element (with 2 degrees of freedom at each node viz, one transverse displacement and one rotation) is presented now. The classical example of circular plate with different edge conditions (simply supported along the edge, clamped along the edge) for which theoretical solution exists is considered for studying the results.

For a circular plate, the curvature can be expressed as

$$\chi_r = \frac{d^2w}{dr^2}$$
$$\chi_\theta = \frac{1}{r}\frac{dw}{dr} \qquad \ldots(3.5)$$

where,

χ_r is the radial curvature
χ_θ is the tangential curvature
w is the deflection
r is the radial distance

The Moment-Curvature relations are given by

$$\begin{Bmatrix} M_r \\ M_\theta \end{Bmatrix} = [D] \begin{Bmatrix} \chi_r \\ \chi_\theta \end{Bmatrix} \qquad \ldots(3.6)$$

where

$$D = \frac{Eh^3}{12(1-v^2)} \begin{bmatrix} 1 & v \\ v & 1 \end{bmatrix}$$

3.3.1 Element Formulation

A 2-noded element, with 3 degrees of freedom at each node, *u, w, w,*$_x$ is considered here. This element is shown in Fig. 3.8. The strain displacement relation is given in eqn. (3.7)

$$\varepsilon = \begin{Bmatrix} \varepsilon_s \\ \varepsilon_\theta \\ \chi_s \\ \chi_\theta \end{Bmatrix} = \begin{Bmatrix} \dfrac{du}{ds} \\ \dfrac{1}{r}(u\cos\phi + w\sin\phi) \\ \dfrac{d^2w}{ds^2} \\ -\dfrac{1}{r}\left(\dfrac{dw}{ds}\right)\cos\phi \end{Bmatrix} \qquad \ldots(3.7)$$

where ε_s, ε_θ are the meridional strain and hoop strain respectively, and other terms are described in eqn. (3.5).

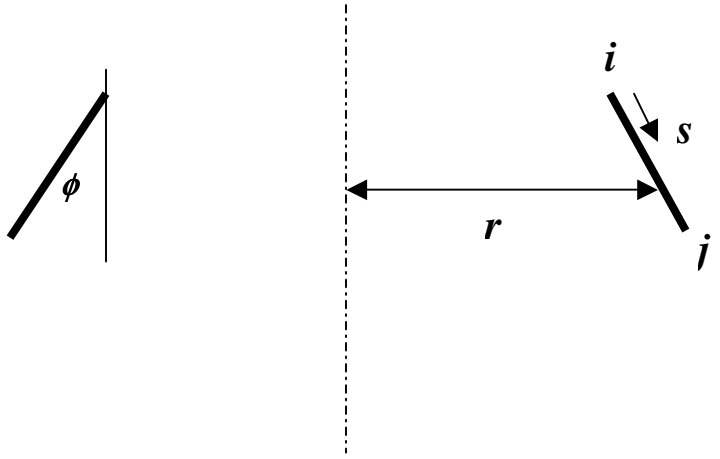

Fig. 3.8 A 2-noded axisymmetric element

The interpolation functions that are used for representing the displacements are given in eqn. (3.8)

$$u = \alpha_1 + \alpha_2 s$$
$$w = \alpha_3 + \alpha_4 s + \alpha_5 s^2 + \alpha_6 s^3 \qquad \ldots(3.8)$$

The stress-strain relation is given is eqn. (3.9)

$$\sigma = \begin{Bmatrix} N_s \\ N_\theta \\ M_s \\ M_\theta \end{Bmatrix} = [D]\varepsilon \qquad \ldots(3.9)$$

where

$$D = \frac{Et}{1-\nu^2}\begin{bmatrix} 1 & \nu & 0 & 0 \\ \nu & 1 & 0 & 0 \\ 0 & 0 & \frac{1}{12}t^2 & \frac{1}{12}\nu t^2 \\ 0 & 0 & \frac{1}{12}\nu t^2 & \frac{1}{12}t^2 \end{bmatrix} = \begin{bmatrix} D_1 & 0 \\ 0 & D_2 \end{bmatrix} \qquad \ldots(3.10)$$

The stiffness matrix is formed using eqn. (3.11)

$$K = \int [B]^T [D][B] dA \qquad \ldots(3.11)$$

$$dA = 2\pi r dr$$

3.3.2 Numerical Experiments and Discussion

This element is now used for studying the results of various axisymmetric structures that can be idealized as shell problems. Typical structures that come under this category include plates(circular/elliptical), pipes, and pressure vessels.

A few cases where an exact closed form solution is available are now considered. A circular plate of radius = 10 in., E=1.0e7 psi, υ =0.3, and t=0.1 in. is subjected to a uniform load of 1 lb/in^2. Two boundary conditions, one with plate clamped along its edge and the other with the plate simply supported along the edge are analysed. The deflection at the centre of the plate is shown in Table 3.2 for the clamped circular plate, and in Table 3.2 for the simply supported circular plate.

Clamped Circular Plate, Uniform Load, C^1 Formulation	
Elements	Deflection
2	0.1714556150
4	0.1706845517
8	0.1706292022
16	0.1706252927
32	0.1706250202
64	0.1706250014
Theory	0.1706250000

Table 3.2 Deflection in a clamped circular plate (uniform load)

Simply Supported Circular Plate, Uniform Load, C^1 Formulation	
Elements	Deflection
2	0.6964556163
4	0.6956845521
8	0.6956292024
16	0.6956252927
32	0.6956250202
64	0.6956250013
Theory	0.6956250000

Table 3.3 Deflection in a simply supported circular plate (uniform load)

The best-fit rule for the case of a circular plate is an interesting one for the reason that there are 2 bending moment components that need to be considered – the radial bending moment and hoop bending moment. Neither of them are a stand-alone best-fit as they are coupled. Hence the best-fit rule needs to consider this. Table 3.4 and 3.5 show clearly that the best-fit rule is obeyed.

The bending moment plots are shown in Fig. 3.9 and Fig. 3.10 for the circular clamped plate and Fig. 3.11 and Fig. 3.12 for a simply supported circular plate. These plots compare the finite element results with theoretical results, Timoshenko and Woinowsky-Krieger (1959).

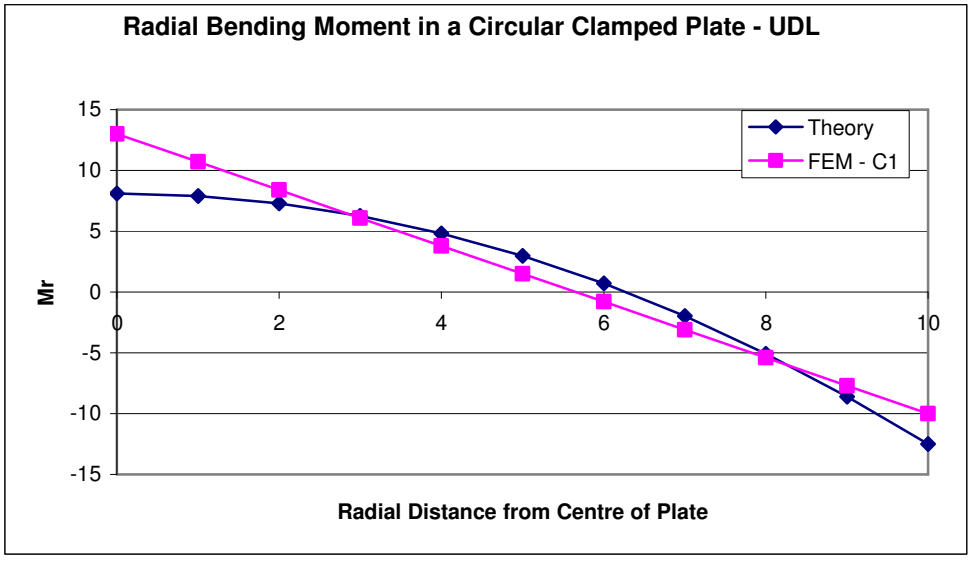

Fig. 3.9 Radial bending moment in a clamped circular plate (uniform load)

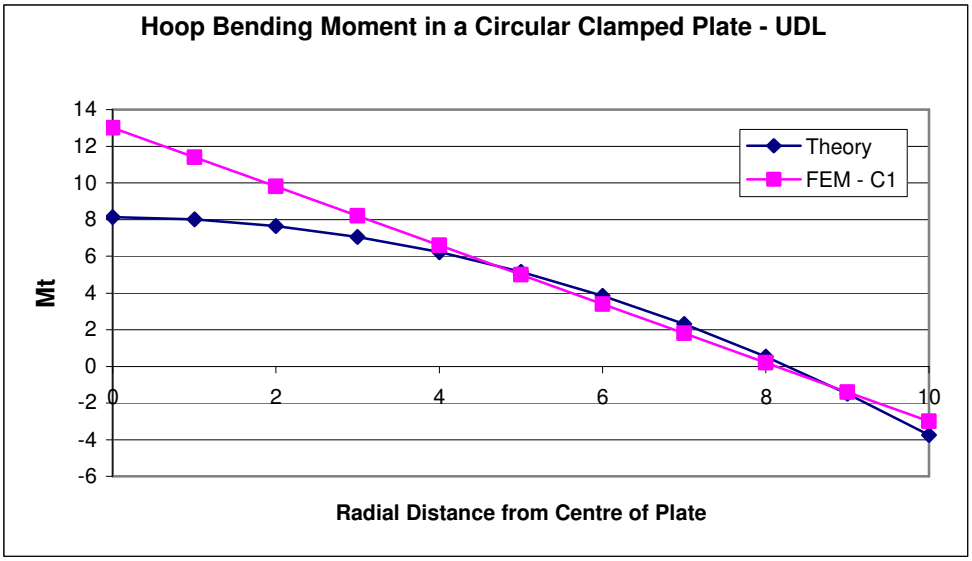

Fig. 3.10 Hoop bending moment in a clamped circular plate (uniform load)

Best-fit for a Circular Clamped Plate - Uniform Load					
Weight	Integration Point	Cr - FEM	Ct - FEM	Cr-Theory	Ct-Theory
0.347855	0.930568	0.009404	-0.00076	0.010905	-0.000915
0.652145	0.669991	0.003713	-0.0036	0.002366	-0.003761
0.347855	0.069432	-0.0094	-0.01016	-0.006726	-0.006792
0.652145	0.330009	-0.00371	-0.00732	-0.004595	-0.006082
Best-fit residual = 0.0000000209514					

Table 3.4 Results of best-fit rule for a clamped circular plate (uniform load)

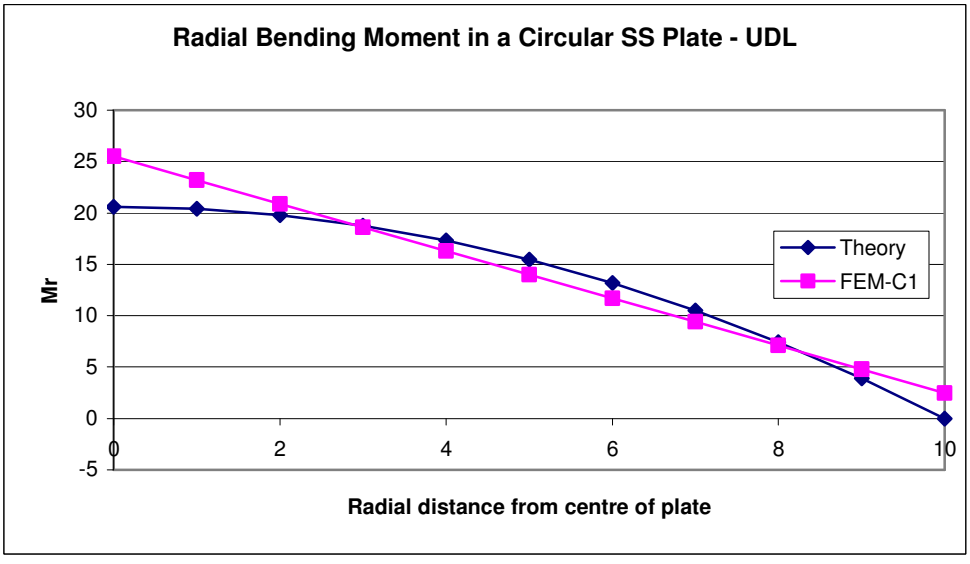

Fig. 3.11 Radial bending moment in a simply supported circular plate (uniform load)

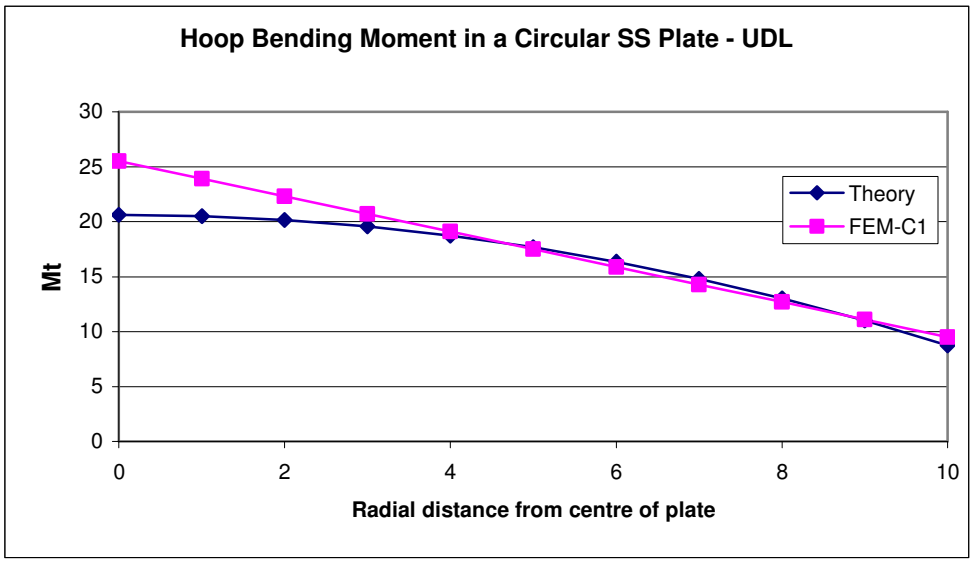

Fig. 3.12 Hoop bending moment in a simply supported circular plate (uniform load)

Best-fit for a Circular SS Plate - Uniform Load					
Weight	Integration Point	Radial Curvature - FEM	Hoop Curvature - FEM	Radial Curvature - Theory	Hoop Curvature - Theory
0.347855	0.930568	-0.001096	-0.011258	0.000405	-0.011415
0.652145	0.669991	-0.006787	-0.014104	-0.008134	-0.014261
0.347855	0.069432	-0.019904	-0.020662	-0.017226	-0.017292
0.652145	0.330009	-0.014213	-0.017816	-0.015095	-0.016582
Best-fit residual = 0.000000013827					

Table 3.5 Results of best-fit rule for a simply supported circular plate (uniform load)

The strain energy for the cases of circular plate for both clamped edge and simply supported edge boundary conditions are tabulated in Table 3.6 and Table 3.7 for various discretisations. The order of convergence for the C^1 formulation is $O(h^4)$, as seen from the plots shown in Fig. 3.13, and 3.14.

Boundedness of Strain Energy, Circular Clamped Plate, Uniform Load	
Elements	C^1 Formulation
2	17.82582805
4	17.86519928
8	17.86764539
16	17.86779849
32	17.86780807
64	17.86780867

Table 3.6 Strain energy boundedness in a clamped circular plate (uniform load)

Boundedness of Strain Energy, Circular Simply Supported Plate, Uniform Load	
Elements	C^1 Formulation
2	100.2926372
4	100.3320087
8	100.3344548
16	100.3346079
32	100.3346175
64	100.3346181

Table 3.7 Strain energy boundedness in a simply supported circular plate (uniform load)

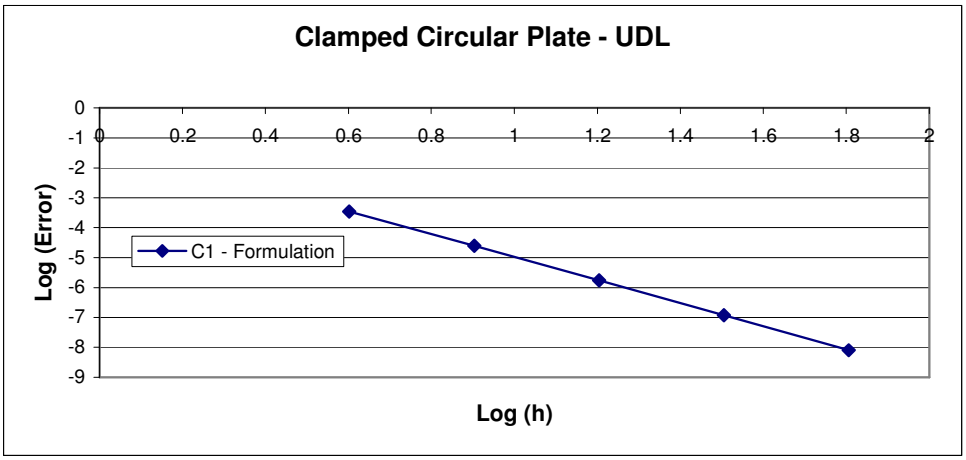

Fig. 3.13 Convergence of deflection in a clamped circular plate (uniform load)

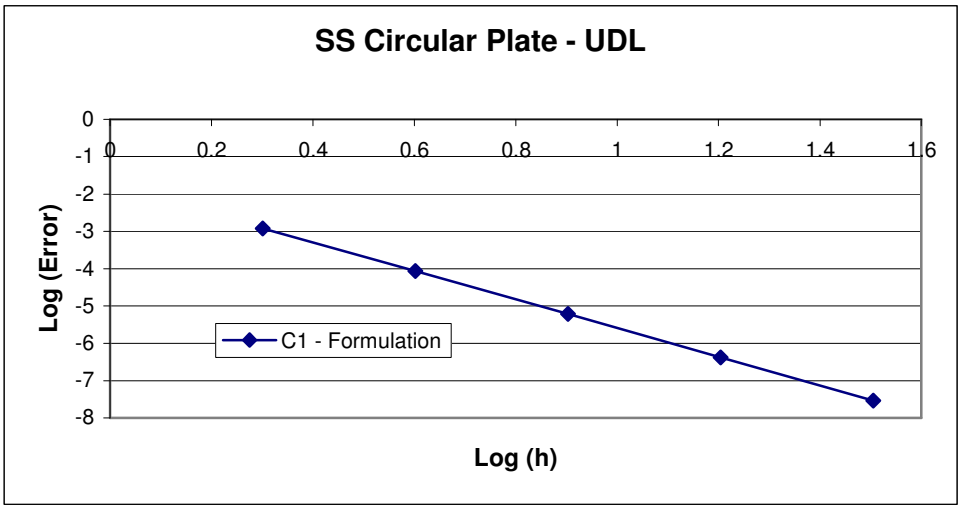

Fig. 3.14 Convergence of deflection in a simply supported circular plate (uniform load)

3.4 Classical Plate Bending Elements

Thin plates have been traditionally solved in the finite element analysis using many types of elements. The pioneering work by Turner *et al.* (1956) showed in essence the application of the finite element method (though the phrase "finite element" was not in existence then). It is to the credit of these pioneers ingenuity in coming up with a generic process which has later been named as the finite element method (in fact by R.W.Clough, one of the co-authors of this publication) that their prophecy "…and the solution offered here is felt to have potential usefulness for finding approximates solutions to many two-dimensional problems in elasticity" came true within a few years of their publication. Melosh (1963) used this process and came up with the stiffness matrices for plate bending problems. Zienkiewicz and Cheung (1965) came up with the applications of the generic finite element method to the analyses of elastic isotropic and orthotropic slab. This period saw a great surge in the development of the finite element method, especially to plate bending problems (Proc. Conferences, 1965, 1968).

Prominent among the different types of plate bending elements are the formulations which are designated as ACM element, reformulated in Brebbia and Connor (1973), and BFS element by Bogner *et al.* (1965). These elements are chosen to examine the 3C concepts, for the reason that the ACM element is a non-conforming element while the BFS element is a conforming element. In this thesis, both of these elements have been formulated and tested for different loading cases and boundary conditions. This section discusses the results of these elements.

3.4.1 ACM Element Formulation

The ACM element has 3 degrees of freedom (displacement w, rotation ∂w/∂x, rotation ∂w/∂y) at each node. This needs 12 polynomial terms which would constitute the shape functions of the element. These 12 polynomial terms are selected so that we can maintain spatial isotropy. The following 12 polynomial terms are used -

$$[1, x, y, x^2, y^2, xy, x^3, x^2y, xy^2, y^3, x^3y, xy^3]$$

The shape functions that are used for the ACM element are given below:

$$N_1 = 2(\eta-1)(\xi-1)(0.5(1+\xi+\eta)-\xi^2-\eta^2)$$

$$N_2 = -a(\eta-1)(\xi-1)(\xi-1)\xi$$

$$N_3 = -b(\eta-1)(\eta-1)(\xi-1)\eta$$

$$N_4 = 2(\eta-1)\xi(\eta^2+\xi^2-1.5\xi-0.5\eta)$$

$$N_5 = -a(\eta-1)\xi^2(\xi-1)$$

$$N_6 = b(\eta-1)(\eta-1)\xi\eta$$

$$N_7 = 2\xi\eta(-\eta^2-\xi^2-0.5+1.5(\xi+\eta)) \qquad \ldots(3.12)$$

$$N_8 = a\,\eta\,\xi^2(\xi-1)$$

$$N_9 = b\,\eta^2\,\xi(\eta-1)$$

$$N_{10} = 2\,\eta(\xi-1)(\eta^2+\xi^2-0.5\xi-1.5\eta)$$

$$N_{11} = a\,\eta\xi(\xi-1)(\xi-1)$$

$$N_{12} = -b\,\eta^2(\xi-1)(\eta-1)$$

where a, and b are the dimensions of the rectangular element, and ξ and η are non-dimensional quantities x/a and y/b respectively.

3.4.2 BFS Element Formulation

The BFS element is an improvement on the ACM element. It has 4 degrees of freedom (displacement *w*, rotation $\partial w/\partial x$, rotation $\partial w/\partial y$, and a cross-twist $\partial^2 w/\partial x \partial y$) at each node. This requires 16 polynomial terms.

$$[1, x, y, x^2, y^2, xy, x^3, x^2y, xy^2, y^3, x^3y, xy^3, x^2y^2, x^3y^2, x^2y^3, x^3y^3]$$

$$\begin{aligned}
N_1 &= f1(\xi)\, f1(\eta) \\
N_2 &= a\, g1(\xi)\, f1(\eta) \\
N_3 &= b\, f1(\xi)\, g1(\eta) \\
N_4 &= a\, b\, g1(\xi)\, g1(\eta) \\
N_5 &= f2(\xi)\, f1(\eta) \\
N_6 &= a\, g2(\xi)\, f1(\eta) \\
N_7 &= b\, f2(\xi)\, g1(\eta) \\
N_8 &= a\, b\, g2(\xi)\, g1(\eta)
\end{aligned} \qquad \ldots(3.13)$$

$$\begin{aligned}
N_9 &= f2(\xi)\, f2(\eta) \\
N_{10} &= a\ g2(\xi)\, f2(\eta) \\
N_{11} &= b\, f2(\xi)\, g2(\eta) \\
N_{12} &= a\ b\ g2(\xi)\, g2(\eta) \\
N_{13} &= f1(\xi)\, f2(\eta) \\
N_{14} &= a\, g1(\xi)\, f2(\eta) \\
N_{15} &= b\, f1(\xi)\, g2(\eta) \\
N_{16} &= a\, b\, g1(\xi)\, g2(\eta)
\end{aligned}$$

where a, and b are the dimensions of the rectangular element, and ξ and η are non-dimensional quantities *x/a* and *y/b* respectively.

$f1(\xi) = 1 - 3\xi^2 + 2\xi^3$

$f2(\xi) = 3\xi^2 - 2\xi^3$

$g1(\xi) = \xi - 2\xi^2 + \xi^3$

$g2(\xi) = \xi^3 - \xi^2$

The inclusion of the additional 4 terms, as compared to the polynomial terms of ACM element, lends inter-element continuity up to the rotation degree of freedom.

3.4.3 Numerical Experiments and Discussion

The convergence study on the plate problem is studied now, where the need for C^1 continuity is important, especially as the ACM element does not have the necessary twist degree of freedom to ensure this degree of conformance. A square plate problem is chosen. Both simply supported and clamped edge conditions are investigated and in turn, the point-load at centre and uniformly distributed loading cases are studied. For these cases, very accurate solutions for the central deflection are known. The plate is divided into elements of equal size, and meshes ranged from 1x1 to 16x16 for one quarter of the plate. The ACM element is used for the solution of the problems of a simply supported rectangular plate subjected to two different loading conditions, one - a uniformly distributed load, and the other - a point load acting at the center of the plate. Results are also tabulated for a clamped plate subjected to the above loads. Due to symmetry, only one quadrant of the plate has been analysed. The boundary conditions used are shown in Figs 3.15 and 3.16. The different meshes used for this analyses are shown in Fig. 3.17 – Fig 3.20. The BFS element is used for analyzing the same problems as was done earlier with the ACM element. The mesh configurations used in this case are also the same as the case of ACM element. The boundary conditions used are shown in Fig. 3.15

and Fig. 3.16, except for the twist degree of freedom which does not exist for the ACM formulation. The mesh discretisation that was used in the analysis is shown in Fig. 3.17- 3.20.

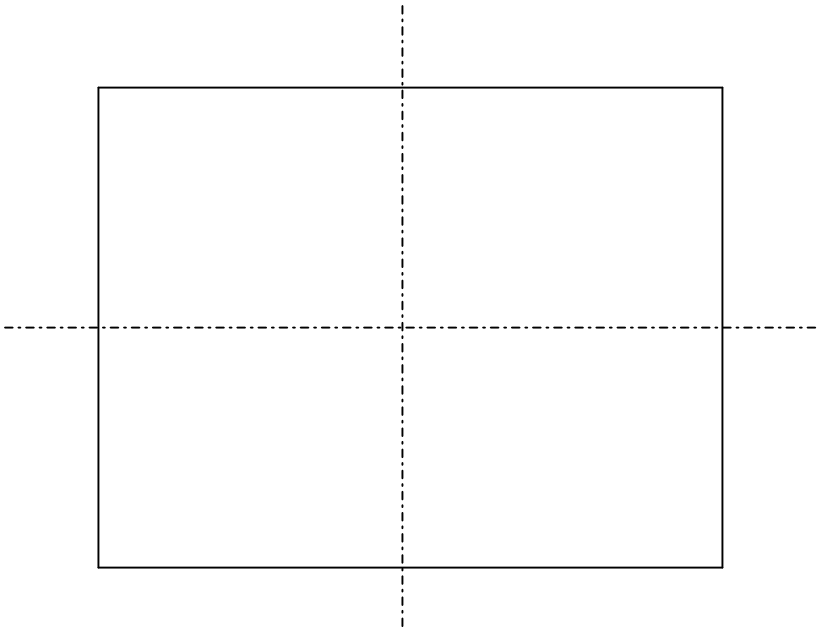

Fig. 3.15 A simply supported plate

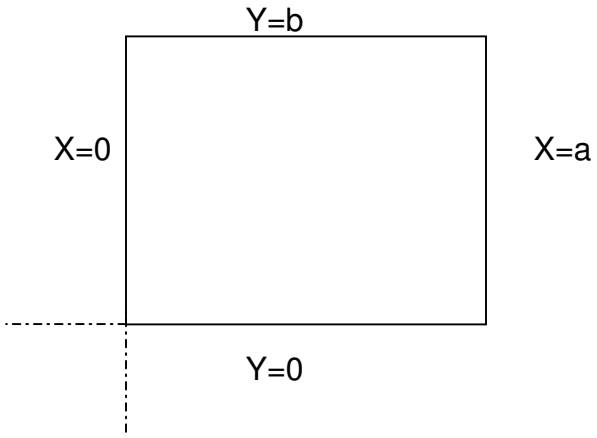

Fig. 3.16 One quadrant of the plate

Boundary Conditions:

1. on the line Y = 0, $\partial w/\partial y = 0$, $\partial^2 w/\partial x \partial y = 0$
2. on the line X = 0, $\partial w/\partial x = 0$, $\partial^2 w/\partial x \partial y = 0$
3. on the line Y = b, $w = 0$, $\partial w/\partial x = 0$
4. on the line X = a, $w = 0$, $\partial w/\partial y = 0$

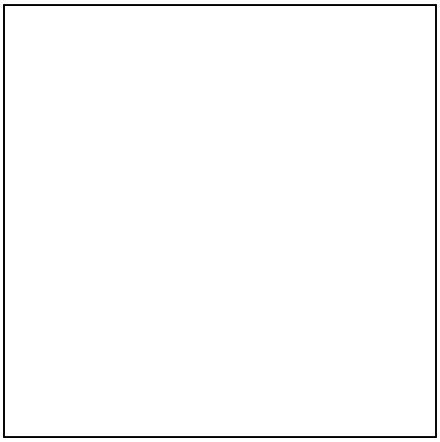

Fig. 3.17 1X1 Mesh

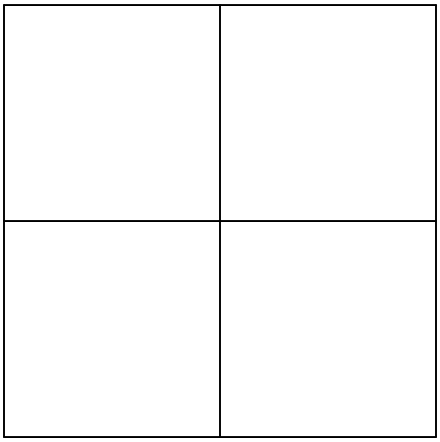

Fig. 3.18 2X2 Mesh

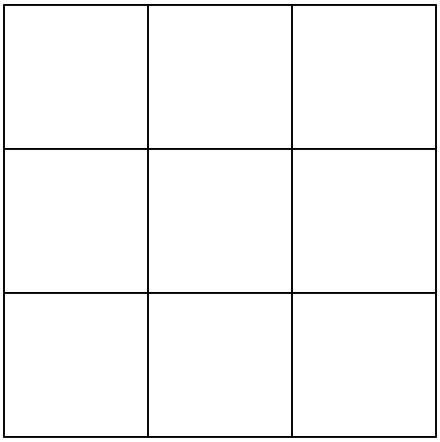

Fig. 3.19 3X3 Mesh

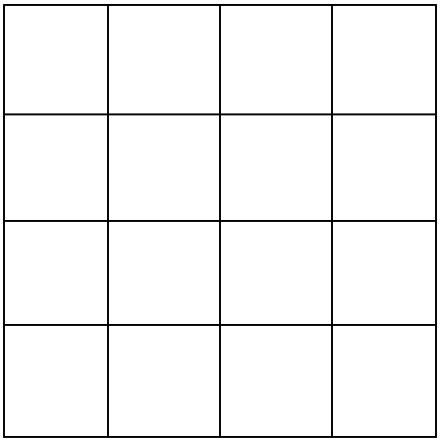

Fig. 3.20 4X4 Mesh

From the best-fit rule, explained in section 2.2, the following relation must hold good.

$$\int \underline{\varepsilon}^{T} (\sigma - \bar{\sigma})\, dV = 0 \qquad \ldots(3.14)$$

where

$\underline{\bar{\varepsilon}}$ *is the finite element strain*

$\bar{\sigma}$ *is the finite element stress*

σ *is the exact stress*

For a plate bending problem, the exact solution in closed form is readily available for a plate simply supported on all the edges (side of the plate=40 units, thickness = 0.4, E = 200000 and Poisson's ratio = 0.3) and subjected to a sinusoidal load, Timoshenko & Woinowsky-Krieger (1959). The results from the finite element solution for the BFS and ACM formulations can now be used for testing the best-fit rule.

The results for the BFS formulation with 1 element modeled for a quarter of the plate are tabulated in Table 3.8. The best-fit integral terms are evaluated at 5 Gaussian Points in each direction. It can be seen that the best-fit residual is zero for this, which confirms that the finite element solution is a best-fit to the exact solution for the BFS formulation. In this example, 5-point numerical integration (Gaussian Integration) was used so that the sinusoidal load variation can be captured more realistically in the formulation of the consistent load vector. The deflection at the center of the plate from the 1-element finite element solution comes out to be 5.664384, as against the exact value of 5.605226 indicating a good solution for a 1-element discretisation.

For further confidence on the results of the 1-element solution, the bending moment M_x and M_{xy} along the diagonal of the plate are compared with the exact solution in Fig. 3.21 and Fig. 3.22

Best-fit Rule for a Simply Supported Plate Subjected to a Sinusoidal Varying Load - BFS Formulation									
Weight	x	y	Theory-cur-x	Theory-cur-y	Theory-cur-xy	FEM-cur-x	FEM-cur-y	FEM-cur-xy	Proj. Theorem
0.229085	0.884617	0.884617	-0.004348	-0.004348	0.060457	-0.004419	-0.004419	0.058572	0.010153
0.229085	0.884617	0.615383	-0.011464	-0.011464	0.022928	-0.011724	-0.011218	0.024011	-0.002528
0.113400	0.884617	0.976545	-0.000903	-0.000903	0.064483	-0.000927	-0.002097	0.063491	0.002547
0.113400	0.884617	0.523455	-0.012227	-0.012227	0.004760	-0.012577	-0.013540	0.005328	-0.003934
0.272287	0.884617	0.750000	-0.008670	-0.008670	0.045720	-0.008792	-0.007819	0.045048	0.005788
0.229085	0.615383	0.884617	-0.011464	-0.011464	0.022928	-0.011218	-0.011724	0.024011	-0.002528
0.229085	0.615383	0.615383	-0.030228	-0.030228	0.008695	-0.029757	-0.029757	0.009842	0.008740
0.113400	0.615383	0.976545	-0.002380	-0.002380	0.024455	-0.002355	-0.005567	0.026029	-0.004551
0.113400	0.615383	0.523455	-0.032241	-0.032241	0.001805	-0.031919	-0.035913	0.002184	-0.020411
0.272287	0.615383	0.750000	-0.022860	-0.022860	0.017339	-0.022316	-0.020740	0.018465	0.021191
0.113400	0.976545	0.884617	-0.000903	-0.000903	0.064483	-0.002097	-0.000927	0.063491	0.002547
0.113400	0.976545	0.615383	-0.002380	-0.002380	0.024455	-0.005567	-0.002355	0.026029	-0.004551
0.056134	0.976545	0.976545	-0.000187	-0.000187	0.068777	-0.000440	-0.000440	0.068820	-0.000087
0.056134	0.976545	0.523455	-0.002539	-0.002539	0.005077	-0.005972	-0.002842	0.005776	-0.001728
0.134785	0.976545	0.750000	-0.001800	-0.001800	0.048765	-0.004174	-0.001641	0.048833	-0.001861
0.113400	0.523455	0.884617	-0.012227	-0.012227	0.004760	-0.013540	-0.012577	0.005328	-0.003934
0.113400	0.523455	0.615383	-0.032241	-0.032241	0.001805	-0.035913	-0.031919	0.002184	-0.020411
0.056134	0.523455	0.976545	-0.002539	-0.002539	0.005077	-0.002842	-0.005972	0.005776	-0.001728
0.056134	0.523455	0.523455	-0.034388	-0.034388	0.000375	-0.038523	-0.038523	0.000485	-0.027248
0.134785	0.523455	0.750000	-0.024382	-0.024382	0.003600	-0.026934	-0.022248	0.004097	-0.003433
0.272287	0.750000	0.884617	-0.008670	-0.008670	0.045720	-0.007819	-0.008792	0.045048	0.005788
0.272287	0.750000	0.615383	-0.022860	-0.022860	0.017339	-0.020740	-0.022316	0.018465	0.021191
0.134785	0.750000	0.976545	-0.001800	-0.001800	0.048765	-0.001641	-0.004174	0.048833	-0.001861
0.134785	0.750000	0.523455	-0.024382	-0.024382	0.003600	-0.022248	-0.026934	0.004097	-0.003433
0.323635	0.750000	0.750000	-0.017288	-0.017288	0.034576	-0.015554	-0.015554	0.034645	0.026283
Best-fit Rule Residual									0.000051

Table 3.8 Results of best-fit rule for a simply supported plate – BFS Formulation (sinusoidal load)

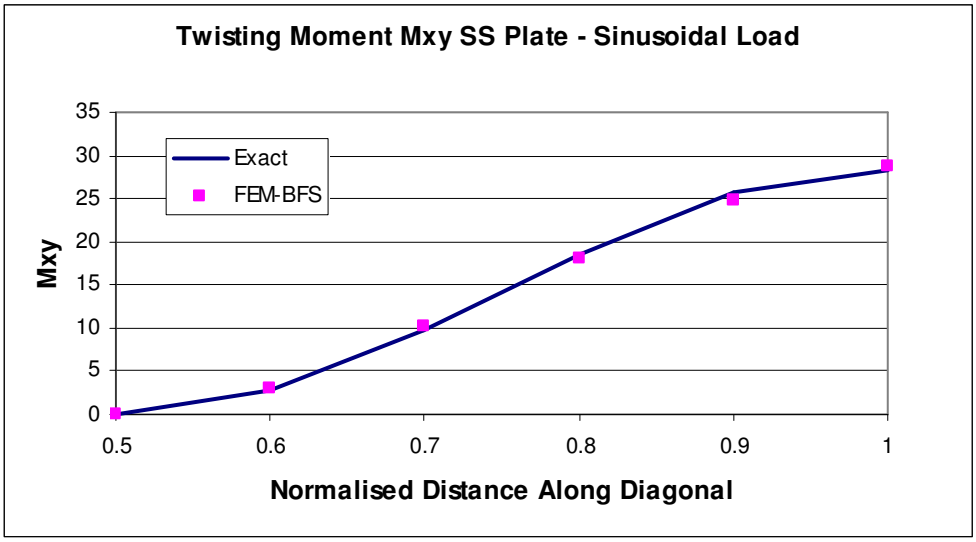

Fig. 3.21 Twisting moment in a simply supported plate, BFS Element (sinusoidal load)

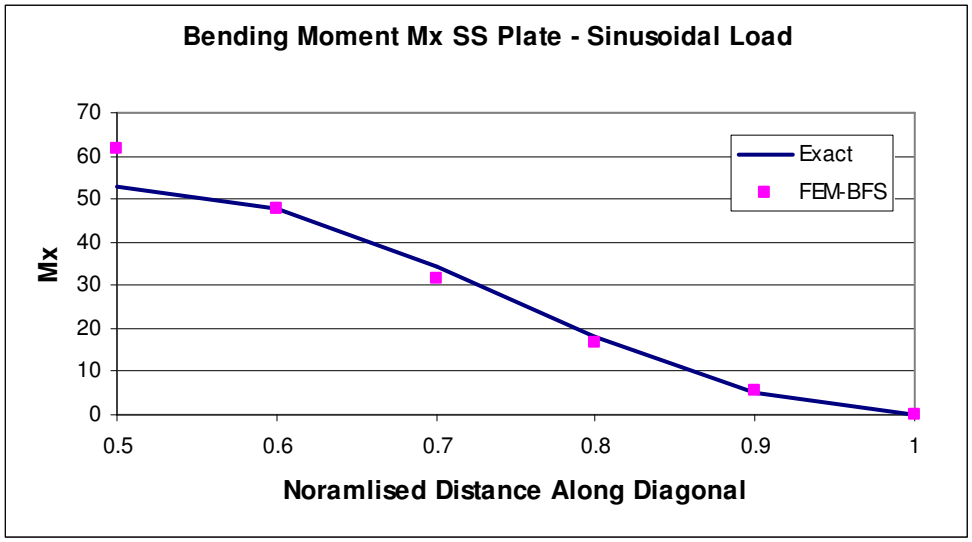

Fig. 3.22 Bending moment in a simply supported plate, BFS Element (sinusoidal load)

The same problem is now solved using the ACM formulation, and the results are tabulated in Table 3.9. It can be seen clearly that the best-fit residual is not zero, indicating that the best-fit rule is violated for the ACM formulation. The results for the deflection at the center of the plate for the 1-element discretisation is 6.975012, as against the exact value of 5.605226. The results for the bending moment and the twisting moment are shown in Fig. 3.23 and Fig. 3.24

Best-fit Rule for a Simply Supported Plate Subjected to a Sinusoidal Varying Load - ACM Formulation									
Weight	x	y	Theory-cur-x	Theory-cur-y	Theory-cur-xy	FEM-cur-x	FEM-cur-y	FEM-cur-xy	Proj. Theorem
0.229085	0.884617	0.884617	-0.004348	-0.004348	0.060457	-0.004371	-0.004371	0.066665	-0.038970
0.229085	0.884617	0.615383	-0.011464	-0.011464	0.022928	-0.014570	-0.008913	0.035668	-0.047991
0.113400	0.884617	0.976545	-0.000903	-0.000903	0.064483	-0.000889	-0.002820	0.072394	-0.027429
0.113400	0.884617	0.523455	-0.012227	-0.012227	0.004760	-0.018052	-0.010464	0.020230	-0.027245
0.272287	0.884617	0.750000	-0.008670	-0.008670	0.045720	-0.009470	-0.006642	0.053816	-0.045464
0.229085	0.615383	0.884617	-0.011464	-0.011464	0.022928	-0.008913	-0.014570	0.035668	-0.047991
0.229085	0.615383	0.615383	-0.030228	-0.030228	0.008695	-0.029711	-0.029711	0.004671	0.012491
0.113400	0.615383	0.976545	-0.002380	-0.002380	0.024455	-0.001812	-0.009400	0.041397	-0.041558
0.113400	0.615383	0.523455	-0.032241	-0.032241	0.001805	-0.036813	-0.034881	-0.010767	-0.051139
0.272287	0.615383	0.750000	-0.022860	-0.022860	0.017339	-0.019312	-0.022141	0.022819	0.021835
0.113400	0.976545	0.884617	-0.000903	-0.000903	0.064483	-0.002820	-0.000889	0.072394	-0.027429
0.113400	0.976545	0.615383	-0.002380	-0.002380	0.024455	-0.009400	-0.001812	0.041397	-0.041558
0.056134	0.976545	0.976545	-0.000187	-0.000187	0.068777	-0.000573	-0.000573	0.078123	-0.016853
0.056134	0.976545	0.523455	-0.002539	-0.002539	0.005077	-0.011647	-0.002127	0.025959	-0.019693
0.134785	0.976545	0.750000	-0.001800	-0.001800	0.048765	-0.006110	-0.001350	0.059545	-0.039706
0.113400	0.523455	0.884617	-0.012227	-0.012227	0.004760	-0.010464	-0.018052	0.020230	-0.027245
0.113400	0.523455	0.615383	-0.032241	-0.032241	0.001805	-0.034881	-0.036813	-0.010767	-0.051139
0.056134	0.523455	0.976545	-0.002539	-0.002539	0.005077	-0.002127	-0.011647	0.025959	-0.019693
0.056134	0.523455	0.523455	-0.034388	-0.034388	0.000375	-0.043218	-0.043218	-0.026206	-0.081324
0.134785	0.523455	0.750000	-0.024382	-0.024382	0.003600	-0.022673	-0.027432	0.007381	-0.009691
0.272287	0.750000	0.884617	-0.008670	-0.008670	0.045720	-0.006642	-0.009470	0.053816	-0.045464
0.272287	0.750000	0.615383	-0.022860	-0.022860	0.017339	-0.022141	-0.019312	0.022819	0.021835
0.134785	0.750000	0.976545	-0.001800	-0.001800	0.048765	-0.001350	-0.006110	0.059545	-0.039706
0.134785	0.750000	0.523455	-0.024382	-0.024382	0.003600	-0.027432	-0.022673	0.007381	-0.009691
0.323635	0.750000	0.750000	-0.017288	-0.017288	0.034576	-0.014391	-0.014391	0.040968	0.006349
Best-fit Rule Residual									-69.4471378

Table 3.9 Results of best-fit rule for a simply supported plate – ACM Formulation (sinusoidal load)

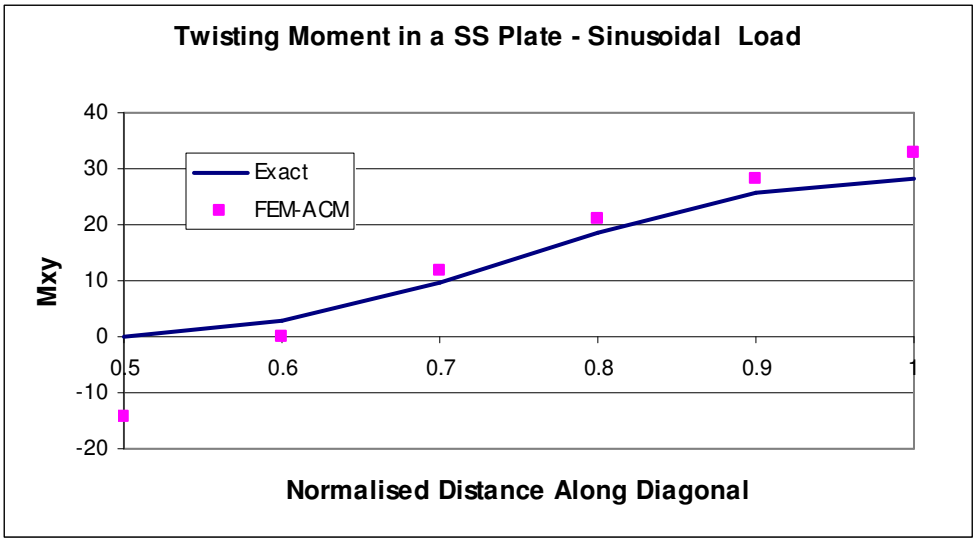

Fig. 3.23 Twisting moment in a simply supported plate, ACM Element (sinusoidal load)

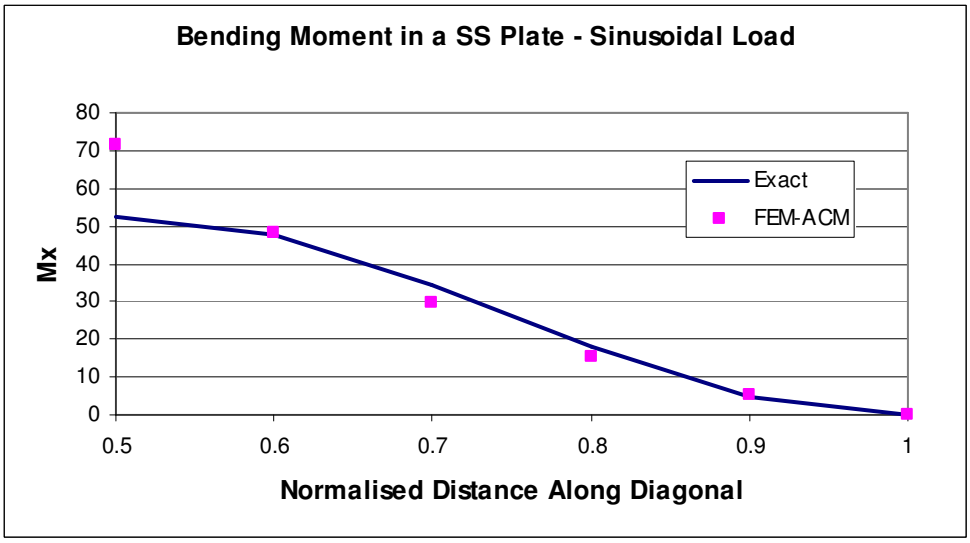

Fig. 3.24 Bending moment in a simply supported plate, ACM Element (sinusoidal load)

It would be interest to see the relative performance of the BFS and ACM element formulations from the point of boundedness of strain energy. A 20x20 mm quarter plate, of 0.4 mm thickness and Poisson's ratio of 0.3, Young's Modulus of 200000 N/mm^2, subjected to different loading/boundary conditions is

considered for this purpose. The results of the strain energy as the mesh is refined are shown in the Tables 3.10 – 3.13.

Simply Supported Plate subject to a UDL		
Elements in one quarter	Strain energy (ACM)	Strain energy (BFS)
1	493.699192	1472.77137
4	1578.98624	1485.95534
16	1511.85256	1487.2168
64	1493.54944	1487.30693

Table 3.10 Comparison of strain energy boundedness in a simply supported plate (uniform load)

Clamped Plate subject to a UDL		
Elements in one quarter	Strain energy (ACM)	Strain energy (BFS)
1	323.153369	289.335021
4	369.417308	339.234146
16	349.731934	339.615331
64	342.528813	340.243312

Table 3.11 Comparison of strain energy boundedness in a clamped plate (uniform load)

Simply Supported Plate subject to a Point Load		
Elements in one quarter	Strain energy (ACM)	Strain energy (BFS)
1	34584.6068	60485.5511
4	67306.7185	62633.8511
16	64583.7893	63165.1815
64	63714.8714	63296.8051

Table 3.12 Comparison of strain energy boundedness in a simply supported plate (point load)

Clamped Plate subject to a point load		
Elements in one quarter	Strain energy (ACM)	Strain energy (BFS)
1	32315.3369	28933.5021
4	33494.1308	29968.9049
16	31682.0648	30465.2347
64	30969.9156	30610.3722

Table 3.13 Comparison of strain energy boundedness in a clamped plate (point load)

It can be observed that in the case of the BFS formulation the strain energy is always bounded, and eqn. (2.30) is valid. The ACM formulation, because of the non-conformance violates this boundedness.

In all cases, the deflections from the BFS element converges from below, showing that the condition expressed in eqn. (2.30) is met, *i.e*. the energy inner product of the approximate solution will always be a lower bound to the exact energy, and hence deflections would converge from below. The results for the BFS element shows $O(h^4)$ convergence, as expected. However, in all these cases, the ACM element shows larger deflections than predicted by theory. That is, the condition expressed in eqn. (2.30) has been violated, and the only explanation for this is that the non-conforming nature of the formulation has introduced extra-variational conditions. Also, the ACM element showed only a degraded h^2 convergence. Fig. 3.25 shows the convergence for the case of the simply supported square plate under uniformly distributed loading conditions. It can be noted that now due to the difference in signs of the error (BFS gives positive errors while ACM gives negative errors), the modulus of the error measure is used for graphical representation. Tables 3.14 – 3.17 compare the results of the ACM and BFS formulations for plates with different boundary conditions.

Simply supported plate with uniform load		
Mesh	ACM	BFS
1X1	0.00070772	0.00057625
2X2	0.00060498	0.00056823
3X3	0.00058443	0.00056790
4X4	0.00057717	0.00056784
8X8	0.00057016	0.00056782
Exact	0.00056749	0.00056749

Table 3.14 Deflection at center of a simply supported plate (uniform load)

Simply supported plate with point load		
Mesh	ACM	BFS
1X1	0.00481672	0.00387108
2X2	0.00430763	0.00400857
4X4	0.00413336	0.00404257
8X8	0.00407775	0.00405100
Exact	0.00405350	0.00405350

Table 3.15 Deflection at center of a simply supported plate (point load)

Clamped plate with uniform load		
Mesh	ACM	BFS
1X1	0.00020682	0.00018517
2X2	0.00019615	0.00017680
3X3	0.00018623	0.00017683
4X4	0.00018226	0.00017729
8X8	0.00017824	0.00017698
Exact	0.00017612	0.00017612

Table 3.16 Deflection at center of a clamped plate (uniform load)

Clamped plate with point load		
Mesh	ACM	BFS
1X1	0.00206818	0.00185174
2X2	0.00214363	0.00191644
4X4	0.00202765	0.00195266
8X8	0.00198207	0.00195906
Exact	0.00195686	0.00195686

Table 3.17 Deflection at centre of a clamped plate subjected (point load)

As can be seen from Fig. 3.24, the BFS element gives a higher rate of convergence with respect to displacements. All theoretical results have been taken from Timoshenko and Woinowsky-Krieger (1959).

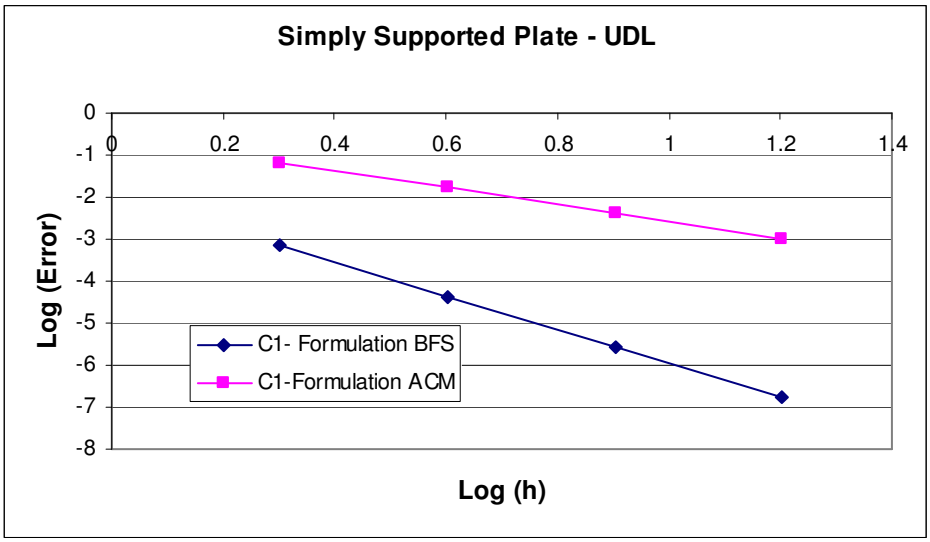

Fig. 3.25 Effect of conformance and non-conformance on displacement convergence (uniform load)

3.5 Closure

In this chapter, a suite of finite elements (beam bending, plate bending, axisymmetric shell elements) has been formulated and studied in detail. The results from the various formulations were used to explain the 3C concepts and the performance of the elements was assessed from energy error perspective for linear elastostatics. It has been shown that the strain energy boundedness and the best-fit rules are violated whenever the element formulation deviates from the 3C concepts. For the plate bending problems, the ACM formulation has been shown to violate the best-fit rule. The results from the ACM formulation also do not show the strain energy boundedness. The ACM formulation has also been found to degrade the rate of convergence of the solution. In all of the above three

measures, the BFS formulation has a perfect score (follows best-fit rule, strain energy is bounded, and the rate of convergence is superior to ACM). Axisymmetric shell formulation was used for the analysis of circular plates with different boundary conditions, and the 3C concepts and energy aspects were studied extensively.

Since the 3C concepts and energy error concepts are derived from first principles, they should hold good for any example, and the examples presented here serve the purpose of demonstration cautioning against indiscriminate use of extra-variational tricks. The results of the studies done across various beam and plate problems are summarized in Table 3.18. This table clearly shows what performance measure is affected for what deviation from the C-concept. These studies are extended to other applications like linear elastodynamics, nonlinear elastostatics and the 3C concepts and energy errors are examined in the subsequent chapters.

Summary of Results for Linear Elastostatics for Classical Beams, Shells & Plates					
Element Formulation	**C-Concept Deviation**	**Example Problem**	**Strain Energy Boundedness**	**Rate of Convergence**	**Best-fit Rule**
C^1 Beam	None	Cantilever beam	✓	✓	✓
		Simply supported beam	✓	✓	✓
BFS Element	None	Simply supported plate	✓	✓	✓
		Clamped plate	✓	✓	✓
ACM Element	Conformance	Simply supported plate	×	↓	×
		Clamped plate	×	↓	×
C^1 Shell	None	Circular simply suported plate	✓	✓	✓
		Circular clamped plate	✓	✓	✓

Table 3.18 3C concepts and performance of various element formulations (linear elastostatics)

Note: ✓ implies that the performance is good/satisfies the respective attribute
× implies that it is a violation of the respective attribute
↓ implies that the performance of the respective attribute is degraded

Chapter-4

Linear Elastostatics for Shear-flexible Beams, Shells and Plates

4.1 Introduction

In this chapter, the 3C concepts of correspondence, consistency and correctness are studied in detail for the linear elastostatics problems of shear-flexible beam, shells and plates. The phenomena of shear locking and membrane locking are explained using consistency concepts. The element formulations cover both isoparametric and anisoparametric elements. The frequently used tactic of reduced integration for alleviating locking is discussed in depth through various examples, and compared with results of full integration and field-consistent formulations. Convergence studies, best-fit rule and boundedness of strain energy are discussed in detail for all the above formulations. The results of the findings are summarized in the closure section of this chapter.

The simplicity of the element formulations associated with a C^0 element made this element very attractive and amenable to many applications. However, when it was realized that for certain class of problems (shear-flexible) the original C^0 formulation was giving spurious results, which was later recognized as various forms of locking, a lot of effort went into understanding the real cause. A quick solution to overcome the problem of locking was to use reduced integration for shear terms in the evaluation of the stiffness matrices, Zienkiewicz *et al.* (1971), Zienkiewicz and Hinton (1976). Bathe and Dvorkin (1985) used different interpolations for the bending and transverse shear strain. The shear strain is averaged out across a patch of four elements, and this eliminates shear locking. Prathap and Bhashyam (1982) used a functional re-constitution technique for the additional stiffness that is present in the exactly integrated element and predict

very accurate *a priori* analytical error models. Hrabok and Hrudey (1984) listed out the C^0 element formulations for plate bending that used different strategies to avoid locking, and with the field remaining active there have been many additions to this work.

Hinton and Huang (1986) presented a comprehensive analysis of different types of formulations that used a shear strain field (which they name it as substitute shear strain fields) to remove locking. Since then lot of research has been done to examine this problem. Briassoulis (1989a) studied the flexural behavior of a Mindlin plate by subjecting the element to polynomial Kirchhoff fields (those that would produce zero transverse shear strain) which are different from the shape functions of the element, and concluded that typical shear locking occurs with lower order elements, and non-typical shear locking (independent of the element thickness ratio) occurs in higher order elements. Briassoulis (1989b) proposed a new element formulation that removed the spurious stiffness matrix terms from the original stiffness matrix and showed that such a maneuver frees the element from all locking mechanisms. Kreja and Cywinski (1988) performed a detailed study of the shear locking in a beam problem and quantify the " spurious stiffness" for different slenderness ratios of the beam. The specific impact of reduced integration on the stiffness matrix terms is identified explicitly.

Tessler (1991) used a higher-order beam theory for bending and stretching on a 2-noded beam element. Quadratic interpolations functions are used for the transverse displacement *w* and the element does not cause shear locking. Shi and Voiyadjis (1991a) formulated a 4-noded element with 3 degrees of freedom at each node, and used higher order interpolation functions for the transverse displacement *w.* This made the element free from shear locking. Paramasivam *et al.* (1992) used a cubic displacement function for *w* and the quadratic displacement function for rotation θ. The beam element is shown to be completely free from shear locking.

The early work of Ahmed *et al.* (1968) on curved thick shells popularized the use of conical shell elements in analysis of axisymmetric structures. Their work used degenerated isoparametric elements and did not use the strain displacement relations for shear-flexible effects. The finite element analysis of shear-flexible axisymmetric shells poses additional challenges. In addition to shear locking, there is a possibility of membrane locking. Venkataramana and Venkateswara Rao (1975) implemented a 2-noded conical shell element with 10 degrees of freedom at each node to analyse moderately thick shells that include shear-flexible effects. This element does not require reduced integration and behaves very well in the limit of thin shell as well and does not produce shear/membrane locking. Zienkiewicz *et al.* (1977) used a 2-noded straight element with reduced integration and overcome the problems of locking.

Mohr (1982) used a 3-noded curved isoparametric axisymmetric shell element with 3 degrees of freedom at each node. A penalty parameter which is a function of the thickness of the shell was used to alleviate shear locking. Ramesh Babu and Prathap (1986), Prathap and Ramesh Babu (1986) used the field-consistency concepts to explain shear and memebrane locking in shear-deformable curved shells. Tessler and Spiridigliozzi (1988) proposed kinematically admissible interpolation functions for the in-plane and translational displacements (which are of higher order than the interpolation function for rotation) to resolve both shear and membrane locking. Shi and Voyiadjis (1991b) used the assumed element strain method to avoid both shear and membrane locking in arches, beams, plates and shells. Paramasivam and Raj Muthiah (1994) introduced a cubic interpolation function for transverse displacement w, and a quadratic function for rotation θ on a 2-noded axisymmetric shell element to get a displacement convergence of $O(h^4)$. This element does not cause shear locking and the additional rotational degree of freedom in the middle of the cone was eliminated by static condensation at the end. Raveendranath *et al.* (1999b) used a formulation that has a cubic polynomial function for the translational

displacement and a quartic polynomial function for the analysis of curved axisymmetric shells. This formulation does not produce shear and membrane locking. Gilewski and Radwanska (1991), Yang *et al.* (2000) provided a comprehensive survey on the elements available for the axisymmetric analysis of shells.

Auricchio and Taylor (1994) used bubble functions for increasing the order of the interpolation function for rotation θ_x and θ_x and formulate an element that is free from shear locking. Singh *et al.* (1998) introduced a 4-noded element with 5 degrees of freedom at each node and developed a lock-free element for the analysis of moderately thick rectangular plates. The interpolation functions for the rotational degrees of freedom are expressed in terms of the element material properties and the element thickness to span ratio. Mac Neal (1998) traced three distinct phases in the history of plate bending elements – the classical Kirchhoff elements from 1961-1970, the lower order Mindlin elements from 1969-1990 and the higher order elements from 1988 onwards, and examined in detail the impact of *p* refinement on shear flexibility of a clamped square plate. Liu *et al.* (2000) developed a 4-noded element that is based on an assembly of four triangular elements. The formulation used anisoparametric interpolation functions and resolved shear locking. Singh *et al.* (2000b) developed a 4-noded shear-flexible element that is based on coupled displacement field derived using the moment-shear equilibrium and in-plane force equilibrium. This element has 6 degrees freedom at each node, and does not cause shear locking. Singh and Venkateswara Rao (2000c) summarized the work done on shear-flexible elements and discussed the merits/demerits of selective integration, field consistency approach and material finite element approach.

Pitkaranta (2000) traced the full history of locking and uses the reduced strain formulation to overcome locking. Bletzinger *et al.* (2000) and Koschnick *et al.* (2005) obtained a shear strain distribution which is free of parasitic shear, through calculation of discrete shear gaps at the nodes and their interpolation

across the element domain and solved problems of a clamped plate and cylindrical shell roof. Rong and Lu (2003) used the concept of the Parametrized Lagrange Multiplier method, and formulated the generalized mixed variational principle and applied this to study shear locking problems in plates and beams, and give a very good interpretation of the two different convergences of the potential energy and the complementary energy solutions. Olovsson *et al.* (2006) suggested moving the quadrature points as a possible way to circumvent certain shear locking problems. Each one of the three shear strain components is averaged in groups of four integration points. This can be thought of as another case of selective/reduced integration or strain smoothing. Choi and Lee (2003) used additional polynomial terms to enrich the interpolation functions. A smart linear combination of these terms when used in the strain displacement relations has been shown to avoid both shear and membrane locking. Ozkul and Ture (2004) used two different elements with 12 and 24 degrees of freedom in each of the elements for the analysis of rectangular and circular plates for different thickness of plates and conclude that the higher order element (with 24 degrees of freedom) has relatively less shear locking. Voyiadjis and Woelke (2006) used alternate fields for representing the displacements and overcome both shear and membrane locking.

The field-consistency approach of Prathap (1984), the enhanced-natural strain approach of Simo and Rifai (1990) the mixed interpolation of tensorial components of Bathe and Dvorkin (1985,1986), all lead to formulations that do not produce shear locking.

More approaches continue to evolve, and the corotational approach has been used with success, Crisfield (1991), Belytschko *et al.* (2000), Urthaler and Reddy (2005). Duarte Filho and Awruch (2004) discussed at length the various methods available in literature to overcome locking, but go ahead with reduced integration and explain clearly the advantage of the corotational approach for addressing the problem of locking. Felippa (2006) discussed the element

stiffness formulation in natural coordinates using the kinematic decomposition of the in-plan motion. This formulation does not cause shear locking. Cen *et al.* (2006) used an independent shear field in conjunction with a fourth-order deflection field in terms of the area coordinates of the element. This formulation is implemented on a 4-node element with 3 degrees of freedom at each node.

Reddy (1997) discussed the concept of consistent interpolation (CI) element and interdependent interpolation (II) element. For the CI case, for the three-noded element there is a differential number of degrees of freedom per node. Though full integration is employed, due to the different degree of interpolation function for the deflection and the slope degrees of freedom, this element does not lock. For the II case, the interpolation functions for the deflection and the slope have common parameters, which are expressed in terms of the nodal degrees of freedom. This formulation uses full integration and produce shear locking-free results for both the CI and II cases.

Mukherjee and Prathap (2001) defined field-consistent and field-inconsistent spaces and use function space approach to predict *a priori* error estimates for shear locking. Mukherjee and Prathap (2002a) used the concepts of functional analysis to compare the response of the 3-noded Timoshenko beam element to that of a 2-noded element and attribute the delayed convergence due to the field-inconsistent shear terms. Singh and Venkateswara Rao (2003) provided a closed form solution for the discretisation error for shear-flexible beams for three different element formulations.

While for isoparametric elements, the field-consistency concepts are fairly well-understood for a variety of applications, (Prathap and Ramesh Babu (1986), Prathap and Naganarayana (1992), Ganapathi *et al.* (2003, 2004), the same cannot be said of anisoparametric elements. In fact the genesis of anisoparametric elements can be traced to the efforts in the 1980's to overcome shear locking, Tessler (1986), Tessler and Spiridigliozzi (1988).

The first detailed investigation of anisoparametric elements from field-consistency point was by Marur and Prathap (2000), where the example of a shear-flexible beam is used for explaining the concept of shear locking. This work examined the consistency and correctness aspects directly, and the correspondence part is brought in indirectly when the order of convergence is discussed. In this example, the inconsistent terms do not produce spurious constraints and hence no shear locking is observed *prima facie*. However, the impact of continuing with this inconsistent term is not studied in detail from a best-fit argument. Additionally, the conditions under which the inconsistent terms could become spurious constraints are not brought out.

None of the above work, and those that are in open literature of shear-deformable curved shells address the correspondence concept explicitly. In the following sections, after introducing briefly the element formulation, the best-fit rule is checked. Later in the chapter, the consistency aspects for different classes of shear-flexible problems (beams, circular plates, curved shells) are examined in detail. In section 2.3, the field-consistency concept was explained and the spurious constraints that may arise due to non-adherence to field-consistency was outlined. In each of the cases, it was shown that it is possible to predict *a priori* from the strain-displacement relations what type of locking (shear locking/membrane locking) would occur under what conditions. Further to this, in this chapter, the use of reduced integration technique to overcome locking is examined and its impact on the correctness and correspondence aspects are investigated.

4.2 Shear-flexible Beam

The shear-flexible beam is an interesting example through which many of the 3C concepts can be clearly understood. The basic differences between the behaviour of an Euler-Bernoulli beam and shear-flexible beam can be found in

many textbooks, *e.g*. Cook *et al.* (1989). The difference lies in the fact that the rotational degree of freedom is an independent degree of freedom, unlike the case in section 3.2 where it was the derivative of the translational displacement. In this section, the focus is on 3C concepts, which is brought in through the study of the same examples that were discussed in section 3.2. For the element formulation of a shear-flexible beam, two approaches can be envisaged. In the first formulation, a 2-noded element with 2 degrees of freedom per node is used. Here, the degrees of freedom are the same as that of the 2-noded element discussed in section 3.2, namely, one translation and one rotation. In the second type of formulation, a 2-noded element with 3 degrees of freedom per node is used. The rotational degree of freedom that is used in the strain displacement relation is still an independent degree of freedom, as will be explained later. This formulation is typical of an anisoparametric formulation.

The anisoparametric element formulation for shear-flexible beams is an interesting formulation that brings out the field-consistency concept in a newer light. The concept of variational correctness is very subtle in this case and it is very easy to miss out the errors that can come in when mixed integration is used for the shear terms.

4.2.1 Strain Displacement Relations

The strain displacement relations for a shear-flexible beam are given by

$$\chi_x = \frac{d\theta_x}{dx}$$
$$\gamma_{xy} = \frac{dw}{dx} - \theta_x \qquad \ldots(4.1)$$

where χ_x is the flexural strain, and γ_{xy} is the shear strain and w is the translational displacement and θ_x is the rotation of plane normal to the neutral axis.

4.2.2 Phenomena of Shear Locking

When the above formulation is used for finding the deflection of a cantilever beam subjected to a tip load, interesting results can be seen. As the beam becomes slender (*l/t* >>20), the deflections as computed from the above formulation do not turn out to be physically correct. It can be seen that for very high *l/t*, the formulation gives totally meaningless values of deflections. These results are tabulated in Table 4.1 for a cantilever beam (E=1.0e6 units, width=1.0 unit, Tip load=1 unit). The deflection at the tip of the cantilever when full integration is used is tabulated under the column F and when mixed integration is used is tabulated under column M.

Comparison of Deflection for a Cantilever between Full & Mixed Integration												
L/t	1 Element		2 Elements		4 Elements		8 Elements		16 Elements		32 Elements	
	F	M	F	M	F	M	F	M	F	M	F	M
100	0.0010	3.0010	0.0038	3.7510	0.0015	3.9385	0.0605	3.9853	0.2316	3.9971	0.7892	4.0000
1000	0.0000	3.0000	0.0000	3.7500	0.0002	3.9375	0.0006	3.9843	0.0002	3.9960	0.0098	3.9990
10000	0.0000	3.0000	0.0000	3.7500	0.0000	3.9372	0.0000	3.9843	0.0000	3.9960	0.0010	3.9990

Table 4.1 Effect of reduced integration on displacement of a shear-flexible cantilever beam (tip load)

4.2.3 Reduced Integration Technique

It was seen in the preceding section, that the results for the cantilever are highly erroneous when used with the full integration on a C^0 element and is not able to get the desired displacements even with a large number of elements. A remedy that has been proposed by Zienkiewicz *et al.* (1971) is to use reduced integration for the terms involving shear strains. The stiffness matrix is now decomposed into two parts, one involving the bending terms and other involving shear terms.

The stiffness matrix is expressed as follows

$$[K]=[K_b]+[K_s] \qquad \ldots(4.2)$$

$$[K]=\int[B_b]^T\,[D_b]\,[B_b]dA+\int[B_s]^T\,[D_s]\,[B_s]dA \qquad \ldots(4.3)$$

where $[B_b]$ represents the strain displacement relations between the bending strains and the displacements, and $[B_s]$ represents the strain displacement relations between the shear strains and the displacements. Similarly, the material matrix, $[D]$ will now be split into $[D_b]$ and $[D_s]$.

The stiffness matrix $[K_b]$ is integrated using the 2X2 Gaussian Quadrature rule and $[K_s]$ is integrated using 1X1 rule. This technique shows very good improvement in the results for the cantilever as seen in Table 4.1

4.2.4 Field-consistent Formulation – Isoparametric Element

The field-consistent formulation for this element was explained in chapter-2. It can be seen from eqn. (4.1) that the shear strain terms involve multiple "fields", with the shear strain comprising the transverse deflection w and the slope θ_x. Field-consistent formulation requires that the interaction between these multiple fields should be in a consistent manner, the violation of which can lead to constraints which manifests in forms like locking, spurious stresses, delayed convergence etc.

From the strain displacement relation in eqn. (4.1), for a 2-noded element (C^0 formulation), the shear strain would comprise of a constant term and a first degree polynomial term. This would make the shear strain "inconsistent" and

would produce spurious strains in certain limits (as the beam becomes slender and slender, or as l/d ratio increases). Field-consistent formulation realizes this and the shear strain is reconstituted upfront in such a manner that the spurious strain does not exist even in the extreme conditions. The reconstituted shear strain for this case is

$$\gamma_{xy} = (b_0 - \frac{a_1}{l}) \qquad \ldots(4.4)$$

4.2.5 Field-consistent Formulation - Anisoparametric Element

The field-consistent formulation for this element was earlier explained in chapter-2. The constraints that need to be met are reproduced below here.

$$\begin{aligned} & b_0 + \frac{b_2}{3} - c_0 \Rightarrow 0 \\ & b_1 - c_1 \Rightarrow 0 \\ & b_2 \Rightarrow 0 \end{aligned} \qquad \ldots(4.5)$$

The first of these 2 equations are field-consistent, as they contain terms coming from both w and θ_x. The third equation has the contribution of only the transverse deflection w, and hence is inconsistent. Despite being inconsistent, if the shear strain terms retain the term b_2, it would not cause any spurious constraint, as this term b_2 does not influence the flexural strain. This is unlike the isoparametric formulation discussed earlier, where the inconsistent shear strain term b_1 in eqn. (2.8) influences the flexural strain and produces a spurious constraint. This uniqueness of anisoparametric formulation for shear-flexible beams thus obviates the necessity for reduced integration or even a field-consistent formulation to alleviate shear locking, as it does not exist. The same would not hold true for curved beams or shells, where anisoparametric formulation would still create a

spurious constraint due to interplay of the field inconsistent terms in the flexural, membrane and shear strains. This was discussed in detail in Section 2.3.

It can be shown that the use of reduced integration or full integration for anisoparametric formulation of a beam problem does not disturb the strain energy. For one element, the shear strain energy for a field-consistent formulation is given by

$$\begin{aligned} U_s &= \frac{1}{2}\int \tau\gamma \, dv \\ &= \frac{\kappa G t b l}{4}\int_{-1}^{1}\left\{\left(b_0 + \frac{b_2}{3} - c_0\right)P_0 + (b_1 - c_1)P_1\right\}^2 d\xi \\ &= GA\left[\frac{1}{2}(b_0 - c_0)^2 + \frac{1}{18}b_2^{\,2} + \frac{2}{3}b_2(b_0 - c_0) + \frac{1}{6}(b_1 - c_1)^2\right] \end{aligned} \qquad \ldots(4.6)$$

When full-integration is employed for evaluating the strain energy (by using 3-point Gaussian Integration), the shear strain energy is given by

$$U_s = \kappa GA\left[\frac{49}{99}(b_0 - c_0)^2 + \frac{27}{275}b_2^{\,2} + \frac{18}{55}b_2(b_0 - c_0) + \frac{9}{55}(b_1 - c_1)^2\right] \qquad \ldots(4.7)$$

When reduced integration is employed (with use of 2-point Gaussian Integration instead of the 3-point integration), the shear strain energy is identical to eqn. (4.6).

The strain energy comparison from eqns. (4.6) and (4.7) will be shown later (in Table 4.3).

The field-consistent formulation for the anisoparametric formulation for shear-flexible beams is discussed now. After Legenderization of the shear strain (explained in section 2.3.2), the contribution of the b_2 in shear strain term in the field-consistent formulation, the following expression for the shear strain is realized as

$$\gamma_{xy} = [b_0 + \frac{b_2}{3} - c_0]P_0 + [b_1 - c_1]P_1 \qquad \ldots(4.8)$$

The strain energy arising from the 3 strain components, shear strain energy U_s, membrane strain energy U_m, and bending strain energy U_b, are as follows

$$U_s = kGAl\left[\left(b_0 + \frac{b_2}{3} - c_0\right)^2 + \frac{1}{3}(b_1 - c_1)^2\right]$$

$$U_m{}^l = EA\frac{a_1^{\,2}}{l} \qquad \ldots(4.9)$$

$$U_b = EI\frac{c_1^{\,2}}{l}$$

The total strain energy is

$$U = U_s + U_m + U_b \qquad \ldots(4.10)$$

It should be noted that in the total strain energy expression shown in eqn. (4.10), the membrane strain energy is also included. For the purpose of obtaining a general stiffness matrix, the membrane strain energy is retained.

The stiffness matrix is obtained from the strain energy by taking

$$\delta U = 0 \qquad \ldots(4.11)$$

which gives

$$[D]\{\delta q\} = 0$$

$$q = \begin{Bmatrix} a_1 \\ b_0 \\ b_1 \\ b_2 \\ c_0 \\ c_1 \end{Bmatrix} \qquad \ldots(4.12)$$

where *[D]* is

$$\begin{bmatrix} \frac{2AE}{l} & 0 & 0 & 0 & 0 & 0 \\ 0 & 2kGAl & 0 & \frac{2}{3}kGAl & 2kGAl & 0 \\ 0 & 0 & \frac{2}{3}kGAl & 0 & 0 & -\frac{2}{3}kGAl \\ 0 & \frac{2}{3}kGAl & 0 & \frac{2}{9}kGAl & -\frac{2}{3}kGAl & 0 \\ 0 & -2kGAl & 0 & -\frac{2}{3}kGAl & 2kGAl & 0 \\ 0 & 0 & -\frac{2}{3}kGAl & 0 & 0 & \frac{2}{3}kGAl + \frac{2EI}{l} \end{bmatrix}$$

The matrix *{q}* can be expressed in terms of the nodal displacements *{d}* as

$$\{q\} = [B]\{d\} \qquad \ldots(4.13)$$

The matrices can be expanded as

$$\begin{Bmatrix} a_1 \\ b_0 \\ b_1 \\ b_2 \\ c_0 \\ c_1 \end{Bmatrix} = \begin{bmatrix} -\frac{1}{2} & 0 & 0 & 0 & \frac{1}{2} & 0 & 0 & 0 \\ 0 & -\frac{3}{4l} & -\frac{1}{4} & 0 & 0 & \frac{3}{4l} & \frac{1}{4} & 0 \\ 0 & 0 & -\frac{1}{2} & 0 & 0 & 0 & \frac{1}{2} & 0 \\ 0 & \frac{3}{4l} & \frac{3}{4} & 0 & 0 & -\frac{3}{4l} & \frac{3}{4} & 0 \\ 0 & 0 & 0 & \frac{1}{2} & 0 & 0 & 0 & \frac{1}{2} \\ 0 & 0 & 0 & -\frac{1}{2} & 0 & 0 & 0 & \frac{1}{2} \end{bmatrix} \begin{Bmatrix} u_1 \\ w_1 \\ \beta_1 \\ \theta_1 \\ u_2 \\ w_2 \\ \beta_2 \\ \theta_2 \end{Bmatrix} \qquad \ldots(4.14)$$

The stiffness matrix is thus

$$K = [B]^T [D][B] \qquad \ldots(4.15)$$

The stiffness matrix can also be formulated using the conventional approach from the strain displacement relations, and using reduced/selective integration technique. This has been historically done to overcome the problem of shear locking. However, for higher order elements, it has been observed that even without reduced/selective integration, shear locking does not occur. These aspects are explained elegantly from a field-consistency formulation by Marur and Prathap (2000). The use of full and reduced/selective integration is examined for the present study of anisoparametric shear-flexible beam, and results are compared against those obtained from the field-consistent formulation.

4.2.6 Numerical Experiments and Discussion

A cantilever beam is considered for evaluating the performance of different element formulations. When reduced integration is used for the shear-flexible beam, the bending moment for the cantilever with uniform load is shown in Fig. 4.1, and the shear force in Fig. 4.2. Following the procedure described in section 3.2.2, the equivalent of eqn. (3.3) for this case comes out to be

$$E = \int [\ \{-wl^2/2 + wlx - wx^2/2\} - C\ ]^2\ dx \qquad \ldots.(4.16)$$

where *C* is the bending moment (constant for this particular case) obtained from the 1-term finite element solution. It can be clearly seen that this does not follow best-fit rule (If it were to follow the best-fit rule, the constant bending moment should have been $wl^2/6$, which is not the case here. For this problem, the length of the beam has been taken as 100 units and the uniform load as 1 unit.

Mukherjee and Prathap (2002b) studied this problem in detail and accounted why the reduced integration (or in this particular case the field-consistent formulation and the reduced integration give identical results), does not satisfy the best-fit rule. There is a stiffening effect produced due to the differing bending moment sensed by the finite element method from the actual bending moment for the C^0 formulation, and hence the finite element results are not the best-fit to the exact solution, but do form a best-fit of the stiffened solution. In this reference, they deal with both 2-noded and 3-noded elements and show that for both of these cases the best-fit is violated. For the anisoparametric element, going with the same reasoning proposed by them, the finite element method senses the applied loading correctly (due to the C^1 formulation that is used) and hence the results would a best-fit, as would be seen shortly.

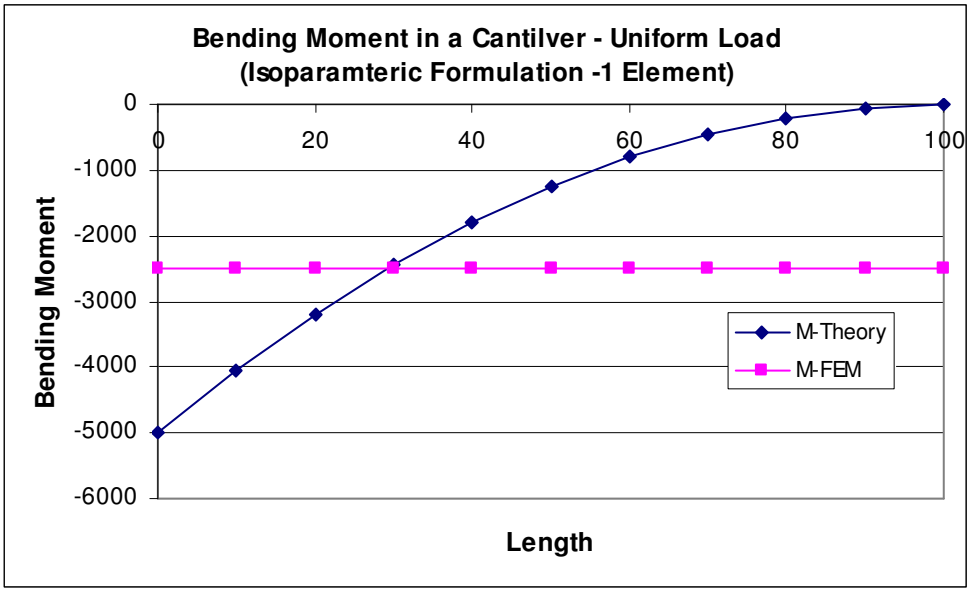

Fig. 4.1 Bending moment in a shear-flexible cantilever beam (uniform load) – Isoparametric element

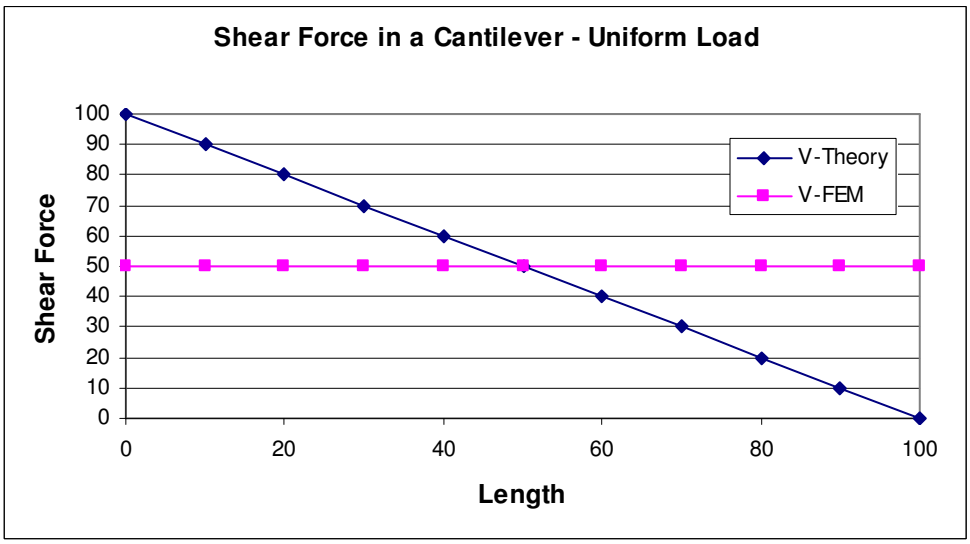

Fig. 4.2 Shear force in a shear-flexible cantilever beam (uniform load) – Isoparametric element

The concepts explained above with the help of a cantilever beam are true for other cases boundary conditions/loading conditions also.

To demonstrate the adherence/violation of the best-fit rule for the C^0 formulation, the same procedure described in section 3.2.2 is followed here as well. The bending moment and shear force along the length of the beam are shown in Figs. 4.3 and 4.4 along with the results obtained using 1 element.

$$E = \int \left\{ [\{ -\frac{1}{2} wl^2 + wlx - \frac{1}{2} \} wx^2 \} - C]^2 \qquad \ldots(4.17)$$

The bending moment C that is constant along the length of the beam, can now be determined by

$$\delta E = 0 \qquad \ldots(4.18)$$

which gives

$$C = -\frac{1}{6} wl^2 \qquad \ldots(4.19)$$

Thus for a cantilever beam subjected to a uniform distributed load, the results of the anisoparametric formulation do show that the best-fit rule is obeyed. It is interesting to note that the shear force obtained from the finite element solution matches with the exact solution (the exact solution for a shear-flexible beam is discussed in Reddy *et al.* (1997)).

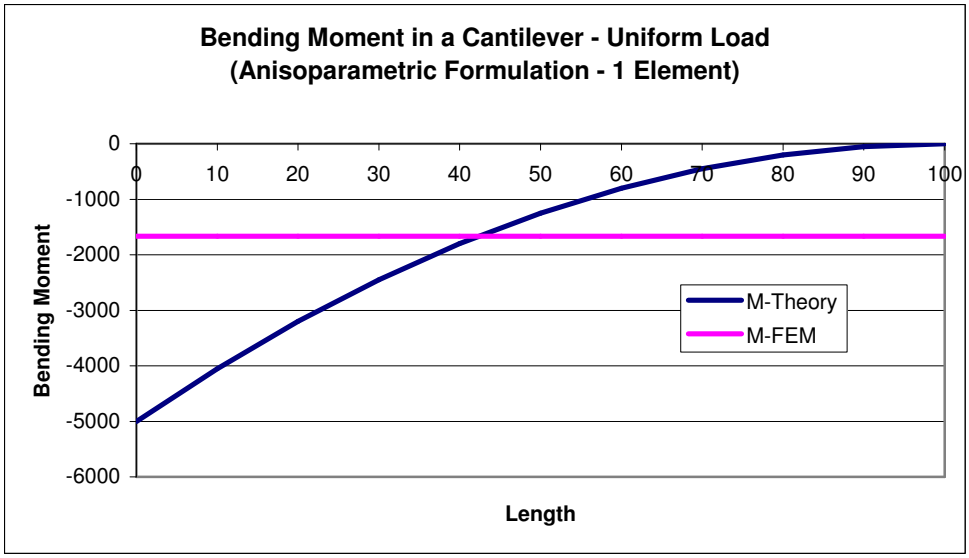

Fig. 4.3 Bending moment in a shear-flexible cantilever beam (uniform load) – Anisoparametric element

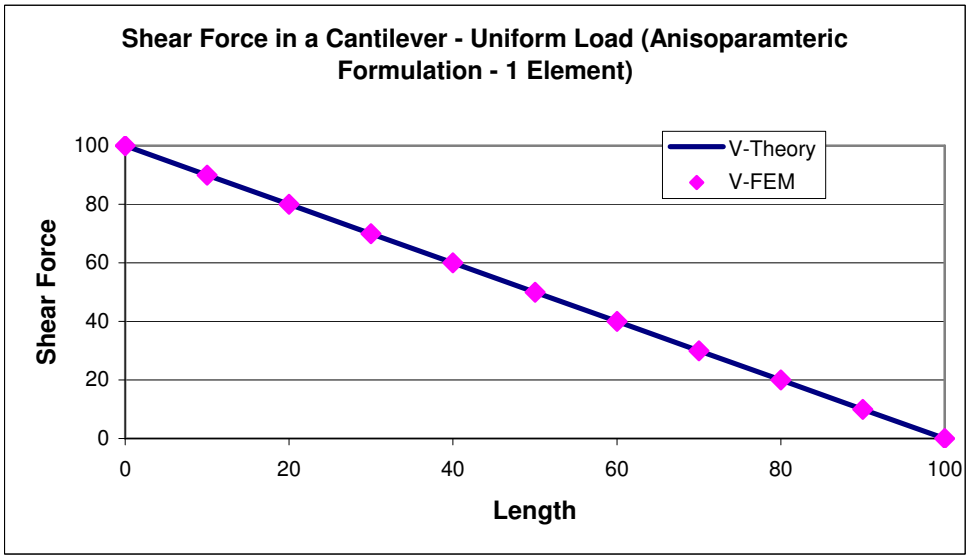

Fig. 4.4 Shear force in a shear-flexible cantilever beam (uniform load) – Anisoparametric Element

A comparison of the results for a simply supported beam subjected to a uniformly distributed load for the field-consistent, full integration and reduced integration formulations is tabulated in Table 4.2. The length of the beam is taken as 100 units, width =1 unit, depth = 1unit, E= 30e6 units, and Poisson's ratio=0.0.

Simply Supported Beam - Uniform Load						
# of Elements	Isoparametric-FC		Isoparametric-FI		Isoparametric-RI	
	Deflection	Strain Energy	Deflection	Strain Energy	Deflection	Strain Energy
2	0.468819	7.080078	0.001316	0.019915	0.468819	7.081163
4	0.507882	8.010864	0.005429	0.085687	0.507882	8.012004
8	0.517648	8.252144	0.021249	0.338837	0.517648	8.253297
16	0.520089	8.313000	0.075881	1.213074	0.520089	8.314156
32	0.520699	8.328248	0.211292	3.379971	0.520699	8.329405
64	0.520852	8.332062	0.381257	6.099822	0.520852	8.333219

Table 4.2 Strain energy boundedness in a shear-flexible simply supported beam (uniform load) – Isoparametric element

This table shows that the field consistent formulation and reduced integration formulations give identical results for the deflection at the center of the beam. The full integration formulation as expected locks, and gives spurious results.

The results of the anisoparametric formulation for a simply supported beam (the dimensions/loading/material properties of the beam remain same) are tabulated in Table 4.3. For the purpose of comparison, the results obtained by using full integration and reduced integration are also tabulated, and as predicted in section 3.4.3, there is no impact on the strain energy and deflection between full and reduced integrations. Till date, this has been the primary driver for the strong advocacy of use of anisoparametric elements.

Simply Supported Beam - Uniform Load						
# of Elements	Anisoparametric-FC		Anisoparametric-FI		Anisoparametric-RI	
	Deflection	Strain Energy	Deflection	Strain Energy	Deflection	Strain Energy
2	0.4948611116	7.9221643674	0.4948610968	7.9221641313	0.4948611116	7.9221643674
4	0.5143923612	8.2273401369	0.5143923459	8.2273398918	0.5143923612	8.2273401369
8	0.5192751736	8.3074487765	0.5192751582	8.3074485291	0.5192751736	8.3074487769
16	0.5204958767	8.3277143549	0.5204958612	8.3277141070	0.5204958767	8.3277143553
32	0.5208010526	8.3327956520	0.5208010370	8.3327954026	0.5208010526	8.3327956521
64	0.5208773465	8.3340669066	0.5208773310	8.3340666597	0.5208773465	8.3340669077

Table 4.3 Strain energy boudedness in a shear-flexible simply supported beam (uniform load) – Anisoparametric Element

The results for a simply supported beam subjected to a uniform load, obtained from field consistent formulation and reduced integration for this case are identical. The convergence of the deflection at the center of the beam is $O(h^2)$, and is shown in Fig. 4.5 and Fig. 4.6. The same plot also shows the high errors when full integration is used. This can be predicted *a priori* using the correspondence concept (best-fit paradigm), as explained in section 3.2.2

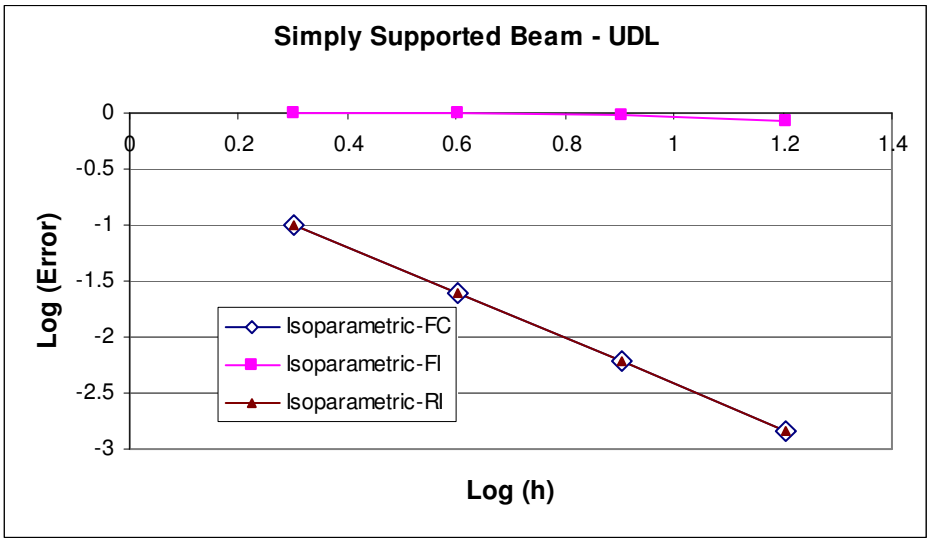

Fig. 4.5 Convergence of deflection in a shear-flexible simply supported beam (uniform load)– Isoparametric element

It can be observed that the deflection at the center of the beam and the strain energy for all the three formulations are the same – which further proves that the anisoparametric formulation is insensitive to locking even when full integration is employed. Fig. 4.6 shows the rate of convergence for all the three formulations, and a comparison with the rate of convergence of the isoparametric reduced integration shows that both ansioparametric full integration and reduced integration case give the same order of convergence as that of isoparametric reduced integration.

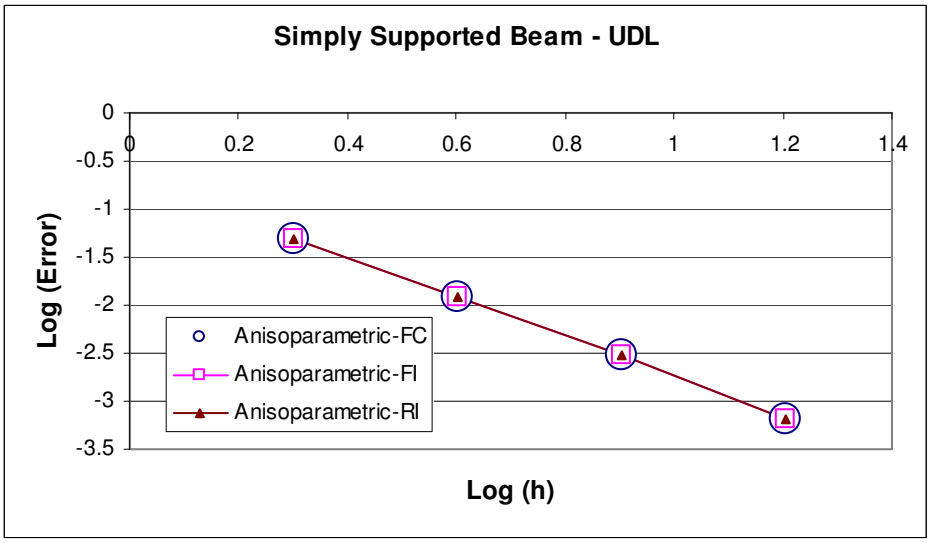

Fig. 4.6 Convergence of deflection in a shear-flexible simply supported beam (uniform load) – Anisoparametric Element

4.3 Axisymmetric Shell Problems

4.3.1 Strain Displacement Relations

Since the slope and rotations are independent, and the strain-displacement relations as given in eqn. (4.20)

$$\varepsilon = \begin{Bmatrix} \varepsilon_s \\ \varepsilon_\theta \\ \chi_s \\ \chi_\theta \\ \gamma \end{Bmatrix} = \begin{Bmatrix} \dfrac{du}{ds} \\ \dfrac{1}{r}(u\cos\phi + w\sin\phi) \\ \dfrac{d\beta}{ds} \\ -\dfrac{1}{r}\beta\cos\phi \\ \dfrac{dw}{ds} - \beta \end{Bmatrix} \qquad \ldots(4.20)$$

4.3.2 Two-noded C^0 Element - Isoparametric Formulation

The interpolation functions that are used for the three displacements are given in eqn. (4.21)

$$\begin{aligned} u &= N_1(\xi)u_1 + N_2(\xi)u_2 \\ w &= N_1(\xi)w_1 + N_2(\xi)w_2 \\ \beta &= N_1(\xi)\beta_1 + N_2(\xi)\beta_2 \end{aligned} \qquad \ldots(4.21)$$

where

$$N_1 = \frac{1}{2}(1-\xi)$$
$$N_2 = \frac{1}{2}(1+\xi)$$

The stress-strain relations are now given by

$$D = \begin{bmatrix} D_1 & 0 & 0 \\ 0 & D_2 & 0 \\ 0 & 0 & D_3 \end{bmatrix} \qquad \ldots(4.22)$$

where D_1, D_2 and D_3 are given as follows:

$$\begin{aligned} D_1 &= \frac{Et}{1-\upsilon^2}\begin{bmatrix} 1 & \nu \\ \nu & 1 \end{bmatrix} \\ D_2 &= \frac{Et^3}{12(1-\nu^2)}\begin{bmatrix} 1 & \nu \\ \nu & 1 \end{bmatrix} \\ D_3 &= \frac{\kappa Et}{2(1+\nu)} \end{aligned} \qquad \ldots(4.23)$$

The stiffness matrix is now formulated, using eqn. (4.15). To overcome shear-locking, reduced integration is used for evaluating all the terms of the stiffness matrix. For this particular case (due to the choice of the linear interpolation functions), the field-consistent formulation and the reduced integration formulation represent the shear term as constant.

$$\bar{\gamma} = Constant \qquad \ldots(4.24)$$

4.3.3 Two-noded C^0 Element - Anisoparametric Formulation

For this element, the interpolation functions that are used are similar to the ones used for the shear-flexible beam element discussed in section 4.2.5 (with cubic polynomial to represent *w*, and linear polynomial to represent *u* and β).

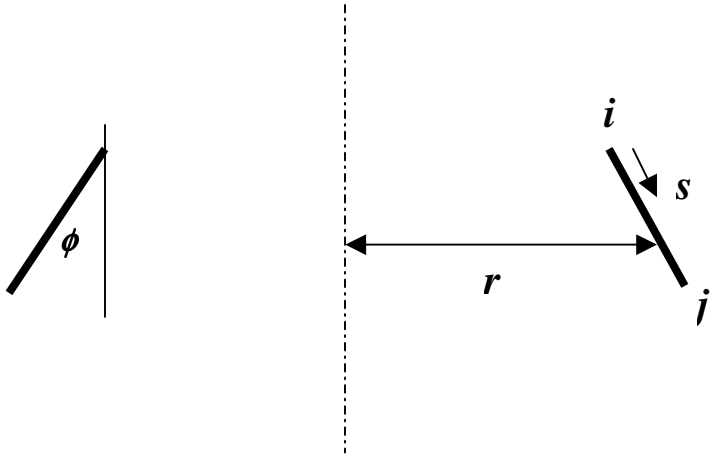

Fig. 4.7 A 2-noded axisymmetric element

4.3.4 Numerical Experiments & Discussion

In the shear-flexible isoparametric formulation for analysis of circular plates, we can clearly see the impact of shear locking when full integration is used. Consider a circular plate of radius = 10 in., E=1.0e7 psi, υ =0.3, and t=0.1 in.

Circular Simply Supported Plate - Uniform Load				
# of Elements	Iso-Reduced (Bending 2, Shear-1, Membrane-1)	Iso-Reduced (Bending 2, Shear-2, Membrane-1)	Iso-Reduced (Bending 2, Shear-1, Membrane-2)	Iso-Full (Bending-2, Shear-2, Membrane-2)
1	0.130762	0.000349	0.130762	0.000349
2	0.400187	0.003929	0.400187	0.003929
4	0.541695	0.024937	0.541695	0.024937
8	0.618232	0.113966	0.618232	0.113966
16	0.657194	0.316628	0.657194	0.316628
32	0.676587	0.509147	0.676587	0.509147

Table 4.4 Deflections in a shear-flexible simply supported circular plate (uniform load) – Isoparametric element

which is subjected to a uniform load of 1 lb/in^2. For the specific case of this plate, there would be no membrane locking even when full integration is used, as the membrane strains for small deformations do not exist. This is clearly seen in Table 4.4, where the effect of selective integration on various strain terms is assessed. The bending moment also matches closely with the theoretical solution as shown in Fig. 4.8.

For a curved shell however, membrane locking occurs in addition to shear locking, due to the interplay of the translational displacement term in the membrane strains. This is seen clearly in Table 4.5.

Open Spherical Dome - Tip Moment				
# of Elements	Iso-Reduced (Bending 2, Shear-1, Membrane-1)	Iso-Reduced (Bending 2, Shear-2, Membrane-1)	Iso-Reduced (Bending 2, Shear-1, Membrane-2)	Iso-Full (Bending-2, Shear-2, Membrane-2)
4	0.0000062420	0.0000008076	0.0000015307	0.0000006201
8	0.0000115792	0.0000019649	0.0000051210	0.0000016611
16	0.0000145522	0.0000041305	0.0000107268	0.0000037763
32	0.0000156918	0.0000077644	0.0000143678	0.0000074420
64	0.0000161062	0.0000120593	0.0000157405	0.0000118625
128	0.0000162678	0.0000148725	0.0000161737	0.0000147974

Table 4.5 Deflections in a shear-flexible open spherical dome subjected to tip moment – Isoparametric element

It has already been shown in section 4.2.9 that the field-consistent formulation gives identical results as that of reduced integration, and hence are not tabulated specifically in the above tables.

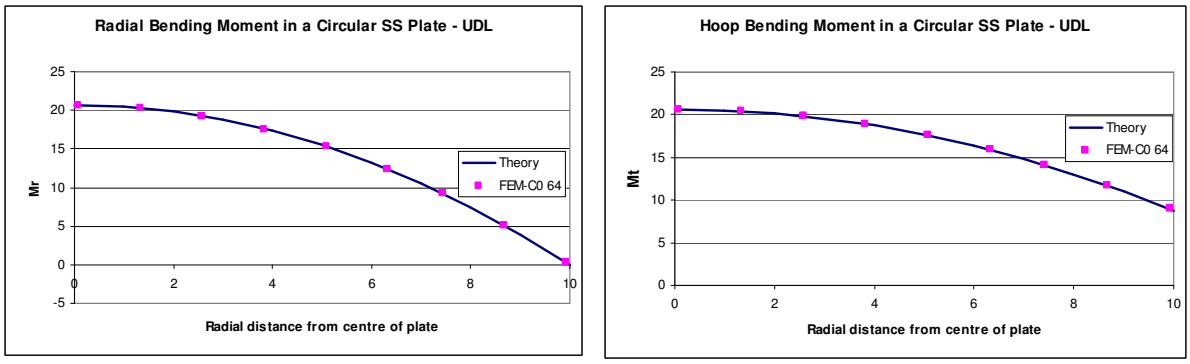

Fig. 4.8 Bending moments in a shear-flexible simply supported circular plate (uniform load) – Isoparametric element

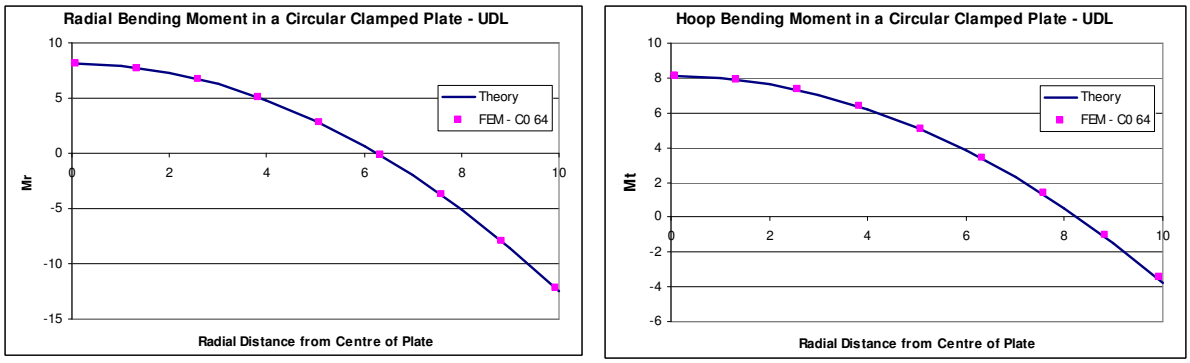

Fig. 4.9 Bending moments in a shear-flexible clamped circular plate (uniform load) – Isoparametric element

For the C^0 formulation, it has already been shown in section 3.5.1.1 that the best-fit rule is violated, and similar reasoning holds good for this as well. For a 1-element discretisation, the radial and hoop bending moments are overlayed with the exact bending moments in Fig. 4.10.

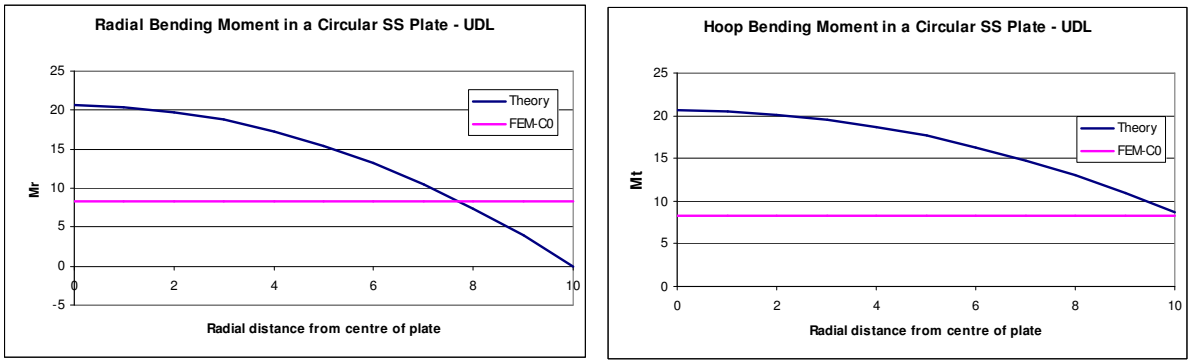

Fig. 4.10 Bending moments in a shear-flexible simply supported circular plate (uniform load) – 1 element solution for isoparametric formulation

Projection Theorem for a Circular Simply Supported Plate - Uniform Load					
Weight	Integration Point	Radial curvature - FEM	Hoop curvature-FEM	Radial curvature-Theory	Hoop curvature-Theory
0.34785485	0.93056816	-0.007000	-0.007000	0.000405	-0.011415
0.65214515	0.66999052	-0.007000	-0.007000	-0.008134	-0.014261
0.34785485	0.06943184	-0.007000	-0.007000	-0.017226	-0.017292
0.65214515	0.33000948	-0.007000	-0.007000	-0.015095	-0.016582
Best-fit Residual = 0.583333					

Table 4.6 Results of best-fit rule for a shear-flexible simply supported circular plate (uniform load) – Isoparametric element

Table 4.6 shows the best-fit residual that should ideally be zero if the best-fit is obeyed. Since it is not zero, it can be concluded that best-fit is violated (due to use of reduced integration in the stiffness matrix).

A 1 element solution for a clamped plate is very inaccurate and predicts bending moment as zero (the nodal displacement components on which the bending moment is computed is zero at both nodes). Hence best-fit rule check for a single element is not valid here, and even for a 2-element solution, the finite element solution is not a best-fit.

The strain energy for the cases of circular plate for both clamped edge and simply supported edge boundary conditions are tabulated in Table 4.7 and Table

4.8 for various discretisations. As expected, the reduced integration and the field consistent formulation give identical results. For both of these formulations the strain energy is bounded.

Boundedness of Strain Energy, Circular Simply Supported Plate, Uniform Load		
Elements	C^0-Selective Integration	C^0-Field Consistent
2	86.52191106	86.52191106
4	96.80393995	96.80393995
8	99.44373769	99.44373769
16	100.11133050	100.11133050
32	100.27875990	100.27875990
64	100.32065130	100.32065140

Table 4.7 Strain energy boundedness in a shear-flexible simply supported circular plate (uniform load) – Isoparametric element

Boundedness of Strain Energy, Circular Clamped Plate, Uniform Load		
Elements	C^0-Selective Integration	C^0-Field Consistent
2	17.22688322	17.22688322
4	17.73745455	17.73745455
8	17.83372042	17.83372042
16	17.85913856	17.85913856
32	17.86563104	17.86563104
64	17.86726365	17.86726365

Table 4.8 Strain energy boundedness in a shear-flexible clamped circular plate (uniform load) – Isoparametric element

The reduced integration and the field consistent formulation give identical results for both the clamped and simply supported circular plates. The order of convergence for the C^1 formulation is $O(h^4)$, while for the C^0 formulation is $O(h^2)$, as seen from the plots shown in Fig. 4.11 and 4.12 . This can be explained from the correspondence concept (on similar lines as done in section 3.2.2). If the displacement fields are chosen so that the finite element strains are complete to the order x^{n-1}, then the finite element solution produces strains that are accurate to $O(h^n)$, energies that are accurate to $O(h^{2n})$ and the errors (in displacements) are removed at the rate of $O(h^{2n})$. Thus for a Timoshenko beam bending problem that is analysed with a 2-noded finite element that has linear interpolation

functions, it can be predicted *a priori* that the displacements would converge at the rate of $O(h^2)$, which is shown in Figs. 4.11 and 4.12.

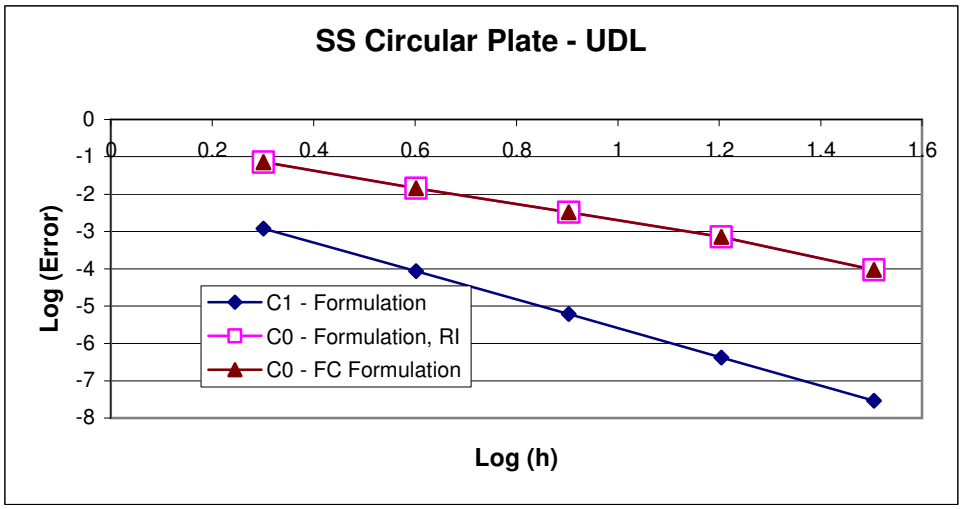

Fig. 4.11 Convergence of deflection in a shear-flexible simply supported circular plate (uniform load) - Isoparametric element

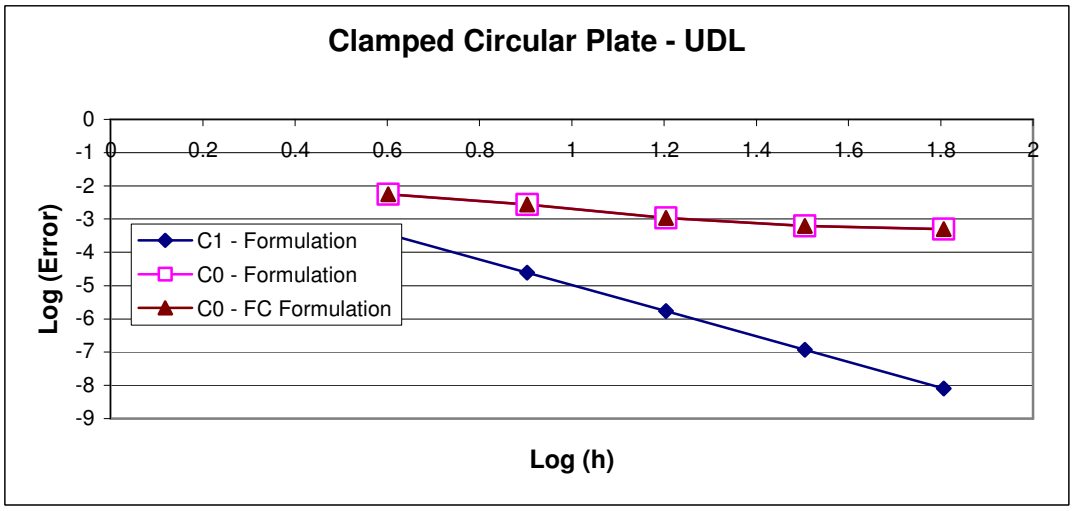

Fig. 4.12 Convergence of deflection in a shear-flexible clamped circular plate (uniform load) – Isoparametric Element

Fig. 4.13 captures the rate of convergence for the problem of an open hemispherical dome subjected to a tip moment (this problem was reported by Grafton and Strome (1963)). The results shown in Table 4.5 are plotted on this chart, and this clearly shows that the analysis case for which reduced integration is used for both shear and membrane terms gives the least error. It is to be noted here that the errors are plotted on the positive side, due to the fact they are converging from above.

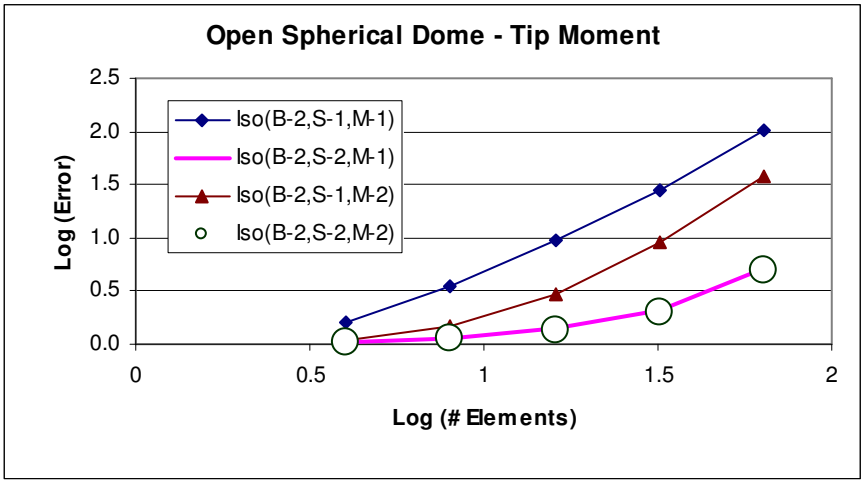

Fig. 4.13 Convergence of deflection in a shear-flexible open spherical dome – Isoparametric Element

For a circular plate subjected to a uniformly distributed load, there is no interplay between the shear and membrane strain terms, and hence no locking is expected due either of these terms, even when full integration is used. This is seen in Table 4.9. The bending moment results match very well with exact solutions as shown in Fig. 4.13.

However, for the case of a general curved shell (*e.g.* a open spherical dome), the membrane and shear strains are coupled, and hence locking is observed when full integration is used as shown in Table 4.10. For the open spherical dome, the membrane locking becomes more significant, and only when reduced integration is used, it gets alleviated.

Simply Supported Circular Plate - Uniform Load					
# of Elements	Aniso-Reduced (Bending-4, Shear-2, Membrane-1)	Aniso-Reduced (Bending-2, Shear-2, Membrane-1)	Aniso-Reduced (Bending-4, Shear-2, Membrane-4)	Aniso-Reduced (Bending-4, Shear-4, Membrane-1)	Aniso-Full (All terms -4)
2	0.668655	0.668829	0.668655	0.668671	0.668671
4	0.689983	0.690004	0.689983	0.689991	0.689991
8	0.694340	0.694342	0.694340	0.694345	0.694345
16	0.695366	0.695366	0.695366	0.695368	0.695368
32	0.695619	0.695619	0.695619	0.695620	0.695620
64	0.695681	0.695682	0.695681	0.695682	0.695682

Table 4.9 Deflections in a shear-flexible simply supported circular plate (uniform load) – Anisoparametric element

Open Spherical Dome - Tip Moment					
# of Elements	Aniso-Reduced (Bending-4, Shear-2, Membrane-1)	Aniso-Reduced (Bending-2, Shear-2, Membrane-1)	Aniso-Reduced (Bending-4, Shear-2, Membrane-4)	Aniso-Reduced (Bending-4, Shear-4, Membrane-1)	Aniso-Full (All terms -4)
4	0.0000681528	0.0000681681	0.0000036086	0.0000681364	0.0000034397
8	0.0000268575	0.0000268579	0.0000085491	0.0000268495	0.0000083776
16	0.0000181831	0.0000181831	0.0000126145	0.0000181804	0.0000125296
32	0.0000165935	0.0000165935	0.0000149957	0.0000165927	0.0000149672
64	0.0000163326	0.0000163326	0.0000159120	0.0000163323	0.0000159042
128	0.0000163247	0.0000163247	0.0000162177	0.0000163246	0.0000162157

Table 4.10 Deflections in a shear-flexible open spherical dome subjected to tip moment – Anisoparametric element

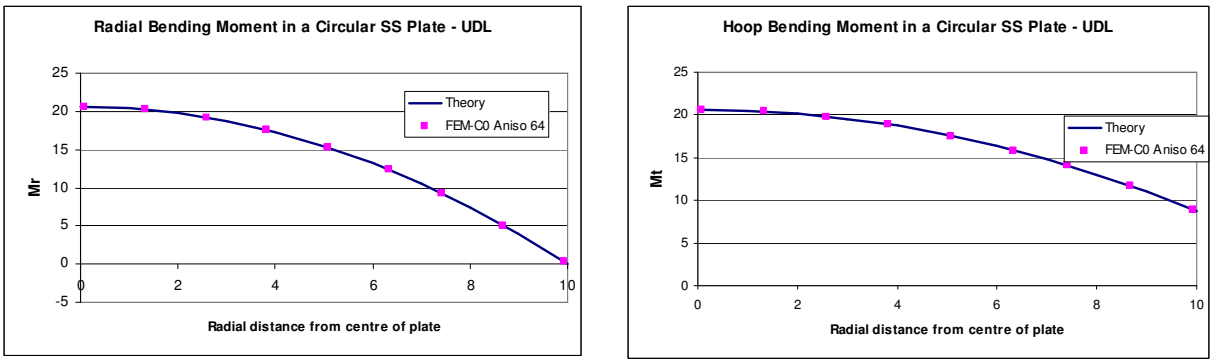

Fig. 4.14 Bending moments in a shear-flexible simply supported circular plate for a uniform load – Anisoparametric element

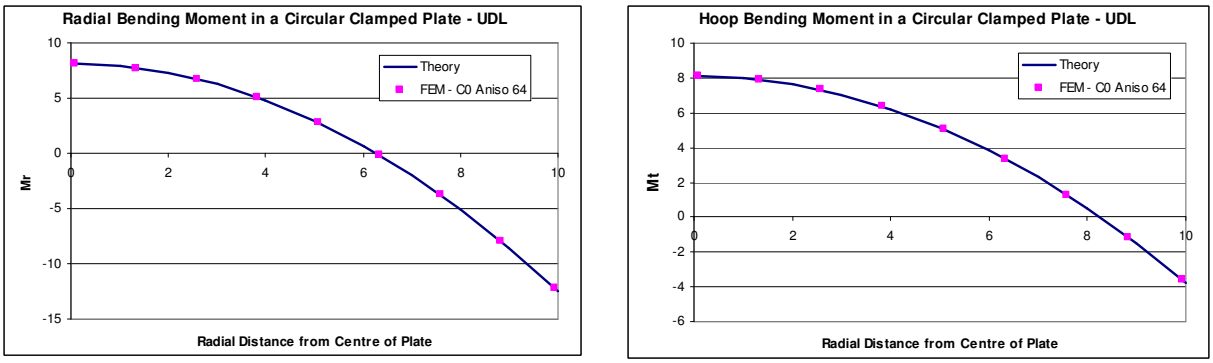

Fig. 4.15 Bending moments in a shear-flexible clamped circular plate for a uniform load – Anisoparametric element

The radial and hoop bending moments for a 1-element discretisation is shown in Fig. 4.15 for clamped plate and Fig. 4.16 for simply supported plate. The best-fit residual in tabulated in Table 4.11 and It can be clearly seen that the best-fit rule is obeyed.

Projection Theorem for a Circular SS Plate - Uniform Load					
Weight	Integration Point	Cr - FEM	Ct - FEM	Cr-Theory	Ct-Theory
0.3478549	0.9305682	-0.010500	-0.010500	0.000405	-0.011415
0.6521451	0.6699905	-0.010500	-0.010500	-0.008134	-0.014261
0.3478549	0.0694318	-0.010500	-0.010500	-0.017226	-0.017292
0.6521451	0.3300095	-0.010500	-0.010500	-0.015095	-0.016582
Numerical Value of the Expression=0.000000147					

Table 4.11 Results of best-fit rule for a shear-flexible simply supported circular plate (uniform load) – Anisoparametric Element

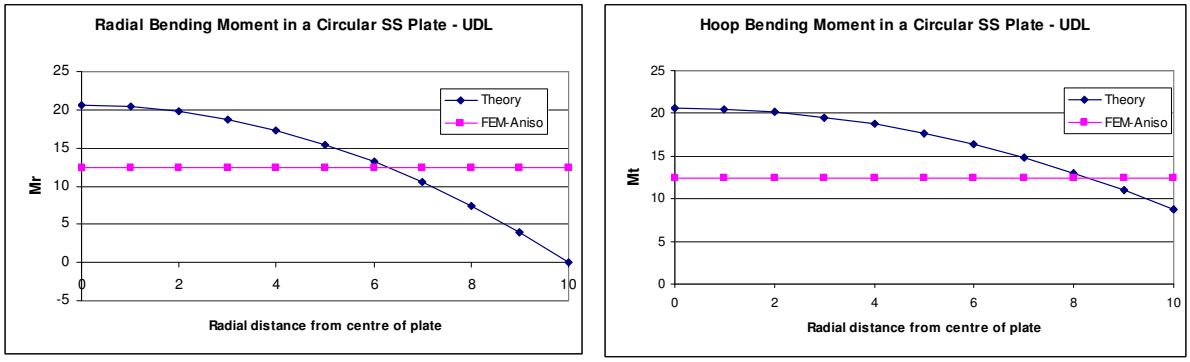

Fig. 4.16 Bending moments in a shear-flexible simply supported circular plate (uniform load) - 1 element solution for anisoparametric formulation

The strain energy boundedness is now studied for the anisoparametric formulation for a circular plate subjected to a uniform load and an open spherical dome subjected to a tip moment. The results are tabulated in Tables 4.12 and 4.13 for the simply supported and open spherical dome.

Simply Supported Circular Plate - Uniform Load; Strain Energy Boundedness					
# of Elements	Aniso-Reduced (Bending-4, Shear-2, Membrane-1)	Aniso-Reduced (Bending-2, Shear-2, Membrane-1)	Aniso-Reduced (Bending-4, Shear-2, Membrane-4)	Aniso-Reduced (Bending-4, Shear-4, Membrane-1)	Aniso-Full (All terms -4)
2	50.822251	50.840037	50.822251	50.819730	50.819730
4	50.634561	50.635877	50.634561	50.630472	50.630472
8	50.368423	50.368507	50.368423	50.362394	50.362394
16	50.248122	50.248128	50.248122	50.239776	50.239776
32	50.205911	50.205906	50.205911	50.194869	50.194869
64	50.194120	50.194123	50.194120	50.179991	50.179991

Table 4.12 Strain energy boundedness in a shear-flexible simply supported circular plate (uniform load) – Anisoparametric element

Open Spherical Dome - Tip Moment; Strain Energy Boundedness					
# of Elements	Aniso-Reduced (Bending-4, Shear-2, Membrane-1)	Aniso-Reduced (Bending-2, Shear-2, Membrane-1)	Aniso-Reduced (Bending-4, Shear-2, Membrane-4)	Aniso-Reduced (Bending-4, Shear-4, Membrane-1)	Aniso-Full (All terms -4)
4	0.761063	0.761408	0.002878	0.760981	0.002590
8	0.168035	0.168040	0.021067	0.167991	0.019710
16	0.101986	0.101986	0.053544	0.101969	0.053357
32	0.094085	0.094085	0.079258	0.094075	0.081517
64	0.093700	0.093700	0.090232	0.093691	0.094134
128	0.094244	0.094244	0.093960	0.094235	0.098674

Table 4.13 Strain energy boundedness in a shear-flexible open spherical dome subjected to a tip moment - Anisoparametric element

It can be seen from Table 4.13 that the boundedness is lost due to use of reduced integration. The rate of convergence for the displacement at the centre of the circular plate subjected to a uniform load is shown in Fig. 4.17 and Fig. 4.18 for simply supported and clamped boundary conditions. It can be observed that the rate of convergence for the anisoparametric formulation is lower than that of the C^1 formulation, and there is no degradation of the anisoparametric element *per se*.

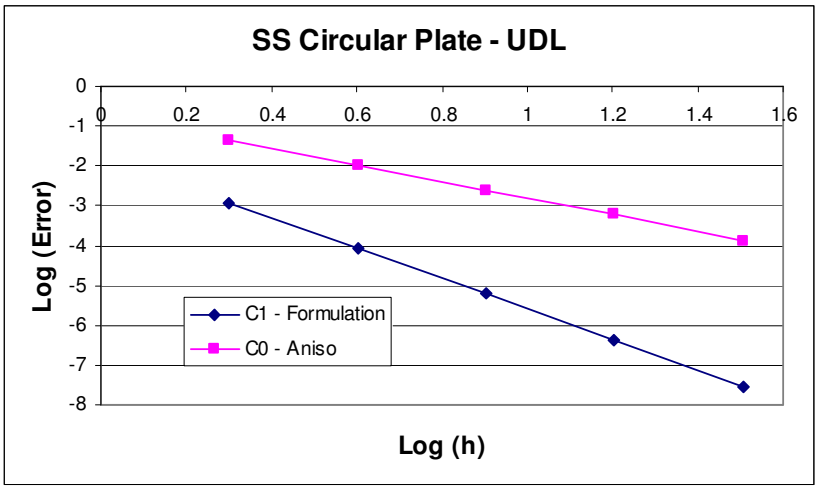

Fig. 4.17 Convergence of deflection in a shear-flexible simply supported circular plate (uniform load) – Anisoparametric element

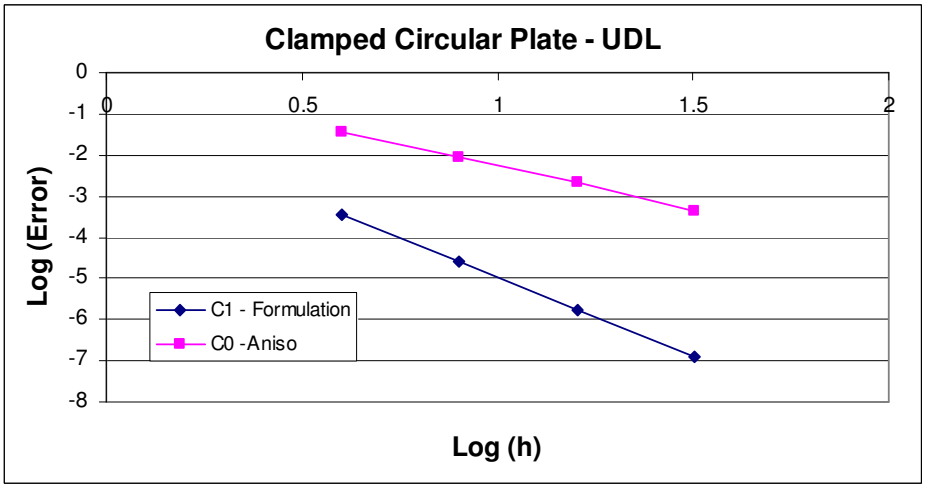

Fig. 4.18 Convergence of deflection in a shear-flexible clamped circular plate (uniform load) – Anisoparametric Element

Fig. 4.19 captures the rates of convergence of anisoparametric formulation for the different combinations of reduced integration for shear and membrane terms. The order of convergence is $O(h^2)$, as predicted from correspondence concept.

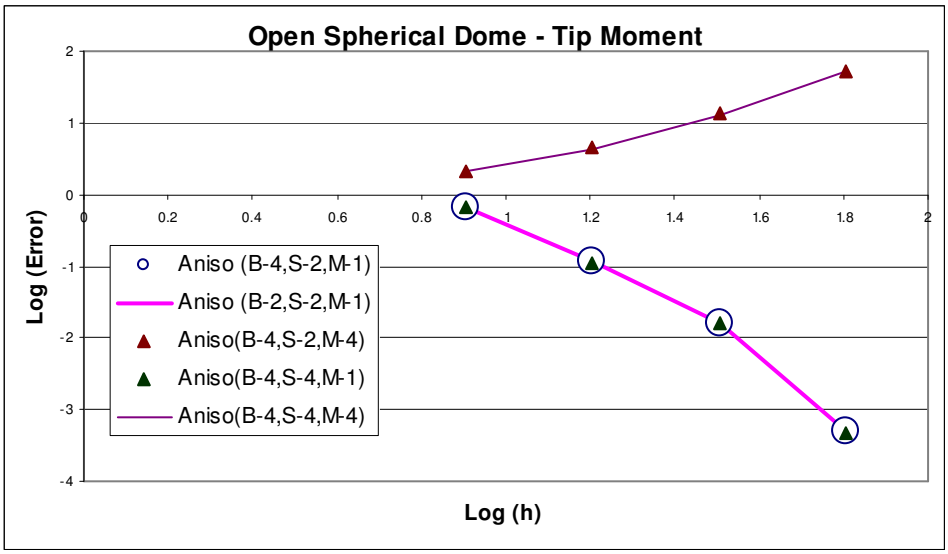

Fig. 4.19 Convergence of deflection in a shear-flexible open spherical dome (tip moment) – Anisoparametric element

4.4 Plate Bending Problems – Isoparametric Formulation

The formulation of the simple and elegant isoparametric element led to the applications of the finite element method to a wide variety of problems, and allowed the mesh to be a generic quadrilateral. For plate bending problems, the formulation of a C^1 element for an arbitrary quadrilateral was not very straight forward, and the isoparametric formulation was very appealing. This led to the development of C^0 elements for plate bending. In this section, the Mindlin theory is used for formulating the C^0 element and its effects on the results are studied. A case is then made for the use of an element that is variationally correct for getting the correct results.

4.4.1 Strain Displacement Relations

In the Mindlin theory of bending, one of the crucial assumptions of the Euler-Bernoulli beam bending theory – lines normal to the neutral axis of the beam remain straight and normal to the neutral axis after bending is relaxed. In the Mindlin theory, the line normal to the neutral axis remains straight, but not necessarily normal to the neutral axis, after bending. This relaxation brings with it, two additional independent degrees of freedom of a node belonging to an element modeling the plate/beam. Thus, the node now has w, θ_x and θ_y as the three independent movements. Due to this, the bending and shear strain terms are now different from those of the Euler-Bernoulli theory, and are as follows.

$$\begin{Bmatrix} \varepsilon_x \\ \varepsilon_y \\ \gamma_{xy} \\ \gamma_{yz} \\ \gamma_{xz} \end{Bmatrix} = \begin{Bmatrix} -z\theta_{x,x} \\ -z\theta_{y,y} \\ -z(\theta_{x,y} + \theta_{y,x}) \\ -\theta_y + w_{,y} \\ -\theta_x + w_{,x} \end{Bmatrix} \qquad \ldots(4.27)$$

Since only first derivative terms are involved in the strain energy expansion, only C^0 continuity is required.

4.4.2 Four-noded C^0 Element – Isoparametric Formulation

The interpolation functions are bi-linear for the case of the four noded element. These functions are –

$$w = N_1 w_1 + N_2 w_2 + N_3 w_3 + N_4 w_4 \qquad \ldots(4.28)$$

where, N_1, N_2, N_3 *and* N_4 are the interpolation functions and w is the transverse displacement of the nodes 1, 2, 3 and 4. Similar expressions for the rotations of the node are

$$\phi = N_1\phi_1 + N_2\phi_2 + N_3\phi_3 + N_4\phi_4 \qquad \ldots(4.29)$$

where the symbol ϕ is generic, denoting both θ_x and θ_y

The same interpolation functions can be used for the geometry

$$x = N_1x_1 + N_2x_2 + N_3x_3 + N_4x_4 \qquad \ldots(4.30)$$

$$y = N_1y_1 + N_2y_2 + N_3y_3 + N_4y_4 \qquad \ldots(4.31)$$

where, x_1, x_2, x_3, x_4 and y_1, y_2, y_3 and y_4 are the geometric locations of the nodes 1, 2, 3 and 4.

$$\begin{aligned} N_1 &= \frac{1}{4}(1-\xi)(1-\eta) \\ N_2 &= \frac{1}{4}(1+\xi)(1-\eta) \\ N_3 &= \frac{1}{4}(1+\xi)(1+\eta) \\ N_4 &= \frac{1}{4}(1-\xi)(1+\eta) \end{aligned} \qquad \ldots(4.32)$$

The stiffness matrix formulation can be found in any standard text book, *e.g.* Cook *et al*. (1989) and is not elaborated here.

Thus all the equations necessary for the formulation of the stiffness matrix are in place. Numerical integration using an appropriate Gaussian Quadrature (2X2) rule is employed for computing these matrices.

The biggest advantage of using isoparametric elements is that complex geometric shapes can also be discretised, which is not at the cost of different interpolation functions for displacement and geometry. Thus, same interpolation functions can be used, making the generation of matrices easier. The transformation of the variable from the natural coordinate system to the element coordinate system is very important here, which is achieved through the Jacobian of the element.

If the mixed integration technique is used here and the stiffness matrix corresponding to the shear strains integrated with the appropriate quadrature as demanded by the terms (in this case 2X2 rule), the element still gives erroneous results. Thus, locking which disappeared in the earlier case has reappeared. Obviously, the mere usage of different rules has to have a deeper mathematical significance. Possibly, the mandatory use of 1X1 rule for the shear strain terms for quadrilateral elements just happens to be the solution to avoid locking. But, this again fails in the case of the 3-corner supported plate problem.

This necessitates the requirement of a more logically supported strategy for analyzing the locking problem. For the quadrilateral elements, the shear strains across the inter-element boundary need to be preserved, and this can not be achieved by a mere Jacobian transformation of the nodal derivatives. Numerous formulations can be found in literature which tackle this transformation of shear strains, and the edge-consistency formulation by Prathap and Somasekhar (1988) is the one which would be discussed next.

4.4.3 Four-noded C^0 Element –Field-consistent/Edge-consistent Element

The shear strains in the plate are a function of both the rotation and the transverse displacement, (see eqn. 4.27). Thus any transformation of the shear strain from a natural coordinate system to a Cartesian coordinate system, should appropriately take care of the transformations of both, rotation and the derivative of the transverse displacement. In the edge consistency formulation, the shear strains across the inter-element boundary are preserved irrespective of the transformation of the coordinate system, Prathap and Somashekar (1988).

When the above edge-consistency formulation is implemented in the C^0 element, the element becomes free of locking. The results for the cantilever with both rectangular and non-rectangular mesh are quite consistent with expected results. Also, this formulation gives the correct results for the 3-corner supported plate as well. The simple and efficient mathematical basis of the edge-consistency formulation has made the implementation of this strategy possible for adaptive mesh refinement of plate bending problems by Mukherjee and Krishnamoorthy (1996)

4.4.4 Numerical Studies and Discussion

The above element formulation is now used to study plates with different loads and boundary conditions. Many of these test cases are well known problems for which analytical solutions exist. To further check the remedy used above, tests on a simply supported square plate were done, Averill and Reddy (1990). The plate is shown in Fig. 4.20, and the results are tabulated in Table 4.14 for the non-dimensionalized displacement at the centre of the plate. Here again it can be observed that the strategy of mixed integration apparently works. Based on the above two test problems, if one concludes that the technique of mixed integration can overcome locking, one would be committing a serious mistake. For, this

technique does not come from a theoretical perspective. It is just a stop-gap solution. It fails in many cases, as discussed in the following sections.

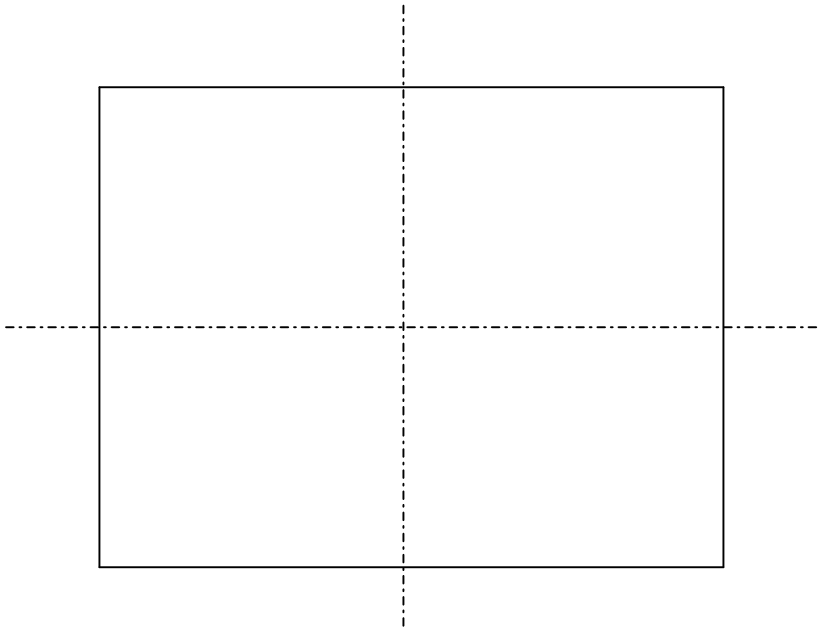

Fig. 4.20 A simply supported plate

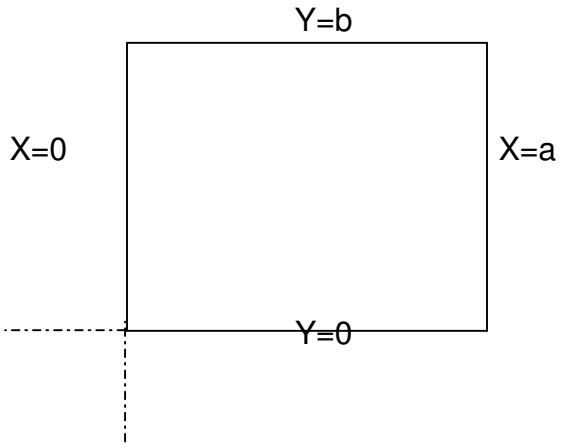

Fig. 4.21 One quadrant of the plate

Boundary Conditions:

1. on the line Y = 0, $\partial w/\partial y = 0$
2. on the line X = 0, $\partial w/\partial x = 0$
3. on the line Y = b, $w = 0$, $\partial w/\partial x = 0$
4. on the line X = a, $w = 0$, $\partial w/\partial y = 0$

Effect of Full Integration and Mixed Integration in a simply supported square plate - uniform load									
a/t	1X1		2X2		4X4		8X8		Exact
	F	M	F	M	F	M	F	M	
100	0.0112	3.5902	0.0478	4.4720	0.1819	4.5549	0.6497	4.5731	4.5720
50	0.0447	3.6352	0.1861	4.5020	0.6516	4.5822	1.8270	4.5996	4.5790
40	0.0695	3.6690	0.2850	4.5245	0.9443	4.6026	2.3353	4.6198	4.5840
20	0.2695	3.9502	0.9794	4.7120	2.3632	4.7728	3.7331	4.7866	4.6250
10	0.9639	5.0752	2.5573	5.4620	3.8835	5.4534	4.5268	5.4538	4.7910

Table 4.14 Effect of reduced integration on displacement in a shear-flexible simply supported square plate (uniform load)

A three-corner supported square plate with a concentrated load at the fourth cornet is studied now (side of the plate=20 units, thickness = 0.4 units, Poisson's ratio = 0.3 and E=200000 units, load=1000 units). This is a standard test recommended in Prathap and Somashekar (1988) for studying the response of the mixed integration technique. Fig. 4.22 shows the plate, supported at the three corners, and load by a concentrated load at the fourth corner. This loading produces a constant twisting moment in the plate and should be captured by any finite element modeling this. The mixed integration formulation fails miserably in this case, giving violet oscillations in the twisting moments. On the contrary, the C^1 element, even with one element modeling the entire plate gives good results. The results are tabulated in Table 4.15. It is also observed that the mixed integration technique fails in the case of non-rectangular elements being used to model a plate/beam.

Three-Corner suported square plate				
# of Elements	Deflection		Twisting Moment	
	F	M	F	M
2x2	243.98	-21.83	499.99	1324.4, 8.07, 895.5
4x4	244.28	248.60	501.63	1268.9, 1330.9
8x8	244.81	256.11	492, 498	596.4, 2060, 1942
16x16	245.81	257.81	477, 493	188, -53811

Table 4.15 Effect of reduced integration on displacement of a shear-flexible 3-corner supported plate (loaded at 4^{th} corner)

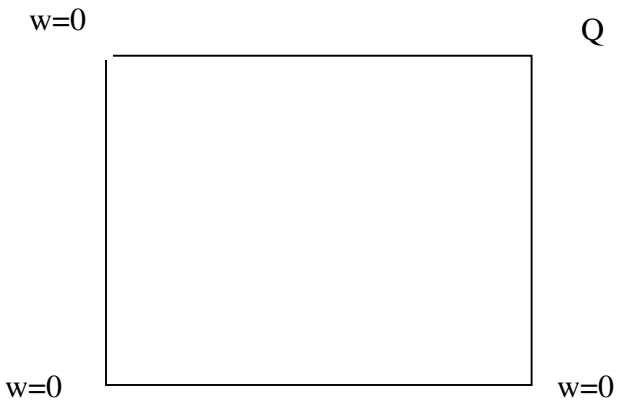

Fig. 4.22 A 3-corner supported plate

(40X40 plate, t=0.4, v=0.3, Load=1000)

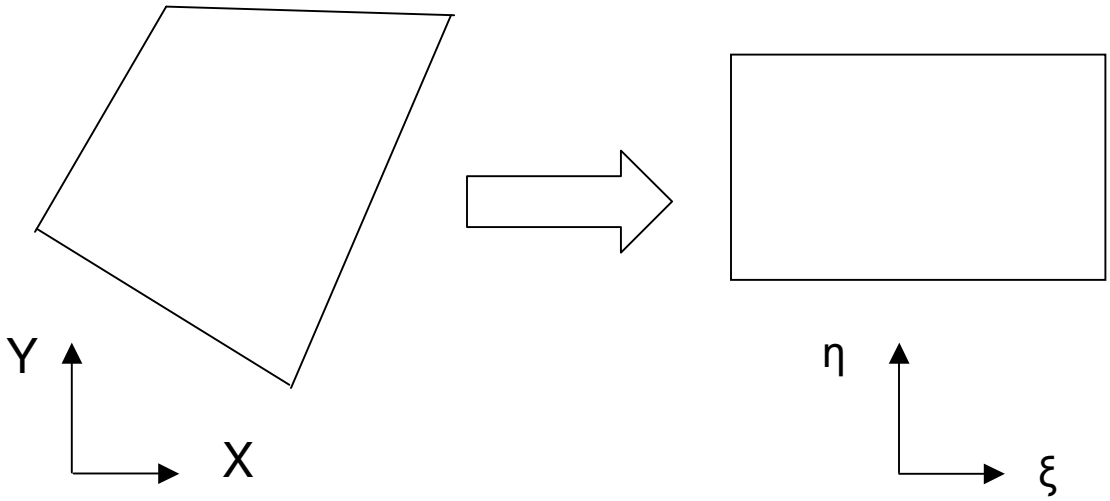

Fig. 4.23 Transformation of a quadrilateral element

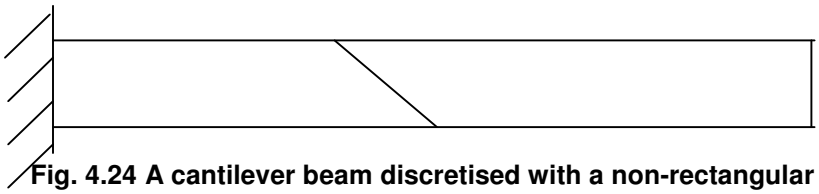

Fig. 4.24 A cantilever beam discretised with a non-rectangular mesh

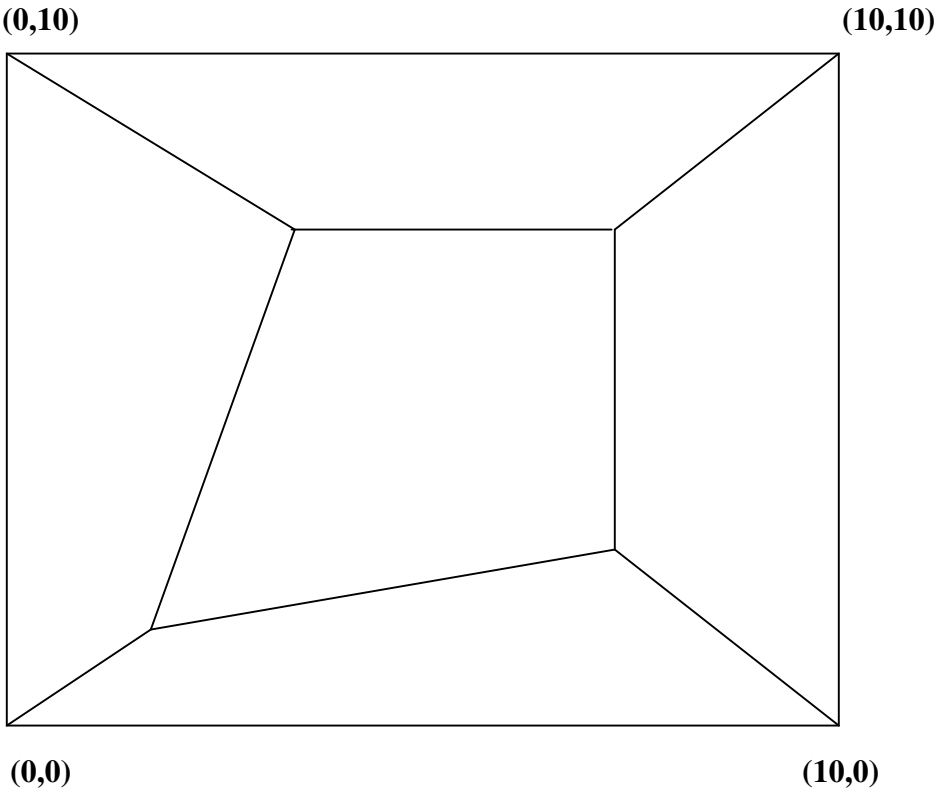

Fig. 4.25 Tests on a patch of elements
(E =1.0E6 units, v = 0.3 units, t =1.0 units)

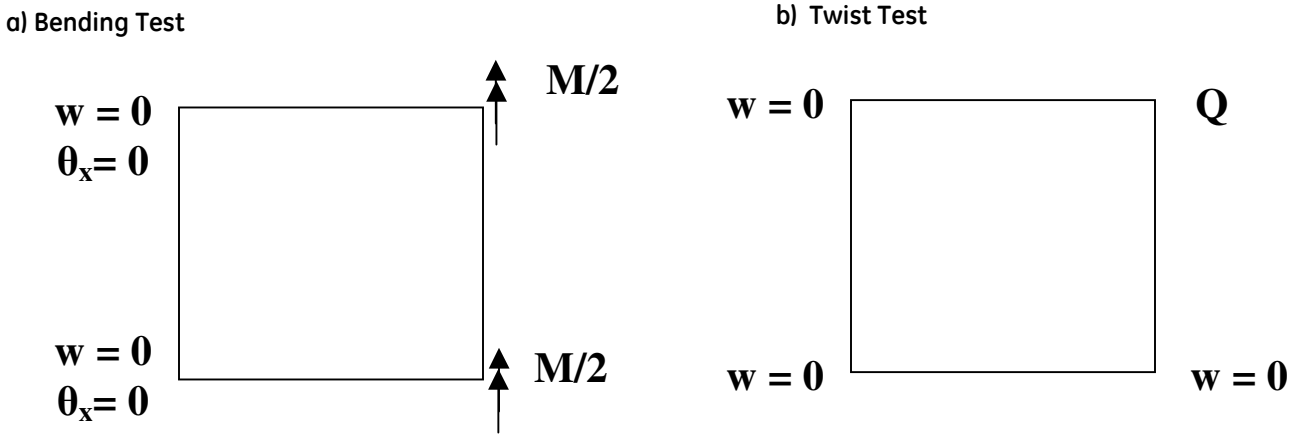

The patch tests are now conducted for studying the element behaviour. To simulate the constant state of strains in a patch of elements, consider the patch shown in Fig. 4.25.

From Tables 4.16 and 4.17, it can be observed that the patch of elements pass the patch test. Now, this element will be used for studying a cantilever with distorted mesh that had earlier produced erroneous results.

Results of Patch Test (Bending Case)		
Element Number	Mx at Centroid	Qx at Centroid
1	0.1	0
2	0.1	0
3	0.1	0
4	0.1	0
5	0.1	0

Table 4.16 Results of patch test (bending case)

Patch Test (Twist Case)	
Element #	Mxy at Centroid
1	0.4999
2	0.4999
3	0.5004
4	0.4999
5	0.4998

Table 4.17 Results of patch test (twist case)

Thus, it can be concluded that the edge-consistency formulation satisfactorily explains the phenomena of locking as evidenced from the results reported above.

There are many other tests to study the behaviour of the element. Here, a square cantilever plate is subjected to a unit moment at the free edge. The schematic is shown in Fig. 4.26. The displacement at the free nodes is found as 6.0, and the moment at the centroid of both the elements as 0.1, confirming the theoretical solutions.

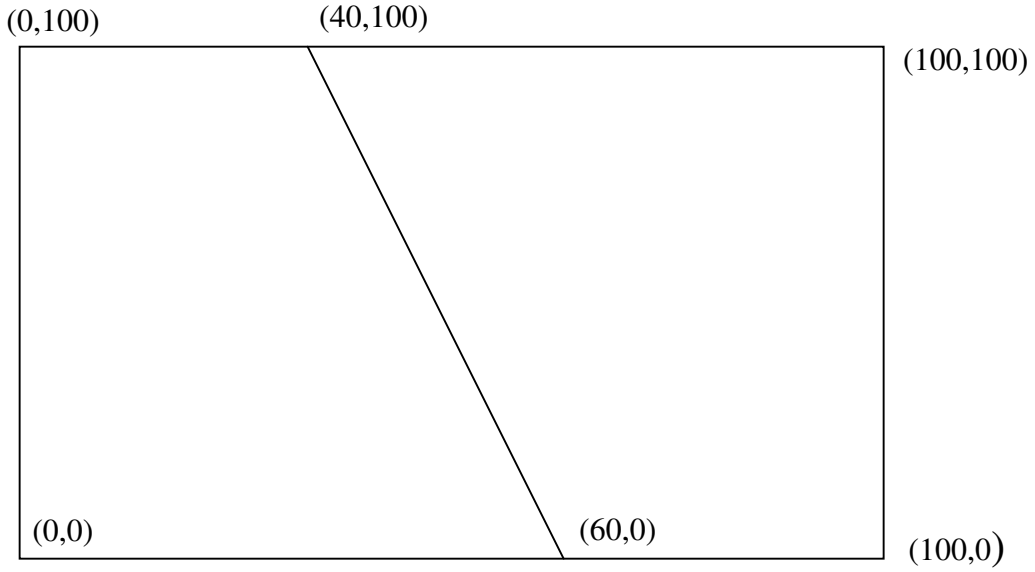

Fig. 4.26 Mesh for a cantilever subjected to a tip moment

It was shown that for a shear-deformable beam using a 2-noded C^0 element violated the best-fit rule is violated. Using similar arguments, the best-fit rule for a shear-deformable plate, for a 4-noded C^0 element is violated (Table 4.18). A detailed study of a square plate simply supported on all four sides (side of plate = 40 units, thickness = 0.4 units, E=200000 units and Poisson's ratio = 0.3) and subjected to a sinusoidal load, (similar to the one described in section 3.4.4) reveals this fact. It is significant to note that the bending moments and the shear forces for these boundary conditions for both classical plate and shear-deformable plate remain the same, Wang *et al.* (2000).

Best-fit Rule for a Simply Supported Plate - Sinusoidal Load, Mindlin Theory, Field-consistent Formulation							
Weight	Theory-Mx	Theory-My	Theory-Mxy	FEM-Mx	FEM-My	FEM-Mxy	Projection
0.121003	0.62422074	0.62422074	28.0338126	2.420564	2.420564	17.46871	0.05374518
0.2268519	2.84144785	2.84144785	24.4963913	4.516958	9.408544	15.02291	0.06686654
0.121003	5.70076103	5.70076103	3.06964055	9.348561	25.51389	9.386043	-0.06919243
0.2268519	4.98141566	4.98141566	13.9729794	7.252167	18.52591	11.83184	-0.03384374
0.2268519	2.84144785	2.84144785	24.4963913	9.408544	4.516958	15.02291	0.06686654
0.4252933	12.934248	12.934248	21.4053363	11.50494	11.50494	12.57712	0.12434232
0.2268519	25.9498189	25.9498189	2.68230074	16.33654	27.61028	6.94025	-0.00787615
0.4252933	22.6753645	22.6753645	12.2098116	14.24015	20.6223	9.386043	0.06802561
0.121003	5.70076103	5.70076103	3.06964055	25.51389	9.348561	9.386043	-0.06919243
0.2268519	25.9498189	25.9498189	2.68230074	27.61028	16.33654	6.94025	-0.00787615
0.121003	52.0627948	52.0627948	0.33611886	32.44188	32.44188	1.303381	0.10055246
0.2268519	45.4932981	45.4932981	1.53001038	30.34549	25.4539	3.749174	0.13810313
0.2268519	4.98141566	4.98141566	13.9729794	18.52591	7.252167	11.83184	-0.03384374
0.4252933	22.6753645	22.6753645	12.2098116	20.6223	14.24015	9.386043	0.06802561
0.2268519	45.4932981	45.4932981	1.53001038	25.4539	30.34549	3.749174	0.13810313
0.4252933	39.7527675	39.7527675	6.96459508	23.35751	23.35751	6.194967	0.21864417
Best-fit Residual = 328.580							

Table 4.18 Results of best-fit rule for a shear-flexible simply supported plate (sinusoidal load)

The Quad-4 element formulated using the field-consistency and edge-consistency concepts gives results that are bounded, and eqn. (2.29) remains valid. The strain energy boundedness is shown in Tables 4.19 – 4.22 for the cases of simply supported and clamped plates subjected to uniform and point loads.

Strain Energy of a SS Plate subject to a UDL		
Elements in one quarter	QUAD-4 (FC)	QUAD-4 (RI)
1	697.013576	923.8573054
4	1272.785107	1273.676536
16	1432.886116	1433.766877
64	1474.271466	1475.149577

Table 4.19 Strain energy boundedness in a shear-flexible simply supported plate (uniform load)

Strain Energy of a SS Plate subject to a Point Load		
Elements in one quarter	QUAD-4 (FC)	QUAD-4 (RI)
1	69701.3576	92385.73054
4	62914.80678	63048.5223
16	63091.35758	63271.26662
64	63329.09561	63559.48348

Table 4.20 Strain energy boundedness in a shear-flexible simply supported plate (point load)

Strain Energy of a Clamped Plate subject to a UDL		
Elements in one quarter	QUAD-4 (FC)	QUAD-4 (RI)
1	0.585000028	1.56
4	265.4208846	266.6395151
16	321.2729319	322.3537074
64	335.9808104	337.0235158

Table 4.21 Strain energy boundedness in a shear-flexible clamped plate (uniform load)

Strain Energy of a Clamped Plate subject to a Point		
Elements in one quarter	QUAD-4 (FC)	QUAD-4 (RI)
1	58.50	188.7600075
4	26527.10	32243.40873
16	29603.15	35601.39303
64	30444.27	36552.04065

Table 4.22 Strain energy boundedness in a shear-flexible clamped plate (point load)

The relationship between shear deformable plates and classical plates has been extensively analyzed by Wang *et al.* (2000). The exact solution obtained using the relationship provided by Wang *et al.* (2000) is used to plot the rate of convergence of the displacements. For a simply supported plate subjected to a uniform load, the convergence of the displacements is shown in Fig. 4.27

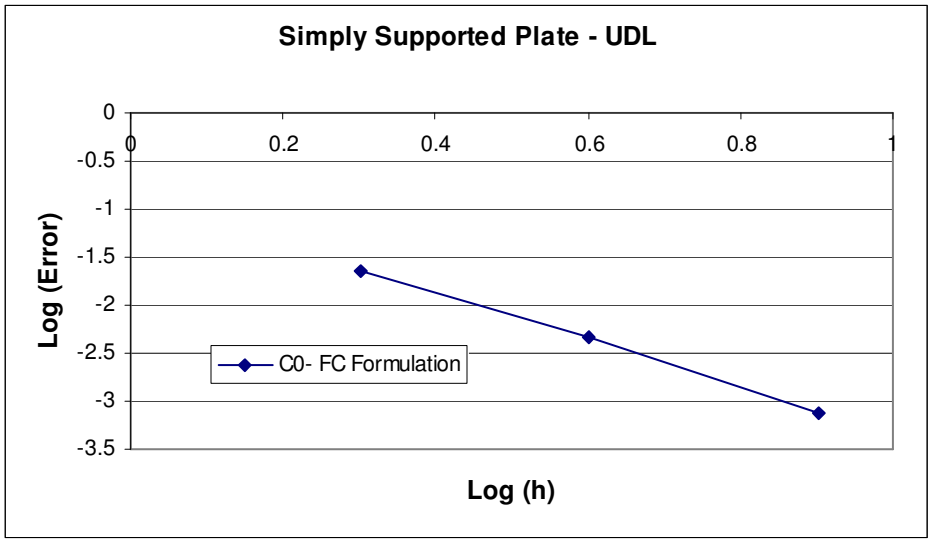

Fig. 4.27 Convergence of displacement in a shear-flexible simply supported plate (uniform load) – Isoparametric FC element

4.5 Plate Bending Problems – Anisoparametric Formulation

4.5.1 Element Formulation

The anisoparametric formulation is now extended to shear-deformable plates. Tessler (1981) uses a conforming element that has the translational displacement interpolated from 9 nodes, and rotational displacements interpolated from 6 nodes. In this thesis, it was felt that since the interpolation functions from a conforming element already exist, they could be leveraged. Thus, the same cubic Hermite shape functions that were used for the BFS element to represent the translational displacement w are used for the Mindlin element as well. The rotational degrees of freedom θ_x and θ_y are represented using bilinear polynomials. The element is shown in Fig.4.28.

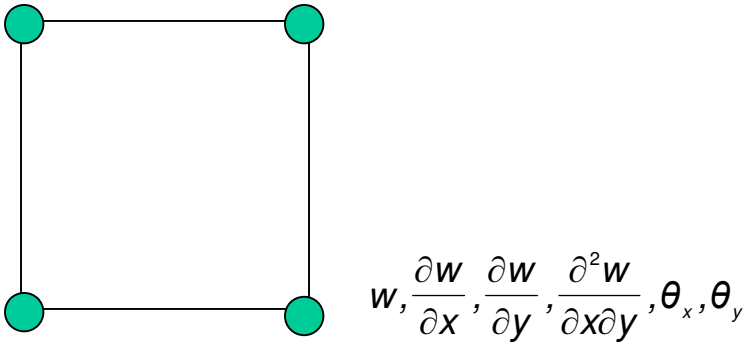

Fig.4.28 4-Noded anisoparametric plate bending element with 6 degrees of freedom at each node

4.5.2 Numerical Studies and Discussion

For this formulation there is no requirement of using reduced integration. This element does not produce any shear locking and the results for the deflection at the centre of a simply supported plate are tabulated in Table 4.23. The results of the 4-noded conforming anisoparametric element for the case of a simply supported plate subjected to a uniform load (side of plate = 40 units, thickness = 0.4 units, E=200000 units and Poisson's ratio = 0.3) are shown in Table 4.22. It should be noted that the boundary conditions now need to specify the twist parameter as well, in addition to the displacement and rotations. The strain energy for a simply supported plate subjected to a uniform load is shown in Table 4.24 for different mesh discretisations.

Anisoparametric Element, SS Plate, UDL		
# Elements	Deflection @ Centre	Theoretical Deflection
2	0.396591021	0.8873
4	0.830990882	
8	0.882934272	
16	0.887099406	

Table 4.23 Deflection at the centre of shear-flexible simply supported plate (uniform load) – Anisoparametric element

Aniso, SS Plate, UDL	
# Elements	Strain Energy
2	649.9243894
4	1386.235237
8	1479.054693
16	1486.947007

Table 4.24 Strain energy boundedness in a shear-flexible simply supported plate (uniform load) - Anisoparametric element

Fig. 4.29 shows the order of convergence for the case of simply supported plate subjected to uniform load. There is no benefit in the order of convergence due to the use of anisoparametric formulation, which was already explained in section 4.2.12. There is no degradation either due to the use of full integration.

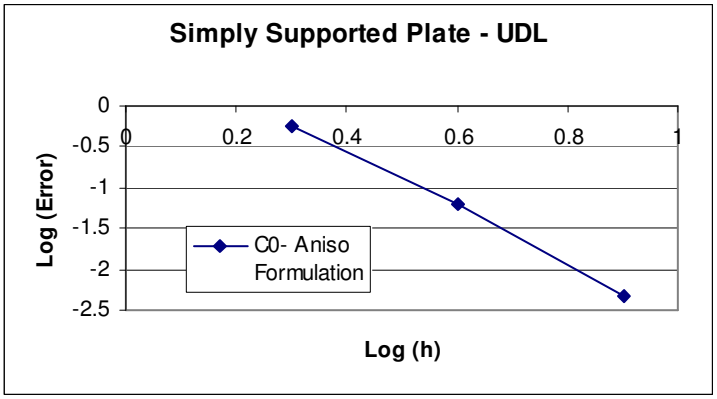

Fig. 4.29 Convergence of displacement in a shear-flexible simply supported plate for a uniform load – Anisoparametric FC element

4.6 Closure

In this chapter, a suite of shear-flexible finite elements (beam bending, plate bending, axisymmetric shell elements) was formulated and studied in detail. Extensive studies were carried out on anisoparametric elements, which have been used so far for overcoming shear locking. It has been conclusively shown

that anisoparametric formulation cannot overcome membrane locking, whereas field-consistency does. The results from the various formulations were used to explain the 3C concepts and the performance of the elements was assessed from energy error perspective for shear-flexible linear elastostatics problems. It has been shown that the strain energy boundedness and the best-fit rules are violated whenever the element formulation deviates from the 3C concepts. For the plate bending problems of shear-deformable plates, the reduced integration technique does not follow the best-fit rule. A novel 4-node conforming anisoparametric plate bending element has been developed and the results are very positive.

Since the 3C concepts and energy error concepts are derived from first principles, they should hold good for any example, and the examples presented here serve the purpose of demonstration cautioning against indiscriminate use of extra-variational tricks. The results of the studies done across various beam, plate and shell problems are summarized in Table 4.25. This table clearly shows what performance measure is affected for what deviation from the 3C concept. These studies are extended to other applications like linear elastodynamics and nonlinear elastostatics and the 3C concepts and energy errors are examined in the subsequent chapters.

Summary of Results for Linear Elastostatics for shear flexible beams,shells and plates					
Element Formulation	**C-Concept Deviation**	**Example Problem**	**Strain Energy Boundedness**	**Rate of Convergence**	**Best-fit Rule**
C^0 Iso - FI	Correctness, Consistency	Cantilever Beam	×	↓	×
		Circular Plate	×	↓	×
		Open Spherical Dome	×	↓	×
		Square Plate	×	↓	×
C^0 Iso - RI	Correctness, Correspondence	Cantilever Beam	✓	✓	×
		Circular Plate	✓	✓	×
		Open Spherical Dome	✓	✓	×
		Square Plate	✓	✓	×
C^0 Aniso - FI	Consistency	Cantilever Beam	✓	✓	✓
		Circular Plate	✓	✓	✓
		Open Spherical Dome	✓	↓	✓
		Square Plate	✓	✓	✓
C^0 Aniso - FC	None	Cantilever Beam	✓	✓	✓
		Circular Plate	✓	✓	✓
		Open Spherical Dome	✓	✓	✓
		Square Plate	✓	✓	✓

Table 4.25 3C concepts and performance of various shear-flexible element formulations

Note: ✓ implies that the performance is good/satisfies the respective attribute

× implies that it is a violation of the respective attribute

↓ implies that the performance of the respective attribute is degraded

Chapter-5

Nonlinear Elastostatics for Classical Beams, Shells and Plates

5.1 Introduction

In chapters three and four, the application of 3C concepts of correspondence, consistency and correctness to linear elastostatics to beams, axisymmetric shells and plates was studied. The consistency concepts were able to remove shear and membrane locking and stress oscillations. The correspondence concepts were able to predict the accuracy of stresses at what are now called Prathap points, Rajendran (2008). The correctness concept showed that the variationally correct formulations were all bounded and the extra-variational formulations like use of non-conforming elements, reduced integration were not necessarily bounded.

In this chapter, the problem of large deformation of beams, shells and plates taken up. This is of interest due to its practical applications in fields as diverse as robotic manipulators, composites, vibrations, piezo-electrics *etc*. Von Karman (1939) gave a review of nonlinear problems which are of practical interest and devotes a whole section to the nonlinear problems in the theory of elasticity due to large deflections. The large deformation problems are nonlinear in nature and require a good understanding of the kinematics of the deformation. The finite element method can be effectively used for the large deformation analysis of structures.

The applications of the stiffness matrix method to the large deflection problems started in late 1950s and early 1960s. Martin (1965) presented a detailed

account of the work done in this early period, and derived the initial stress stiffness matrix for a plate bending element.

Brebbia and Connor and (1969) used a nonconforming element for the large deflection analysis of a clamped plate and a clamped cylindrical panel. A mixed procedure - linearized equations for a limited number of load steps and then correction with Newton-Raphson method is employed. Mallett and Marcal (1968) laid out a framework for linear incremental method for the geometric nonlinear analysis, and derived the incremental matrices for typical elements. Rajasekaran and Murray (1974) brought out the restrictions on the incremental matrices, naming them as adequate, inadequate matrices and derive them for typical elements.

Wood and Zienkiewicz (1977) used a total Lagrangian formulation for the large deflection analysis of structures. A modified isoparametric element with reduced integration is used. Mattiason (1981) analysed the large deformation behavior of beam using the elliptic integral approach, and tabulated the results for various loads. Surana (1982) used a total Lagrangian formulation for axisymmetric shell elements in which the displacements are nonlinear functions of nodal rotations. Linear, parabolic and cubic isoparametric elements are used in the formulation.

Yuan and Liang (1989) presented an updated Lagrangian formulation for geometric nonlinear analysis of axisymmetric shell problems using a degenerated isoparametric shell element. The formulation also incorporated the corotational concepts. Narayanan and Krishnamoorthy (1990) used both updated and total Lagrangian formulation for the geometric nonlinear analysis of 3D beams. The incremental matrices of Rajasekaran and Murray (1974) are used in the formulation. Liu and Surana (1993) presented a geometric nonlinear formulation for the axisymmetric curved shell based on p-version elements. The element displacement field is made hierarchical and derived from Lagrangian family of interpolation functions. Little (1999) studied the large deflection

behaviour of thin, elastic plates expressing the lateral displacement as a series, each term of which involves the product of a sinusoidal term in the longitudinal direction, and a polynomial term in the transverse direction. Pai *et al.* (2000) presented a total-Lagrangian displacement-based finite-element formulation for general anisotropic beams undergoing large displacements and rotations. Zhang and Chueng (2003) used a refined non-conforming triangular plate/shell element for geometric non-linear analysis of plates/shells using the total Lagrangian/updated Lagrangian approach for geometric non-linear analysis.

The concept of co-rotational formulation has been successfully used in the large deformation problems, and is now covered in advanced books on finite element analysis, *e.g.* Crisfield (1991), Belytschko *et al.* (2000), Felippa (2005). Urthaler and Reddy (2005) used the co-rotational concept for the analysis of planar beams for both small and large deformations. Li (1997,1998) used an approach which is similar to the co-rotational formulation.

Geometrical nonlinear finite element formulations are prone to a mild form of membrane locking. The possibility of membrane locking in a geometrically nonlinear formulation as in the Von Karman moderately large deflection theory is less well known. The phenomenon of locking (in the form of delayed convergence and spurious stress oscillations) for linear formulations was discussed at length in chapters 2 and 4. However, there are very few studies on locking type behaviour in nonlinear problems. It is not unusual to consider these non-linear locking (where the inconsistency originates from the nonlinear displacement term in the membrane strain component) to be of the same provenance as membrane locking (where the inconsistency emerges from a linear term involving the curvature). So far no studies have been undertaken on the interpretation of the use of 3C concepts to the applications of such nonlinear problems. Most of the books on nonlinear analysis of structures, Palazotto and Dennis (1992), Sathyamoorthy (1997), do not cover the membrane locking.

Kikuchi and Aizawa (1982) were the first to demonstrate that in the finite element geometrically nonlinear formulation, a form of locking appears which could be removed by a technique called partial field description or by reduced integration. Yunhua (1998) and Laulusa and Reddy (2004) used consistency or reduced integration to resolve the locking issue in similar nonlinear problems. Reddy (2004) returned to this problem recently and used a “similarity” argument to rationalize the use of reduced integration on the non-linear strain displacement term so that lock-free solutions could be obtained for beam (Euler-Bernoulli and Timoshenko) and plate formulations. In these publications, the specific aspects of the membrane locking associated with large deformation problems was not dealt with. Zhu and Chen (1997) used a combination of one-order and two-order interpolation for displacement *w* instead of three-order interpolation, and overcome the membrane locking in the geometric nonlinear analyses of thin plates. Choi and Lee (2003) discussed the various assumed strain formulations that are used to alleviate the membrane locking in large deformation problems- and add the hierarchical non-conforming terms to the membrane component to make the nonlinear strain field consistent and thereby avoid locking. Reese *et al.* (2000) proposed a combination of reduced integration plus stabilization concept with the stabilization factors being computed on the basis of the enhanced strain method, to remove locking. Zhang and Cheung (2003) used a lower-order displacement function in the non-linear term in order to avoid membrane locking. Asta and Zona (2002) used two additional internal nodes for improving axial translations only to overcome the membrane locking of beam problems. Nanakorn and Vu (2006) used a similar technique by adding a degree of freedom at the center of the element to increase the order of the interpolation of the axial displacement.

In this chapter the field-consistency approach is used to explain membrane locking. First, the conventional approach for the geometrically nonlinear problems using the incremental matrices of Mallett and Marcal (1968), Rajasekaran and Murray (1974) is discussed for an Euler-Bernoulli beam. The simplest two-node

classical beam element (Euler-Bernoulli Formulation) is used to elucidate the principles involved. It is shown that reduced integration can produce an accurate element free of locking and stress oscillations. The use of reduced integration and partial field consistency is shown to alleviate the membrane locking. The field-consistency formulation for the large deflection analysis is laid out for an Euler-Bernoulli beam, axisymmetric shell and Kirchhoff plate. The concepts of field-consistency for membrane strain are brought out and the required matrices for the solution of the nonlinear analyses are formulated. Three carefully chosen beam problems are solved and the results of the field-consistent formulation and compared the results with other formulations. The field-consistent formulation for a Kirchhoff plates using the classical plate elements developed in chapter-3 is explained and the results of this formulation for plates with different boundary conditions (simply supported, clamped *etc*.) and loadings (uniform load, point load *etc*.) are discussed. For the case of Kirchhoff plate, the field-consistent formulation though in principle can be applied, the nature of the shape functions that need to be used for ensuring the C^1 continuity make the formulation complex. Since membrane locking is not expected in plates, there is no need for use of selective integration either. The conventional formulation is employed here and the results are discussed for plates with different boundary conditions (simply supported, clamped *etc*.) and loadings (uniform load, point load *etc*.).

5.2 Large Deformation Analyses of Euler-Bernoulli Beams

5.2.1 Strain-displacement relations

The strain-displacement relations for the geometrically nonlinear analysis of a long slender beam, from Euler-Bernoulli beam bending theory are as follows:

$$\varepsilon_x = \frac{du}{dx} + \frac{1}{2}\left(\frac{dw}{dx}\right)^2 \qquad \ldots(5.1)$$

and

$$\chi_x = \frac{d^2w}{dx^2} \qquad \ldots(5.2)$$

where ε_x is the membrane strain in the axial direction, and χ_x is the curvature.

5.2.2 Incremental Matrices

The strain energy when expressed in terms of the above strain-displacement relations takes the form, Mallett & Marcal (1968).

$$U = \int_V d^T \left[\frac{K}{2} + \frac{K^{N1}}{6} + \frac{K^{N2}}{12} \right] d \; dV \qquad \ldots(5.3)$$

where U is the strain energy, d is the displacement matrix, K is the linear stiffness matrix, K^{N1} and K^{N2} are nonlinear stiffness matrices, which are functions of the displacements.

The equilibrium equation for a given load increment can be expressed in the following form:

$$\left\{ [K] + \left[\frac{K^{N1}}{2} \right] + \left[\frac{K^{N2}}{3} \right] \right\} \{d\} = \lambda \{F\} \qquad \ldots(5.4)$$

where λ is the load increment for the force matrix F.

The above equation is a nonlinear equation which can be solved using Newton-Raphson iterative technique. The tangent stiffness matrix which is required for this purpose is given by

$$\left\{ [K] + \left[K^{N1} \right] + \left[K^{N2} \right] \right\} \{\Delta d\} = \Delta\lambda \{F\} \qquad \ldots(5.5)$$

and

$$[K^{N1}] = \int [B^N]^T [N^1][B^N] dx \qquad \ldots(5.6)$$

where

$$[N^1] = AE \begin{bmatrix} 0 & \frac{dw}{dx} \\ \frac{dw}{dx} & \frac{du}{dx} \end{bmatrix}$$

$$[B^N] = \begin{Bmatrix} \frac{du}{dx} \\ \frac{dw}{dx} \end{Bmatrix}$$

and

$$[K^{N2}] = \int [B^N]^T [N^2][B^N] dx \qquad \ldots(5.7)$$

where

$$[N^2] = AE \begin{bmatrix} 0 & 0 \\ 0 & 1.5\left(\frac{dw}{dx}\right)^2 \end{bmatrix}$$

The reduced integration technique involves using numerical integration with one Gaussian point for the evaluation of matrices K^{N1} and K^{N2}.

5.2.3 Preliminary Numerical Studies

In this section, the study will be restricted to examining how locking phenomenon can appear in the large deformation formulation of a simple beam element. The application of field-consistency to remove locking will be taken up in section 5.2.6.

The incremental matrices derived above are used for the large deformation analysis of beams with various boundary conditions. To start with, 2 special

cases of hinged-hinged beam and pinned-pinned beam are chosen. These 2 examples have recently been examined in detail by Reddy (2004). For a clear understanding of the nonlinear response of the beam at an element level, it would be good to discretise the beam in to 2 elements.

A uniform beam of length L = 100 units, cross section dimensions of 1 x 1 units, made of a material with E = 30 x 10^6 units that is simply supported at both ends subjected to a uniformly distributed load of intensity q per unit length (Reddy 2004) is considered. The units are consistently chosen, so that the exact deflection at the middle of the beam in linear bending theory is 0.5208, when q = 1. In linear bending theory, where the beam is assumed to undergo pure bending (*i.e.* there is no axial deformation), it is immaterial to consider whether the beam is allowed free movement in the axial direction (*i.e.* u) at the supported ends, Fig. 5.1. However, in non-linear bending, this is a crucial distinction. Hence the case where there is no axial restraint at both ends is designated by the hinged-hinged (HH) condition, and where there is full restraint by the pinned-pinned (PP) condition. In the former case, it is inextensional bending, which is largely of a linear nature, and in the latter case, it is bending with extension. Both of these cases are modeled with two versions of the EB element. The first version which will have locking uses 2 point integration for bending energy and extensional energy (this is referred as the EB2x2 element) while the second version which will be lock free according to our foregoing analysis will use 2 point integration for bending energy but only 1 point integration for the extensional energy (the EB2x1 element). Using symmetry, half of the beam is modeled with equal length elements (Reddy 2004).

The HH case is ideal to test the consistency aspect of the problem. As a nonlinear beam element formulation is being used, a correct model should be able to recover the purely linear bending response under increasing load. This is possible only if the element can ensure that the inextensional axial condition (*i.e.* as there is no axial restraint at both ends, no axial force should develop) is

consistently recovered throughout. Table 5.1 shows the deflection under the load as q increases from 1 to 10, when half of the beam is modeled with four equal length elements. Results from Reddy (2004) are also shown. It is clear that the EB2x1 model is able to capture the linear behaviour exactly but the EB2x2 model shows an additional stiffening due to the inability of the model to capture the zero axial force consistently.

5.2.4 Reduced Integration Formulation

This is a clear indication that the EB2x2 model is unable to recover the zero axial force condition consistently due to the presence of the inconsistent terms described in section 2.3.3 by eqn. 2.21. Fig. 5.2 now shows the variation of axial force for the same problem when 2 EB2x2 elements are used. The sampling strategy must now be carefully interpreted. Using the original strain-displacement functions (eqn. 5.1) would show a complex quartic oscillation of the axial force. Fig. 5.3 shows the variation of axial force for $q = 1$ when half of the the HH beam is modeled with 2 EB2x1 elements. It is seen that when the axial force is sampled at the Gauss point, it predicts the exact zero value expected accurately. Also shown for effect is the variation in axial force when the displacements are used directly in the nonlinear membrane strain (eqn. 5.1) showing the complex quartic variation. It is this variation that accounts for the additional stiffening effect seen if a 2x2 integration strategy is used. As a 2 pt. integration rule has been used for the evaluation of the extensional energy, the first level of filtering is shown in Fig. 5.3 by sampling the stresses at the Gauss points corresponding to the 2 pt. rule and then extrapolating linearly (EL-1, EL-2). A very curious result emerges. It is seen that filtering this stress further by sampling this linear variation at the centroid will produce the correct axial force. The constant term is consistently recovered and only this should be used in the evaluation of the stiffness matrix. A higher order rule will introduce spurious energies that cause the additional stiffening. It will be shown in later sections that the field-consistency argument does exactly this.

Fig. 5.1 A hinged-hinged beam

(E=3000000 N/mm^2, L = 100 mm, D= 1 mm, B = 1 mm)

q	Present		Reddy (2004)	
	2x2	2x1	2x2	2x1
1	0.5108	0.5208	0.5108	0.5208
2	0.9738	1.0417	0.9739	1.0417
3	1.3764	1.5625	1.3764	1.5625
4	1.7265	2.0833	1.7265	2.0833
5	2.0351	2.6042	2.0351	2.6042
6	2.3115	3.1250	2.3116	3.1250
7	2.5624	3.6458	2.5630	3.6458
8	2.7926	4.1667	2.7930	4.1667
9	3.0060	4.6875	3.0060	4.6875
10	3.2051	5.2083	3.2051	5.2083

Table 5.1. Deflection at centre of a hinged-hinged beam (uniform load) – Large deflection analysis

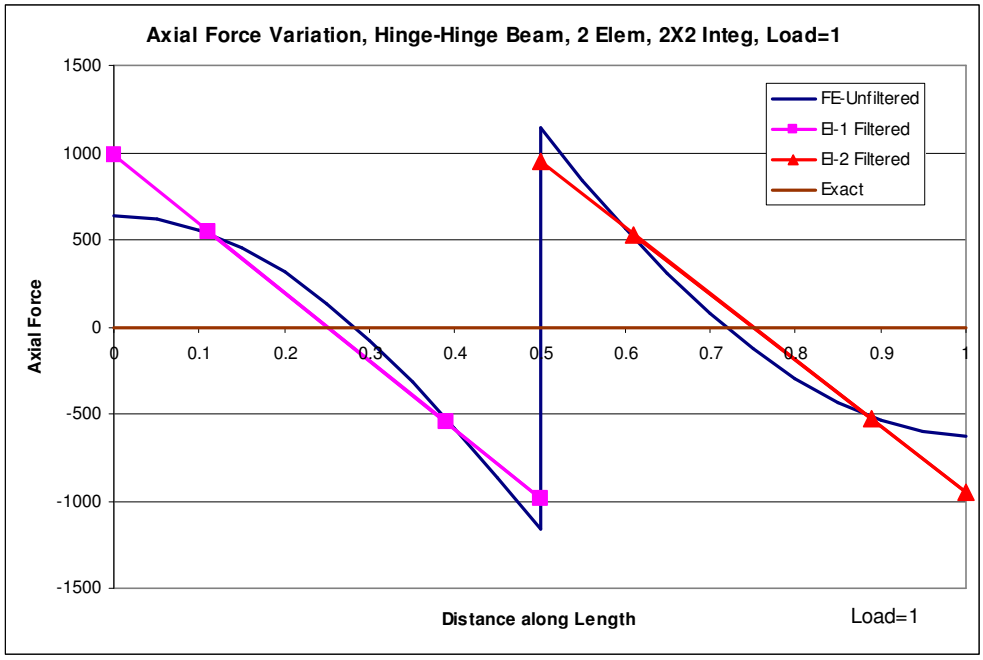

Fig. 5.2 Axial force in a hinged-hinged beam (uniform load) – Large deflection analysis, Full Integration

Fig. 5.3 Axial force in a hinged-hinged beam (uniform load) – Large deflection analysis, Reduced Integration

Figures 5.4 and 5.5 show the bending moment predictions from EB2x2 and EB2x1 models of the hinged-hinged Beam with $q = 1$. It is seen that the EB2x1 model of the problem, even though it incorporates the geometrical non-linearity due to moderately large deformation, produces predictions for the bending moment variation for each element which is exactly a best-fit of the analytically exact solution (this can be proved using the process explained in 2.3.3). This implies that there are only local errors and no global errors (pollution errors). This is true even as the load increases (computations were done up to $q = 10$). Thus, the EB2x1 element is variationally correct in the sense of the projection theorem of Strang and Fix (1973).

These exercises are now repeated for the pinned-pinned (PP) condition. The PP case is ideal to examine the significance of the consistency aspect of the

problem where the nonlinear action becomes important. The use of the nonlinear beam element formulation should now recover a nonlinear bending response under increasing load. The geometry of the beam, the material properties and the boundary conditions are shown in Fig. 5.6. Table 5.2 shows the deflection under the load as *q* increases from 1 to 10, when half of the beam is modeled with four equal length elements. Results from Reddy (2004) are also shown. It is clear that the EB2x1 model is able to capture the nonlinear behaviour exactly (consider Reddy (2004) as the benchmark for this problem) but the EB2x2 model now shows only a hardly noticeable additional stiffening. This is because the inconsistent forces excited contribute negligible energy compared to the primary axial force generated due to the immovable ends.

Fig. 5.5 shows the variation of axial force for the same problem when 2 EB2x2 elements are used. The variation over the element shows how field-inconsistency excites spurious oscillations. Note that now the element does not sample the correct stress at the centroid, nor does the filtering strategy (level 1 corresponding to removal of the linear and quadratic oscillations) give the correct stress. This is indicative of the small error seen in the deflections in Table 5 2. Figures 5.7 and 5.8 shows how the axial force predictions vary as load *q* increases for EB2x2 and EB2x1. For comparison is shown a solution using 1000 elements from ANSYS® (2008) is assumed as the exact solution. It is seen that EB2x1 gives very nearly the exact answer while EB2x2 gives answers (after filtering) which are reasonably close. The variation of the bending moment along the length of the beam is shown in Fig. 5.9 for EB2x2, and in Fig. 5.10 for EB2x1. For the HH case, it was seen earlier that the bending moment variation for each element was exactly a best-fit of the analytically exact solution However, this is no longer true in the presence of locking (EB2x2 element) and the best-fit rule is violated. There are now global errors (Prathap and Mukherjee 2004) seen as the jump in the bending stress from the best-fit value with each element and across element nodes.

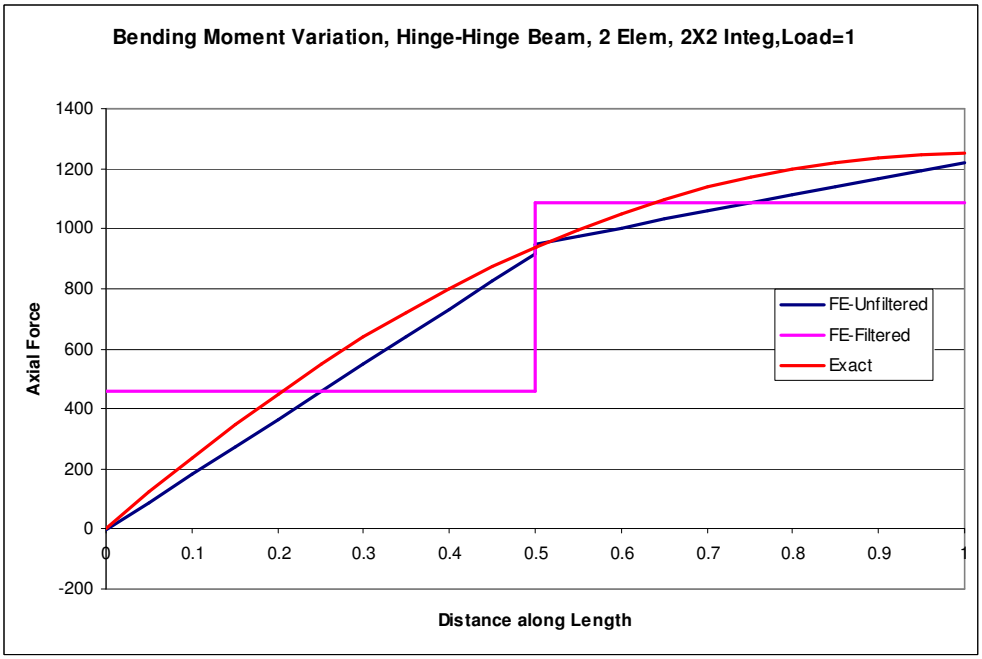

Fig. 5.4 Bending moment in a hinged-hinged beam (uniform load) – Large deflection analysis, Full Integration

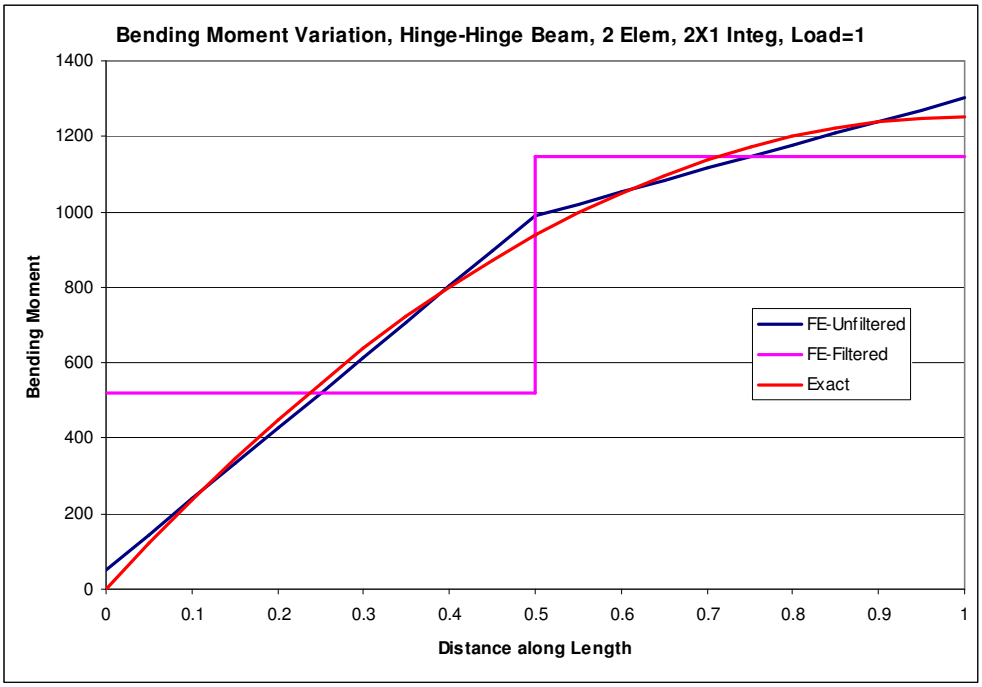

Fig. 5.5 Bending moment in a hinged-hinged beam (uniform load) – Large deflection analysis, Reduced Integration

Fig. 5.6 A pinned-pinned beam

q	Present		Reddy (2004)	
	2x2	2x1	2x2	2x1
1	0.3668	0.3687	0.3669	0.3687
2	0.5424	0.5466	0.5424	0.5466
3	0.6601	0.6663	0.6601	0.6663
4	0.7510	0.7591	0.7510	0.7591
5	0.8263	0.8361	0.8263	0.8361
6	0.8912	0.9027	0.8912	0.9027
7	0.9485	0.9617	0.9485	0.9617
8	1.0002	1.0150	1.0002	1.0150
9	1.0473	1.0638	1.0473	1.0638
10	1.0908	1.1089	1.0908	1.1089

Table 5.2 Deflection at centre of a pinned-pinned beam (uniform load) – Large deflection analysis

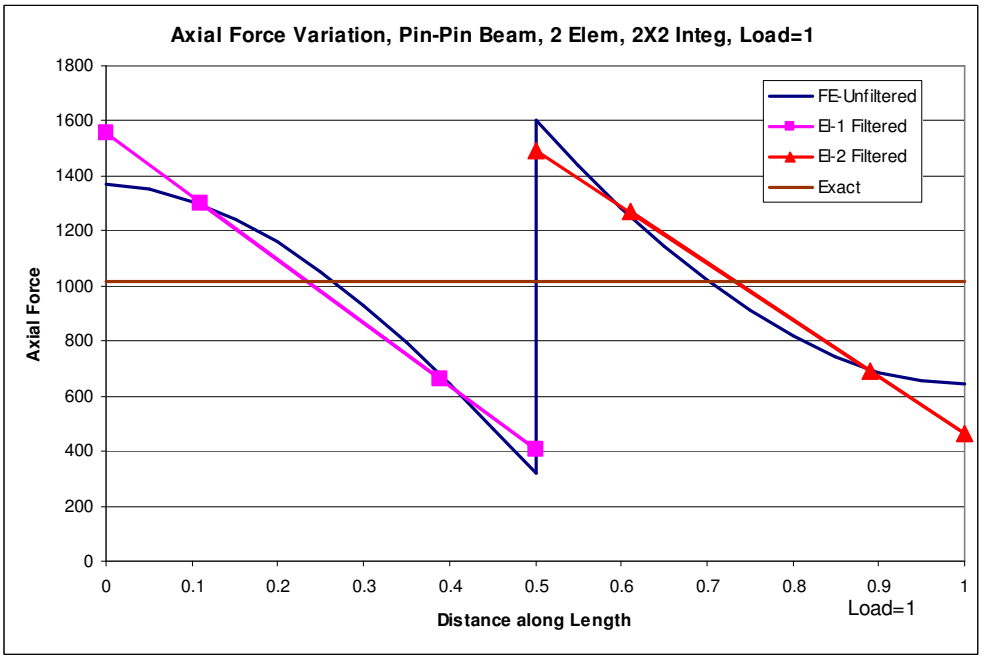

Fig. 5.7 Axial force in a pinned-pinned beam (uniform load) – Large deflection analysis, Full Integration

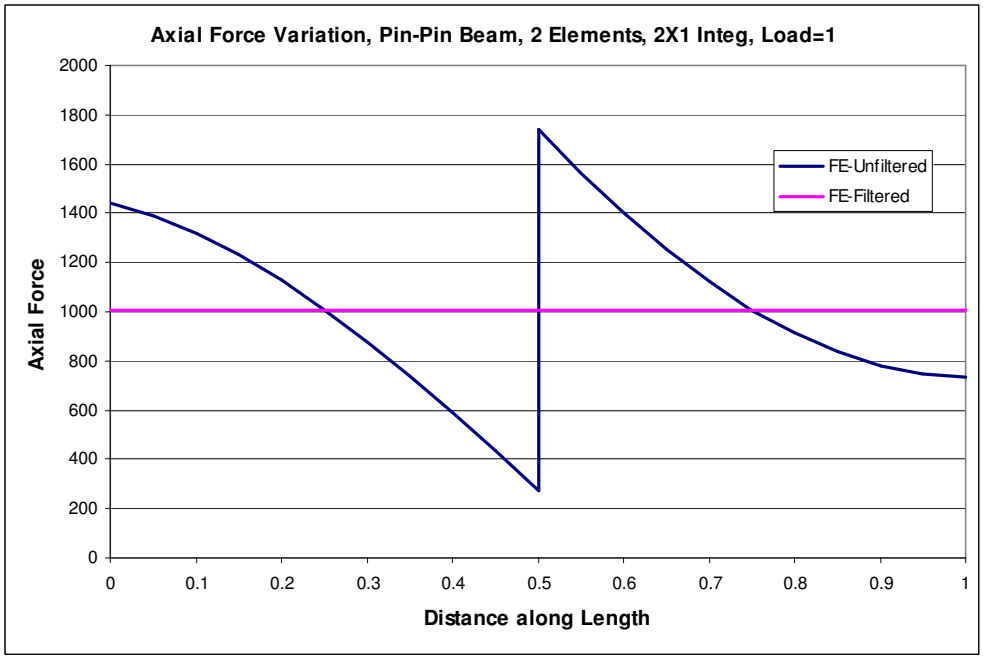

Fig. 5.8 Axial force in a pinned-pinned beam (uniform load) – Large deflection analysis, Reduced Integration

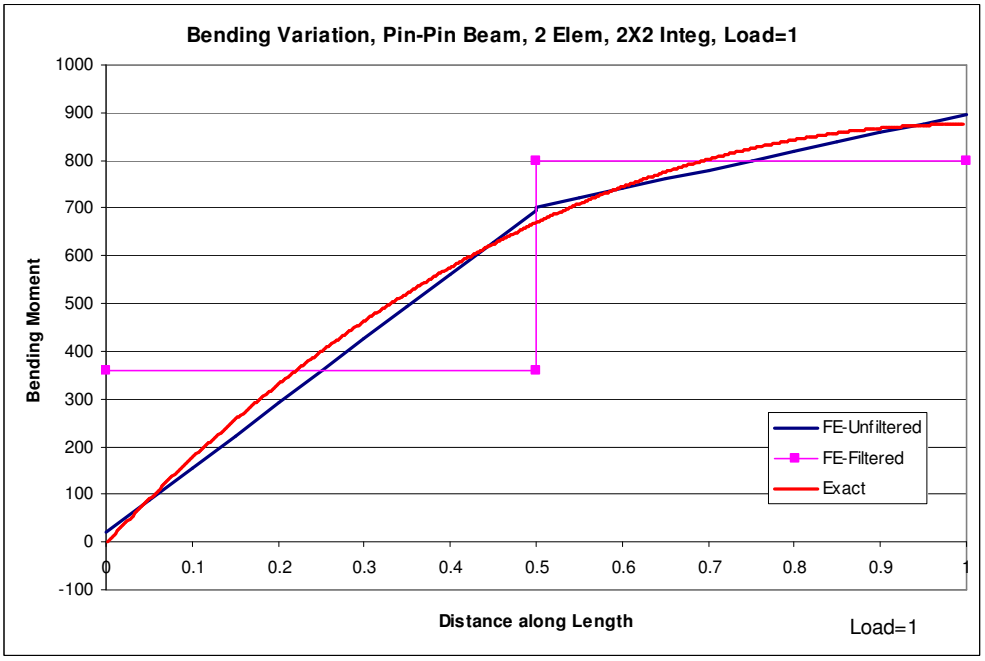

Fig. 5.9 Bending moment in a pinned-pinned beam (uniform load) – Large deflection analysis, Full Integration

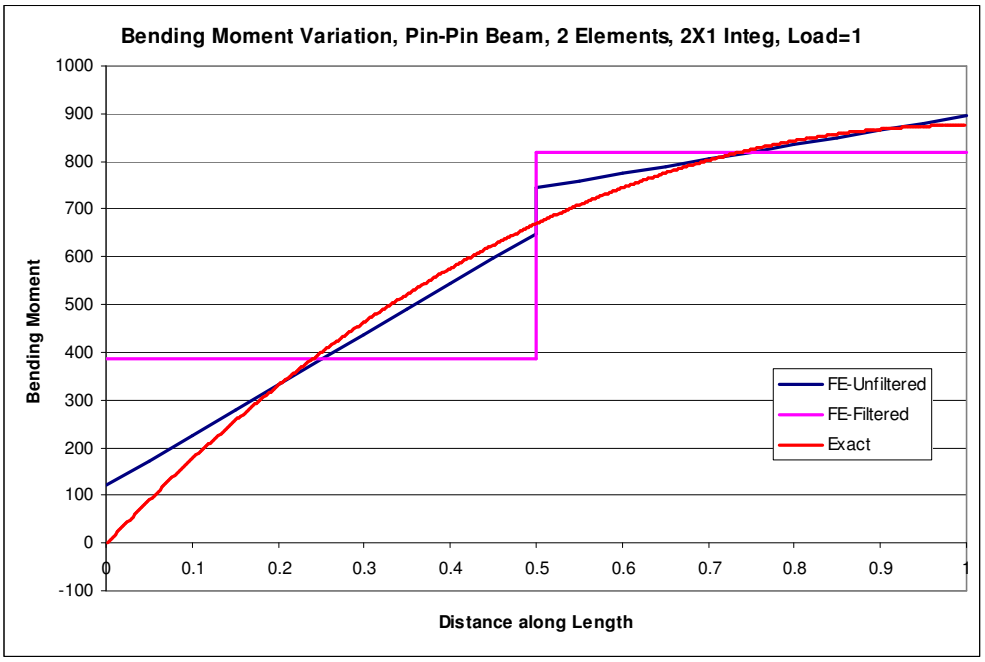

Fig. 5.10 Bending moment in a pinned-pinned beam (uniform load) – Large deflection analysis, Reduced Integration

For the pinned-pinned case, the exact solution is not known. Though various solutions exist, they are all approximate and even a highly refined finite element solution from a commercial finite element software does have some small errors. This is the best that can be used for studying the best-fit rule for this case and it is seen that it is not exactly zero, but very close to zero with the errors due to the non-availability of the exact solution.

Both of the above examples show the impact of the integration-points on the results, and the hinged-hinged beam brought out how a spurious axial force is produced due to incorrect use of the integration-points. This phenomena is called membrane locking, and is significant for large deformation problems. The examples shown above have now laid a case for a requirement of understanding of the phenomena of membrane locking during the element formulation level itself, and in the next sections 2 element formulations are described that explain the membrane locking and the solutions for eliminating the same, using the field-

consistency concepts. Muralikrishna and Prathap (2006) report a detailed study on this.

5.2.5 Partial Field-Consistent Formulation

In this formulation, $w_{,x}$ is assumed to be constant and is represented by eqn. (5.8). This approach was followed by Kikuchi and Aizawa (1982).

$$w_{,x} = \frac{1}{2}(w_2 - w_1) \qquad \ldots(5.8)$$

This is very easy to implement in the algorithm for the nonlinear solution through the incremental matrices approach of Mallett and Marcal (1968).

5.2.6 Full Field-Consistent Formulation

The field-consistent concept of element formulation of Prathap (1984) is extended to the case of membrane strain energy. For the case of the large deformation, the process of the field-consistent representation of the membrane strain is similar. The strain term that is now being focused is the membrane strain ε_x, which has the multiple "fields". From eqn. (5.1), the membrane strain is

$$\varepsilon_x = \frac{du}{dx} + \frac{1}{2}\left(\frac{dw}{dx}\right)^2 \qquad \ldots(5.9)$$

and

$$\begin{aligned} u &= a_0 + a_1\xi \\ \theta &= c_0 + c_1\xi \\ \frac{dw}{dx} &= b_0 + b_1\xi + b_2\xi^2 \end{aligned} \qquad \ldots(5.10)$$

where

$$b_0 = \frac{3}{4l}(w_2 - w_1) - (\theta_2 + \theta_1)$$
$$b_1 = \frac{1}{2}(\theta_2 - \theta_1) \qquad \ldots(5.11)$$
$$b_2 = \frac{3}{4l}(w_1 - w_2) + \frac{3}{4}(\theta_2 + \theta_1)$$

Using the concepts of field-consistency outlined in section 2.3.3, the field-consistent membrane strain is

$$\varepsilon_x = a_1 + \left[\frac{1}{2}b_0^{\,2} + \frac{1}{6}b_1^{\,2} + \frac{1}{10}b_2^{\,2} + \frac{1}{3}b_0 b_2\right] \qquad \ldots(5.12)$$

This expression is now used for computing the membrane strain energy, which now includes both linear and nonlinear deformations. The strain energy now involves nonlinear terms, and the solution of the equations requires the secant stiffness and tangent stiffness matrices in addition to the linear stiffness matrix that was derived earlier. The secant stiffness matrix is derived from

$$\delta U = 0 \qquad \ldots(5.13)$$

where U has the nonlinear terms as well. This leads to the following equations

$$[D_s]\{\delta q_s\} = 0$$

$$q_s = \begin{Bmatrix} a_1 \\ b_0 \\ b_1 \\ b_2 \end{Bmatrix} \qquad \ldots(5.14)$$

The matrix $\{q_s\}$ can be expressed in terms of the nodal displacements as

$$\{q_s\} = [B_s]\{d\} \qquad \ldots(5.15)$$

where

$$[B_s] = \begin{bmatrix} -\frac{1}{2} & 0 & 0 & \frac{1}{2} & 0 & 0 \\ 0 & -\frac{3}{4l} & -\frac{1}{4} & 0 & \frac{3}{4l} & \frac{1}{4} \\ 0 & 0 & -\frac{1}{2} & 0 & 0 & \frac{1}{2} \\ 0 & \frac{3}{4l} & \frac{3}{4} & 0 & -\frac{3}{4l} & \frac{3}{4} \end{bmatrix}$$

and

$$\{d\} = \begin{Bmatrix} u_1 \\ w_1 \\ \theta_1 \\ u_2 \\ w_2 \\ \theta_2 \end{Bmatrix}$$

The secant stiffness matrix is

$$K_s = [B_s]^T [D_s][B_s] \qquad \ldots(5.16)$$

$$[D_s] = EAl \begin{bmatrix} 2 & b_0 + \frac{b_2}{3} & \frac{b_1}{3} & \frac{b_2}{5} + \frac{b_0}{3} \\ b_0 + \frac{b_2}{3} & a_1 + g_0 & 0 & \frac{1}{3}(a_1 + g_0) \\ \frac{b_1}{3} & 0 & \frac{1}{3}(a_1 + g_0) & 0 \\ \frac{b_2}{5} + \frac{b_0}{3} & \frac{1}{3}(a_1 + g_0) & 0 & \frac{1}{5}(a_1 + g_0) \end{bmatrix}$$

where

$$g_0 = b_0^{\,2} + \frac{b_1^{\,2}}{3} + \frac{b_2^{\,2}}{5} + \frac{2}{3} b_0 b_2$$

The tangent stiffness matrix is derived on similar lines, using

$$\delta^2 U = 0 \qquad \ldots(5.17)$$

which gives the tangent stiffness matrix as

$$K_T = [B_s]^T [D_T] [B_s] \qquad \ldots(5.18)$$

where

$$[D_T] = AEl \begin{bmatrix} 2 & 2x_1 & 2x_2 & 2x_3 \\ 2x_1 & 2x_1^{\,2} + 2a_1 + g_0 & 2x_1 x_2 & 2x_1 x_3 + \frac{1}{3}(2a_1 + g_0) \\ 2x_2 & 2x_1 x_2 & 2x_2^{\,2} + \frac{1}{3}(2a_1 + g_0) & 2x_2 x_3 \\ 2x_3 & 2x_1 x_3 + \frac{1}{3}(2a_1 + g_0) & 2x_2 x_3 & 2x_3^{\,2} + \frac{1}{5}(2a_1 + g_0) \end{bmatrix}$$

and

$$x_1 = b_0 + \frac{1}{3} b_2$$

$$x_2 = \frac{1}{3} b_1$$

$$x_3 = \frac{1}{5} b_2 + \frac{1}{3} b_0$$

The above formulations are now used for studying the large deformation behaviour of a hinged-hinged beam, pinned-pinned beam and clamped-clamped beam. In addition to the comparison of deflections, axial forces and bending moments, the rates of convergence and strain-energy boundedness are also discussed.

5.2.6 Numerical Experiments and Discussion

Table 5.3 augments the results of Table 5.1 for the various formulations where locking is removed. The KA element is based in partial approximation of the displacement $w_{,x}$. The FC element is based on application of the field-consistency concept (Note that in section 5.2.2, a reduced integration approach was used). The ANSYS® (2008) results are based on a 1000 element discretisation (BEAM3 element is used). JNR elements are based on reduced integration, Reddy (2004). It can be seen that in this linear problem (nonlinearity is not induced as there are no membrane forces due to hinged-hinged condition), the KA, FC and JNR formulations capture the linearity of the problem (deflections for load=10 are exactly 10 times the deflection for load=1). This is confirmed by the axial force shown in Table 5.4.

Hinged-Hinged Beam								
Load	Max. Vertical Deflection at Centre				Max. Axial Displacement			
	KA	FC	ANSYS	JNR	KA	FC	ANSYS	JNR
1	0.520833	0.520833	0.520692	0.520833	0.003330	0.003373	0.003370	0.003373
2	1.041667	1.041667	1.040545	1.041667	0.013319	0.013491	0.013461	0.013491
3	1.562500	1.562500	1.558739	1.562500	0.029969	0.030355	0.030213	0.030355
4	2.083333	2.083333	2.074449	2.083333	0.053277	0.053965	0.053531	0.053965
5	2.604167	2.604167	2.587074	2.604167	0.083246	0.084320	0.083286	0.084320
6	3.125000	3.125000	3.095785	3.125000	0.119874	0.121420	0.119317	0.121421
7	3.645833	3.645833	3.599968	3.645833	0.163162	0.165267	0.161436	0.165268
8	4.166667	4.166667	4.099017	4.166667	0.213109	0.215859	0.209430	0.215860
9	4.687500	4.687500	4.592349	4.687500	0.269717	0.273196	0.263062	0.273197
10	5.208333	5.208333	5.079442	5.208333	0.332983	0.337279	0.322078	0.337281

Table 5.3 Comparison of deflection at the center of a hinged-hinged beam (uniform load) – Large deflection analysis

Hinged-Hinged Beam								
Load	Max. Bending Moment at Centre				Max. Axial Force			
	KA	FC	ANSYS	JNR	KA	FC	ANSYS	JNR
1	-1263.0	-1263.0	-1250.0	-1263.0	0	0	0.8	Zero @ centre of each element
2	-2526.0	-2526.0	-2498.0	-2526.0	0	0	3.3	
3	-3789.1	-3789.1	-3742.0	-3789.1	0	0	7.5	
4	-5052.1	-5052.1	-4981.0	-5052.1	0	0	13.3	
5	-6315.1	-6315.1	-6213.0	-6315.1	0	0	20.7	
6	-7578.1	-7578.1	-7437.0	-7578.1	0	0	29.7	
7	-8841.2	-8841.2	-8651.0	-8841.2	0	0	40.2	
8	-10104.2	-10104.2	-9854.0	-10104.2	0	0	52.4	
9	-11367.2	-11367.2	-11045.0	-11367.2	0	0	66.0	
10	-12630.2	-12630.2	-12222.0	-12630.2	0	0	81.0	

Table 5.4 Comparison of maximum forces in a hinged-hinged beam (uniform load) – Large deflection analysis

Table 5.5 and 5.6 give the deflection and results for a pinned-pinned beam. Here there is a significant amount of nonlinearity. The FC (with 128 elements) and ANSYS® (2008) results (with 1000 elements) are closest to each other, both at displacement and force levels. This is also seen in Fig. 5.11 and 5.12 where the force distribution obtained from various formulations are compared. The Von Karman theory of moderately large deformation predicts constant axial force throughout the length of the element. This is captured only by the FC/KA/RI formulations (Fig. 5.12). This is also seen for the clamped-clamped case in Fig. 5.13 – the FC/KA/RI formulations give a constant axial force throughout the length of the element.

Pinned-Pinned Beam								
Load	Max. Vertical Deflection at Centre				Max. Axial Displacement			
	KA	FC	ANSYS	JNR	KA	FC	ANSYS	JNR
1	0.370203	0.368466	0.368467	0.368733	0.000567	0.000556	0.000556	0.000569
2	0.548789	0.545390	0.545397	0.546556	0.001261	0.001232	0.001233	0.001261
3	0.668467	0.663943	0.663958	0.666265	0.001887	0.001842	0.001844	0.001885
4	0.760865	0.755490	0.755514	0.759090	0.002464	0.002403	0.002407	0.002459
5	0.837257	0.831194	0.831228	0.836144	0.003003	0.002928	0.002934	0.002995
6	0.902999	0.896358	0.896402	0.902705	0.003513	0.003425	0.003433	0.003503
7	0.961082	0.953941	0.953996	0.961718	0.004000	0.003899	0.003909	0.003987
8	1.013357	1.005776	1.006000	1.015008	0.004468	0.004354	0.004367	0.004452
9	1.061057	1.053081	1.053000	1.063788	0.004919	0.004793	0.004809	0.004900
10	1.105046	1.096712	1.097000	1.108910	0.005356	0.005218	0.005237	0.005334

Table 5.5 Comparison of deflection at the center of a pinned-pinned beam (uniform load) Large deflection analysis

Pinned-Pinned Beam								
Load	Max. Bending Moment at Centre				Max. Axial Force			
	KA	FC	ANSYS	JNR	KA	FC	ANSYS	JNR
1	-888.3	-884.2	-875.8	-880.3	1012.2	1015.7	1015.7	1014.4
2	-1301.5	-1293.9	-1282.6	-1282.0	2231.3	2232.1	2232.1	2228.5
3	-1570.3	-1560.7	-1548.0	-1539.8	3319.2	3316.4	3317.0	3310.5
4	-1773.1	-1762.3	-1749.0	-1732.0	4309.6	4303.2	4303.3	4295.2
5	-1937.6	-1926.0	-1912.0	-1886.3	5228.5	5218.5	5219.0	5208.5
6	-2076.9	-2064.9	-2051.0	-2015.7	6092.2	6078.9	6080.0	6066.9
7	-2198.4	-2186.2	-2172.0	-2127.3	6911.8	6895.2	6896.0	6881.4
8	-2306.5	-2294.2	-2280.5	-2225.7	7694.9	7675.2	7675.6	7659.7
9	-2404.1	-2392.0	-2378.0	-2313.7	8447.3	8424.5	8425.0	8407.3
10	-2493.4	-2481.4	-2468.0	-2393.4	9173.2	9147.5	9149.0	9128.7

Table 5.6 Comparison of maximum forces in a pinned-pinned beam (uniform load) Large deflection analysis

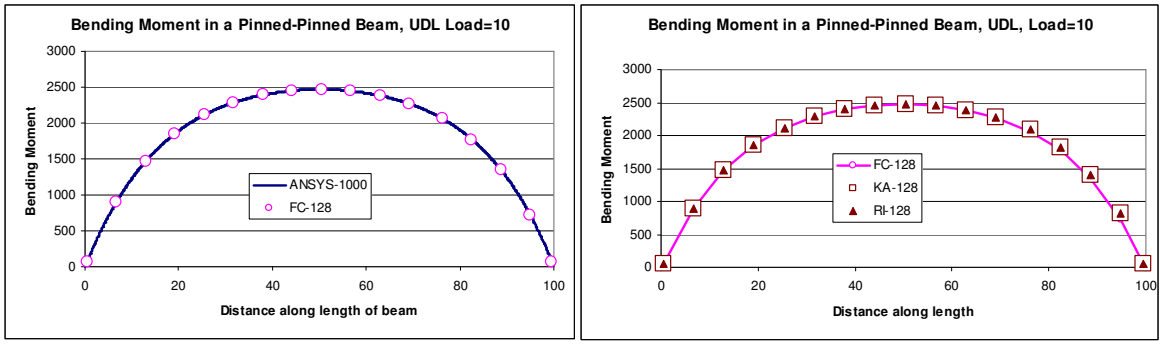

Fig. 5.11 Bending moment in a pinned-pinned beam (uniform load), Large deflection analysis – Comparison of various formulations

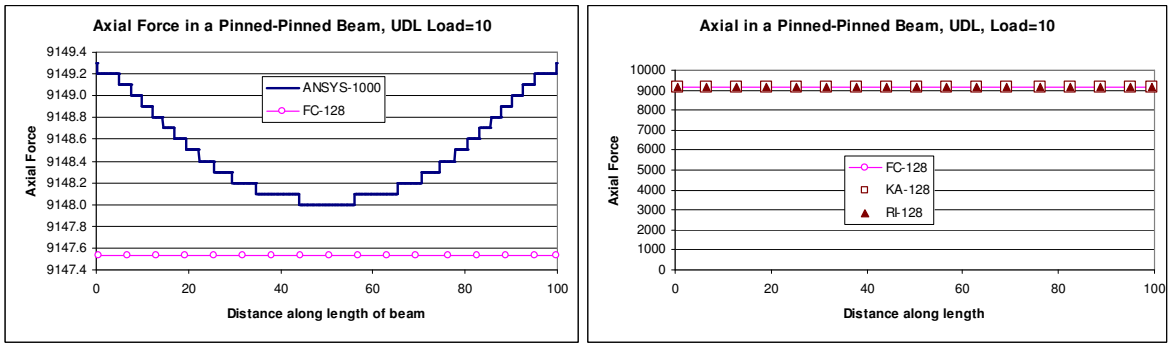

Fig. 5.12 Axial force in a pinned-pinned beam (uniform load), Large deflection analysis – Comparison of various formulations

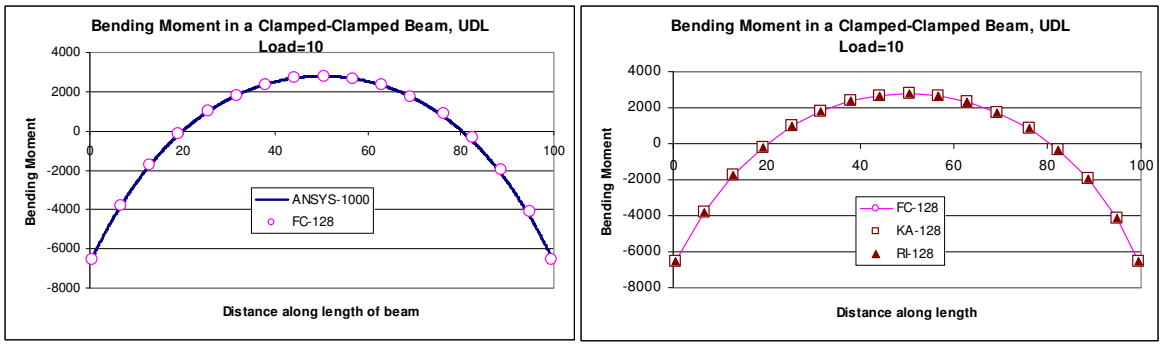

Fig. 5.13 Bending moment in a clamped-clamped beam (uniform load), Large deflection analysis – Comparison of various formulations

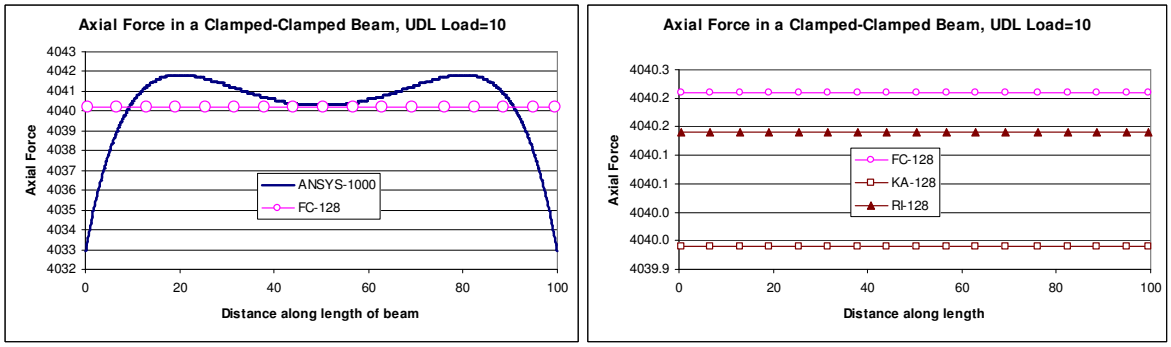

Fig. 5.14 Axial force in a clamped-clamped beam (uniform load), Large deflection analysis – Comparison of various formulations

The behaviour of the rate of convergence of the deflections for the above cases is discussed now. It is pertinent to note that the total deflection is the sum of two parts, one coming due to the linear portion, and the other due to the nonlinear portion, as shown in Fig. 5.15. The load-deflection line shown in blue colour in Fig. 5.15 is due to the linear behaviour of the beam due to small deflection theory. The load-deflection line shown in magenta colour is the total deflection at the centre of the beam from large deflection theory. The difference in the deflection of the beam for a give load due to small deflection and large deflection theory is due to the stress stiffening of the beam (due to the axial forces that are generated from the nonlinear axial strains). The total deflection of the beam needs to be separated out into linear and nonlinear portions, as the behaviour of the convergence for these two portions could be different. This fact is often confounded in most of the current error norms that are used in the adaptive mesh

refinement strategies, *e.g.* Lee and Bathe (1994), Hernandez *et al.* (1999, 2003), Izzuddin *et al.* (2004). More on this would be discussed in the succeeding sections of this chapter and the next chapter.

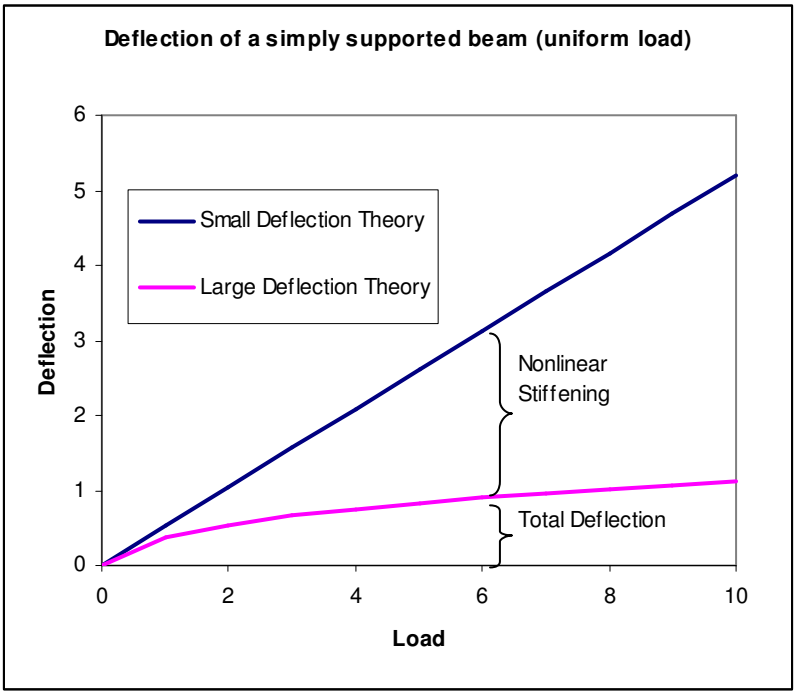

Fig. 5.15 Linear and nonlinear deflections in a simply supported beam (uniform load)

For the field-consistent formulation for the hinged-hinged case where there is no nonlinearity, the rate of convergence is the same as that of the linear deformation.

It is possible to establish the rate of convergence *a priori*, as follows. The displacement field for a general 1-D problem can be represented as

$$u = a_0 + a_1 x + a_2 x^2 + ... + a_n x^n + O(h^{n+1}) \qquad \ldots(5.19)$$

The discretised field is represented by element size h, and there are n elements, ($n+1$ nodes).

The strain field is now represented by

$$\varepsilon = \frac{du}{dx} = a_1 + 2a_2x + ... + na_nx^{n-1} + O(h^n) \quad \ldots(5.20)$$

The strain-energy for this case is given by

$$U = \frac{1}{2}\int \sigma\, \varepsilon\, dv = \frac{1}{2}E\int \varepsilon^2 dv \quad \ldots(5.21)$$

$$\varepsilon^2 = a_1^{\,2} + 4a_2^{\,2}x^2 + ... + n^2a_n^{\,2}x^{2(n-1)} + O(h^{2n}) \quad \ldots(5.22)$$

Thus the order of convergence of the energy (and the displacement) is $O(h^{2n})$. For a 2-noded element where u is represented by a first-order polynomial, this comes out to be $O(h^2)$ for membrane displacement. As with EB element where cubic functions are used for w, and the bending strain terms ($w_{,xx}$) are of linear order, the accuracy of w should be $O(h^4)$. In Fig. 5.16 – 5.18, it can be seen that only the FC formulation gives the ideal performance of $O(h^4)$. It can also be noticed notice that all three formulations, FC/RI/KA give positive E^+, implying that the convergence is from above. This becomes clear when the strain energy boundedness of the various formulations is studied in the next sections.

The error is defined as follows:

$$E^+ = \frac{w_{exact} - w_{fem}}{w_{exact}} \quad \ldots(5.23)$$

where

E^+ is the error in the deflections, with the + sign indicates that the finite element solution is converging from above (lower bound).

w_{exact} is the exact solution

w_{fem} is the solution from the finite element analysis

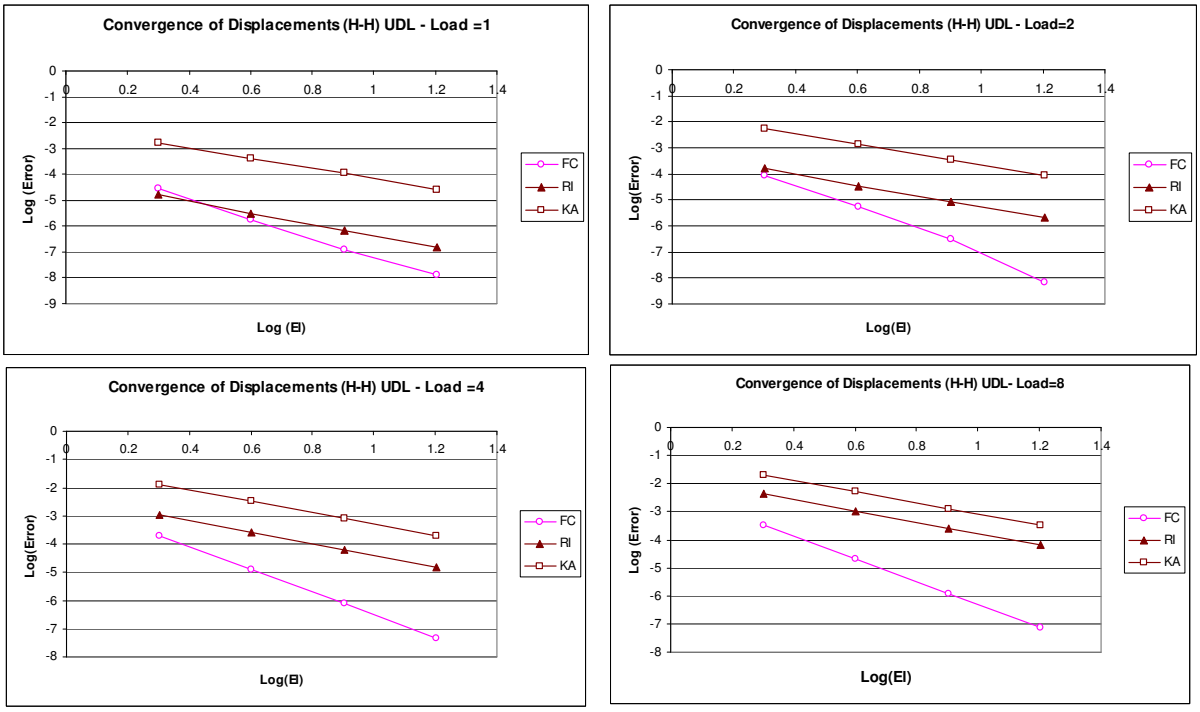

Fig. 5.16 Convergence of displacement in a hinged-hinged beam (uniform load), Large deflection analysis - Comparison of various formulations

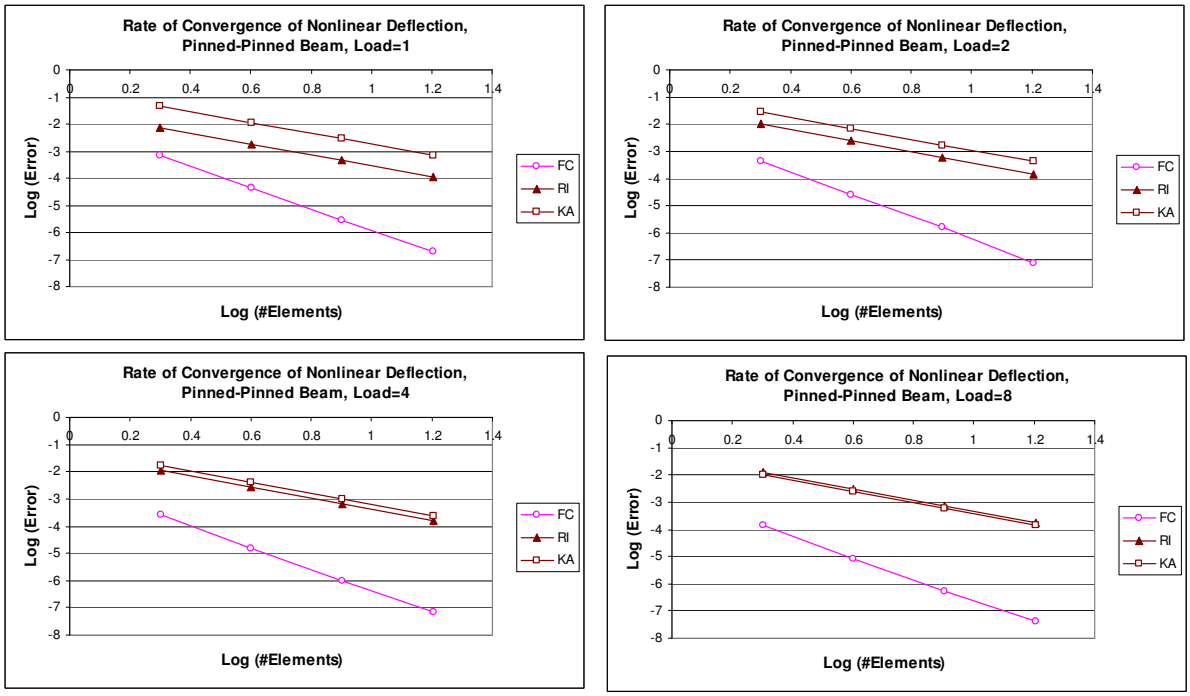

Fig. 5.17 Convergence of displacement in a pinned-pinned beam (uniform load), Large deflection analysis - Comparison of various formulations

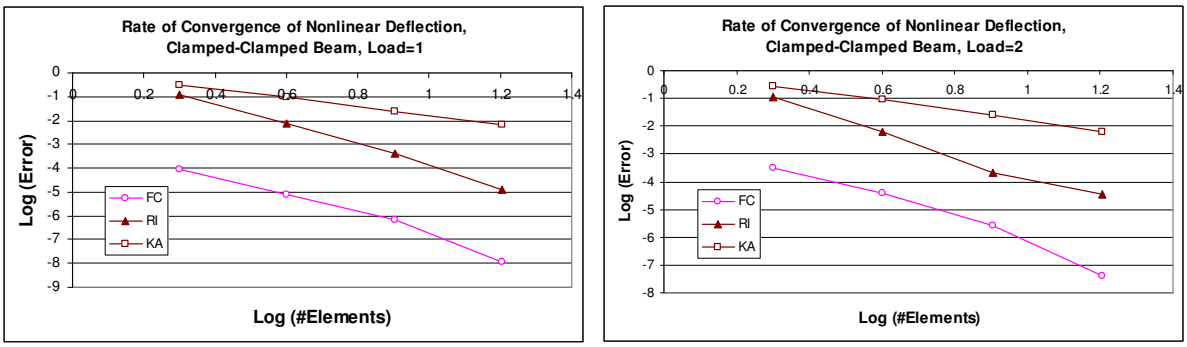

Fig. 5.18 Convergence of displacement in a clamped-clamped beam (uniform load), Large deflection analysis - Comparison of various formulations

It can be clearly seen from Fig. 5.16 – 5.18 that the field-consistent formulation gives higher rate of convergence than the reduced integration or the partial field-consistent formulation.

For the hinged-hinged beam, the strain energy for the beam for different load cases and mesh discretisations are tabulated in Table 5.7. These results are obtained from the field consistent formulation, and for this case of load/boundary conditions, the KA formulation and RI formulations give identical results.

Strain Energy Boundedness in a Hinged-Hinged Beam, FC Formulation							
Load	2 Elements	4 Elements	8 Elements	16 Elements	32 Elements	64 Elements	Theory
1	16.655816	16.665989	16.666624	16.666664	16.666667	16.666667	16.666667
2	66.623264	66.663954	66.666497	66.666656	66.666666	66.666667	66.666667
3	149.902344	149.993897	149.999619	149.999976	149.999999	150.000000	150.000000
4	266.493057	266.655816	266.665989	266.666624	266.666664	266.666666	266.666667
5	416.395401	416.649713	416.665607	416.666600	416.666663	416.666667	416.666667
6	599.609377	599.975586	599.998474	599.999905	599.999994	600.000001	600.000000
7	816.134986	816.633437	816.664590	816.666537	816.666659	816.666667	816.666667
8	1065.972226	1066.623265	1066.663954	1066.666497	1066.666656	1066.666664	1066.666667
9	1349.121099	1349.945070	1349.996567	1349.999786	1349.999987	1349.999998	1350.000000
10	1665.581603	1666.598851	1666.662428	1666.666402	1666.666650	1666.666666	1666.666667

Table 5.7 Strain energy boundedness in a hinged-hinged beam (uniform load) - FC formulation, Large deflection analysis

For the particular case of hinged-hinged beam, the strain energy from all the three formulations, field-consistent, reduced-integration and partial field-consistent formulations give identical results.

For the case of a pinned-pinned beam, the strain energy for different loads and mesh discretisations are summarized in Table 5.8 for the FC formulation, in Table 5.9 for the KA formulation and Table 5.10 for the RI formulation. It can be seen that only the FC formulation gives guaranteed lower bound of the strain energy, and also shows the fastest convergence. The same trend is seen for the case of clamped-clamped beam as shown below.

Strain Energy Boundedness in a Pinned-Pinned Beam, FC Formulation							
Load	2 Elements	4 Elements	8 Elements	16 Elements	32 Elements	64 Elements	ANSYS
1	10.090221	10.092873	10.093047	10.093058	10.093058	10.093058	10.093200
2	26.728881	26.734314	26.734701	26.734726	26.734728	26.734728	26.735300
3	45.746059	45.755335	45.756042	45.756089	45.756092	45.756092	45.757500
4	66.485848	66.499963	66.501093	66.501168	66.501173	66.501173	66.503800
5	88.647739	88.667498	88.669143	88.669253	88.669260	88.669261	88.673500
6	112.044444	112.070491	112.072732	112.072883	112.072893	112.072894	112.079000
7	136.543484	136.576332	136.579243	136.579441	136.579454	136.579455	136.589000
8	162.044435	162.084498	162.088144	162.088394	162.088410	162.088411	162.101000
9	188.467726	188.515334	188.519776	188.520083	188.520102	188.520104	188.536000
10	215.748309	215.803725	215.809019	215.809387	215.809411	215.809413	215.830000

Table 5.8 Strain energy boundedness in a pinned-pinned beam (uniform load) - FC formulation, Large deflection analysis

Strain Energy Boundedness in a Pinned-Pinned Beam, KA Formulation							
Load	2 Elements	4 Elements	8 Elements	16 Elements	32 Elements	64 Elements	ANSYS
1	10.357490	10.160307	10.109954	10.097287	10.094116	10.093323	10.093200
2	27.633965	26.960076	26.791183	26.748850	26.738259	26.735611	26.735300
3	47.403387	46.166516	45.858847	45.781794	45.762518	45.757699	45.757500
4	68.967078	67.113134	66.654353	66.539488	66.510753	66.503568	66.503800
5	92.011521	89.495929	88.876168	88.721016	88.682201	88.672496	88.673500
6	116.343034	113.125757	112.336404	112.138810	112.089376	112.077014	112.079000
7	141.825132	137.868911	136.902169	136.660184	136.599641	136.584501	136.589000
8	168.354536	163.624058	162.472724	162.184554	162.112452	162.094422	162.101000
9	195.849472	190.310908	188.968249	188.632219	188.548138	188.527113	188.536000
10	224.243109	217.863822	216.323491	215.938028	215.841573	215.817453	215.830000

Table 5.9 Strain energy boundedness in a pinned-pinned beam (uniform load) - KA formulation, Large deflection analysis

Strain Energy Boundedness in a Pinned-Pinned Beam, RI Formulation							
Load	2 Elements	4 Elements	8 Elements	16 Elements	32 Elements	64 Elements	ANSYS
1	10.149294	10.106008	10.096246	10.093852	10.093257	10.093108	10.093200
2	27.194340	26.838218	26.759992	26.741008	26.736295	26.735119	26.735300
3	47.064980	46.049956	45.827741	45.773895	45.760536	45.757203	45.757500
4	69.122290	67.088923	66.644399	66.536757	66.510055	66.503393	66.503800
5	93.073155	89.655970	88.909628	88.728974	88.684166	88.672986	88.673500
6	118.734893	113.564589	112.436190	112.163140	112.095420	112.078523	112.079000
7	145.978347	138.682845	137.091627	136.706678	136.611210	136.587390	136.589000
8	174.705660	164.910730	162.775527	162.259083	162.131011	162.099057	162.101000
9	204.839341	192.169005	189.408328	188.740721	188.575169	188.533865	188.536000
10	236.316071	220.392903	216.924991	216.086492	215.878570	215.826695	215.830000

Table 5.10 Strain energy boundedness in a pinned-pinned beam (uniform load) - RI formulation, Large deflection analysis

For the case of a clamped-clamped beam, the strain energy for different loads and mesh discretisations are summarized in Table 5.11 for the FC formulation, in Table 5.12 for the KA formulation and Table 5.13 for the RI formulation. For reference, the strain energy from a commercial finite element software ANSYS® (2008) using a discretisation of 1000 BEAM3 elements has also been tabulated.

Strain Energy Boundedness in a Clamped-Clamped Beam, FC Formulation							
Load	2 Elements	4 Elements	8 Elements	16 Elements	32 Elements	64 Elements	ANSYS
1	2.736249	2.746412	2.747048	2.747087	2.747090	2.747090	2.747240
2	10.610864	10.651588	10.654149	10.654309	10.654319	10.654320	10.654300
3	22.820017	22.912784	22.918673	22.919042	22.919065	22.919067	22.919000
4	38.460553	38.629646	38.640534	38.641219	38.641262	38.641265	38.642100
5	56.764292	57.037712	57.055624	57.056758	57.056829	57.056833	57.056200
6	77.155263	77.564529	77.591847	77.593584	77.593693	77.593699	77.592400
7	99.222178	99.801568	99.840979	99.843497	99.843656	99.843666	99.841600
8	122.673755	123.459486	123.513925	123.517420	123.517640	123.517653	123.515000
9	147.301221	148.330754	148.403353	148.408035	148.408330	148.408349	148.403000
10	172.951743	174.263267	174.357313	174.363407	174.363791	174.363816	174.357000

Table 5.11 Strain energy boundedness in a clamped-clamped beam (uniform load) - FC formulation, Large deflection analysis

Strain Energy Boundedness in a Clamped-Clamped Beam, KA Formulation							
Load	2 Elements	4 Elements	8 Elements	16 Elements	32 Elements	64 Elements	ANSYS
1	2.745455	2.749412	2.747849	2.747291	2.747141	2.747103	2.747240
2	10.741231	10.693586	10.665321	10.657145	10.655031	10.654498	10.654300
3	23.372367	23.088236	22.965143	22.930827	22.922022	22.919806	22.919000
4	39.874921	39.073108	38.757538	38.670863	38.648698	38.643125	38.642100
5	59.522020	57.893622	57.280806	57.113767	57.071126	57.060410	57.056200
6	81.709740	78.968280	77.960484	77.686869	77.617085	77.599552	77.592400
7	105.969264	101.872734	100.384375	99.980976	99.878127	99.852290	99.841600
8	131.946997	126.301590	124.259420	123.706021	123.564930	123.529485	123.515000
9	159.377932	152.033458	149.374917	148.653855	148.469969	148.423770	148.403000
10	188.062215	178.905011	175.576217	174.671872	174.441143	174.383168	174.357000

Table 5.12 Strain energy boundedness in a clamped-clamped beam (uniform load) - KA formulation, Large deflection analysis

Strain Energy Boundedness in a Clamped-Clamped Beam, RI Formulation							
Load	2 Elements	4 Elements	8 Elements	16 Elements	32 Elements	64 Elements	ANSYS
1	2.732118	2.746155	2.747033	2.747087	2.747090	2.747090	2.747240
2	10.554574	10.648326	10.654043	10.654328	10.654326	10.654322	10.654300
3	22.593348	22.901204	22.918825	22.919275	22.919136	22.919085	22.919000
4	37.910634	38.606602	38.642754	38.642289	38.641562	38.641342	38.642100
5	55.746852	57.006412	57.063854	57.059857	57.057669	57.057047	57.056200
6	75.556080	77.535823	77.612211	77.600476	77.595530	77.594166	77.592400
7	96.961063	99.793301	99.881487	99.856431	99.847067	99.844529	99.841600
8	119.700975	123.495195	123.584084	123.539027	123.523300	123.519085	123.515000
9	143.592084	148.438398	148.513835	148.441249	148.416990	148.410536	148.403000
10	168.501561	174.474180	174.519679	174.411390	174.376258	174.366962	174.357000

Table 5.13 Strain energy boundedness in a clamped-clamped beam (uniform load) - RI formulation, Large deflection analysis

The sweep test is a very convenient technique to study at a meta-level the effect of the discretisation of the problem. It is a very effective tool for mesh sensitivity studies. In a sweep test, the position of the nodes are varied geometrically and so become one more parameter for discretisation. For the current beam problem, if the beam is discretised in to 2 elements (giving rise to a total of 3 nodes), the sweep test can be conducted by keeping the geometrical positions of the first and third node fixed, and varying the geometrical position of the 2nd node, as shown in Fig. 5.19. In this manner, the position of the middle node becomes one more parameter in the discretisation, and is varied from 0 – 50.

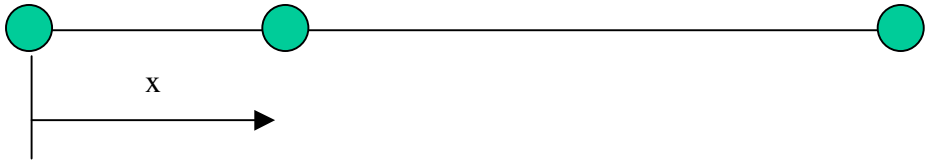

Fig. 5.19 Sweep-Test in a beam – The position of 2nd node (x) is varied

The results of the sweep test for a pinned-pinned beam from the FC/RI/KA formulations are shown in Fig. 5.20. It can be seen that it is the FC formulation that is most insensitive to the sweep test for all loads. Indeed, what can be concluded from Fig. 5.20 is that a 1-element solution (as x approaches 0 or 50) is as accurate as the 2 element solution. Also, for the RI/KA formulations, the error in the strain energy increases with increase in load while the FC formulation is insensitive. In Fig. 5.20, the “exact” strain energy is shown in red line, and the FC formulation is always bounded for all loads, whereas the RI/KA formulations do not remain bounded.

Fig. 5.21 shows the results of the sweep test for a clamped-clamped case. The results from FC formulation show guaranteed boundedness of strain energy, which is not the case with the KA formulation for this specific case. Unlike the case of pinned-pinned beam, the 1-element solution from FC formulation has higher errors for all the load cases.

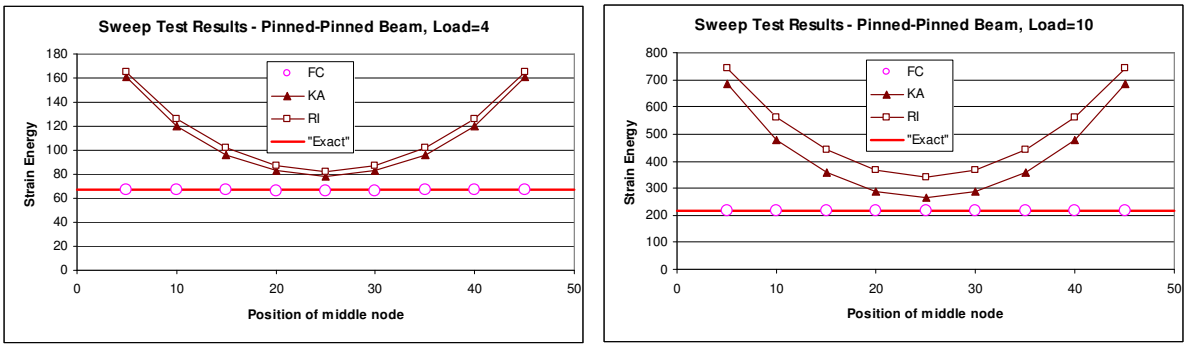

Fig. 5.20 Sweep-Test in a pinned-pinned beam (uniform load), Large deflection analysis - Comparison of various formulations

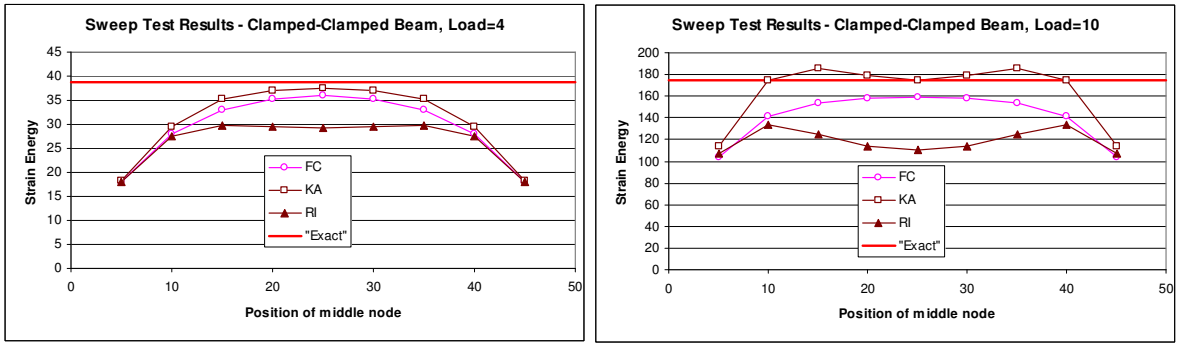

Fig. 5.21 Sweep-Test in a clamped-clamped beam (uniform load), Large deflection analysis - Comparison of various formulations

5.3 Large Deformation Analysis of Circular Plates

5.3.1 Strain-displacement relations

The strain-displacement relations for the case of large deflections of a circular plate are given in Timoshenko and Woinowsky-Krieger (1959):

$$\varepsilon_r = \frac{du}{du} + \frac{1}{2}\left(\frac{dw}{dr}\right)^2$$

$$\varepsilon_\theta = \frac{u}{r} \qquad \ldots(5.24)$$

$$\chi_r = \frac{d^2w}{dr^2}$$

$$\chi_\theta = \frac{1}{r}\frac{dw}{dr}$$

5.3.2 Incremental Matrices

The incremental matrices for this case have been derived in this thesis on the lines explained by Rajasekaran and Murray (1974). These matrices come out to be

$$\left[N^1\right] = \begin{bmatrix} 0 & 0 & C_{11}w,r \\ 0 & 0 & C_{12}w,r \\ C_{11}w,r & C_{12}w,r & C_{11}u,r + C_{12}\dfrac{u}{r} \end{bmatrix}$$

$$\left[N^2\right] = \begin{bmatrix} 0 & 0 & 0 \\ 0 & 0 & 0 \\ 0 & 0 & 1.5C_{11}w,r^2 \end{bmatrix} \qquad \ldots(5.25)$$

where

$$C_{11} = \frac{Et}{1-\nu^2}, C_{12} = \nu C_{11}, C_{13} = \frac{(1-\nu)}{2}C_{11}$$

and

$$\left[B^N\right]^T = \begin{bmatrix} u,r & \dfrac{u}{r} & w,r \end{bmatrix} \qquad \ldots(5.26)$$

These incremental matrices are generic in nature and can be applied to different element formulations.

5.3.3 Numerical Experiments and Discussion

The case of a circular plate undergoing axisymmetric large deflection is now studied in detail using a 2-noded element with 3 degrees of freedom at each node (1 in-plane axial displacement, 1 transverse displacement and rotation). This is a one-dimensional problem and the same element that has been used in chapter-3 for linear elastostatics is used.

The results from the above formulation for the case of a circular plate simply supported on the edges (radius = 10 in., E=1.0e7 psi, υ =0.3, and t=0.1 in. is subjected to a uniform load of 1 lb/in^2) are shown in Table 5.14. The results of the approximate solution are based on the formula in eqn. (5.27) Timoshenko and Woinowsky-Kreiger (1959).

$$\frac{w}{h} + A\left(\frac{w}{h}\right)^3 = B\frac{q}{E}\left(\frac{a}{h}\right)^4 \qquad \ldots(5.27)$$

where

w is the translational deflection

h is the thickness of the plate

a is the radius of the circular plate

q is the uniform load

A, B are constants that depend on the boundary conditions (*A*=1.852 and *B* =0.696 for a simply supported plate, *A*=0.471 and *B*=0.171 for a clamped plate)

Deflection at centre of a simply supported circular plate - uniform load			
Load	ANSYS	C^1 Formulation	Approximate solution
0.1	0.048075	0.048075	0.044813
0.2	0.070373	0.070371	0.069054
0.3	0.085126	0.085122	0.085131
0.4	0.096427	0.096423	0.097462
0.5	0.105719	0.105714	0.107621
0.6	0.113684	0.113678	0.116350
0.7	0.120699	0.120692	0.124056
0.8	0.126996	0.126988	0.130989
0.9	0.132731	0.132723	0.137315
1	0.138012	0.138002	0.143150

Table 5.14 Deflection in a simply supported circular plate (uniform load) - Large deflection analysis

The membrane forces and bending moments shown in Fig. 5.22 – Fig. 5.25 for the case of both simply supported and clamped circular plate match very well with results from commercial finite element software ANSYS® (2008) (element SHELL51 is used), and gives confidence on the results predicted by the elements developed herein.

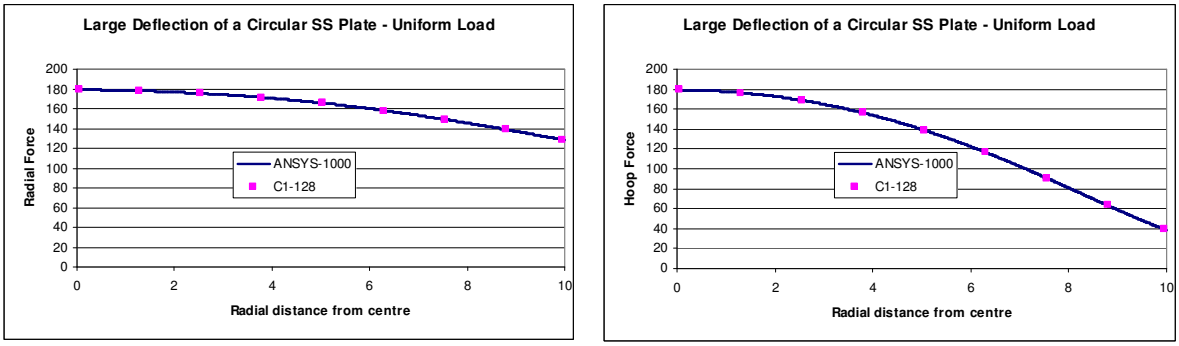

Fig. 5.22 Membrane forces in a simply supported circular plate (uniform load) – Large deflection analysis

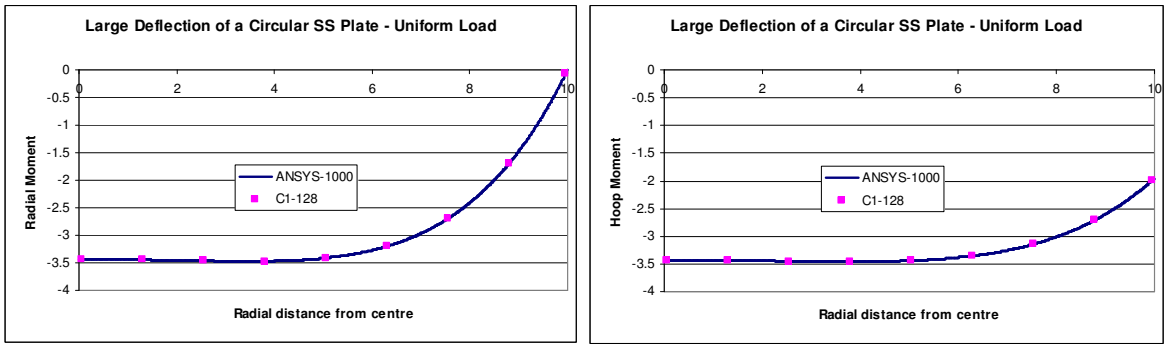

Fig. 5.23 Bending moments in a simply supported circular plate (uniform load) – Large deflection analysis

Deflection at centre of a circular clamped plate - uniform load			
Load	ANSYS	C^1 Formulation	Approximate solution
0.1	0.016810	0.016803	0.016177
0.2	0.032283	0.032283	0.031917
0.3	0.045884	0.045883	0.045972
0.4	0.057679	0.057678	0.058311
0.5	0.067960	0.067958	0.069165
0.6	0.077024	0.077020	0.078801
0.7	0.085114	0.085109	0.087449
0.8	0.092416	0.092410	0.095292
0.9	0.099074	0.099067	0.102470
1	0.105198	0.105190	0.109093

Table 5.15 Deflection in a clamped circular plate (uniform load) - Large deflection analysis

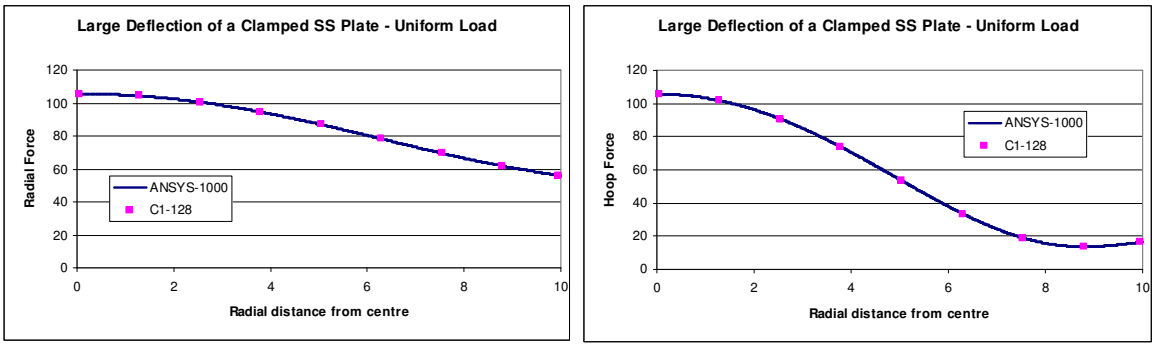

Fig. 5.24 Membrane forces in a clamped circular plate (uniform load) - Large deflection analysis

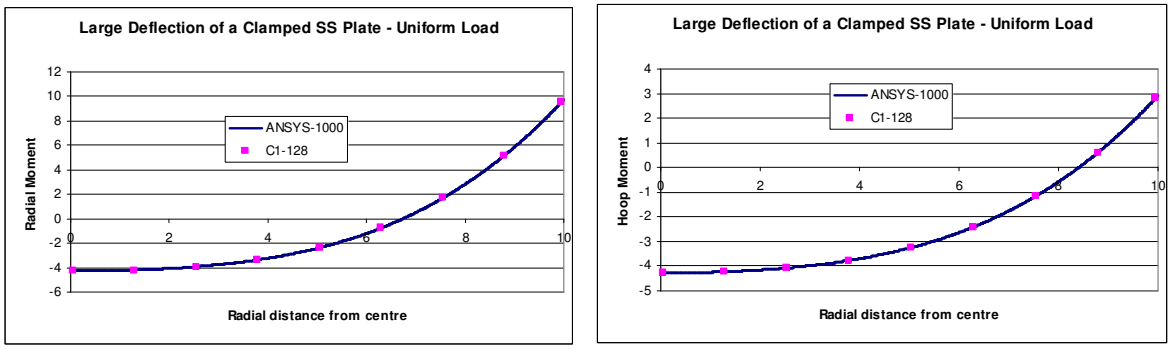

Fig. 5.25 Bending moments in a clamped circular plate (uniform load) - Large deflection analysis

As explained earlier, the total deflection of the plate can be considered to have a linear and a nonlinear portion. The behaviour of each of these portions is distinctly different. The linear portion was already studied in chapter-3 where it was shown to converge at $O(h^4)$, and the same is seen here. The order of convergence of the nonlinear portion for the simply supported circular plate is close to $O(h^2)$ as shown in Fig. 5.26, and the total deflection follows the same as the nonlinear portion. For the case of clamped circular plate as well, a similar behaviour is seen in Fig. 5.27

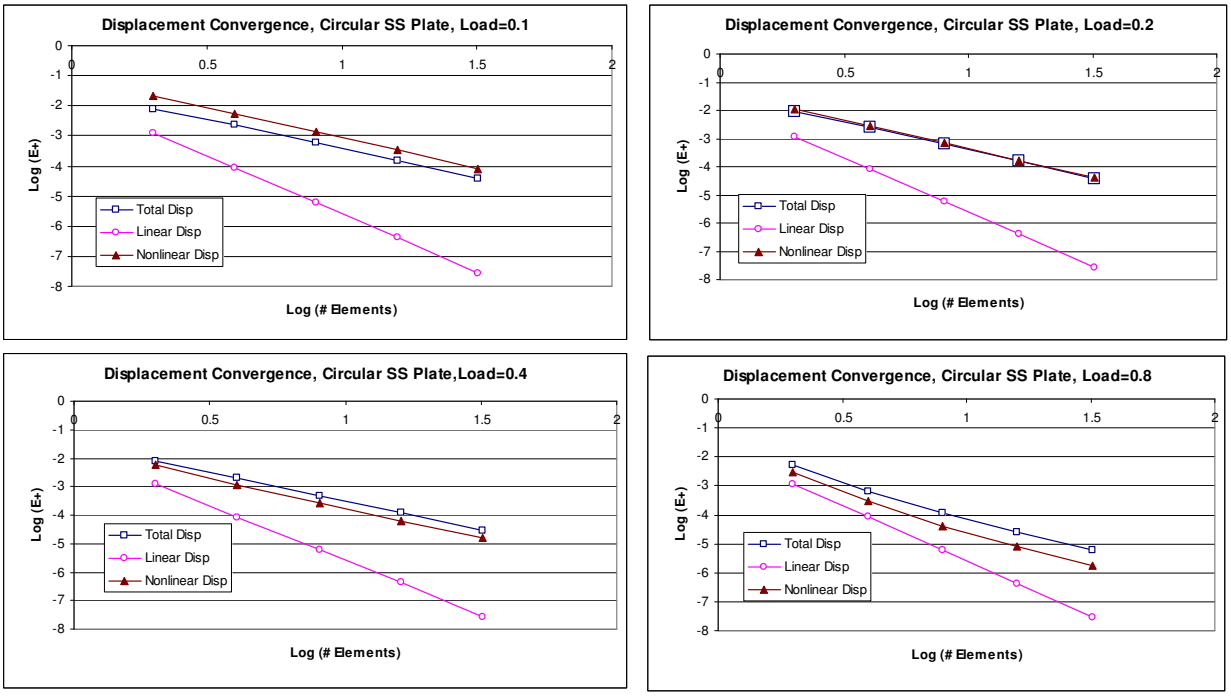

Fig. 5.26 Convergence of displacement in a simply supported circular plate (uniform load) - Large deflection analysis

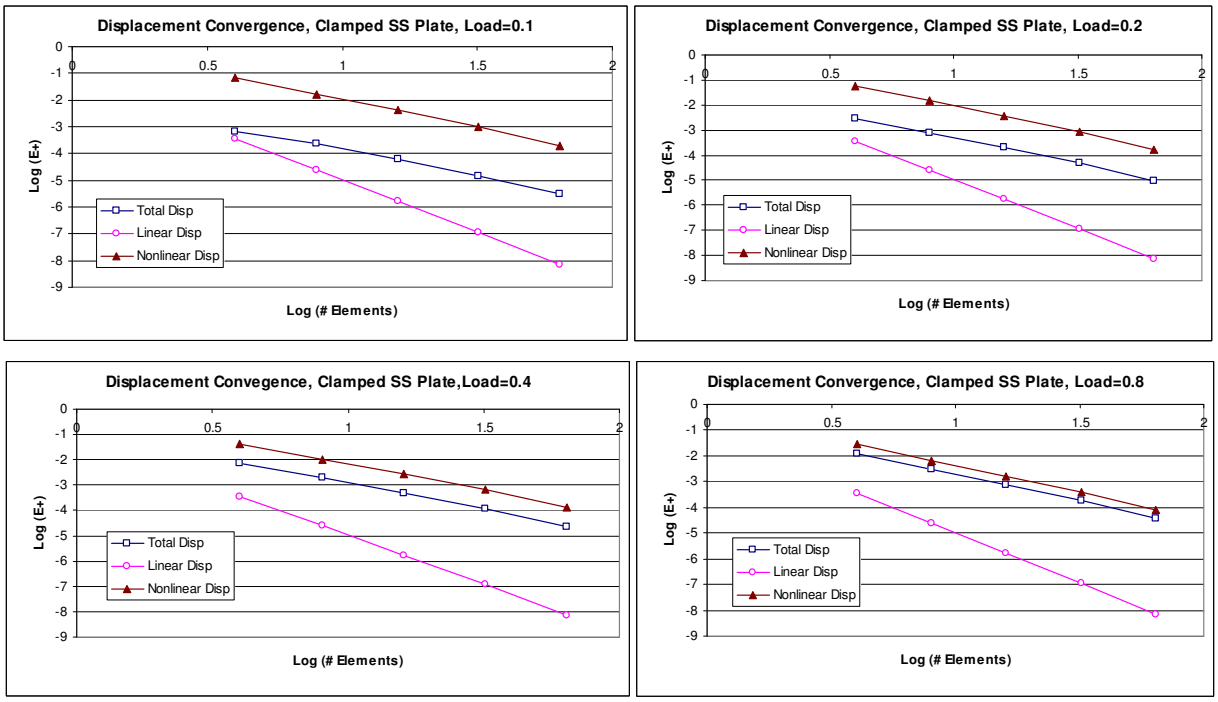

Fig. 5.27 Convergence of displacement in a clamped circular plate (uniform load) - Large deflection analysis

Table 5.16 and 5.17 show the results of the strain energy for different discretisations for simply supported and clamped circular plates, and the boundedness of the results can be seen clearly.

Strain Energy in a Simply Supported Circular Plate - Uniform Load, Large Deflections, C^1 Formulation								
Load	2 Elements	4 Elements	8 Elements	16 Elements	32 Elements	64 Elements	128 Elements	ANSYS
0.1	0.292087	0.295847	0.296963	0.297257	0.297331	0.297351	0.297353	0.297347
0.2	0.766620	0.779989	0.784037	0.785136	0.785415	0.785485	0.785501	0.785476
0.3	1.308681	1.334463	1.342417	1.344614	1.345173	1.345316	1.345350	1.345320
0.4	1.900115	1.940317	1.952938	1.956464	1.957377	1.957607	1.957667	1.957630
0.5	2.532368	2.588598	2.606540	2.611612	2.612927	2.613262	2.613341	2.613260
0.6	3.200064	3.273663	3.297502	3.304314	3.306088	3.306535	3.306648	3.306590
0.7	3.899383	3.991512	4.021769	4.030490	4.032771	4.033346	4.033495	4.033410
0.8	4.627432	4.739112	4.776255	4.787051	4.789881	4.790596	4.790784	4.790710
0.9	5.381918	5.514057	5.558521	5.571543	5.574968	5.575835	5.576052	5.575990
1	6.160965	6.314387	6.366570	6.381957	6.386017	6.387052	6.387306	6.387250

Table 5.16 Strain energy boundedness in a simply supported circular plate (uniform load) – Large deflection analysis

Strain Energy in a Clamped Circular Plate - Uniform Load, Large Deflections, C^1 Formulation								
Load	2 Elements	4 Elements	8 Elements	16 Elements	32 Elements	64 Elements	128 Elements	ANSYS
0.1	0.086761	0.087429	0.087552	0.087579	0.087588	0.087592	0.087600	0.087646
0.2	0.324424	0.330798	0.332274	0.332618	0.332707	0.332727	0.332728	0.332710
0.3	0.670541	0.691837	0.697370	0.698663	0.698990	0.699075	0.699094	0.699050
0.4	1.091968	1.137362	1.150329	1.153330	1.154097	1.154290	1.154336	1.154260
0.5	1.568404	1.645270	1.669121	1.674587	1.675985	1.676334	1.676426	1.676290
0.6	2.087694	2.201684	2.239775	2.248414	2.250622	2.251180	2.251318	2.251120
0.7	2.642187	2.797710	2.853258	2.865738	2.868927	2.869731	2.869934	2.869660
0.8	3.226739	3.427374	3.503460	3.520423	3.524746	3.525840	3.526120	3.525760
0.9	3.837685	4.086463	4.186049	4.208109	4.213731	4.215152	4.215516	4.215040
1	4.472272	4.771860	4.897790	4.925554	4.932619	4.934414	4.934859	4.934290

Table 5.17 Strain energy boundedness in a clamped circular plate (uniform load) – Large deflection analysis

The results of the sweep test for a simply supported circular plate are shown in Fig. 5.28. For all the load cases, the sweep test results show that the strain energy is bounded and is fairly insensitive to the position of the 2nd node. Also, a 1-element solution gives a fairly accurate prediction of the results (strain energy). Similar behaviour is seen for the case of the clamped circular plate as shown in Fig. 5.29.

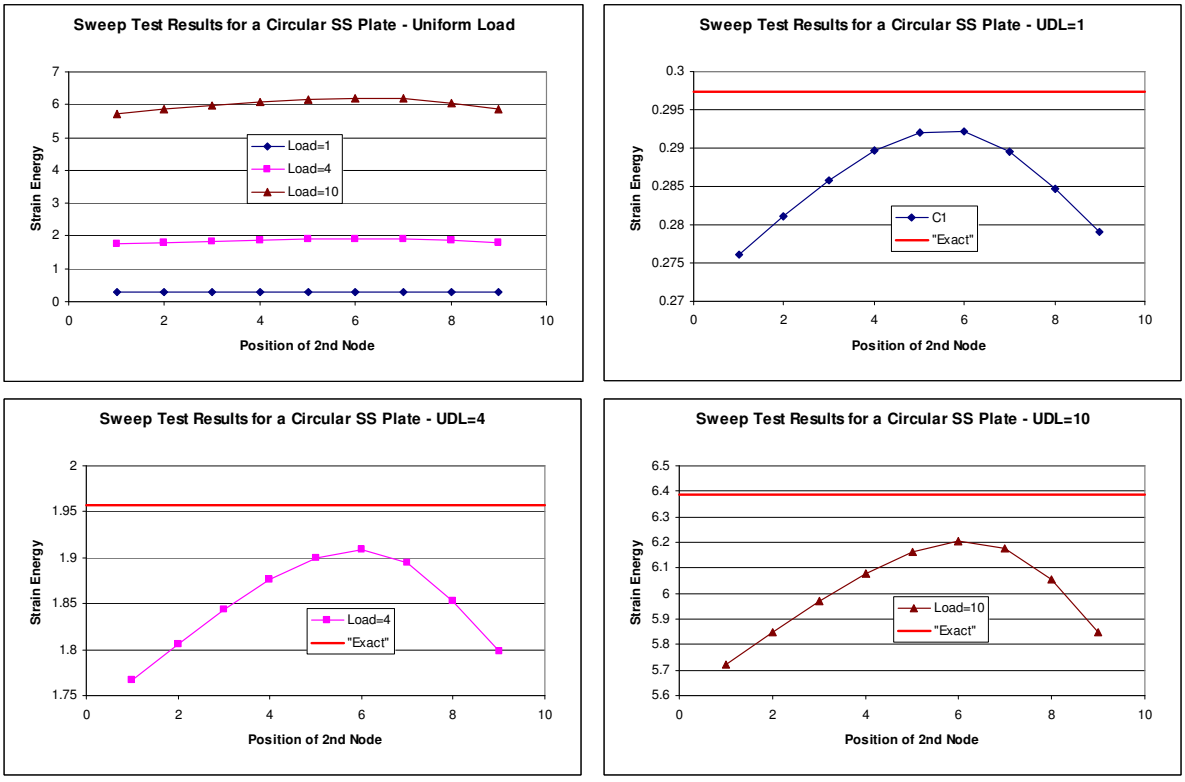

Fig. 5.28 Sweep-Test in a simply supported circular plate (uniform load) – Large deflection analysis

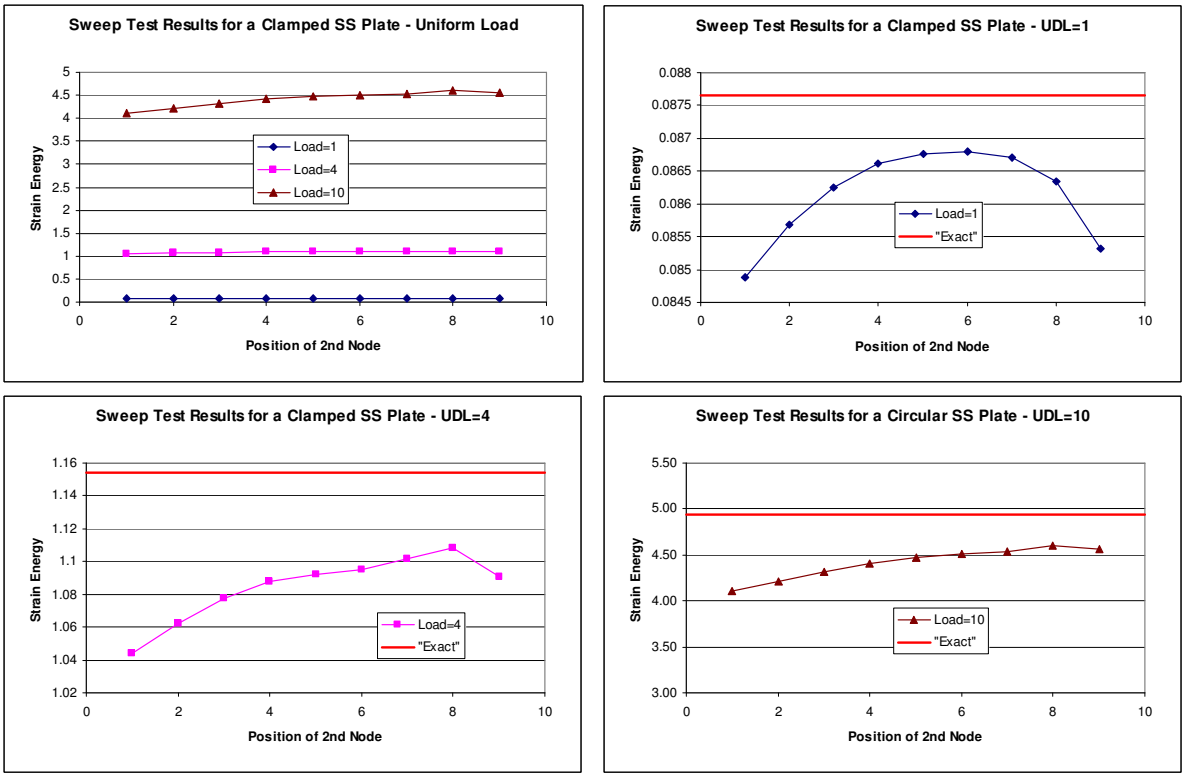

Fig. 5.29 Sweep-Test in a clamped circular plate (uniform load) – Large deflection analysis

5.4 Large Deformation Analysis of Classical Plates

5.4.1 Strain-displacement relations

The Von Karman strain displacement relations for the case of large deflections of a rectangular plate are given in Timoshenko and Woinowsky-Krieger (1959)

$$\boldsymbol{\varepsilon} = \begin{Bmatrix} \varepsilon_x \\ \varepsilon_y \\ \gamma_{xy} \\ \chi_x \\ \chi_y \\ \chi_{xy} \end{Bmatrix} = \begin{Bmatrix} \dfrac{\partial u}{\partial x} \\ \dfrac{\partial u}{\partial y} \\ \dfrac{\partial u}{\partial y} + \dfrac{\partial v}{\partial x} \\ \dfrac{\partial^2 w}{\partial x^2} \\ \dfrac{\partial^2 w}{\partial y^2} \\ 2\dfrac{\partial^2 w}{\partial x \partial y} \end{Bmatrix} + \begin{Bmatrix} \dfrac{1}{2}\left(\dfrac{\partial w}{\partial x}\right)^2 \\ \dfrac{1}{2}\left(\dfrac{\partial w}{\partial y}\right)^2 \\ \left(\dfrac{\partial w}{\partial x}\right)\left(\dfrac{\partial w}{\partial y}\right) \\ 0 \\ 0 \\ 0 \end{Bmatrix} \qquad \ldots(5.28)$$

5.4.2 Incremental Matrices - BFS Formulation

The BFS element was described earlier in chapter-3 for applications to linear elastostatics. The same element is leveraged for considering the nonlinear effects, with additional degrees of freedom (in addition to the 4 degrees of freedom at each node that was used in chapter-3, this has 2 more – 1 for in-plane displacement *u* and the other for in-displacement *v*. Both *u* and *v* have bilinear interpolation functions). The incremental matrices for the BFS element formulation can be derived on same lines as described in section 5.2. The N^1 and N^2 matrices are as follows:

$$\left[N^1\right]=\begin{bmatrix} 0 & 0 & 0 & 0 & C_{11}w,x & C_{12}w,y \\ 0 & 0 & 0 & 0 & C_{33}w,y & C_{33}w,x \\ 0 & 0 & 0 & 0 & C_{33}w,y & C_{33}w,x \\ 0 & 0 & 0 & 0 & C_{12}w,x & C_{22}w,y \\ C_{11}w,x & C_{33}w,y & C_{33}w,y & C_{12}w,x & C_{11}u,x+C_{12}v,y & C_{33}(u,y+v,x) \\ C_{12}w,y & C_{33}w,x & C_{33}w,x & C_{22}w,y & C_{33}(u,y+v,x) & C_{12}u,x+C_{22}v,y \end{bmatrix} \quad \ldots(5.29)$$

and

$$\left[N^2\right]=\begin{bmatrix} 0 & 0 & 0 & 0 & 0 & 0 \\ 0 & 0 & 0 & 0 & 0 & 0 \\ 0 & 0 & 0 & 0 & 0 & 0 \\ 0 & 0 & 0 & 0 & 0 & 0 \\ 0 & 0 & 0 & 0 & A & B \\ 0 & 0 & 0 & 0 & B & C \end{bmatrix}$$

where

$$A=\frac{3}{2}C_{11}w,x^2+\frac{1}{2}C_{12}w,y^2+C_{33}w,y^2$$
$$B=2C_{33}w,x\,w,y+C_{12}w,x\,w,y$$
$$C=\frac{3}{2}C_{11}w,y^2+\frac{1}{2}C_{12}w,x^2+C_{33}w,x^2$$

$$C_{11}=\frac{Et}{1-\nu^2},C_{12}=\nu C_{11},C_{13}=\frac{(1-\nu)}{2}C_{11}$$

and

$$\left[B^N\right]^T=\begin{bmatrix} u,x & u,y & v,x & v,y & w,x & w,y \end{bmatrix} \quad \ldots(5.30)$$

5.4.3 Incremental Matrices – ACM Formulation

The ACM element described in chapter-3 is now used for large deformation studies. The incremental matrices for the ACM element formulations are similar to those obtained for the BFS formulation, with the only difference being the interpolation function w (the interpolation functions for the other displacement components u and v are bilinear and the same as that of BFS).

5.4.4 Numerical Experiments & Discussion

The results for the case of a simply supported plate (20x20 mm quarter plate, 0.4 mm thickness and Poisson's ratio of 0.3, Young's Modulus of 200000 N/mm^2) are shown in Table 5.18, where the results are compared with ANSYS® (2008) (with 1000 elements of SHELL63). Unlike the case of beam problems where membrane locking required, large deflections of plates do not produce membrane locking, and hence there is no requirement of using reduced integration to overcome locking. Table 5.18 compares the results obtained from both reduced and full integration, and they are very close.

Large deformation of simply supported plate UDL			
Load	BFS Deflection, FI	BFS Deflection, RI	ANSYS Deflection
1	0.377013161	0.377006729	0.378168
2	0.505197558	0.505162039	0.506211
3	0.590699941	0.590631297	0.591338
4	0.657072729	0.656969829	0.657296
5	0.712270478	0.712132989	0.712085
6	0.760025623	0.759853495	0.759453
7	0.802414808	0.802208108	0.801477
8	0.840723182	0.840482025	0.839444
9	0.875806578	0.875531096	0.874208
10	0.908266402	0.907956731	0.906367

Table 5.18 Deflection in a simply supported plate (uniform load) - Large deflection analysis, BFS Element

The membrane forces and bending moments obtained from this element are compared with the results from ANSYS® (2008) in Fig. 5.30 and Fig. 5.31 and seen to match very closely.

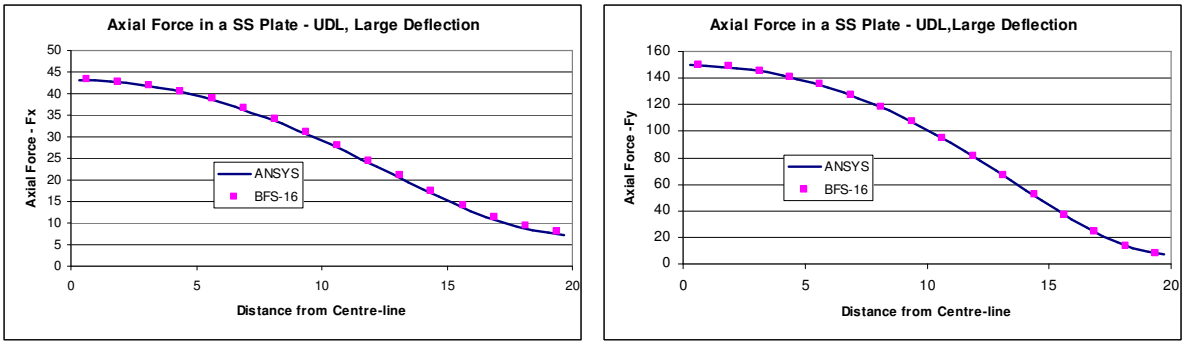

Fig. 5.30 Membrane forces in a simply supported square plate (uniform load) - Large deflection analysis, BFS Element

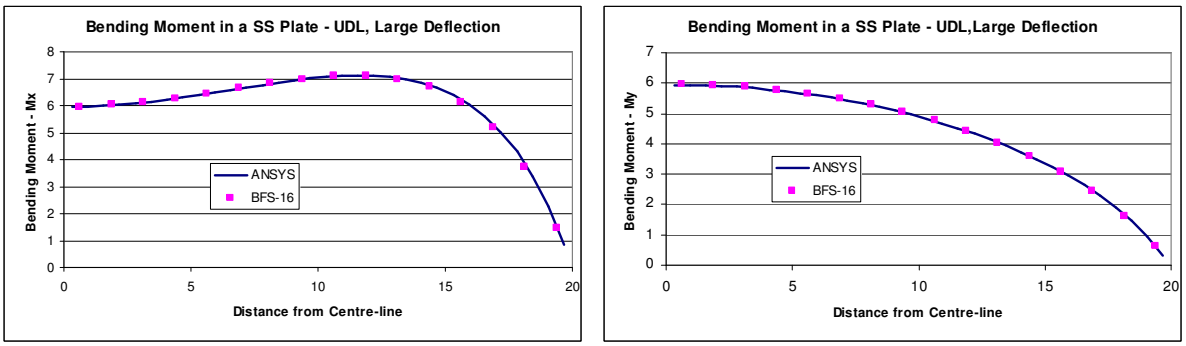

Fig. 5.31 Bending moments in a simply supported square plate (uniform load) - Large deflection analysis, BFS Element

The above observations of a simply supported plate are also noted for a clamped plate. Table 5.19 shows the impact of using reduced and full integration, and as observed for the case of a simply supported plate, there is very little impact. Fig. 5.32 and Fig. 5.33 show the comparison of the membrane forces and bending moments with ANSYS® (2008) and are seen to match well.

The convergence of displacements as explained earlier is studied for total, linear and nonlinear displacements individually and shown in Fig. 5.34 for a simply supported plate. The order of convergence of the linear portion is $O(h^4)$, and for the nonlinear portion is $O(h^2)$. The results for a clamped plate are shown in Fig. 5.35

Large deformation of clamped plate UDL			
Load	BFS Deflection, FI	BFS Deflection, RI	ANSYS Deflection
1	0.23372499	0.233724871	0.23399
2	0.374670511	0.374669981	0.37529
3	0.471039704	0.471038591	0.471923
4	0.545089425	0.545087619	0.546175
5	0.605880967	0.605878381	0.60713
6	0.657870017	0.657866572	0.659257
7	0.703566819	0.703562444	0.705075
8	0.744525658	0.744520282	0.746142
9	0.78177705	0.781770607	0.783492
10	0.816040456	0.816032879	0.817848

Table 5.19 Deflection in a clamped plate (uniform load) - Large deflection analysis, BFS Element

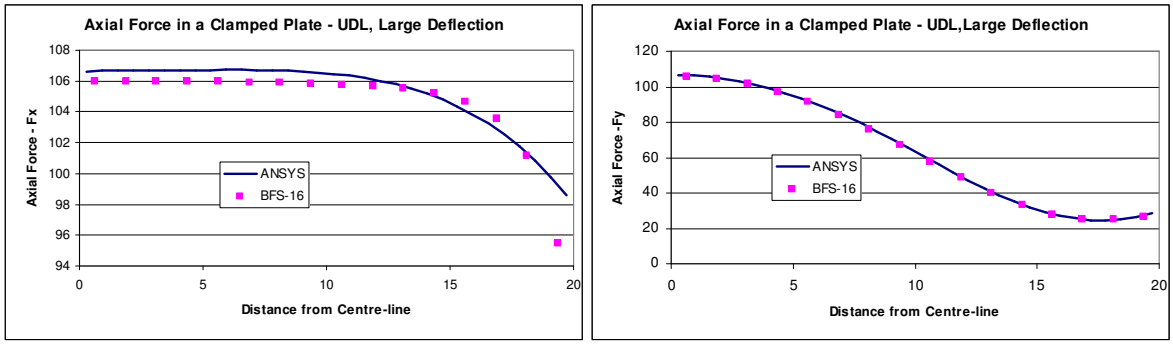

Fig. 5.32 Membrane forces in a clamped square plate (uniform load) - Large deflection analysis, BFS Element

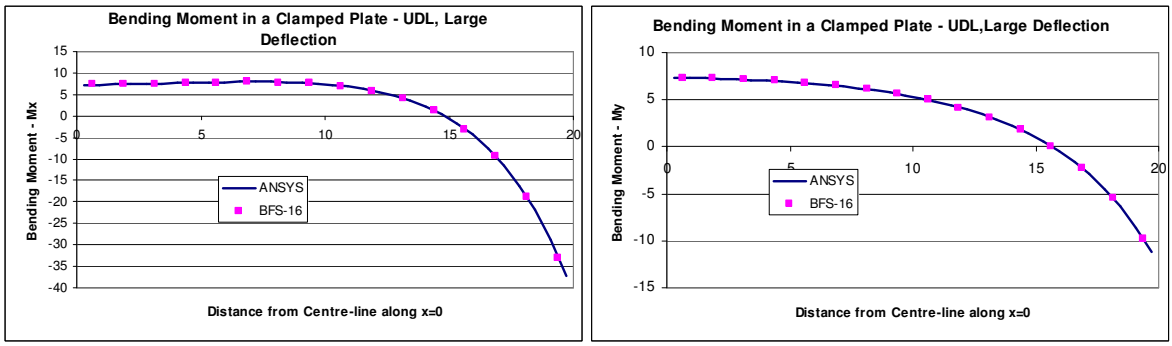

Fig. 5.33 Bending moments in a clamped square plate (uniform load) - Large deflection analysis, BFS Element

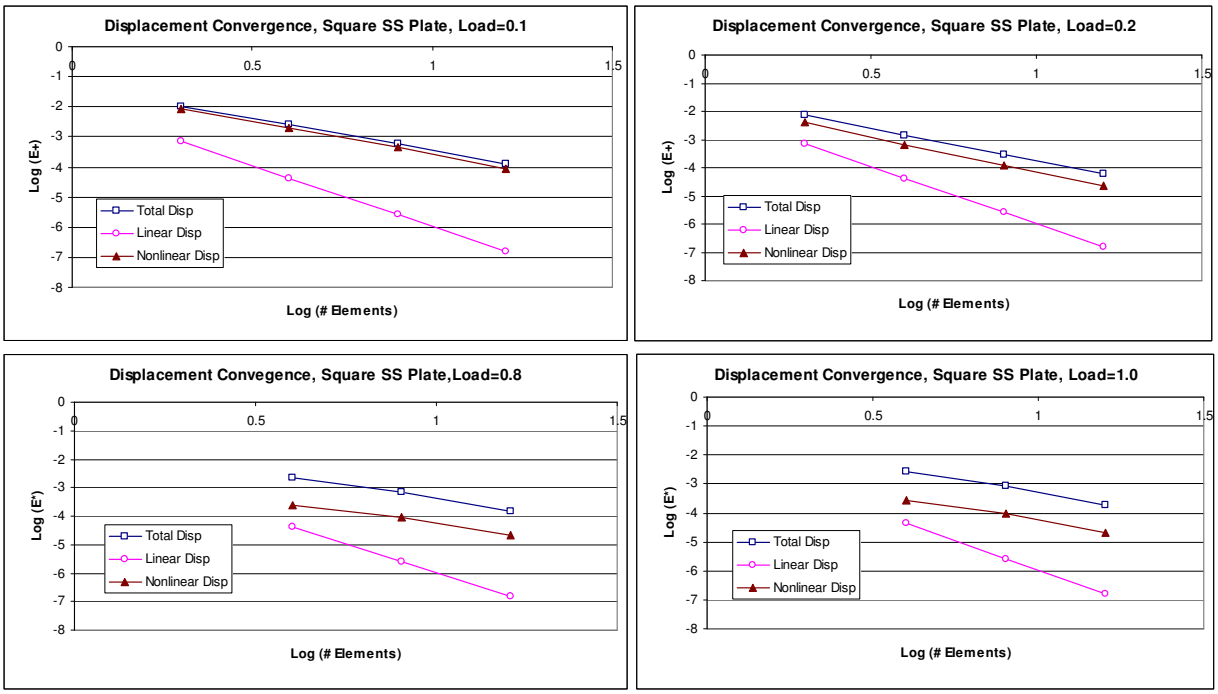

Fig. 5.34 Convergence of displacement in a simply supported square plate (uniform load) - Large deflection analysis, BFS Element

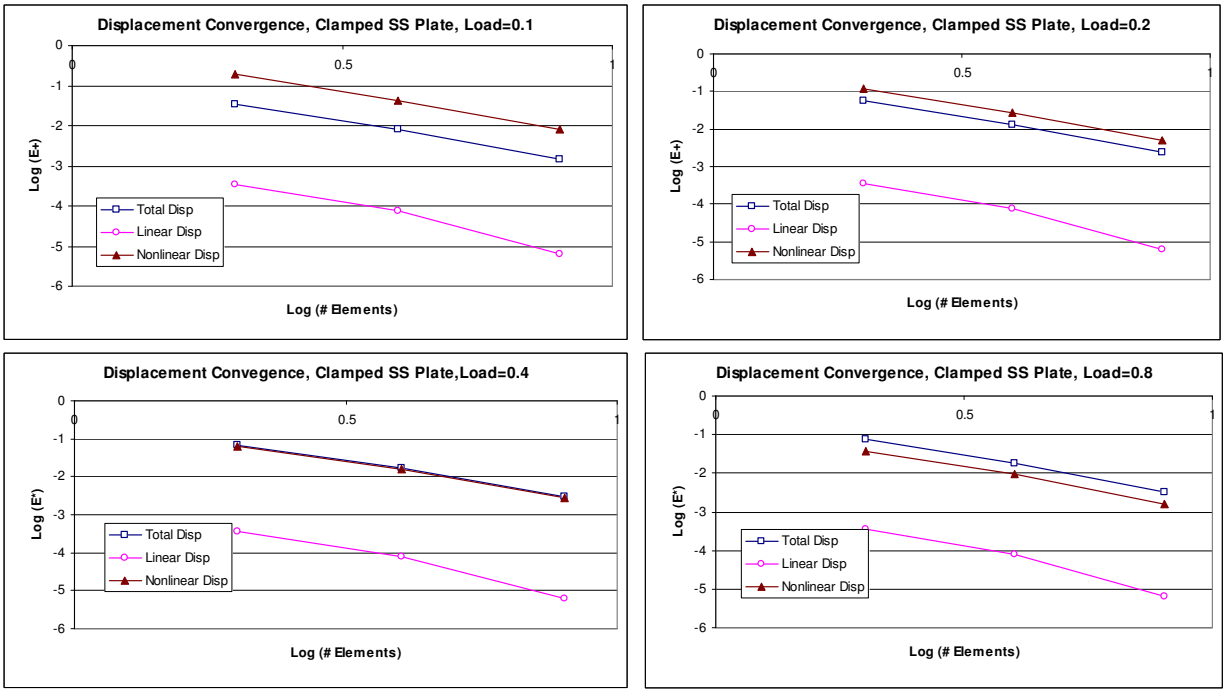

Fig. 5.35 Convergence of displacement in a clamped square plate (uniform load) - Large deflection analysis, BFS Element

Tables 5.20 and 5.21 show the results of the strain energy for different mesh discretisations for both simply supported and clamped plate conditions. The boundedness of the strain energy can be seen clearly from these tables.

Strain Energy in a SS Plate - Uniform Load, Large Deflection, BFS Formulation-FI					
Load	2x2	4x4	8x8	16x16	ANSYS
1	9.211876608	9.435422246	9.500580527	9.518244326	9.53038
2	22.63628006	23.27367949	23.47282543	23.52904922	23.566
3	38.13015706	39.27060018	39.64235107	39.75035081	39.8208
4	55.20819333	56.91487357	57.487508	57.65756195	57.769
5	73.60212652	75.92492776	76.72087509	76.96148084	77.1208
6	93.1360034	96.11661885	97.15454114	97.47298871	97.6865
7	113.6835644	117.3581041	118.6540387	119.0567407	119.33
8	135.1488811	139.5493865	141.1174392	141.6101391	141.949
9	157.4560993	162.6115038	164.4643007	165.0522134	165.463
10	180.5434356	186.4802125	188.6292097	189.3171205	189.804

Table 5.20 Strain energy boundedness in a simply supported plate (uniform load) - Large deflection analysis, BFS Element

Strain Energy in a Clamped Plate - Uniform Load, Large Deflection, BFS FI Formulation					
Load	2x2	4x4	8x8	16x16	ANSYS
1	5.164471942	5.432095087	5.499312185	5.513503679	5.52249
2	15.310932	16.45433398	16.83764179	16.91888107	16.9636
3	27.58707808	29.93366882	30.86153396	31.05986026	31.1628
4	41.30512028	45.07842959	46.74049987	47.10283659	47.2838
5	56.15670283	61.54362933	64.09921022	64.67115006	64.9488
6	71.95871582	79.12717266	82.71143786	83.53758818	83.9298
7	88.58720741	97.69241157	102.421351	103.545413	104.069
8	105.951686	117.1390354	123.1133375	124.5781275	125.25
9	123.9827119	137.3893912	144.6974563	146.5449102	147.381
10	142.6250616	158.3810899	167.1013663	169.3725415	170.389

Table 5.21 Strain energy boundedness in a clamped plate (uniform load) - Large deflection analysis, BFS Element

The sweep test for a plate problem is conceptually similar to that of a beam problem. The mesh here would comprise of 4 elements, and sweeping is done along the diagonal of the plate, as shown in Fig. 5.36. The results of the sweep test for large deformation analysis of simply supported and clamped plates using the BFS element are shown in Fig. 5.37 and Fig. 5.38, and it can be clearly seen that the strain energy is bounded.

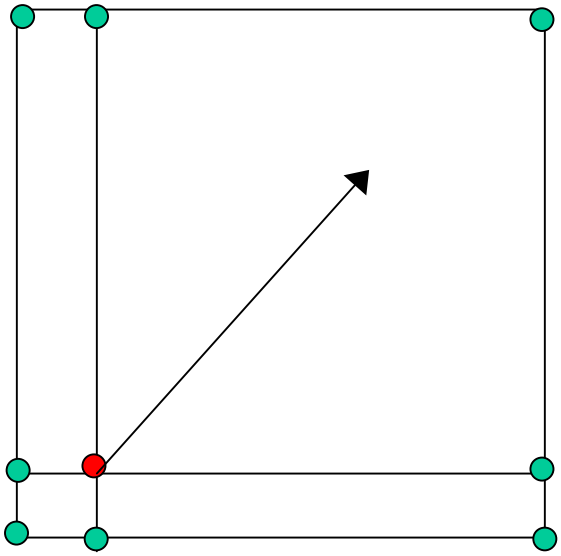

Fig. 5.36 Sweep-Test in a plate (The position of the centre-node shown in red colour is swept along the diagonal)

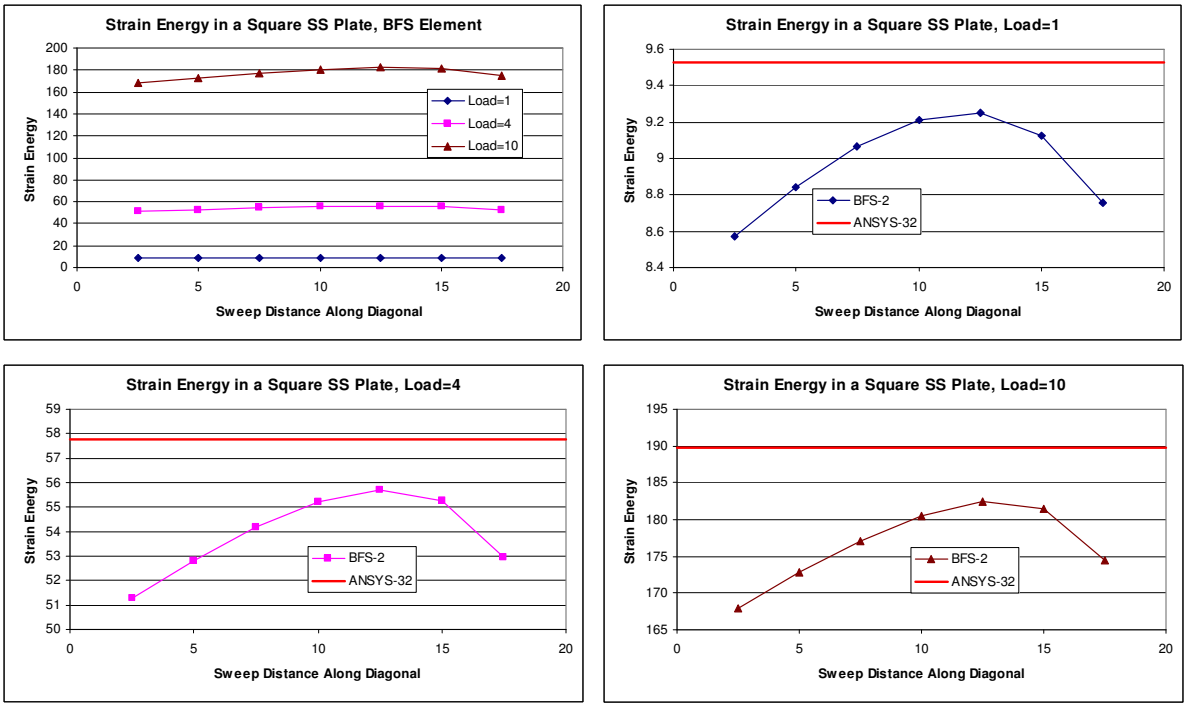

Fig. 5.37 Sweep-Test in a simply supported square plate (uniform load) - Large deflection analysis, BFS Element

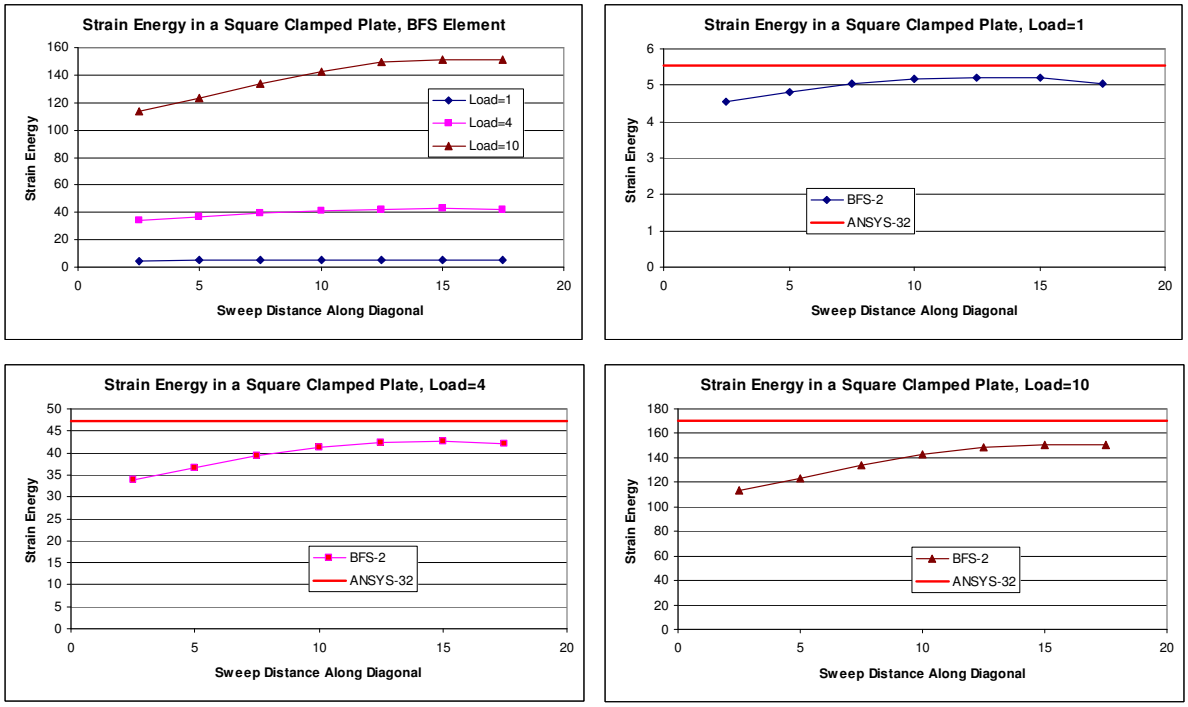

Fig. 5.38 Sweep-Test in a clamped square plate (uniform load) - Large deflection analysis, BFS Element

The above studies are now repeated for the ACM element. Table 5.22 gives the deflection at the centre of a simply supported square plate subjected to a uniform load. For the ACM formulation also, it can be seen that full-integration and reduced-integration give very close results, confirming that membrane locking in large deformation of plate problems is not significant. The membrane forces and bending moments for the ACM element for the case of simply supported plate are shown in Fig. 5.39 and Fig. 5.40.

Large Deflection of a SS Plate - UDL (ACM Formulation)			
Load	Full-Integration (5x5)	Reduced-Integration (2x2)	ANSYS Deflection
1	0.377978	0.377994	0.378168
2	0.505925	0.505933	0.506211
3	0.591012	0.591086	0.591338
4	0.656948	0.657107	0.657296
5	0.711724	0.711972	0.712085
6	0.759081	0.759417	0.759453
7	0.801098	0.801519	0.801477
8	0.839057	0.839560	0.839444
9	0.873814	0.874394	0.874208
10	0.905967	0.906620	0.906367

Table 5.22 Deflection in a simply supported plate (uniform load) - Large deflection analysis, ACM Element

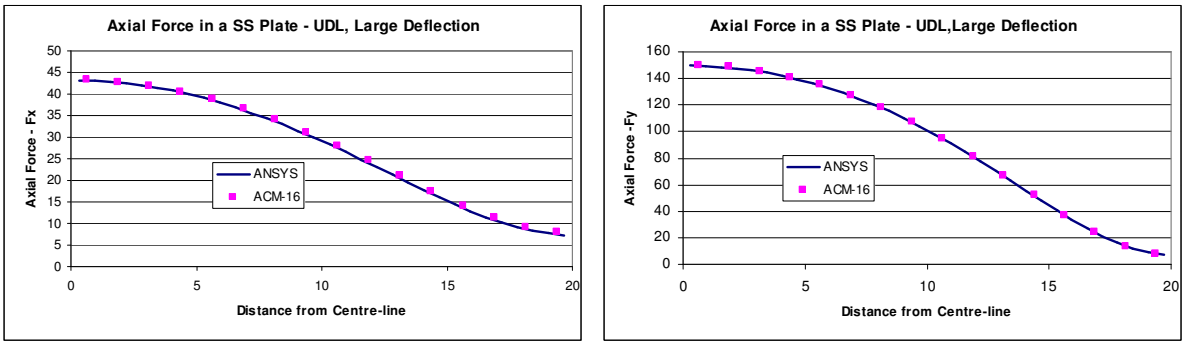

Fig. 5.39 Membrane forces in a simply supported square plate (uniform load) - Large deflection analysis, ACM Element

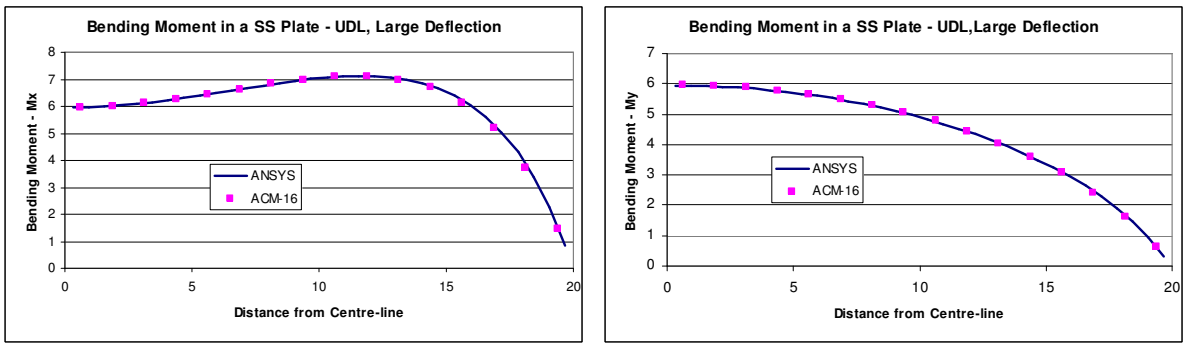

Fig. 5.40 Bending Moments in a simply supported square plate (uniform load) - Large deflection analysis, ACM Element

The deflection at the centre of a clamped plate using ACM element are shown in Tab.5.23. The membrane forces and bending moments are shown in Fig. 5.41 and Fig. 5.42.

Large Deflection of a Clamped Plate - UDL (ACM Formulation)			
Load	Full-Integration (5x5)	Reduced-Integration (2x2)	ANSYS Deflection
1	0.235145	0.235140	0.233990
2	0.376195	0.376177	0.375290
3	0.472227	0.472192	0.471923
4	0.545780	0.545726	0.546175
5	0.606003	0.605928	0.607130
6	0.657389	0.657293	0.659257
7	0.702466	0.702348	0.705075
8	0.742798	0.742658	0.746142
9	0.779421	0.779259	0.783492
10	0.813060	0.812875	0.817848

Table 5.23 Deflection in a clamped plate (uniform load) - Large deflection analysis, ACM Element

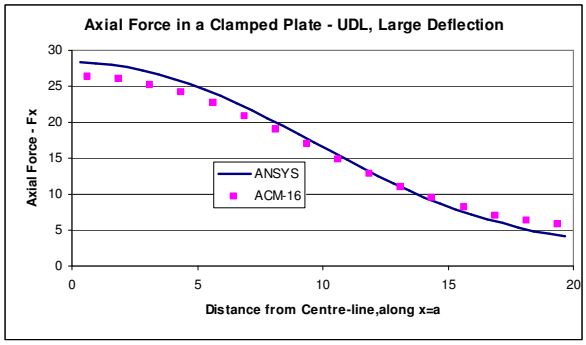

Fig. 5.41 Membrane forces in a clamped square plate (uniform load) - Large deflection analysis, ACM Element

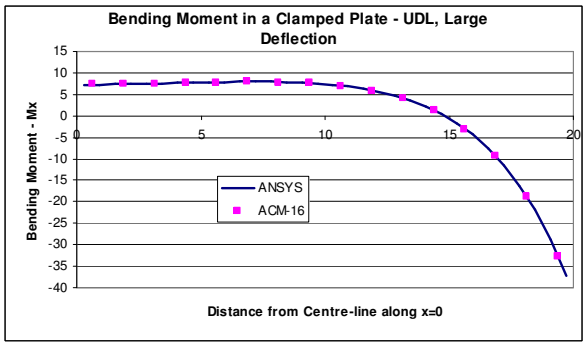

Fig. 5.42 Bending moments in a clamped square plate (uniform load) - Large deflection analysis, ACM Element

The convergence of displacements for the simply supported plate is shown in Fig. 5.43 for various load cases, and in Fig. 5.44 for a clamped plate. When compared with similar convergence studies obtained from BFS element (Fig. 5.34 and Fig. 5.35), the ACM element shows relatively higher errors.

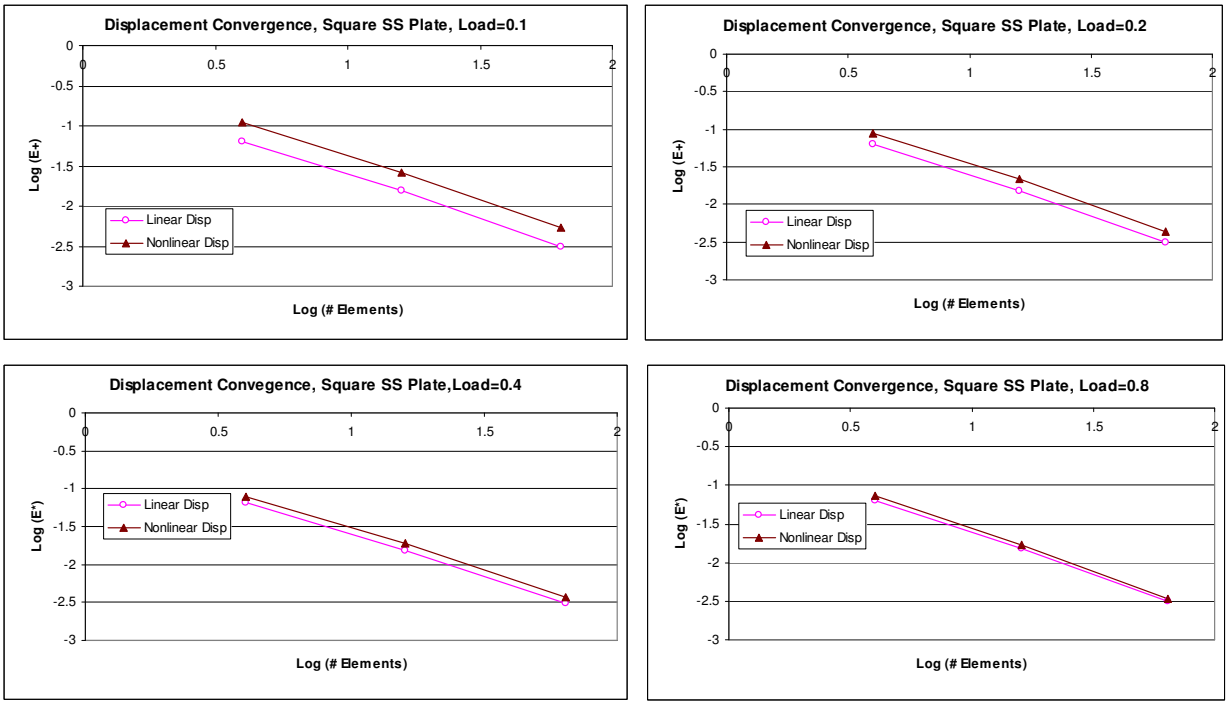

Fig. 5.43 Convergence of displacement in a simply supported square plate (uniform load) - Large deflection analysis, ACM Element

For the ACM element for large deflection studies, the strain energy remains bounded for both simply supported and clamped plate conditions, as shown in Table 5.24 and Table 5.25

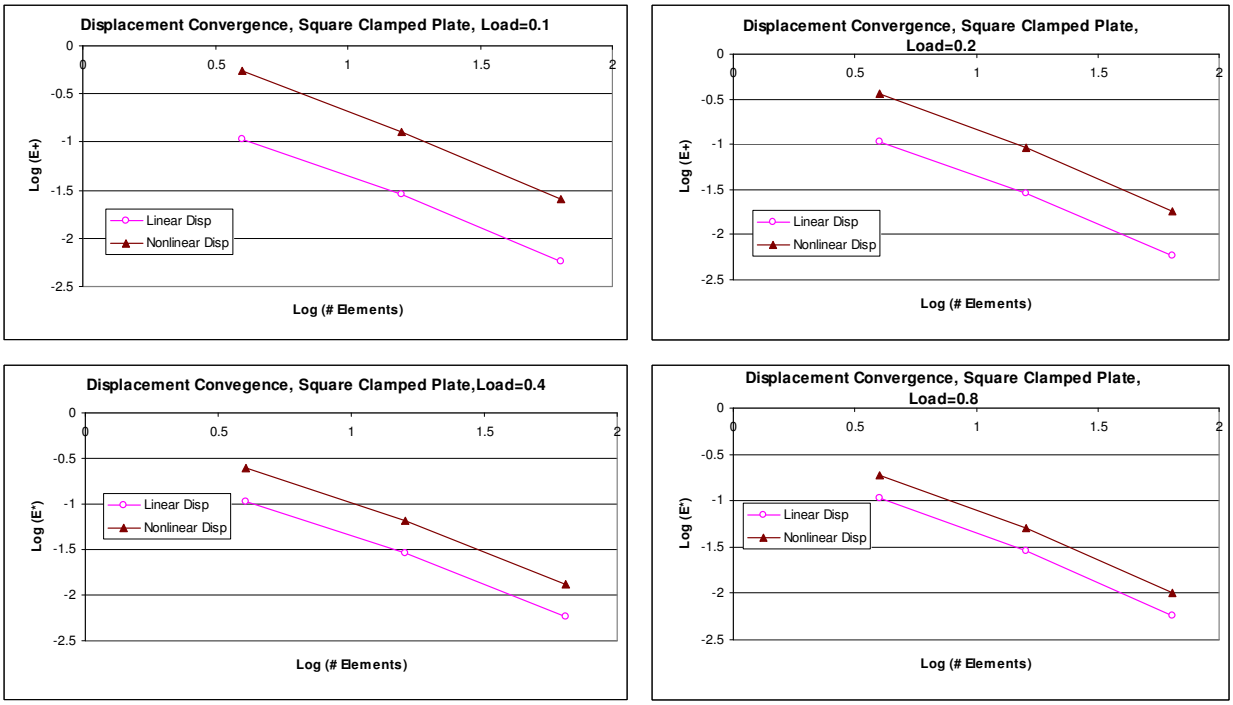

Fig. 5.44 Convergence of displacement in a clamped square plate (uniform load) - Large deflection analysis, ACM Element

Strain Energy in a SS Plate - Uniform Load, Large Deflection, ACM Formulation-FI					
Load	2x2	4x4	8x8	16x16	ANSYS
1	9.204844	9.436274	9.500853	9.518315	9.530380
2	22.558461	23.261609	23.469876	23.528311	23.566000
3	37.977683	39.248092	39.636929	39.748996	39.820800
4	54.977171	56.883422	57.480106	57.655718	57.769000
5	73.288732	75.885392	76.711819	76.959234	77.120800
6	92.736665	96.069495	97.144061	97.470400	97.686500
7	113.194999	117.303666	118.642303	119.053856	119.330000
8	134.568081	139.487766	141.104576	141.606996	141.949000
9	156.780298	162.542738	164.450411	165.048840	165.463000
10	179.770080	186.404276	188.614375	189.313541	189.804000

Table 5.24 Strain energy boundedness in a simply supported plate (uniform load) - Large deflection analysis, ACM Element

The results of the sweep-test using the ACM element for the large deflection studies of a simply supported plate subjected to a uniform load are shown in Fig. 5.45. For all the loads considered here, the strain energy remains bounded.

Strain Energy in a Clamped Plate - Uniform Load, Large Deflection, ACM Formulation-					
Load	2x2	4x4	8x8	16x16	ANSYS
1	5.411510603	5.519581882	5.522874963	5.5194886	5.52249
2	15.6733099	16.59600245	16.87686196	16.92885517	16.9636
3	27.98906103	30.10509881	30.91011316	31.0722124	31.1628
4	41.72211697	45.27371754	46.7970252	47.11722093	47.2838
5	56.57923782	61.76161997	64.16342071	64.68752093	64.9488
6	72.38314075	79.36808731	82.78335236	83.55597262	83.9298
7	89.01249372	97.95686999	102.5010441	103.5658521	104.069
8	106.3780875	117.4277293	123.2008787	124.6006598	125.25
9	124.4111397	137.7029697	144.7928952	146.5695684	147.381
10	143.0567707	158.7201223	167.2047327	169.3993516	170.389

Table 5.25 Strain energy boundedness in a clamped plate (uniform load) - Large deflection analysis, ACM Element

However, for the case of a clamped plate subjected to a uniform load, the sweep-test for the ACM element shows a cross-over, as can be seen from Fig. 5.46. This is a measure of the robustness of the element and clearly indicates that the ACM element (due to its non-conforming nature) does not pass the sweep-test.

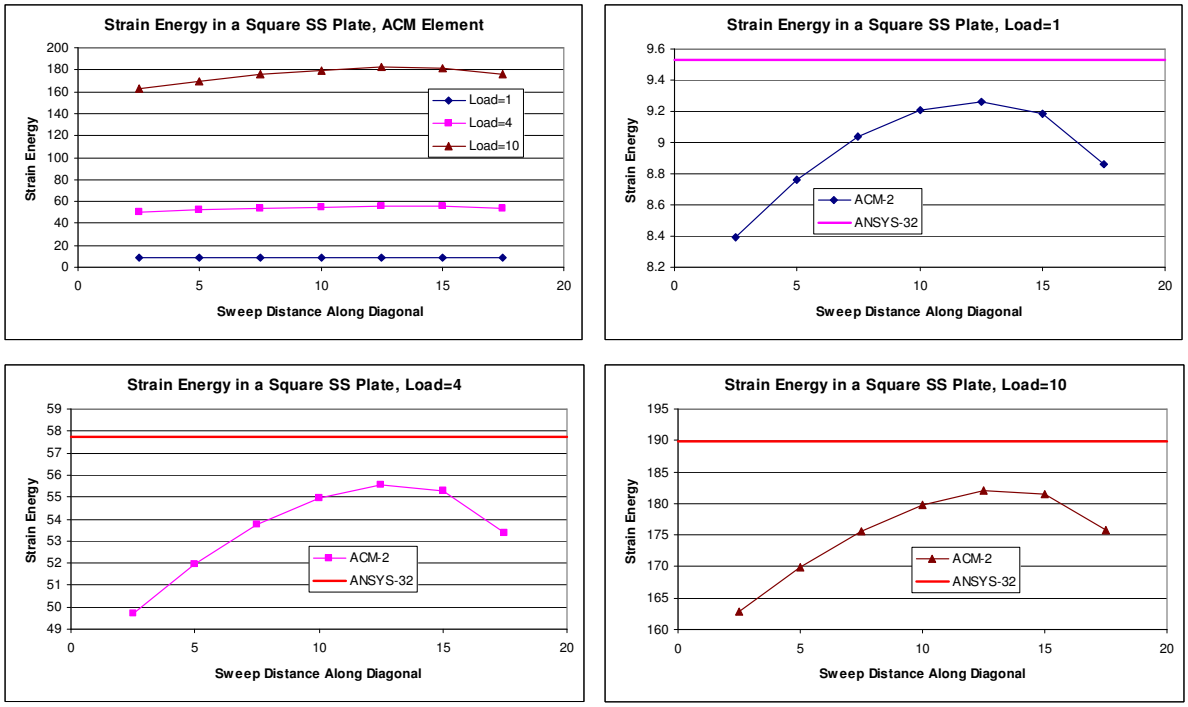

Fig. 5.45 Sweep-Test in a simply supported square plate (uniform load) - Large deflection analysis, ACM Element

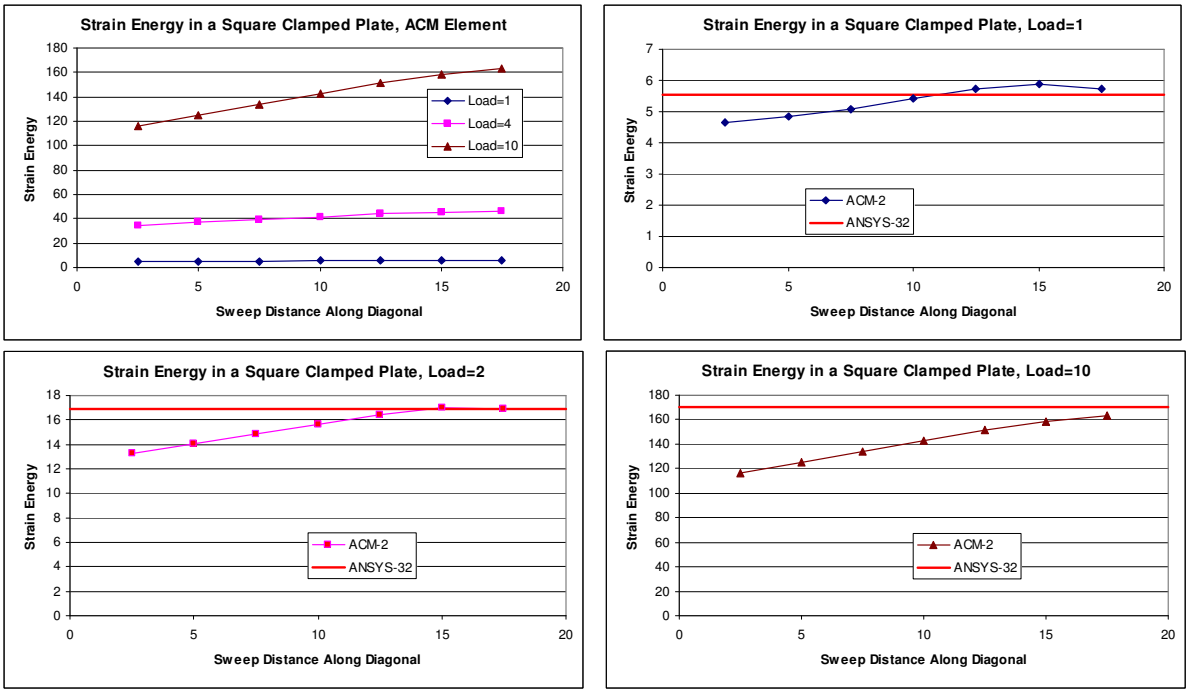

Fig. 5.46 Sweep-Test in a clamped square plate (uniform load) – Large deflection analysis, ACM Element

5.5 Closure

In this chapter, the use of field-consistent formulation for the large deformation analyses of Euler-Bernoulli beam, axisymmetric plate and Kirchhoff plate were presented. This formulation eliminates membrane locking that is normally associated with this class of problems. Alternate mechanisms of overcoming the locking phenomena were examined, and compared with the field-consistent formulation. Since the field-consistent formulation is derived from first-principles, it is variationally correct, and the results clearly bring this out. For shell and plate bending problems, membrane locking due to the nonlinear terms has not been observed, and hence there is no need for additional steps in the element formulations. Table 5.26 summarizes the results of the various element formulations on different example problems that were presented in this chapter.

Summary of Results for Nonlinear Elastostatics for Classical Beams, Shells & Plates					
Element Formulation	**C-Concept Deviation**	**Example Problem**	**Strain Energy Boundedness**	**Rate of Convergence**	**Sweep-Test**
C^1 Beam	None	Pinned-Pinned Beam	✓	✓	✓
		Hinged-Hinged Beam	✓	✓	✓
		Clamped-Clamped Beam	✓	✓	✓
C^1 Beam	Correctness	Pinned-Pinned Beam	×	↓	✓
		Hinged-Hinged Beam	✓	↓	✓
		Clamped-Clamped Beam	×	↓	×
C^1 Shell	None	Circular simply supported plate	✓	✓	✓
		Circular clamped plate	✓	✓	✓
BFS Element	None	Simply supported plate	✓	✓	✓
		Clamped plate	✓	✓	✓
ACM Element	Conformance	Simply supported plate	✓	↓	✓
		Clamped plate	✓	↓	×

Table 5.26 3C concepts and performance of various element formulations (large deflections)

Note: ✓ implies that the performance is good/satisfies the respective attribute

× implies that it is a violation of the respective attribute

↓ implies that the performance of the respective attribute is degraded

Chapter-6

Nonlinear Elastostatics for Shear-flexible Beams, Shells and Plates

6.1 Introduction

The large deformation of beams, shells and plates based on classical theory was discussed in the earlier chapter. In this chapter, the large deformation of shear-flexible beams, shells and plates based on Timoshenko and Reissner-Mindlin theories are discussed. The geometric nonlinear analysis of shear-flexible beams has many unique challenges, like both shear and membrane locking. Independently, the two phenomena of shear and membrane locking have been researched a lot, and many solutions have been offered to overcome them.

Pica *et al.* (1980) provided a geometric nonlinear formulation of a Mindlin plate and present results for 4-noded element, 8-noded serendipity elemnt and 9-noded Lagrangian elements. Reduced integration is used for shear terms for the 4-noded element. Dvorkin and Bathe (1984) introduced separate interpolations for the shear strain component for the 4-noded shell element and perform the nonlinear analysis of thick and thin shells. Oliver and Onate (1984) presented a total Lagrangian formulation for the large displacement/large rotation analysis of 3D shell problems considering the shear deformation effects. Haefner and Willam (1984) used one-point integration for the shear terms in the formulation of the stiffness matrix in their analysis of large deflection of shear-flexible beams. Their total Lagrangian approach considered moderate rotations of the beam as well. Li *et al.* (1984) enforced discrete Kirchhoff constraints in the thin plate limit to suppress the transverse shear energy and used this method for the geometric nonlinear analysis of plates and shells. Oliver and Onate (1986) presented a

unified approach for the geometric nonlinear analysis of arches, frames and axisymmetric shells that included shear deformation effects. A 3-noded element with reduced integration is used in this formulation. Dvorkin *et al.* (1988) studied the nonlinear behaviour of a Timoshenko beam using total Lagrangian formulation for curved beam elements that includes the effect of large rotation increments.

Narayanan and Krishnamoorthy (1989) used a one-point integration for terms associated with shear strains in their geometric nonlinear analysis of mindlin plates/shells. The incremental matrices of Rajasekaran and Murray (1974) are used in this formulation. Shi and Voyiadjis (1991c) used a quasi-conforming element and updated Lagrangian formulation in the geometric nonlinear analysis of plates. Cubic polynomials are employed for the interpolation of the transverse displacement *w*. Liu and Surana (1995) presented a three noded axisymmetric finite element formulation for the geometric nonlinear analysis of laminated composites. *p*-version hierarchicial interpolation functions up to order 7 are used.

Singh *et al.* (1993) used a 4-noded rectangular element with 14 degrees of freedom at each node for the large deflection analysis of shear-deformable plates. Cubic interpolation functions are used for all the translational displacements. The interpolation functions for the transverse displacement *w* are separated into components coming from bending and shear. Sita Thankam *et al.* (2003) used a displacement field that is derived from force and moment equilibrium conditions and call their formulation as material finite element formulation which is used in the large deflection analysis of laminated plates. Zhang and Kim (2006) used a 4-noded element with 5 and 6 degrees of freedom at each node for the geometric nonlinear analysis of laminated composites. Bilinear polynomial functions are used in the interpolation functions for all the translational displacements. Drilling degrees of freedom are used for the element formulation with 6 degrees of freedom per node. Natural shear strain is used for overcoming shear locking.

The concept of co-rotational formulation has been successfully used in the large deformation problems for shear-flexible structures also. Urthaler and Reddy (2005) used the co-rotational concept for the analysis of shear-flexible beams for both small and large deformations.

Ibrahimbegovic (1995) provided a cure for overcoming the locking by using one higher order hierarchical term for the displacement interpolation over the corresponding rotation interpolation. Yunhua (1998) used the field-consistency concept for a shear-flexible beam element, which eliminated the shear and membrane locking. To make the membrane strain field-consistent, Yunhua (1998) chose a higher order (5^{th} order polynomial) displacement function for the axial displacement for a 2-noded element, which makes the formulation complex. All of these approaches work fine for overcoming the membrane locking. Laulusa and Reddy (2004) studied the shear and membrane locking in nonlinear composite beams. They use linear, quadratic and cubic elements and study the effect of using reduced integration for overcoming the shear and membrane locking for beams with different boundary conditions/cross-sections. Agarwal *et al.* (2006) introduced a statically exact solution for the construction of interpolation function for the geometric nonlinear analysis of a shear deformable beam. This element does not require use of reduced integration for overcoming shear locking.

In this chapter the field-consistency approach is used to explain locking in shear-flexible structures undergoing large deflections. The field-consistency formulation for the large deflection analysis is laid out for a shear-flexible beam, an axisymmetric shell and a Mindlin plate. For the one-dimensional problem of bending of a shear flexible beam, two types of elements are chosen for close study – a 2-noded isoparametric element and a 2-noded anisoparametric element (where the interpolation functions for the transverse displacement are

cubic and that for the axial displacement are linear – section 2.3.2 in this thesis) to demonstrate how the field-consistency concepts help to understand the membrane locking. The case of the large deformation formulation of an isoparametric 2-noded element (where the interpolation functions for both the transverse displacement and axial displacement are linear) does not produce any membrane locking (though it causes shear locking) is a matter of simplification of this more generic case of anisoparametric formulation. The concepts of field-consistency for the shear and membrane strain are brought out and the required matrices for the solution of the nonlinear analyses are formulated. Three carefully chosen beam problems are solved and the results of the field-consistent formulation and compared the results with other formulations. The field-consistent formulation for a Mindlin plate element is explained and the results of this formulation for plates with different boundary conditions (simply supported, clamped *etc*.) and loadings (uniform load, point load *etc*.) are discussed. The conventional formulation is employed here and the results are discussed for plates with different boundary conditions (simply supported, clamped *etc*.) and loadings (uniform load, point load *etc*).

6.2 Large Deformation Analyses of Beams – Isoparametric Formulation

6.2.1 – Strain Displacement Relations

For a Timoshenko beam, the nonlinear strain displacement relations become

$$\begin{aligned} \varepsilon_x &= \frac{du}{dx} + \frac{1}{2}\left(\frac{dw}{dx}\right)^2 \\ \chi_x &= \frac{d\theta_x}{dx} \\ \gamma_{xy} &= \frac{dw}{dx} - \theta_x \end{aligned} \qquad \ldots(6.1)$$

6.2.2 Element Matrices

The incremental matrices were explained in section 5.2.2 and are similar for the case of shear-flexible case. The reduced integration technique involves using numerical integration with one Gaussian point for the evaluation of matrices K^{N1} and K^{N2}.

6.2.3 Partial Field-Consistent Formulation

In this formulation, $w_{,x}$ is assumed to be constant and is represented by eqn. (4.8). This approach was followed by Kikuchi and Aizawa (1982).

$$w_{,x} = \frac{1}{2}(w_2 - w_1) \qquad \ldots(6.2)$$

This is very easy to implement in the algorithm for the nonlinear solution through the incremental matrices approach of Mallett and Marcal (1968).

6.2.4 Full Field-Consistent Formulation

The field-consistent concept of element formulation of Prathap (1984) is extended to the case of membrane strain energy. For the case of the large deformation of classical EB beam, the field-consistent formulation was elaborated in section 4.2. The formulation of the tangent and secant stiffness matrices for a Timoshenko beam is very similar.

The secant stiffness matrix is derived from

$$\delta U = 0 \qquad \ldots(6.3)$$

where U has the nonlinear terms as well. This leads to the following equations

$$[D_s]\{\delta q_s\} = 0 \qquad \ldots(6.4)$$

$$q_s = \begin{Bmatrix} a_1 \\ b_0 \\ b_1 \\ b_2 \end{Bmatrix}$$

where

$$\{q_s\} = [B_s]\{d\} \qquad \ldots(6.5)$$

$$[B_s] = \begin{bmatrix} -\frac{1}{2} & 0 & 0 & 0 & \frac{1}{2} & 0 & 0 & 0 \\ 0 & -\frac{3}{4l} & -\frac{1}{4} & 0 & 0 & \frac{3}{4l} & \frac{1}{4} & 0 \\ 0 & 0 & -\frac{1}{2} & 0 & 0 & 0 & \frac{1}{2} & 0 \\ 0 & \frac{3}{4l} & \frac{3}{4} & 0 & 0 & -\frac{3}{4l} & \frac{3}{4} & 0 \end{bmatrix}$$

and

$$\{d\} = \begin{Bmatrix} u_1 \\ w_1 \\ \beta_1 \\ \theta_1 \\ u_2 \\ w_2 \\ \beta_2 \\ \theta_2 \end{Bmatrix}$$

The secant stiffness matrix is

where $$K_s = [B_s]^T [D_s][B_s] \quad \ldots(6.6)$$

$$[D_s] = EAl \begin{bmatrix} 2 & b_0 + \frac{b_2}{3} & \frac{b_1}{3} & \frac{b_2}{5} + \frac{b_0}{3} \\ b_0 + \frac{b_2}{3} & a_1 + g_0 & 0 & \frac{1}{3}(a_1 + g_0) \\ \frac{b_1}{3} & 0 & \frac{1}{3}(a_1 + g_0) & 0 \\ \frac{b_2}{5} + \frac{b_0}{3} & \frac{1}{3}(a_1 + g_0) & 0 & \frac{1}{5}(a_1 + g_0) \end{bmatrix}$$

and

$$g_0 = b_0^{\,2} + \frac{b_1^{\,2}}{3} + \frac{b_2^{\,2}}{5} + \frac{2}{3} b_0 b_2$$

The tangent stiffness matrix is derived on similar lines, using

$$\delta^2 U = 0 \quad \ldots(6.7)$$

Which gives the tangent stiffness matrix as

$$K_T = [B_s]^T [D_T][B_s] \quad \ldots(6.8)$$

where

$$[D_T] = AEl \begin{bmatrix} 2 & 2x_1 & 2x_2 & 2x_3 \\ 2x_1 & 2x_1^{\,2} + 2a_1 + g_0 & 2x_1 x_2 & 2x_1 x_3 + \frac{1}{3}(2a_1 + g_0) \\ 2x_2 & 2x_1 x_2 & 2x_2^{\,2} + \frac{1}{3}(2a_1 + g_0) & 2x_2 x_3 \\ 2x_3 & 2x_1 x_3 + \frac{1}{3}(2a_1 + g_0) & 2x_2 x_3 & 2x_3^{\,2} + \frac{1}{5}(2a_1 + g_0) \end{bmatrix}$$

and

$$x_1 = b_0 + \frac{1}{3}b_2$$

$$x_2 = \frac{1}{3}b_1$$

$$x_3 = \frac{1}{5}b_2 + \frac{1}{3}b_0$$

6.2.5 Numerical Experiments and Discussion

As in the earlier chapter, these matrices are used on the following beam problems:

1. A hinged-hinged beam
2. A pinned-pinned beam
3. A clamped-clamped beam

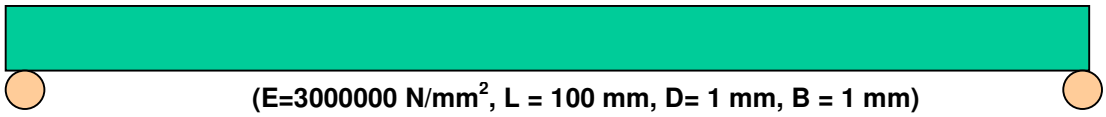

(E=3000000 N/mm^2, L = 100 mm, D= 1 mm, B = 1 mm)

Fig. 6.1 A hinged-hinged beam

Fig. 6.2 A pinned-pinned beam

Fig. 6.3 A clamped-clamped beam

These examples are chosen for their simplicity and for the specific case of the hinged-hinged beam, where there is no nonlinear behaviour (as both the supports are free to move axially, resulting in zero axial force), it will be interesting to see the prediction of the results by the above field-consistent formulation. The results for the deflection at the centre of the hinged-hinged beam obtained from the field-consistent formulation are tabulated in Table 6.1. It

can be clearly seen that this formulation predicts the results as expected (with no nonlinearity).

Shear Felxible Beam, 2-Noded Isoparamteric, Hinged-Hinged Beam, UDL, FC Formulation						
Load	2 Elements	4 Elements	8 Elements	16 Elements	32 Elements	Theory
1	0.46883681	0.50789931	0.51766493	0.52010634	0.52071669	0.5208
2	0.93767361	1.01579861	1.03532986	1.04021267	1.04143338	1.0416
3	1.40651042	1.52369792	1.55299479	1.56031901	1.56215006	1.5624
4	1.87534722	2.03159722	2.07065972	2.08042535	2.08286675	2.0832
5	2.34418403	2.53949653	2.58832465	2.60053168	2.60358344	2.604
6	2.81302083	3.04739583	3.10598958	3.12063802	3.12430013	3.1248
7	3.28185764	3.55529514	3.62365451	3.64074436	3.64501682	3.6456
8	3.75069444	4.06319444	4.14131944	4.16085069	4.16573351	4.1664
9	4.21953125	4.57109375	4.65898437	4.68095703	4.6864502	4.6872
10	4.68836806	5.07899306	5.17664931	5.20106337	5.20716688	5.208

Table 6.1 Deflection at the center of a hinged-hinged shear-flexible beam (uniform load) - FC formulation, Large deflection analysis

The field-consistent formulation and the reduced integration formulation for this case give identical results. The axial force in the beam is given is shown in Fig. 6.4, and is zero throughout the length. This is expected as both of the supports are free to move and hence do not generate any axial force in the beam.

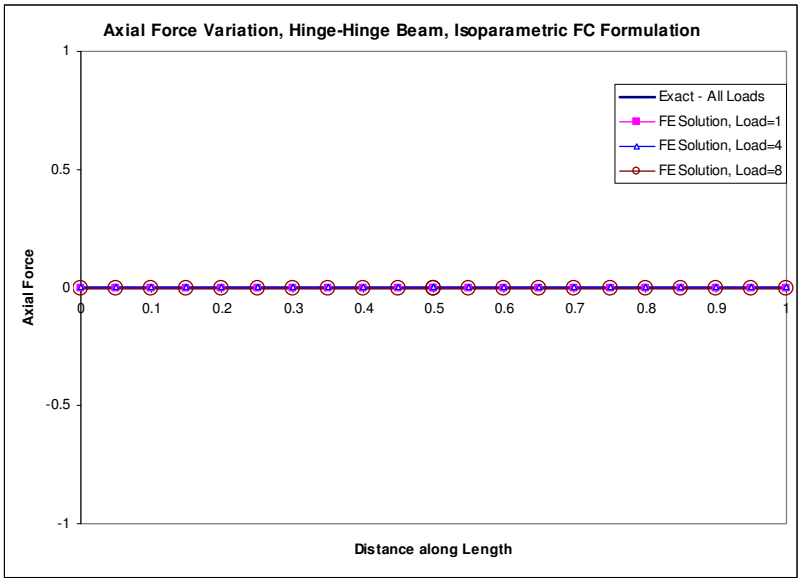

Fig. 6.4 Axial force in a hinged-hinged shear-flexible beam (uniform load) - FC formulation, Large deflection analysis

The bending moment along the length of the beam is shown in Fig. 6.5, and for this formulation it is constant within each element. For the case of the hinged-

hinged beam, the bending moment for the shear-flexible and Euler-Bernoulli formulations are the same, Reddy *et al.* (1997).

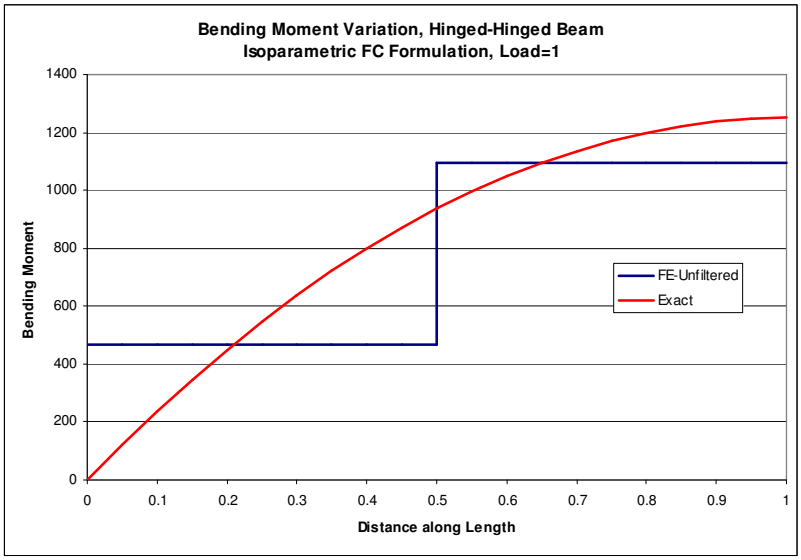

Fig. 6.5 Bending moment in a hinged-hinged shear-flexible beam (uniform load) - FC formulation, Large deflection analysis

This is not a best-fit (for the same reason that was explained in section 4.2.6). The behaviour of the rate of convergence of the deflections for the above cases is discussed now. It is pertinent to note that the total deflection is the sum of two parts, one coming due to the linear portion, and the other due to the nonlinear portion. This needs to be separated out as the behaviour of the convergence for these two portions could be different. This fact is often confounded in most of the current error norms that are used in the adaptive mesh refinement strategies, Lee and Bathe (1994). More of this will be discussed in the subsequent sections.

Shear Felxible Beam, 2-Noded Isoparamteric, Pinned-Pinned Beam, UDL, FC formulation						
Load	2 Elements	4 Elements	8 Elements	16 Elements	32 Elements	Exact
1	0.35442304	0.3653667	0.36772825	0.36829703	0.3684379	0.368466664
2	0.53771461	0.54389601	0.54504526	0.54531092	0.54537602	0.545396738
3	0.66142753	0.66368392	0.6638973	0.66393217	0.66393978	0.663957739
4	0.7570825	0.75619261	0.75567628	0.75553223	0.75549533	0.75551383
5	0.83621348	0.83268529	0.83157055	0.83128039	0.83120717	0.831228249
6	0.90433672	0.89851869	0.89689524	0.89648131	0.89637735	0.89640237
7	0.96453918	0.95668485	0.95461794	0.95409645	0.9539658	0.953995728
8	1.01873379	1.00903668	1.00657608	1.00595935	1.00580509	1.00584067
9	1.06819393	1.05680728	1.05399235	1.05329012	1.05311465	1.05315647
10	1.11381326	1.10086202	1.09772478	1.09694492	1.09675022	1.09679873

Table 6.2 Deflection at the center of a pinned-pinned shear-flexible beam (uniform load)- FC formulation, Large deflection analysis

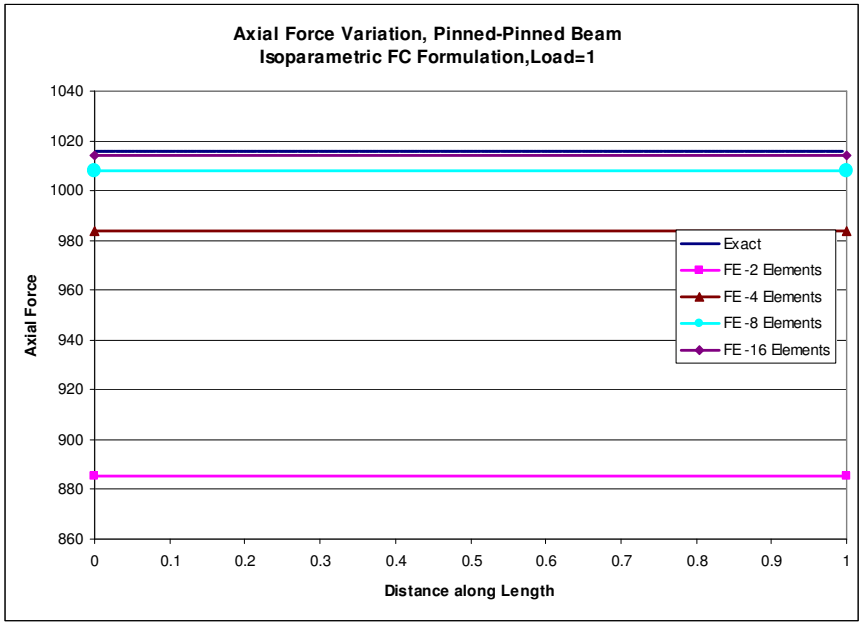

Fig. 6.6 Axial force in a pinned-pinned shear-flexible beam (uniform load)- FC formulation, Large deflection analysis

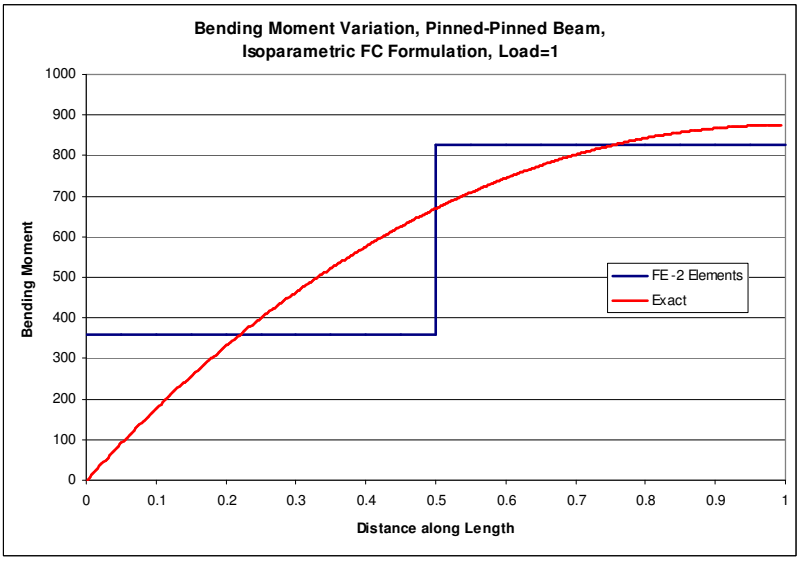

Fig. 6.7 Bending moment in a pinned-pinned shear-flexible beam (uniform load)- FC formulation, Large deflection analysis

Shear Felxible Beam, 2-Noded Isoparamteric, Clamped-Clamped Beam, UDL, FC formulation						
Load	2 Elements	4 Elements	8 Elements	16 Elements	32 Elements	Exact
1	0.07803342	0.09715929	0.10187778	0.10305252	0.10334588	0.10336217
2	0.15502493	0.19104788	0.19962474	0.20173752	0.20226369	0.202282463
3	0.23006391	0.27935372	0.29053506	0.29325279	0.29392732	0.293941173
4	0.30245961	0.36102266	0.37363051	0.37665474	0.37740288	0.377407594
5	0.37176899	0.43597167	0.44911167	0.45222693	0.45299541	0.452975019
6	0.4377742	0.50465231	0.51772063	0.52078849	0.52154351	0.521500557
7	0.5004334	0.56772436	0.5803413	0.583279	0.5840006	0.583934339
8	0.5598265	0.62587552	0.63781498	0.64057601	0.64125313	0.641164863
9	0.61610823	0.67974115	0.69087674	0.69343708	0.69406415	0.693950545
10	0.66947286	0.7298776	0.74014592	0.74249522	0.74306996	0.742934251

Table 6.3 Deflection at the center of a clamped-clamped shear-flexible beam (uniform load)- FC formulation, Large deflection analysis

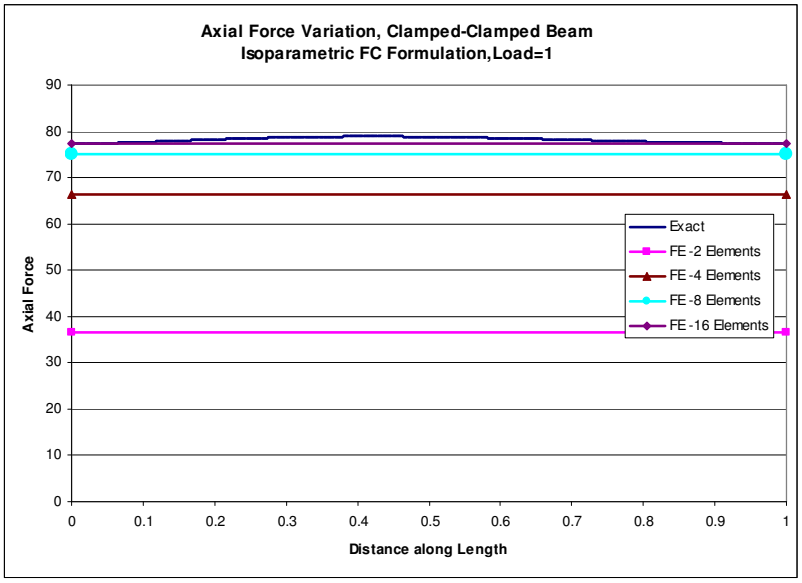

Fig. 6.8 Axial force in a clamped-clamped shear-flexible beam (uniform load)- FC formulation, Large deflection analysis

For the field-consistent formulation for the hinged-hinged case where there is no non-linearity, the rate of convergence is the same as that of the linear deformation $O(h^2)$, which is what is seen in Fig. 6.10 (as the interpolation functions that are used for u and θ_x are linear – refer to section 4.2.6)

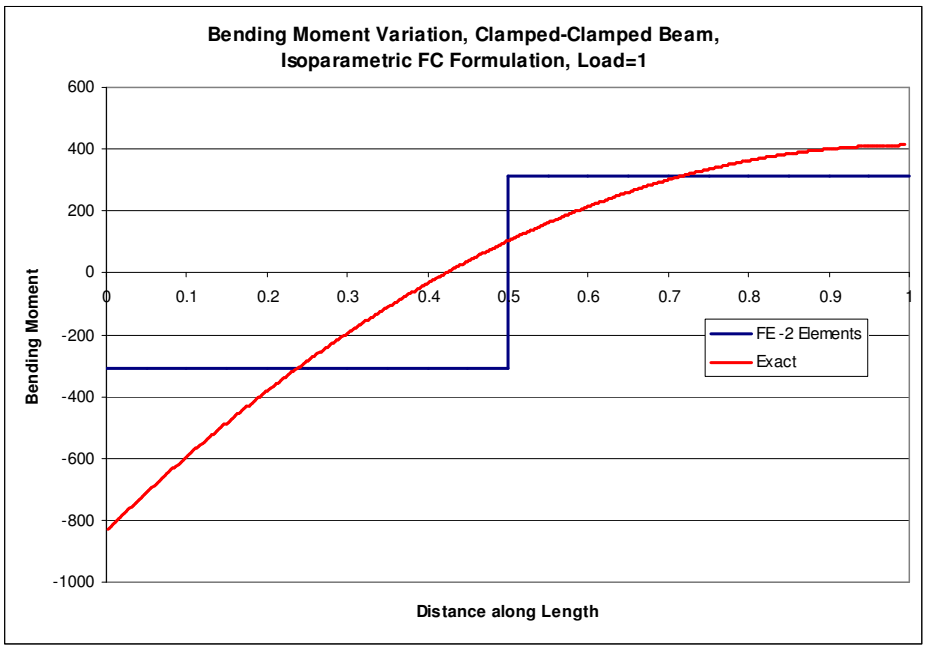

Fig. 6.9 Bending moment in clamped-clamped shear-flexible beam (uniform load)- FC formulation, Large deflection analysis

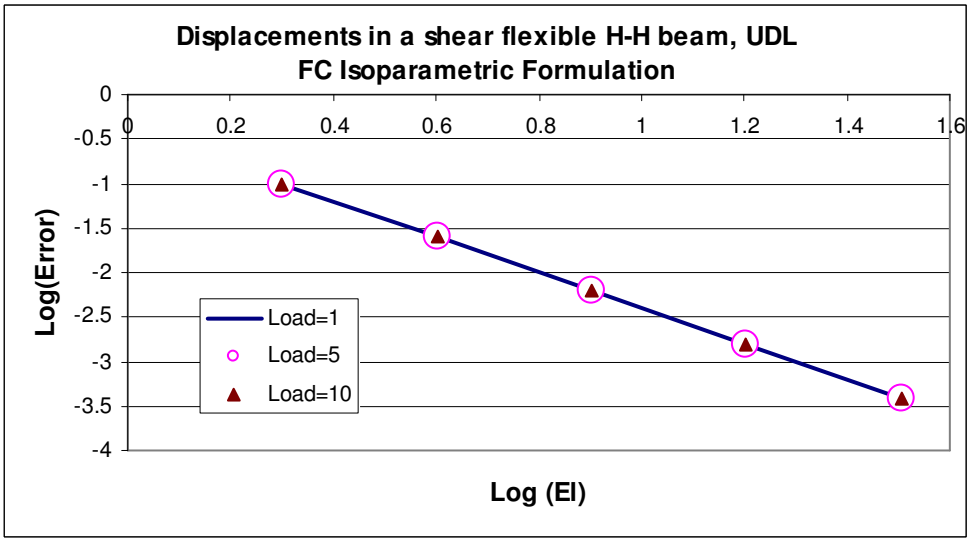

Fig. 6.10 Convergence of displacement in a hinged-hinged shear-flexible beam (uniform load)- FC formulation, Large deflection analysis

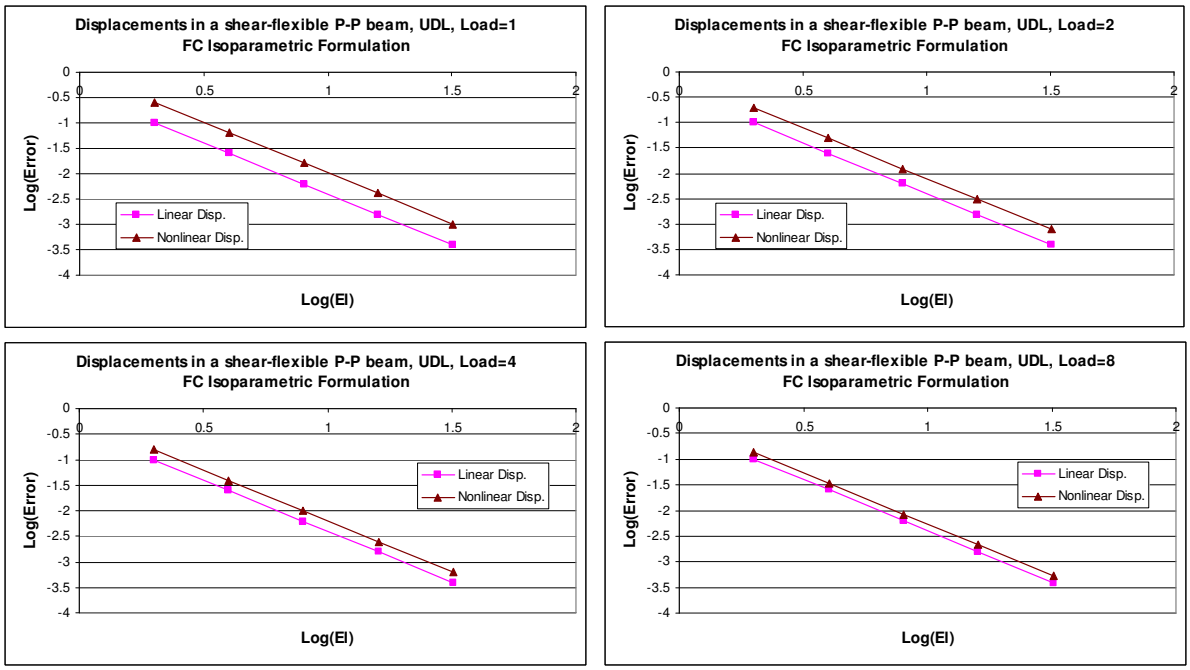

Fig. 6.11 Convergence of displacement in a pinned-pinned shear-flexible beam (uniform load)- FC formulation, Large deflection analysis

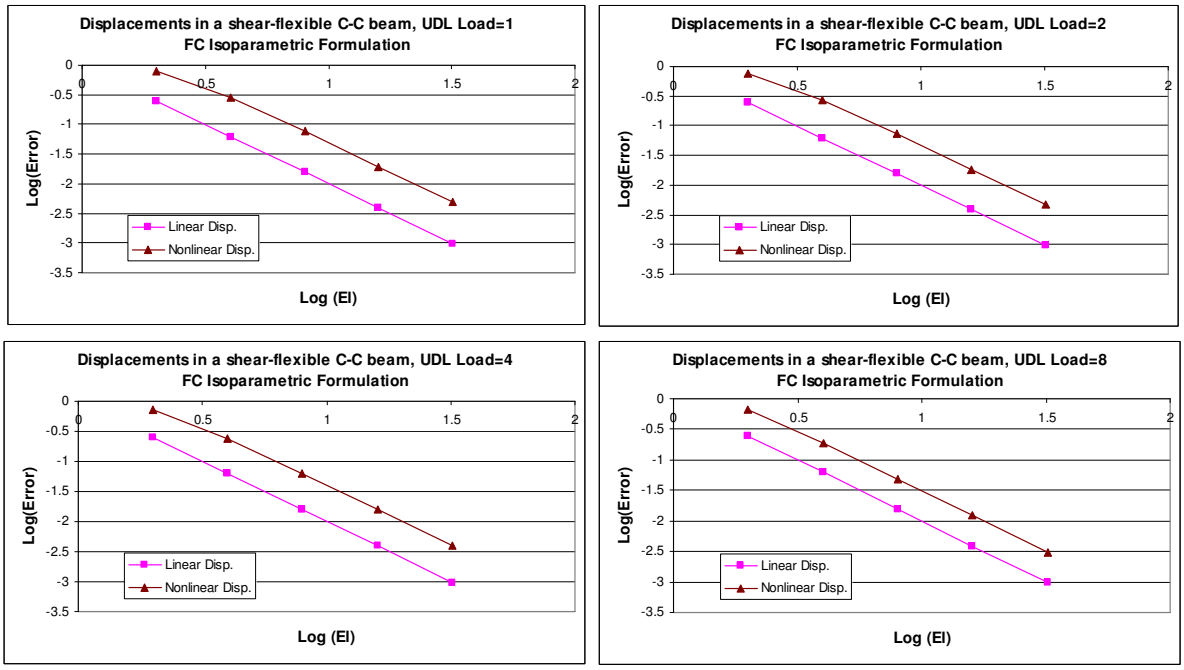

Fig. 6.12 Convergence of displacement in a clamped-clamped shear-flexible beam (uniform load)- FC formulation, Large deflection analysis

The boundedness of the total strain energy can be seen clearly in Tables 6.4 – 6.6 for the cases of H-H, P-P and C-C beams. Due to coupling of shear/membrane/bending terms, the boundedness of the individual components of the strain energy (bending/shear) is not seen.

Strain Energy for Hinged-Hinged Beam, Uniform Load, Field-Consistent Isoparametric Formulation												
Load	Elements=4				Elements=16				Elements=512			
	Shear	Memb.	Bend.	Total	Shear	Memb.	Bend.	Total	Shear	Memb.	Bend.	Total
1	0.003	0.000	16.022	16.025	0.003	0.000	16.626	16.629	0.003	0.000	16.667	16.670
2	0.011	0.000	64.087	64.098	0.012	0.000	66.504	66.516	0.012	0.000	66.667	66.678
3	0.026	0.000	144.196	144.221	0.026	0.000	149.634	149.660	0.026	0.000	150.000	150.026
4	0.046	0.000	256.348	256.393	0.046	0.000	266.016	266.062	0.046	0.000	266.666	266.712
5	0.071	0.000	400.543	400.614	0.072	0.000	415.650	415.722	0.072	0.000	416.666	416.738
6	0.103	0.000	576.782	576.885	0.104	0.000	598.536	598.640	0.104	0.000	599.999	600.103
7	0.140	0.000	785.065	785.204	0.142	0.000	814.674	814.816	0.142	0.000	816.665	816.806
8	0.182	0.000	1025.391	1025.573	0.185	0.000	1064.064	1064.249	0.185	0.000	1066.664	1066.849
9	0.231	0.000	1297.760	1297.991	0.234	0.000	1346.706	1346.940	0.234	0.000	1349.997	1350.231
10	0.285	0.000	1602.173	1602.458	0.289	0.000	1662.600	1662.889	0.289	0.000	1666.663	1666.952

Table 6.4 Strain energy boundedness in a hinged-hinged shear-flexible beam (uniform load) - FC formulation, Large deflection analysis

Strain Energy for Pinned-Pinned Beam, Uniform Load, Field-Consistent Isoparametric Formulation												
Load	Elements=4				Elements=16				Elements=512			
	Shear	Memb.	Bend.	Total	Shear	Memb.	Bend.	Total	Shear	Memb.	Bend.	Total
1	0.001	1.6134	8.31545	9.93039	0.001	1.7133	8.3687	10.0834	0.00147	1.71997	8.37202	10.0935
2	0.003	7.9634	18.4938	26.4605	0.003	8.2845	18.4302	26.718	0.00328	8.30583	18.4258	26.7349
3	0.005	17.73	27.6258	45.3614	0.005	18.296	27.4302	45.7315	0.00496	18.3338	27.4172	45.756
4	0.007	29.991	35.9684	65.9658	0.007	30.812	35.6485	66.4675	0.00655	30.8668	35.6275	66.5008
5	0.008	44.236	43.7298	87.9738	0.008	45.322	43.2953	88.6253	0.00807	45.3937	43.2668	88.6686
6	0.01	60.146	51.0442	111.2	0.01	61.504	50.5038	112.018	0.00954	61.5939	50.4685	112.072
7	0.011	77.501	58.0012	135.513	0.011	79.138	57.3625	136.512	0.01098	79.2465	57.3209	136.578
8	0.013	96.138	64.6638	160.815	0.012	98.062	63.9333	162.008	0.01239	98.189	63.8857	162.087
9	0.014	115.93	71.0782	187.026	0.014	118.15	70.2612	188.425	0.01379	118.297	70.2081	188.519
10	0.015	136.79	77.2792	214.084	0.015	139.3	76.3807	215.7	0.01516	139.47	76.3223	215.808

Table 6.5 Strain energy boundedness in a pinned-pinned shear-flexible beam (uniform load) - FC formulation, Large deflection analysis

Strain Energy for Clamped-Clamped Beam, Uniform Load, Field-Consistent Isoparametric Formulation												
Load	Elements=4				Elements=16				Elements=512			
	Shear	Memb.	Bend.	Total	Shear	Memb.	Bend.	Total	Shear	Memb.	Bend.	Total
1	0.003	0.0073	2.53414	2.54429	0.003	0.01	2.72409	2.73695	0.00286	0.01021	2.73681	2.74988
2	0.011	0.1094	9.81158	9.93202	0.011	0.1469	10.461	10.6191	0.01113	0.14969	10.5038	10.6646
3	0.024	0.5003	21.0224	21.5466	0.024	0.656	22.1744	22.8544	0.02403	0.66727	22.2484	22.9397
4	0.041	1.3959	35.2057	36.6426	0.041	1.7854	36.7248	38.5509	0.04069	1.81308	36.8199	38.6737
5	0.061	2.9698	51.5016	54.5325	0.06	3.7106	53.1768	56.9479	0.06042	3.76236	53.2789	57.1016
6	0.084	5.3341	69.244	74.6621	0.083	6.5276	70.8634	77.4738	0.08269	6.60969	70.9589	77.6513
7	0.109	8.5479	87.9552	96.6123	0.107	10.274	89.3383	99.7192	0.10713	10.3909	89.4165	99.9145
8	0.136	12.633	107.304	120.073	0.134	14.95	108.31	123.394	0.1335	15.1055	108.363	123.602
9	0.165	17.586	127.065	144.817	0.162	20.537	127.591	148.289	0.16163	20.7333	127.612	148.507
10	0.196	23.391	147.085	170.672	0.192	27.005	147.056	174.252	0.19138	27.244	147.042	174.478

Table 6.6 Strain energy boundedness in a clamped-clamped shear-flexible beam (uniform load) - FC formulation, Large deflection analysis

The sweep-test is conducted on similar lines as explained in section 5.2.6, and the results are shown in Fig. 6.13 for hinged-hinged beam which shows the boundedness of the strain energy for all load cases. Fig. 6.14 shows the results of the sweep-test for a pinned-pinned beam which also shows the boundedness of the strain energy for all load cases. The results of the sweep-test for a clamped-clamped beam are shown in Fig. 6.15, which is on similar lines as that of pinned-pinned and hinged-hinged cases.

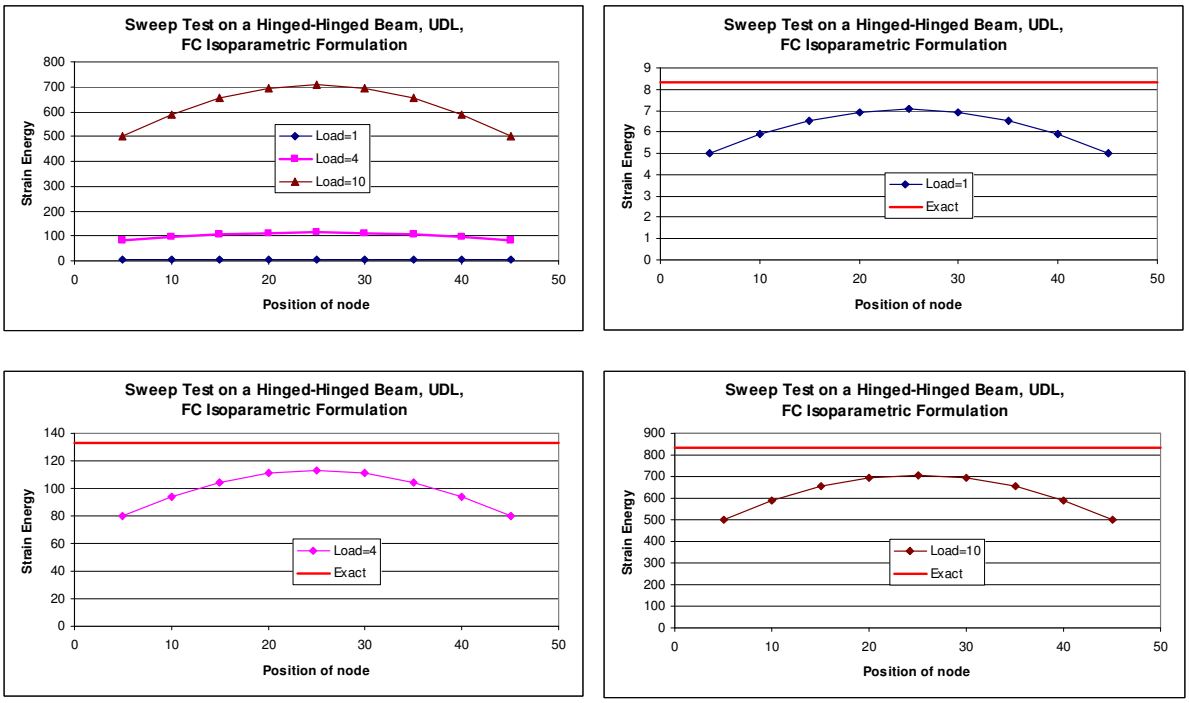

Fig. 6.13 Sweep-Test in a hinged-hinged shear-flexible beam (uniform load) - FC formulation, Large deflection analysis

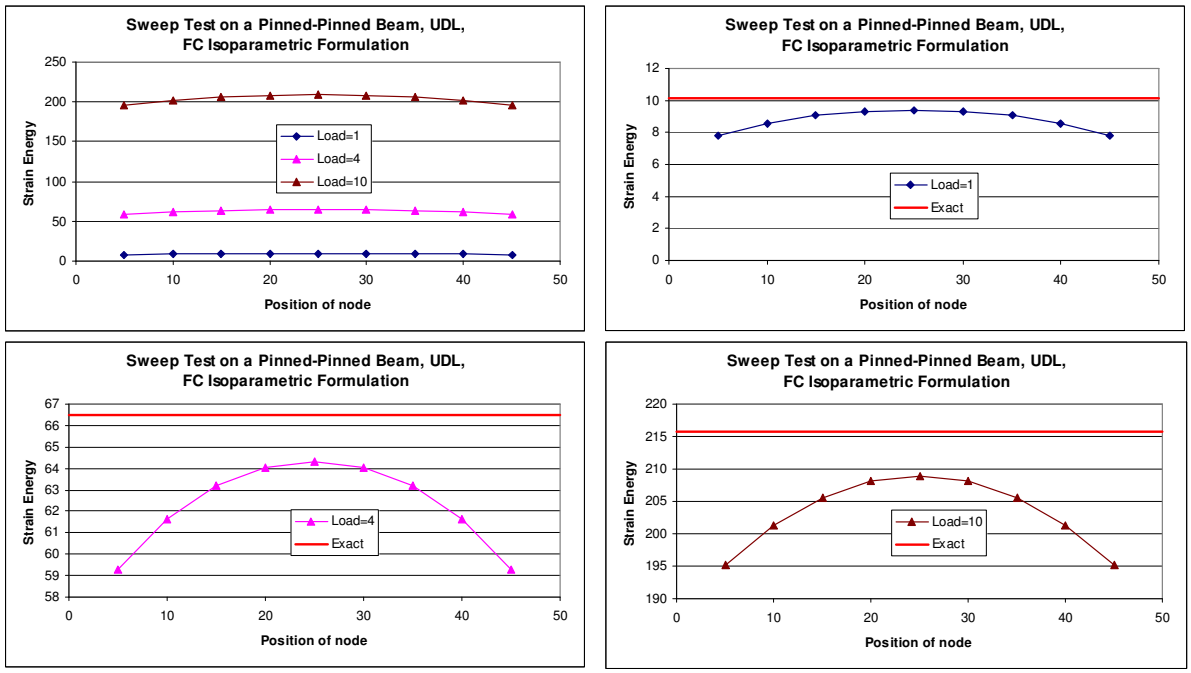

Fig. 6.14 Sweep-Test in a pinned-pinned shear-flexible beam (uniform load) - FC formulation, Large deflection analysis

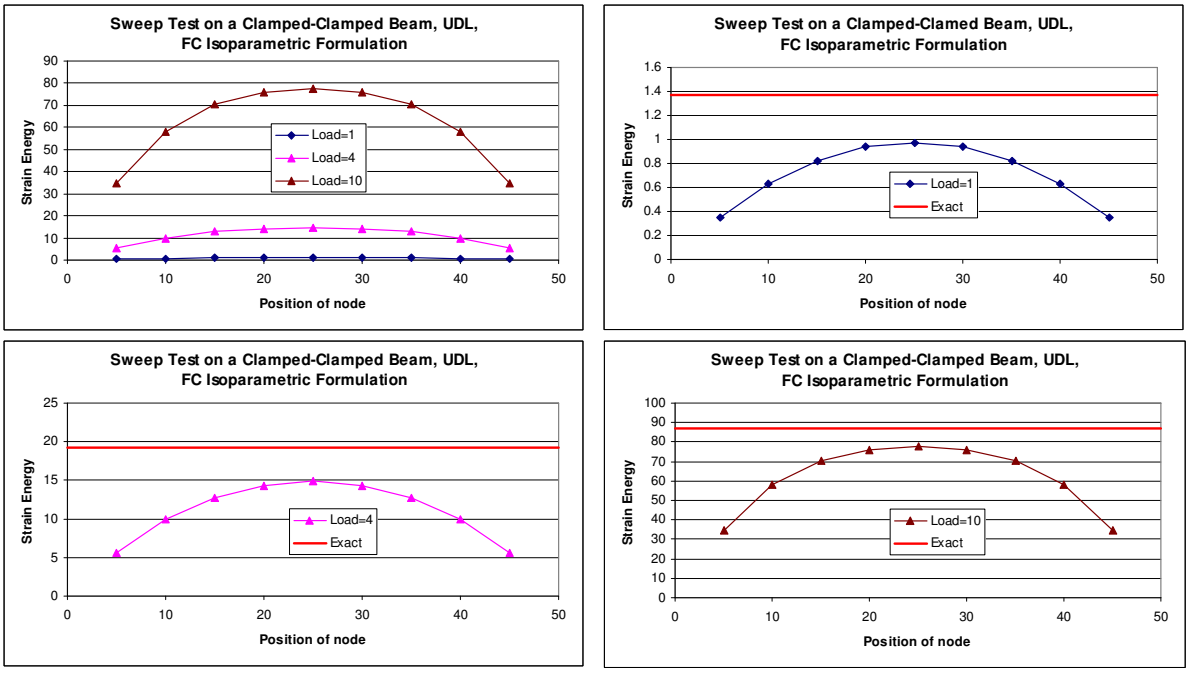

Fig. 6.15 Sweep-Test in a clamped-clamped shear-flexible beam (uniform load) - FC formulation, Large deflection analysis

6.3. Large Deformation Analysis of Beams - Anisoparametric Formulation

The anisoparametric element formulation has already been explained in sections 2.3, 4.2.5, and is briefly recaptured here without getting into details. This is a 2-noded element, with 4 degrees of freedom at each of the nodes (axial displacement u, transverse deflection w, derivative of the transverse deflection β, and independent slope θ_x). The reason for choosing an additional degree of freedom derivative of the transverse deflection β, is to have a higher order interpolation function for the transverse deflection w which now has cubic interpolation functions, and hence the anisoparametric formulation results (the other two variables, u and θ_x will have linear interpolation functions).

For the aniosparametric formulation, the two strain terms that have the multiple fields are studied carefully using the following notation

$$\begin{aligned} u &= a_0 + a_1\xi \\ \theta &= c_0 + c_1\xi \\ \frac{dw}{dx} &= b_0 + b_1\xi + b_2\xi^2 \end{aligned} \qquad \ldots(6.9)$$

The strain energy arising from the 3 strain components, shear strain energy U_s, membrane strain energy U_m, and bending strain energy U_b, are as follows

$$U = U_s + U_m + U_b \qquad \ldots(6.10)$$

The field-consistent representation of the shear strain was already discussed in detail in section 2.7. The field-consistent strain terms for anisoparametric formulation was explained in section 2.3.3. It is of interest to note that there are 2 field-consistencies that are ensured in this formulation – shear and membrane. The field-consistent shear term is explained in section 2.3.2, and for a straight

beam problem, the field-inconsistent shear term is innocuous and does not produce any spurious constraint. As a result, the use of full or reduced integration for the shear terms does not result in any significant impact on the displacements, as shown in Table 4.3 and 4.9. For the membrane strains, the field-consistency becomes more important as it has the potential to cause a spurious constraint as will be seen now.

6.3.1 Element Matrices

The element matrices remain similar to the matrices derived in section 6.2.4, as the nonlinear membrane strain terms remain the same in anisoparametric formulation as well. The additional degree of freedom for the anisoparametric element was actually considered in the derivations there.

6.3.2 Numerical Experiments and Discussion

The above formulations are now used for studying a hinged-hinged, pinned-pinned and clamped-clamped beam on similar lines of section 5.2. Table 6.7 shows the deflection at the centre of a shear-flexible hinged-hinged beam, where there is no nonlinearity. The results simulate this linear behaviour accurately. The axial force is shown in Fig. 6.16, and can be seen to be zero for all the load cases.

Shear Flexible Hinged-Hinged Beam, UDL, Anisoparametric FC Formulation						
Load	2 Element	4 Element	8 Element	16 Element	32 Element	Theory
1	0.49487847	0.51440972	0.51929253	0.52051324	0.52081841	0.5208
2	0.98975695	1.02881944	1.03858507	1.04102648	1.04163683	1.0416
3	1.48463542	1.54322917	1.5578776	1.56153971	1.56245524	1.5624
4	1.97951389	2.05763889	2.07717014	2.08205295	2.08327365	2.0832
5	2.47439236	2.57204861	2.59646267	2.60256619	2.60409207	2.604
6	2.96927084	3.08645833	3.11575521	3.12307943	3.12491048	3.1248
7	3.46414931	3.60086806	3.63504774	3.64359267	3.6457289	3.6456
8	3.95902778	4.11527778	4.15434028	4.1641059	4.16654731	4.1664
9	4.45390625	4.6296875	4.67363281	4.68461914	4.68736572	4.6872
10	4.94878473	5.14409722	5.19292535	5.20513238	5.20818414	5.208

Table 6.7 Deflection at the center of a hinged-hinged shear-flexible beam (uniform load) - FC Anisoparametric formulation, Large deflection analysis

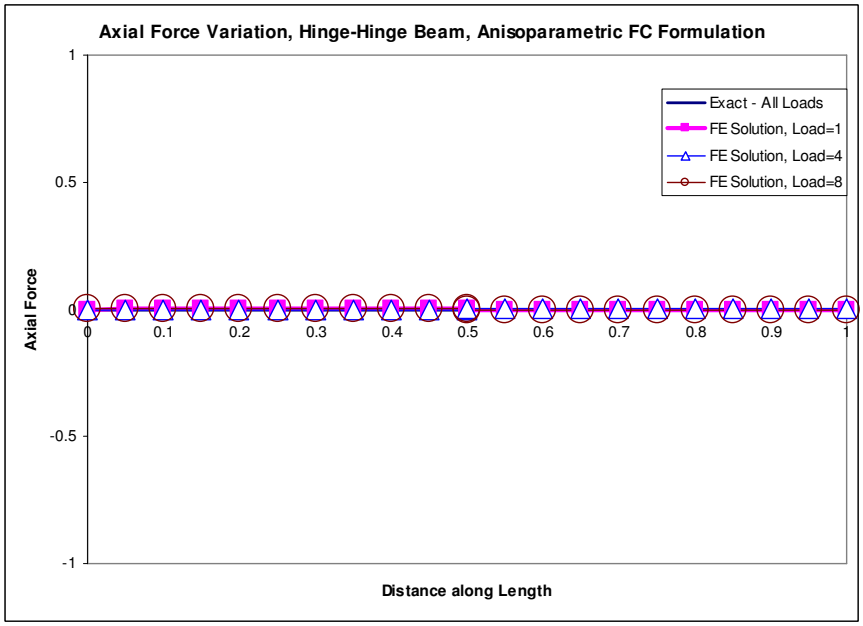

Fig. 6.16 Axial force in a hinged-hinged shear-flexible beam (uniform load)- FC Anisoparametric formulation, Large deflection analysis

The bending moment is shown in Fig. 6.17, and in this case the bending moment is a best-fit, and can be seen both pictorially in Fig. 6.17 and can be proven analytically.

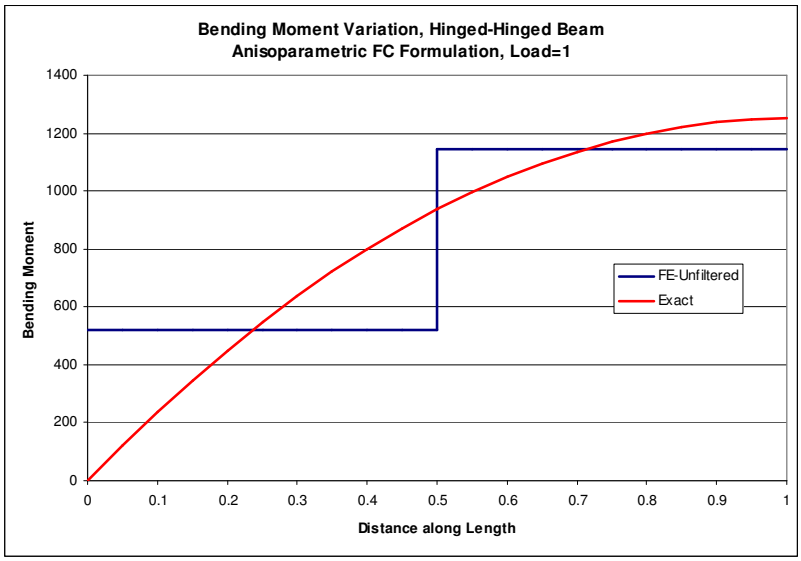

Fig. 6.17 Bending moment in a hinged-hinged shear-flexible beam (uniform load) - FC Anisoparametric formulation, Large deflection analysis

For the pinned-pinned case, the deflection at the centre of the beam is tabulated in Table 6.8 for all the load cases. The exact solution corresponds to the solution obtained from a commercial finite element software ANSYS® (2008), where the beam was discretised into a large number of elements (in this case it was 1000 elements of BEAM3 element).

Shear Felxible Beam, 2-Noded Anisoparamteric, Pinned-Pinned Beam, UDL, FC formulation						
Load	2 Element	4 Element	8 Element	16 Element	32 Element	Exact
1	0.36001996	0.36650394	0.36799775	0.3683635	0.36845446	0.368467
2	0.53812584	0.54378255	0.54500579	0.54530039	0.54537335	0.545397
3	0.65778395	0.66263923	0.66363019	0.66386506	0.66392298	0.663958
4	0.7502228	0.75442431	0.75523302	0.75542137	0.75546761	0.755514
5	0.82666984	0.83032276	0.83098304	0.83113373	0.83117052	0.831228
6	0.89247073	0.89564959	0.89618505	0.89630421	0.89633311	0.896402
7	0.95061254	0.95337263	0.95380064	0.95389279	0.95391492	0.953996
8	1.00294542	1.00532959	1.0056635	1.00573208	1.00574832	1.005841
9	1.05070077	1.05274338	1.05299379	1.05304154	1.05305257	1.053156
10	1.09474286	1.09647221	1.09664777	1.09667691	1.09668329	1.096799

Table 6.8 Deflection at the center of a pinned-pinned shear flexible beam (uniform load)-FC Anisoparametric formulation, Large deflection analysis

The axial force for this case is shown in Fig. 6.18, and bending moment in Fig. 6.19. In the absence of a theoretical exact solution for the axial force and bending moment for a pinned-pinned beam, the best-fit rule is not evaluated here.

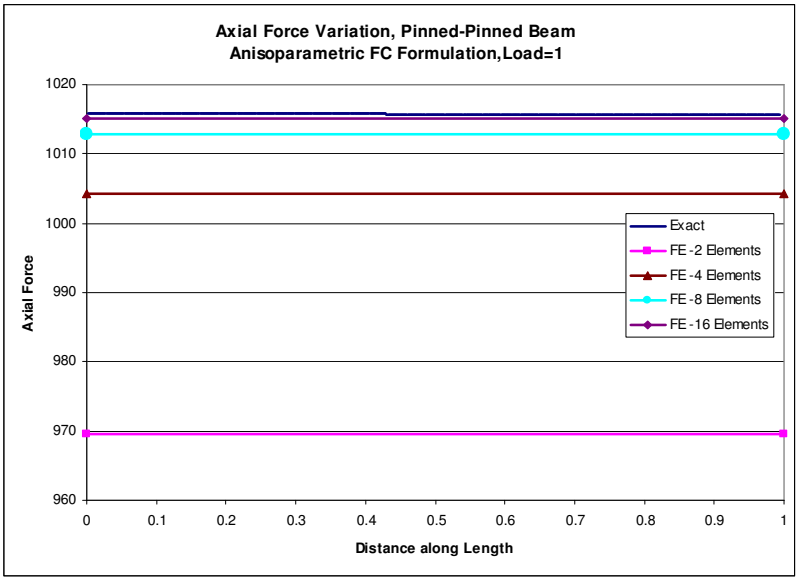

Fig. 6.18 Axial force in a pinned-pinned shear-flexible beam (uniform load)-FC Anisoparametric formulation, Large deflection analysis

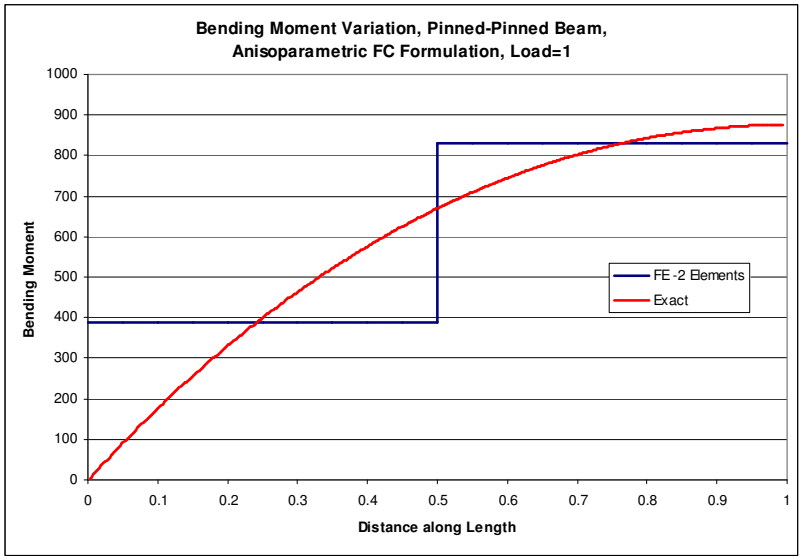

Fig. 6.19 Bending Moment in a pinned-pinned shear-flexible beam (uniform load)- FC Anisoparametric formulation, Large deflection analysis

The deflection in a clamped-clamped beam is shown in Table 6.9 for all the load cases. Here again, the exact solution is from ANSYS® (2008) (BEAM3 element). It can be seen that the results from a relatively less number of elements form the anisoparametric element match closely with ANSYS® (2008) results. The axial force in the beam is shown in Fig. 6.20 for various load cases. Fig. 6.21 shows the bending moment in the beam along the length.

Shear Felxible Beam, 2-Noded Anisoparamteric, Clamped-Clamped Beam, UDL, FC						
Load	2 Element	4 Element	8 Element	16 Element	32 Element	Exact
1	0.07789669	0.0970903	0.10185769	0.10304731	0.10334457	0.103362
2	0.1539893	0.19055105	0.19948243	0.20170076	0.20225442	0.202282
3	0.22685274	0.27791641	0.29013173	0.29314917	0.29390123	0.293941
4	0.29562423	0.35818515	0.37285028	0.37645531	0.37735275	0.377408
5	0.35996601	0.43141572	0.44788111	0.45191375	0.45291676	0.452975
6	0.41991393	0.49819812	0.51600307	0.52035293	0.52143422	0.521501
7	0.47571876	0.55929465	0.57812493	0.58271854	0.58386006	0.583934
8	0.52772863	0.61545939	0.63510286	0.63989172	0.64108164	0.641165
9	0.57631702	0.66736726	0.68768005	0.69263197	0.69386247	0.693951
10	0.62184447	0.71559646	0.73647986	0.74157322	0.74283906	0.742934

Table 6.9 Deflection at the center of a clamped-clamped shear flexible beam (uniform load) FC Anisoparametric formulation, Large deflection analysis

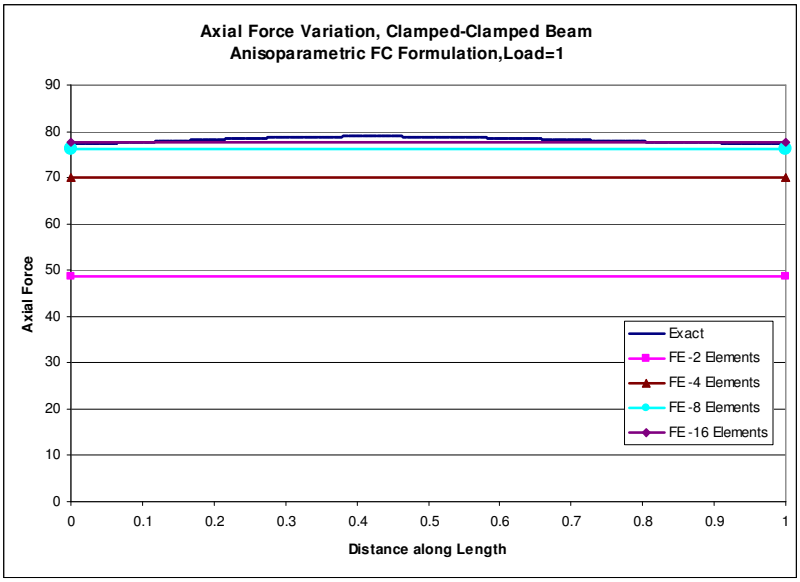

Fig. 6.20 Axial force in a clamped-clamped shear-flexible beam (uniform load) FC Anisoparametric formulation, Large deflection analysis

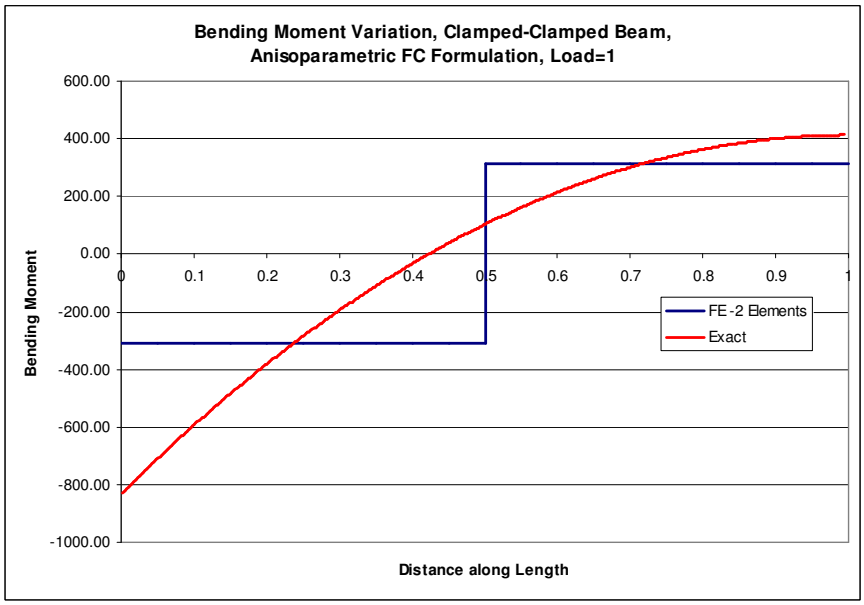

Fig. 6.21 Bending moment in a clamped-clamped shear-flexible beam (uniform load), FC Anisoparametric formulation, Large deflection analysis

The convergence of the displacements in a hinged-hinged beam are shown in Fig. 6.22. Since there is no nonlinearity in this case, the displacement convergence is shown only for the linear case and is of $O(h^2)$, as expected. This

is also independent of the load. The convergence of displacements for pinned-pinned beam and clamped-clamped beam are shown in Fig. 6.23 and Fig. 6.24.

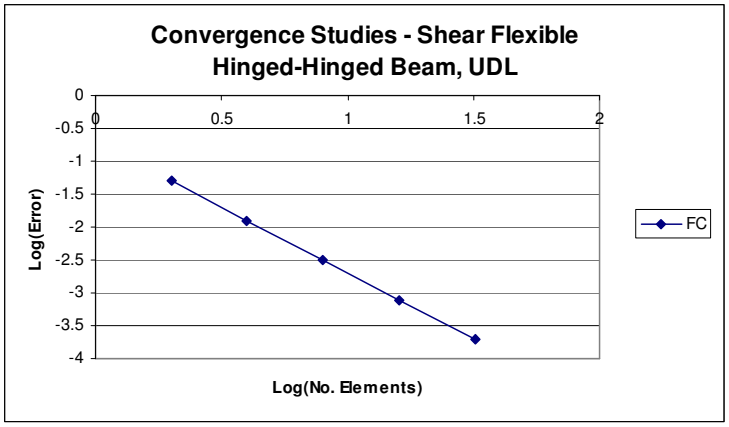

Fig. 6.22 Convergence of displacement in a hinged-hinged shear flexible beam (uniform load) FC Anisoparametric formulation, Large deflection analysis

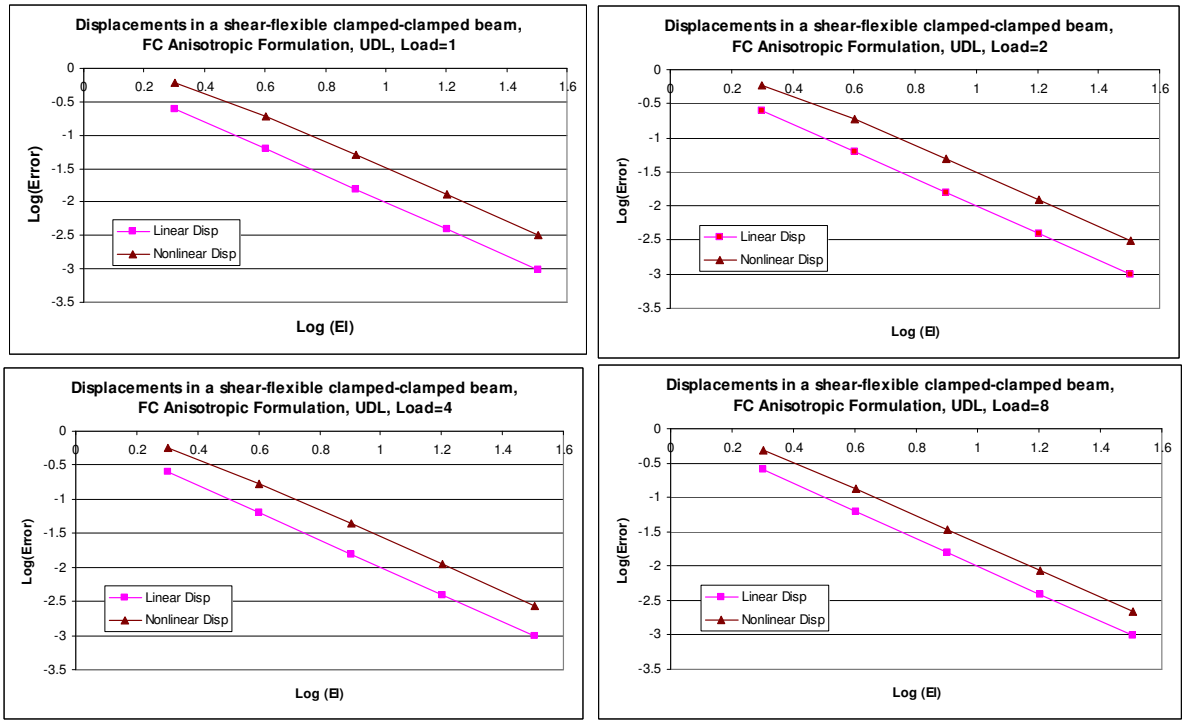

Fig. 6.23 Convergence of displacement in a pinned-pinned shear flexible beam (uniform load) FC Anisoparametric formulation, Large deflection analysis

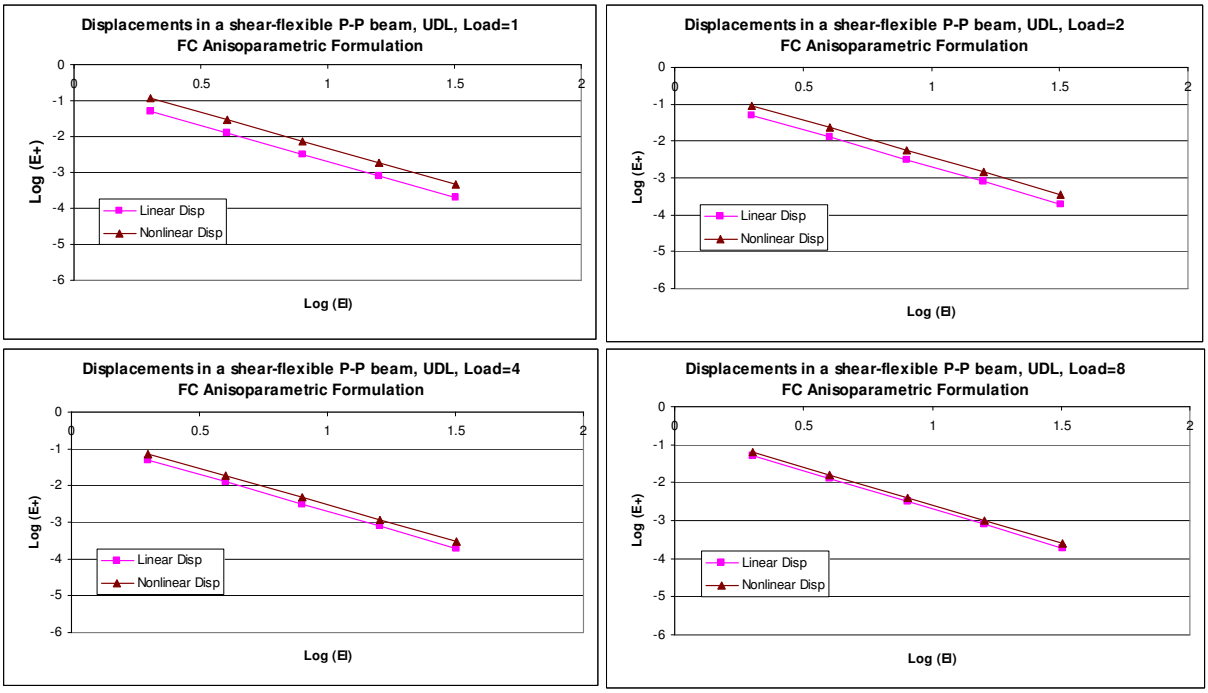

Fig. 6.24 Convergence of displacement in a clamped-clamped shear flexible beam (uniform load) FC Anisoparametric formulation, Large deflection analysis

The strain energy in a hinged-hinged beam for various load cases and element discretisations is tabulated in Table 6.10. It can be seen clearly that the total strain energy remains bounded for all the load cases.

Strain Energy for Hinged-Hinged Beam, Uniform Load, Field-Consistent Anisoparametric Formulation												
Load	Elements=4				Elements=16				Elements=512			
	Shear	Memb.	Bend.	Total	Shear	Memb.	Bend.	Total	Shear	Memb.	Bend.	Total
1	0.003	0.000	16.452	16.455	0.003	0.000	16.653	16.656	0.003	0.000	16.667	16.670
2	0.012	0.000	65.809	65.821	0.012	0.000	66.612	66.624	0.012	0.000	66.667	66.678
3	0.026	0.000	148.071	148.097	0.026	0.000	149.878	149.904	0.026	0.000	150.000	150.026
4	0.046	0.000	263.238	263.284	0.046	0.000	266.450	266.496	0.046	0.000	266.666	266.713
5	0.072	0.000	411.309	411.381	0.072	0.000	416.328	416.400	0.072	0.000	416.666	416.739
6	0.104	0.000	592.285	592.389	0.104	0.000	599.512	599.616	0.104	0.000	600.000	600.104
7	0.142	0.000	806.166	806.308	0.142	0.000	816.003	816.144	0.142	0.000	816.666	816.808
8	0.185	0.000	1052.951	1053.137	0.185	0.000	1065.799	1065.984	0.185	0.000	1066.666	1066.851
9	0.234	0.000	1332.642	1332.876	0.234	0.000	1348.902	1349.137	0.234	0.000	1349.999	1350.233
10	0.289	0.000	1645.237	1645.526	0.289	0.000	1665.311	1665.601	0.289	0.000	1666.665	1666.955

Table 6.10 Strain energy boundedness in a hinged-hinged beam (uniform load)-FC Anisoparametric formulation, Large deflection analysis

For the pinned-pinned beam the shear strain energy and the bending strain energy converge from above for all load cases, as seen in Table 6.11. For the clamped-clamped case, it can be seen from Table 6.12 that the shear strain energy converges from above, and the bending and membrane strain energy converge from below. The reason for the above behaviour is attributed to the exclusion of higher-order Legendre terms in the field-consistent formulation.

Strain Energy for Shear-Flexible Pinnned-Pinned Beam, Field-Consistent Anisoparametric Formulation												
Load	Elements=4				Elements=16				Elements=512			
	Shear	Memb.	Bend.	Total	Shear	Memb.	Bend.	Total	Shear	Memb.	Bend.	Total
1	0.001	1.681	8.381	10.063	0.001	1.717	8.373	10.092	0.001	1.720	8.372	10.093
2	0.003	8.191	18.527	26.721	0.003	8.299	18.432	26.734	0.003	8.306	18.426	26.735
3	0.005	18.145	27.616	45.766	0.005	18.322	27.429	45.756	0.005	18.334	27.417	45.756
4	0.007	30.609	35.917	66.533	0.007	30.851	35.645	66.503	0.007	30.867	35.627	66.501
5	0.008	45.070	43.643	88.722	0.008	45.373	43.290	88.672	0.008	45.394	43.267	88.669
6	0.010	61.208	50.926	112.144	0.010	61.570	50.497	112.076	0.010	61.594	50.469	112.072
7	0.011	78.800	57.857	136.668	0.011	79.219	57.354	136.583	0.011	79.247	57.321	136.578
8	0.013	97.684	64.496	162.193	0.012	98.157	63.923	162.093	0.012	98.189	63.886	162.087
9	0.014	117.735	70.891	188.640	0.014	118.261	70.250	188.525	0.014	118.297	70.208	188.519
10	0.016	138.853	77.076	215.944	0.015	139.432	76.368	215.815	0.015	139.471	76.322	215.808

Table 6.11 Strain energy boundedness in a pinned-pinned beam (uniform load)- FC Anisoparametric formulation, Large deflection analysis

Strain Energy for Clamped-Clamped Beam, Uniform Load, Field-Consistent Anisoparametric Formulation												
Load	Elements=4				Elements=16				Elements=512			
	Shear	Memb.	Bend.	Total	Shear	Memb.	Bend.	Total	Shear	Memb.	Bend.	Total
1	0.003	0.008	2.531	2.542	0.003	0.010	2.724	2.737	0.003	0.010	2.737	2.750
2	0.011	0.122	9.762	9.894	0.011	0.148	10.457	10.616	0.011	0.150	10.504	10.665
3	0.024	0.551	20.810	21.385	0.024	0.660	22.159	22.843	0.024	0.667	22.248	22.940
4	0.041	1.520	34.663	36.224	0.041	1.794	36.687	38.521	0.041	1.813	36.820	38.674
5	0.061	3.201	50.446	53.708	0.060	3.726	53.104	56.891	0.060	3.762	53.279	57.102
6	0.084	5.698	67.505	73.287	0.083	6.551	70.746	77.381	0.083	6.610	70.959	77.651
7	0.109	9.059	85.386	94.554	0.107	10.306	89.168	99.582	0.107	10.391	89.416	99.914
8	0.136	13.295	103.784	117.216	0.134	14.991	108.080	123.205	0.134	15.106	108.363	123.602
9	0.166	18.398	122.494	141.058	0.162	20.587	127.295	148.043	0.162	20.733	127.612	148.507
10	0.197	24.345	141.382	165.923	0.192	27.063	146.689	173.944	0.191	27.244	147.042	174.477

Table 6.12 Strain energy boundedness in a clamped-clamped beam (uniform load)- FC Anisoparametric formulation, Large deflection analysis

The results of the sweep-test for a hinged-hinged beam are shown in Fig. 6.25, where the strain energy remains bounded for all the load cases. For the pinned-pinned beam, the results of the sweep-test are shown in Fig. 6.26, and as discussed in the preceding paragraph, the convergence is not from below (and hence not bounded) for all the load cases. The results of the sweep-test for the

clamped-clamped beam are shown in Fig. 6.27 and the total strain energy is bounded.

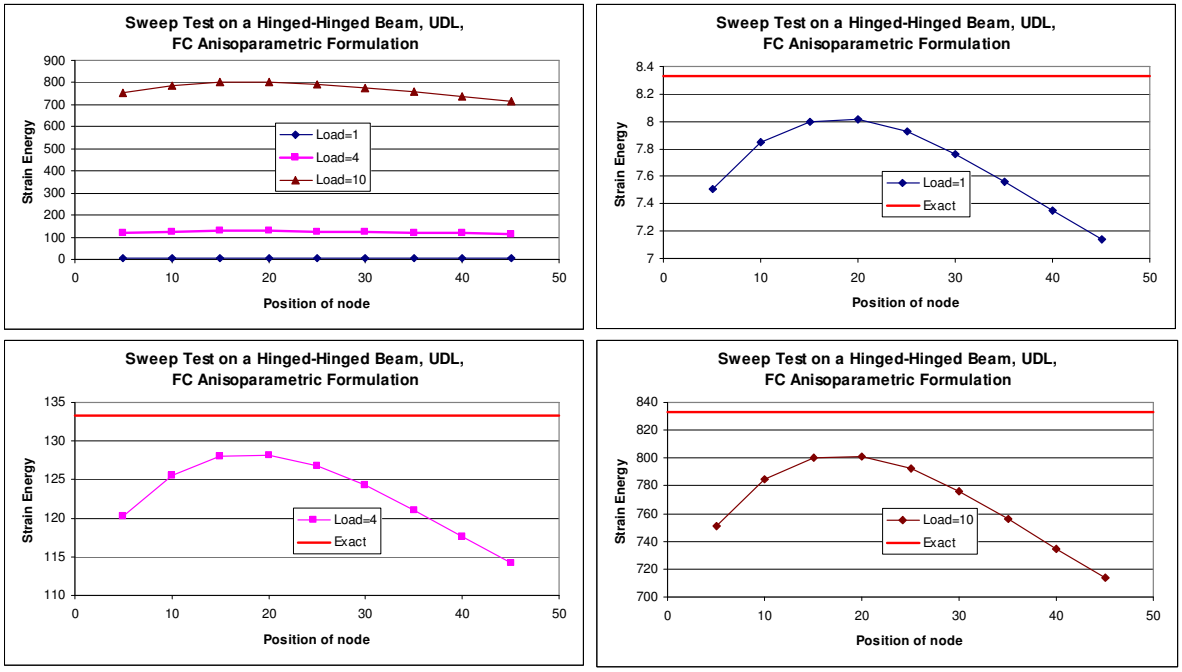

Fig. 6.25 Sweep-Test in a hinged-hinged shear-flexible beam (uniform load)- FC Anisoparametric formulation, Large deflection analysis

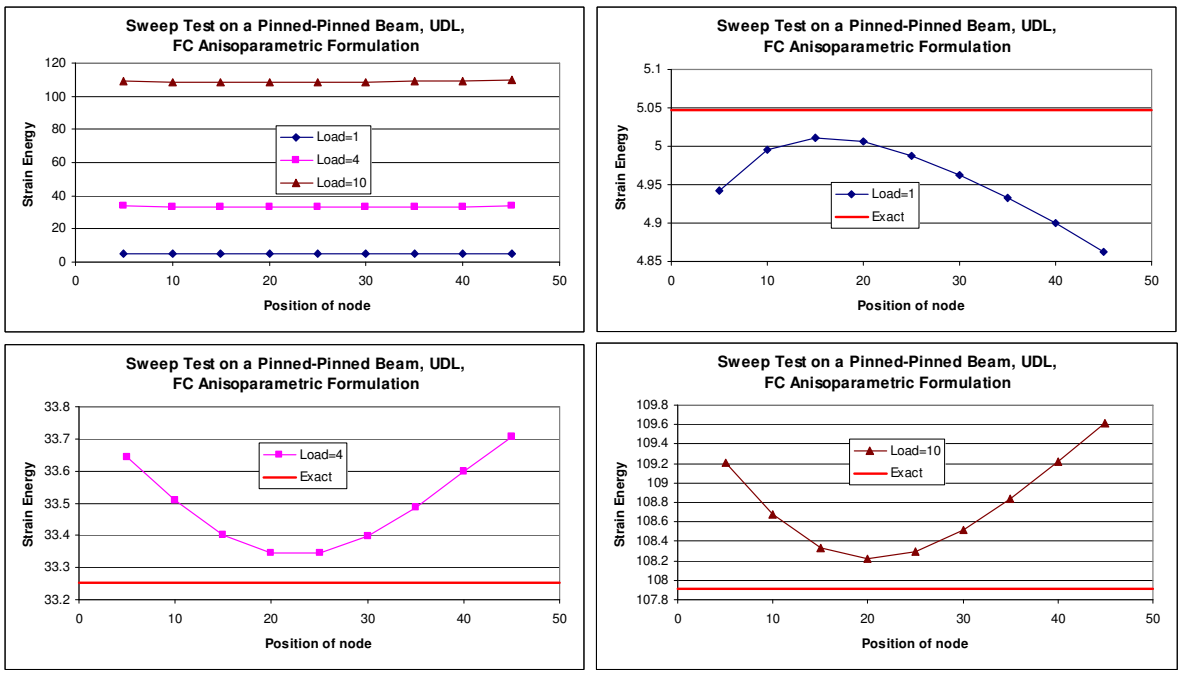

Fig. 6.26 Sweep-Test in a pinned-pinned shear-flexible beam (uniform load)- FC Anisoparametric formulation, Large deflection analysis

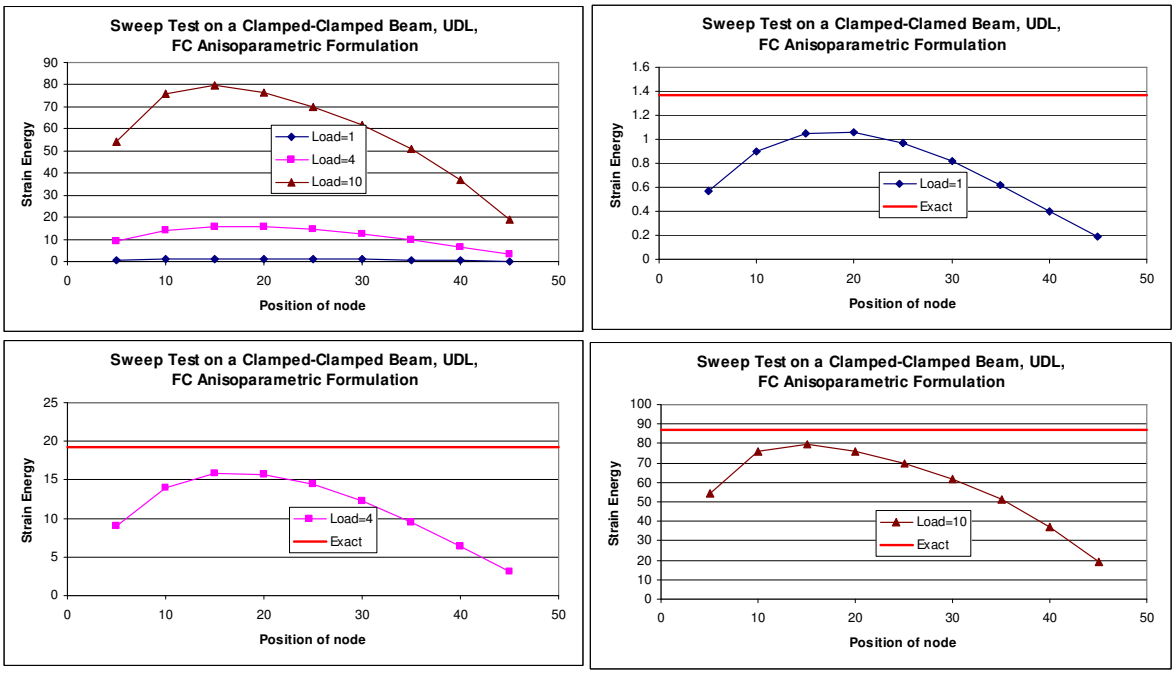

Fig. 6.27 Sweep-Test in a clamped-clamped shear-flexible beam (uniform load)- FC Anisoparametric formulation, Large deflection analysis

The anisoparametric formulation for large deflection problems makes a good case for detailed study of impact of selective integration, which has been historically used to overcome the problem of shear locking. For large deflection problems, it has already been shown in section 2.3.3 that membrane locking occurs due to field-inconsistent membrane strains. This is typically overcome through use of reduced integration. In the present study, full and reduced/selective integration are used for the large deflection analysis of anisoparametric shear flexible beams. Here, the nonlinear incremental matrices, $[K^{N1}]$ and $[K^{N2}]$, are computed using full and reduced/selective integration. This results in the following four cases for the formulation of the stiffness matrices (which includes both linear and nonlinear strains).

1. Full integration for the linear shear strain, and full integration for the nonlinear membrane strain.
2. Reduced integration for the linear shear strain, and full integration for the nonlinear membrane strain.
3. Full integration for the linear shear strain, and reduced integration for the nonlinear membrane strain.
4. Reduced integration for the linear shear train, and reduced integration for the nonlinear membrane strain.

For the present case of anisoparametric beam element, full integration for the linear shear strain terms requires 3-point Gaussian quadrature. For reduced integration for the linear shear stress terms, 2-point Gaussian quadrature is used. For the nonlinear membrane strain terms, full integration requires use of 4-point Gaussian quadrature for evaluating $[K^{N1}]$, and 5-point Gaussian quadrature for evaluating $[K^{N2}]$, while for reduced integration 1-point Gaussian quadrature is used for evaluating both $[K^{N1}]$ and $[K^{N2}]$. The examples of a hinged-hinged beam, pinned-pinned beam, and clamped-clamped beam will now be used for the studying the 4 cases of the different numerical integration schemes that were explained in the preceding paragraph.

The results for the displacement in a hinged-hinged beam for the above 4 cases are shown in Table 6.13. The results from cases 3, 4 and field-consistent formulations are very close, as expected (The impact of using either full integration or reduced integration on the shear strain terms for this anisoparametric beam element is insignificant, as it does not generate any spurious constraint, unlike the case for membrane strain where there is a spurious constraint which needs to be relieved only by reduced integration or field-consistent formulation). It can be observed that the effect of the load on the displacement at the center of the beam is not linear, for cases 1 and 2 where full integration is employed for membrane strains. This is in violation of the physics of the hinged-hinged beam, where there is no axial force and hence no nonlineartiy

is to be expected. This nonlinearity is primarily caused due to the use of full integration for the membrane strain terms which generates a spurious axial force as shown in Fig. 6.28. The stress oscillations also can be seen in Fig. 6.28. Cases 1 and 2 are seen to follow a similar trend, and cases 3 and 4 follow a similar trend. This is expected as the impact of reduced or full integration on the shear terms is minimal. Similar behaviour is seen in the bending moment plot shown in Fig. 6.29.

Comparison of Deflection at the centre of a Hinged-Hinged Beam, 8 Elements						
Load	S-FI, M-FI	S-RI, M-FI	S-FI, M-RI	S-RI, M-RI	FC	Theory
1	0.516619	0.516621	0.519293	0.519293	0.519293	0.520800
2	1.018249	1.018294	1.038585	1.038585	1.038585	1.041600
3	1.494247	1.494485	1.557877	1.557878	1.557878	1.562400
4	1.939638	1.940320	2.077169	2.077170	2.077170	2.083200
5	2.353812	2.355205	2.596460	2.596463	2.596463	2.604000
6	2.738579	2.740902	3.115751	3.115755	3.115755	3.124800
7	3.096722	3.100125	3.635041	3.635048	3.635048	3.645600
8	3.431204	3.435774	4.154331	4.154340	4.154340	4.166400
9	3.744805	3.750580	4.673619	4.673633	4.673633	4.687200
10	4.039991	4.046977	5.192906	5.192925	5.192925	5.208000

Table 6.13 Deflection at the center of a hinged-hinged shear flexible beam (uniform load) – Comparison of Anisoparametric formulations, Large deflection analysis

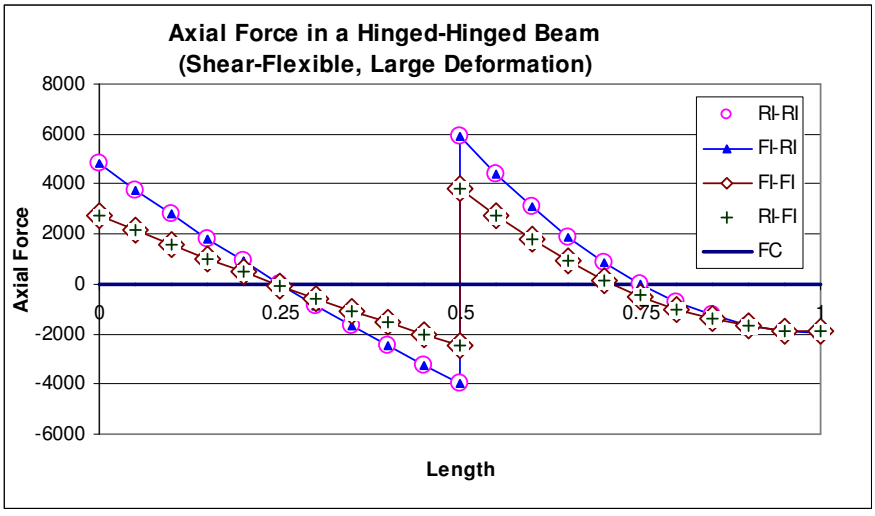

Fig. 6.28 Axial force in a hinged-hinged shear-flexible beam (uniform load) – Comparison of Anisoparametric formulations, Large deflection analysis

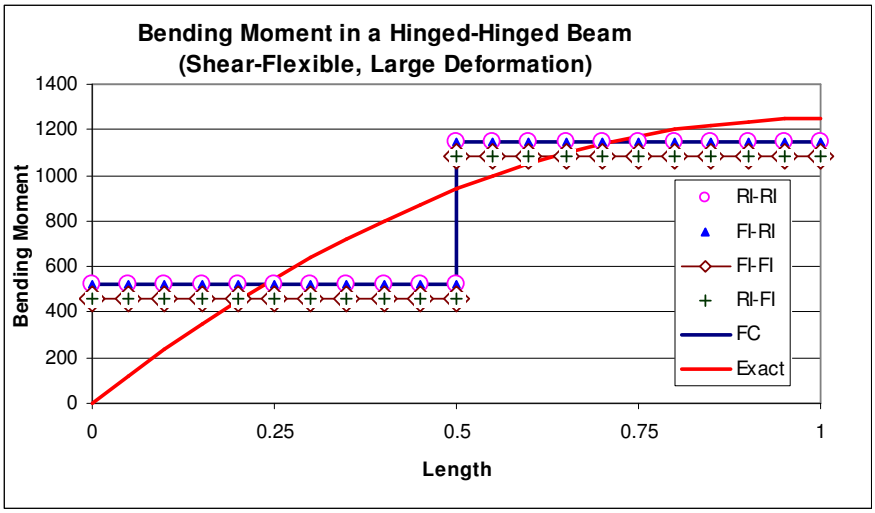

Fig. 6.29 Bending moment in a hinged-hinged shear-flexible beam (uniform load) – Comparison of Anisoparametric formulations, Large deflection analysis

The displacements in a pinned-pinned beam are shown in Table 6.14. It is interesting to note that case-4 gives higher displacements due to use of reduced integration for both shear and membrane strain terms (which causes a softening effect leading to higher displacements).

Comparison of Deflection at the centre of a Pinned-Pinned Beam, 8 Elements						
Load	S-FI, M-FI	S-RI, M-FI	S-FI, M-RI	S-RI, M-RI	FC	Theory
1	0.367578461	0.367578676	0.368452018	0.369536302	0.36799775	0.368467
2	0.544220181	0.544220972	0.545936322	0.550633704	0.54500579	0.545397
3	0.662623499	0.662624953	0.664918939	0.674262096	0.66363019	0.663958
4	0.754077782	0.754079906	0.756818846	0.771298294	0.75523302	0.755514
5	0.829721546	0.829724321	0.832829406	0.852733908	0.83098304	0.831228
6	0.894844764	0.894848164	0.898267593	0.923789186	0.89618505	0.896402
7	0.952400737	0.95240473	0.956101911	0.987378514	0.95380064	0.953996
8	1.004218026	1.004222581	1.008170329	1.045306364	1.0056635	1.005841
9	1.051513433	1.05151852	1.055695882	1.098773492	1.05299379	1.053156
10	1.095140873	1.095146462	1.09953683	1.148622549	1.09664777	1.096799

Table 6.14 Deflection at the center of a pinned-pinned shear flexible beam (uniform load) – Comparison of Anisoparametric formulations, Large deflection analysis

The axial force and bending moment plots are shown in Fig. 6.30 and Fig. 6.31. Once again cases 1,2 and cases 3,4 show similar trends.

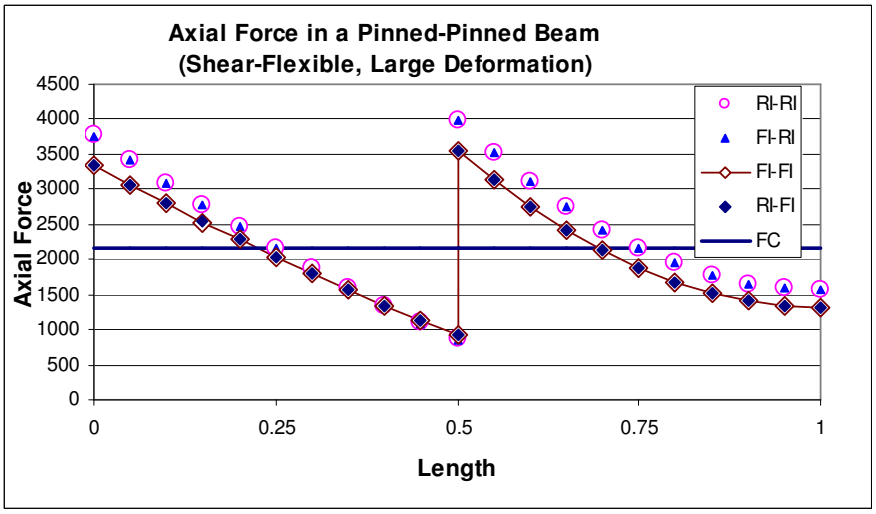

Fig. 6.30 Axial force in a pinned-pinned shear-flexible beam (uniform load) – Comparison of Anisoparametric formulations, Large deflection analysis

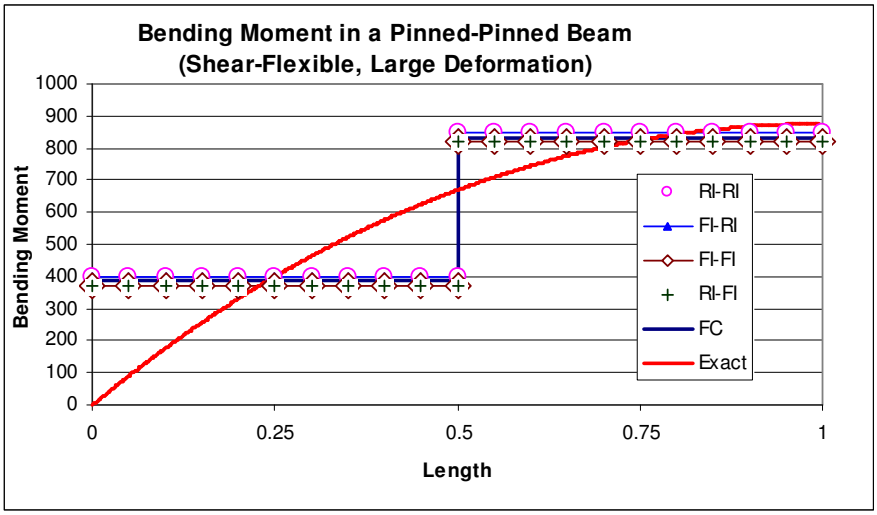

Fig. 6.31 Bending moment in a pinned-pinned shear-flexible beam (uniform load) – Comparison of Anisoparametric formulations, Large deflection analysis

The deflection in a clamped-clamped beam is tabulated in Table 6.15. The axial force is shown in Fig. 6.32 and the bending moment in Fig. 6.33. There is very

little difference between the 4 cases, as the stiffening axial force that is generated is very less compared to a pinned-pinned beam.

Comparison of Deflection at the centre of a Clamped-Clamped Beam, 8 Elements						
Load	S-FI, M-FI	S-RI, M-FI	S-FI, M-RI	S-RI, M-RI	FC	Theory
1	0.101837	0.101840	0.101875	0.101877	0.101858	0.103362
2	0.199352	0.199357	0.199620	0.199623	0.199482	0.202282
3	0.289771	0.289779	0.290529	0.290549	0.290132	0.293941
4	0.372164	0.372175	0.373626	0.373703	0.372850	0.377408
5	0.446812	0.446828	0.449112	0.449304	0.447881	0.452975
6	0.514528	0.514548	0.517731	0.518107	0.516003	0.521501
7	0.576242	0.576265	0.580366	0.580995	0.578125	0.583934
8	0.632821	0.632849	0.637859	0.638808	0.635103	0.641165
9	0.685016	0.685048	0.690944	0.692275	0.687680	0.693951
10	0.733451	0.733487	0.740241	0.742009	0.736480	0.742934

Table 6.15 Deflection at the center of a clamped-clamped shear flexible beam (uniform load) – Comparison of Anisoparametric formulations, Large deflection analysis

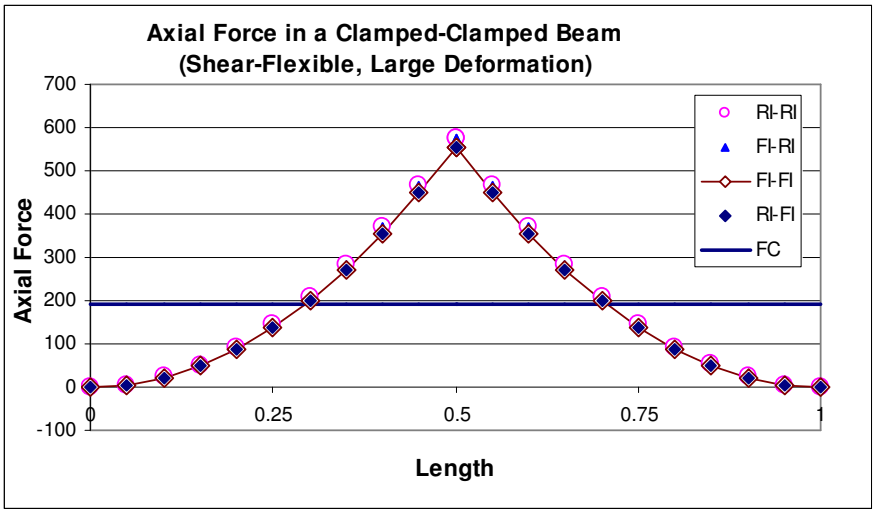

Fig. 6.32 Axial force in a clamped-clamped shear-flexible beam (uniform load) – Comparison of Anisoparametric formulations, Large deflection analysis

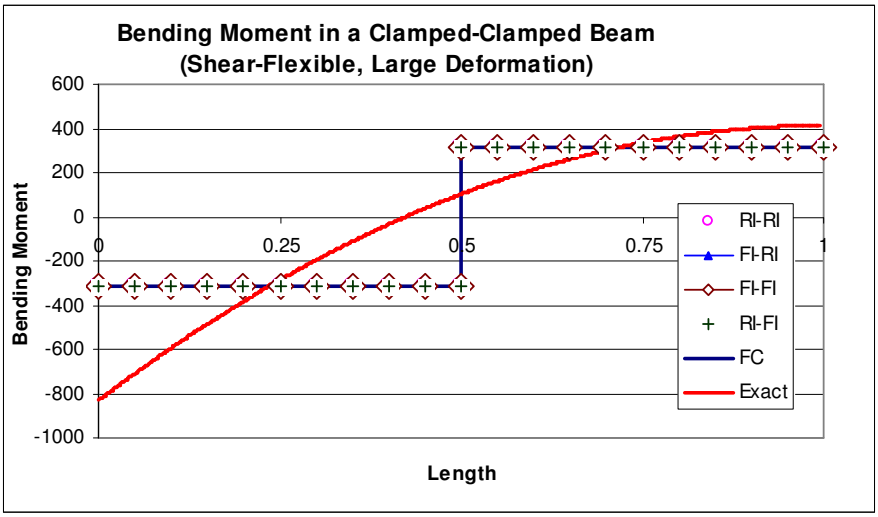

Fig. 6.33 Bending moment in a clamped-clamped shear-flexible beam (uniform load) – Comparison of Anisoparametric formulations, Large deflection analysis

The convergence of displacements for the hinged-hinged, pinned-pinned and clamped-clamped conditions are shown in Fig. 6.34, Fig. 6.35 and Fig. 6.36 respectively for load =10. Errors for cases 1 and 2 are higher due to use of full integration for the membrane strain terms. For the pinned-pinned beam, case-4, the errors are the highest (due to compounding of errors from use of reduced integration for both shear and membrane strains.

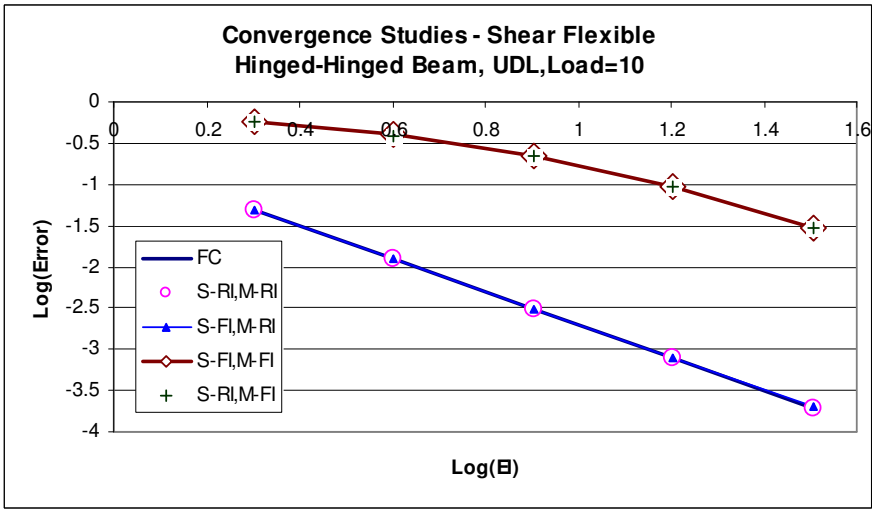

Fig. 6.34 Convergence of displacement in a hinged-hinged shear-flexible beam (uniform load) – Comparison of Anisoparametric formulations, Large deflection analysis

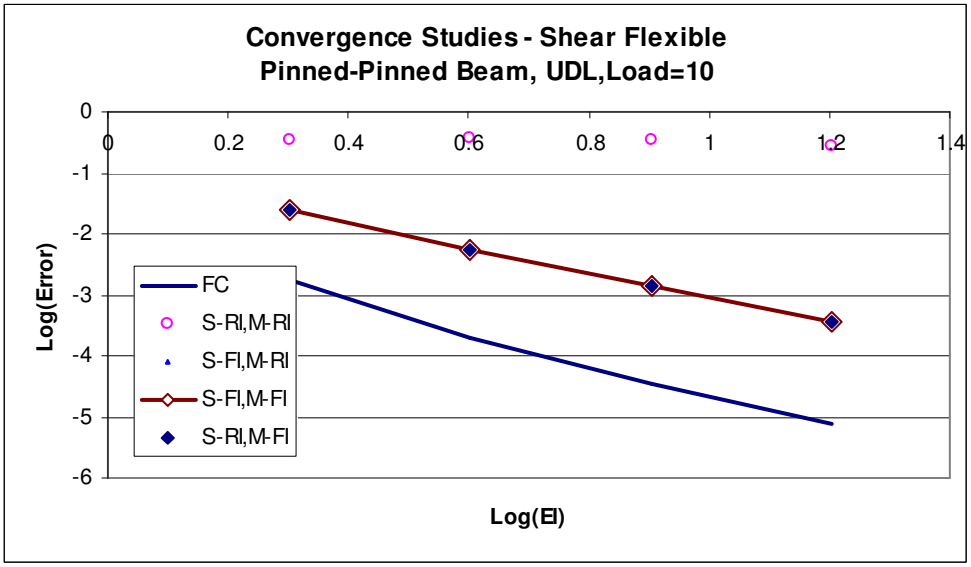

Fig. 6.35 Convergence of displacement in a pinned-pinned shear-flexible beam (uniform load) – Comparison of Anisoparametric formulations, Large deflection analysis

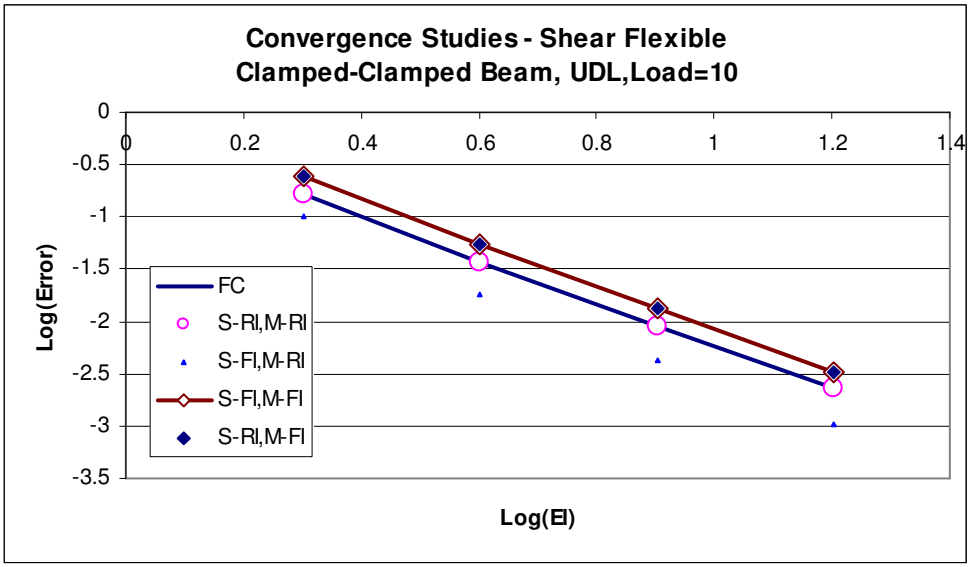

Fig. 6.36 Convergence of displacement in a clamped-clamped shear-flexible beam (uniform load) – Comparison of Anisoparametric formulations, Large deflection analysis

The boundedness of strain energy for the hinged-hinged beam are shown in Table 6.16. For all the four cases, the strain energy converges from below.

Strain Energy for H-H Beam, UDL, Shear-FI, Membrane-FI						
Load	2 El	4 El	8 El	16 El	32 El	Exact
1	7.192	7.982	8.241	8.311	8.329	8.333
2	24.167	29.638	32.215	33.041	33.263	33.333
3	46.087	60.862	70.043	73.613	74.651	75.000
4	70.939	98.616	119.446	129.151	132.243	133.333
5	97.837	141.107	178.309	198.585	205.703	208.333
6	126.323	187.281	244.903	280.754	294.622	300.000
7	156.129	236.478	317.898	374.490	398.526	408.333
8	187.081	288.255	396.286	478.682	516.892	533.333
9	219.056	342.296	479.306	592.302	649.165	675.000
10	251.965	398.365	566.375	714.433	794.766	833.333

Strain Energy for H-H Beam, UDL, Shear-RI, Membrane-FI						
Load	2 El	4 El	8 El	16 El	32 El	Exact
1	7.192	7.982	8.241	8.311	8.329	8.333
2	24.172	29.644	32.217	33.041	33.263	33.333
3	46.109	60.897	70.062	73.617	74.651	75.000
4	70.996	98.729	119.518	129.166	132.245	133.333
5	97.949	141.359	178.490	198.627	205.709	208.333
6	126.511	187.738	245.260	280.844	294.635	300.000
7	156.415	237.208	318.495	374.657	398.551	408.333
8	187.486	289.325	397.186	478.956	516.936	533.333
9	219.602	343.770	480.561	592.719	649.236	675.000
10	252.674	400.301	568.032	715.026	794.871	833.333

Strain Energy for H-H Beam, UDL, Shear-FI, Membrane-RI						
Load	2 El	4 El	8 El	16 El	32 El	Exact
1	7.922	8.228	8.308	8.328	8.333	8.333
2	31.690	32.911	33.231	33.312	33.332	33.333
3	71.302	74.049	74.770	74.952	74.998	75.000
4	126.759	131.642	132.924	133.248	133.329	133.333
5	198.061	205.690	207.693	208.200	208.327	208.333
6	285.208	296.194	299.078	299.807	299.990	300.000
7	388.199	403.152	407.078	408.071	408.320	408.333
8	507.035	526.566	531.693	532.990	533.315	533.333
9	641.716	666.434	672.923	674.564	674.976	675.000
10	792.241	822.757	830.768	832.794	833.302	833.333

Strain Energy for H-H Beam, UDL, Shear-RI, Membrane-RI						
Load	2 El	4 El	8 El	16 El	32 El	Exact
1	7.922	8.228	8.308	8.328	8.333	8.333
2	31.690	32.911	33.231	33.312	33.332	33.333
3	71.302	74.049	74.770	74.952	74.998	75.000
4	126.759	131.642	132.924	133.248	133.329	133.333
5	198.061	205.691	207.694	208.200	208.327	208.333
6	285.208	296.195	299.079	299.808	299.991	300.000
7	388.200	403.154	407.079	408.072	408.321	408.333
8	507.037	526.568	531.695	532.992	533.317	533.333
9	641.719	666.438	672.927	674.568	674.980	675.000
10	792.245	822.763	830.774	832.800	833.309	833.333

Table 6.16 Strain energy boundedness in a hinged-hinged shear flexible beam (uniform load) – Comparison of Anisoparametric formulations, Large deflection analysis

For the case of a pinned-pinned beam, the strain energy is summarized in Table 6.17. When reduced integration is used for the membrane strain terms, the strain energy converges from above. In fact when reduced integration is used for both shear and membrane strain terms, it was already seen in Table 6.14 that the displacements are higher due to softening effect. The same is now seen in the strain energy as well, where the strain energy is seen to be high for this case. The strain energy for the case of a clamped-clamped beam is summarized in Table 6.18. For all of the 4 cases, the strain energy converges from below.

Strain Energy for P-P Beam, UDL, Shear-FI, Membrane-FI						
Load	2 El	4 El	8 El	16 El	32 El	Exact
1	4.853	4.996	5.034	5.043	5.046	5.047
2	12.886	13.237	13.334	13.359	13.365	13.368
3	22.062	22.651	22.819	22.863	22.874	22.879
4	32.059	32.913	33.163	33.228	33.245	33.252
5	42.735	43.874	44.214	44.304	44.327	44.337
6	53.998	55.442	55.880	55.997	56.026	56.040
7	65.786	67.551	68.095	68.240	68.277	68.295
8	78.050	80.153	80.809	80.984	81.029	81.051
9	90.753	93.207	93.981	94.189	94.242	94.268
10	103.865	106.683	107.580	107.822	107.883	107.915

Strain Energy for P-P Beam, UDL, Shear-RI, Membrane-FI						
Load	2 El	4 El	8 El	16 El	32 El	Exact
1	4.853	4.996	5.034	5.043	5.046	5.047
2	12.886	13.237	13.334	13.359	13.365	13.368
3	22.062	22.651	22.820	22.863	22.874	22.879
4	32.061	32.913	33.163	33.228	33.245	33.252
5	42.737	43.875	44.215	44.304	44.327	44.337
6	54.001	55.443	55.881	55.997	56.026	56.040
7	65.790	67.553	68.096	68.240	68.277	68.295
8	78.056	80.156	80.809	80.984	81.029	81.051
9	90.761	93.211	93.982	94.189	94.242	94.268
10	103.874	106.688	107.581	107.822	107.883	107.915

Strain Energy for P-P Beam, UDL, Shear-FI, Membrane-RI						
Load	2 El	4 El	8 El	16 El	32 El	Exact
1	5.126	5.066	5.052	5.048	5.047	5.047
2	13.837	13.479	13.397	13.377	13.372	13.368
3	23.821	23.102	22.940	22.901	22.891	22.879
4	34.708	33.599	33.350	33.289	33.274	33.252
5	46.338	44.816	44.476	44.393	44.373	44.337
6	58.613	56.660	56.225	56.119	56.093	56.040
7	71.465	69.063	68.529	68.400	68.368	68.295
8	84.843	81.976	81.339	81.185	81.147	81.051
9	98.705	95.357	94.615	94.436	94.392	94.268
10	113.019	109.175	108.325	108.119	108.068	107.915

Strain Energy for P-P Beam, UDL, Shear-RI, Membrane-RI						
Load	2 El	4 El	8 El	16 El	32 El	Exact
1	5.127	5.072	5.078	5.150	5.416	5.047
2	13.848	13.529	13.601	14.172	16.201	13.368
3	23.854	23.245	23.518	25.148	30.824	22.879
4	34.776	33.886	34.506	37.774	49.046	33.252
5	46.453	45.298	46.416	51.911	70.753	44.337
6	58.788	57.389	59.157	67.472	95.871	56.040
7	71.713	70.092	72.662	84.395	124.350	68.295
8	85.176	83.357	86.884	102.632	156.150	81.051
9	99.137	97.143	101.781	122.148	191.240	94.268
10	113.562	111.418	117.323	142.910	229.596	107.915

Table 6.17 Strain energy boundedness in a pinned-pinned shear flexible beam (uniform load) – Comparison of Anisoparametric formulations, Large deflection analysis

Strain Energy for C-C Beam, UDL, Shear-FI, Membrane-FI						
Load	2 El	4 El	8 El	16 El	32 El	Exact
1	0.967	1.269	1.348	1.368	1.373	1.374
2	3.754	4.928	5.230	5.307	5.326	5.327
3	8.080	10.614	11.254	11.416	11.456	11.460
4	13.623	17.912	18.979	19.247	19.314	19.321
5	20.104	26.465	28.028	28.419	28.518	28.528
6	27.310	36.001	38.118	38.647	38.781	38.796
7	35.088	46.321	49.047	49.728	49.900	49.921
8	43.329	57.285	60.673	61.517	61.729	61.758
9	51.954	68.792	72.891	73.910	74.167	74.202
10	60.907	80.767	85.627	86.832	87.136	87.179

Strain Energy for C-C Beam, UDL, Shear-RI, Membrane-FI						
Load	2 El	4 El	8 El	16 El	32 El	Exact
1	0.967	1.270	1.348	1.368	1.373	1.374
2	3.755	4.929	5.231	5.307	5.326	5.327
3	8.081	10.615	11.255	11.416	11.456	11.460
4	13.626	17.915	18.980	19.247	19.314	19.321
5	20.110	26.469	28.029	28.420	28.518	28.528
6	27.319	36.006	38.120	38.649	38.781	38.796
7	35.102	46.329	49.051	49.730	49.900	49.921
8	43.348	57.296	60.678	61.519	61.730	61.758
9	51.979	68.806	72.898	73.913	74.168	74.202
10	60.939	80.786	85.635	86.835	87.138	87.179

Strain Energy for C-C Beam, UDL, Shear-FI, Membrane-RI						
Load	2 El	4 El	8 El	16 El	32 El	Exact
1	0.974	1.272	1.349	1.368	1.373	1.374
2	3.859	4.966	5.241	5.309	5.327	5.327
3	8.544	10.772	11.298	11.427	11.459	11.460
4	14.873	18.320	19.089	19.276	19.322	19.321
5	22.664	27.264	28.240	28.475	28.533	28.528
6	31.733	37.328	38.468	38.740	38.807	38.796
7	41.909	48.304	49.565	49.865	49.940	49.921
8	53.040	60.035	61.386	61.707	61.786	61.758
9	64.994	72.409	73.823	74.160	74.244	74.202
10	77.664	85.339	86.800	87.149	87.236	87.179

Strain Energy for C-C Beam, UDL, Shear-RI, Membrane-RI						
Load	2 El	4 El	8 El	16 El	32 El	Exact
1	0.975	1.272	1.349	1.368	1.373	1.374
2	3.859	4.966	5.241	5.310	5.331	5.327
3	8.545	10.773	11.299	11.435	11.495	11.460
4	14.875	18.320	19.096	19.311	19.470	19.321
5	22.666	27.266	28.260	28.576	28.940	28.528
6	31.736	37.333	38.514	38.962	39.681	38.796
7	41.911	48.314	49.653	50.278	51.539	49.921
8	53.041	60.054	61.534	62.392	64.409	61.758
9	64.996	72.439	74.054	75.208	78.217	74.202
10	77.665	85.386	87.137	88.656	92.908	87.179

Table 6.18 Strain energy boundedness in a clamped-clamped shear flexible beam (uniform load) – Comparison of Anisoparametric formulations, Large deflection analysis

The results of the sweep-test for a hinged-hinged beam are shown in Fig. 6.37. For all the load cases, there is no cross-over of the strain energy curve. The field consistent formulations is the least sensitive to the position of the node.

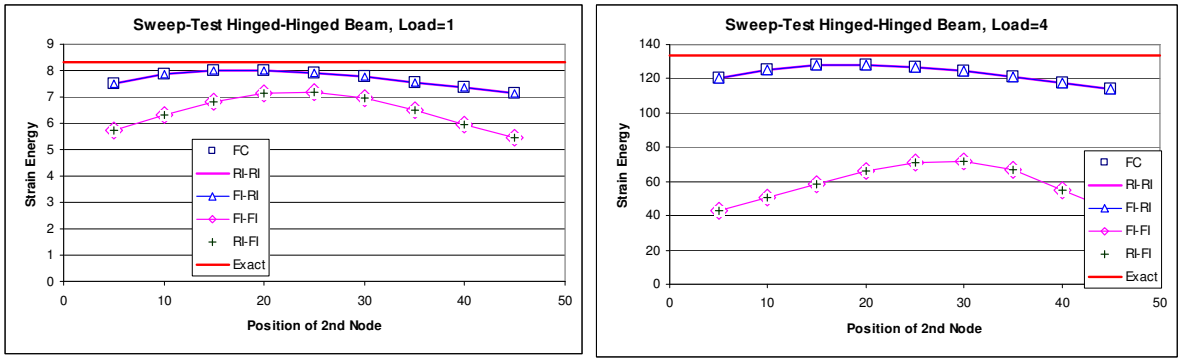

Fig. 6.37 Sweep-Test in a hinged-hinged shear-flexible beam (uniform load) – Comparison of Anisoparametric formulations, Large deflection analysis

For the case of a pinned-pinned, the sweep-test results are shown in Fig. 6.38. It is the field-consistent formulation that shows steady response with respect to the position of the middle node. When reduced integration is used, the strain energy in fact converges from above.

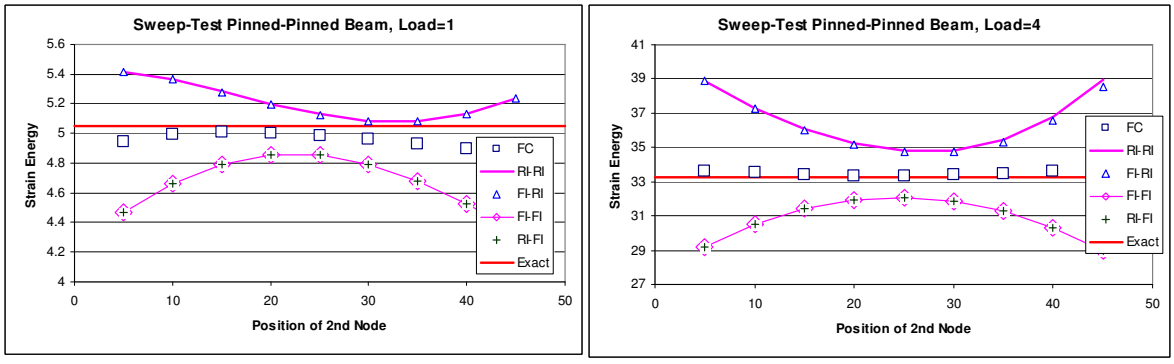

Fig. 6.38 Sweep-Test in a pinned-pinned shear-flexible beam (uniform load) – Comparison of Anisoparametric formulations, Large deflection analysis

Fig. 6.39 shows the results of the sweep-test for a clamped-clamped beam. For this beam, the axial forces that are produced are relatively small as compared to

a pinned-pinned beam, and the results from all the 4 cases and the field-consistent formulation lie very close to each other.

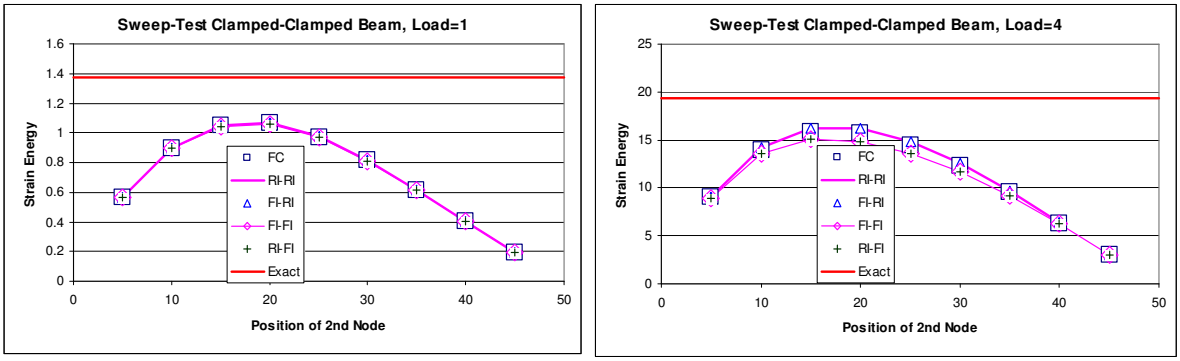

Fig. 6.39 Sweep-Test in a clamped-clamped shear-flexible beam (uniform load) – Comparison of Anisoparametric formulations, Large deflection analysis

Table 6.19 summarizes the gist of the results of all of the above analysed conditions, and it can be seen clearly that the field-consistent formulation gives the best results.

Summary of Results - Large Deformation of Shear-Flexible Beams			
Case	Shear	Membrane	Impact
1	Full	Full	Generally produces a stiffer solution; Generates a spurious axial force for a hinged-hinged beam;
2	Reduced	Full	Generally produces a stiffer solution; Generates a spurious axial force for a hinged-hinged beam;
3	Full	Reduced	Causes a softening effect; No spurious axial force for a hinged-hinged beam;
4	Reduced	Reduced	Causes a softening effect; No spurious axial force for a hinged-hinged beam; Loses boundedness for the pinned-pinned case.

Table 6.19 Summary of results for shear flexible beams due to use of selective integration in Anisoparametric formulations, Large deflection analysis

6.4 Large Deformation Analysis of Circular Plates - Isoparametric Formulation

6.4.1 Strain Displacement Relations

The strain-displacement relations for the case of large deflections of a circular plate are given by

$$\begin{aligned} \varepsilon_r &= \frac{du}{du} + \frac{1}{2}\left(\frac{dw}{dr}\right)^2 \\ \varepsilon_\theta &= \frac{u}{r} \\ \chi_r &= \frac{d^2w}{dr^2} \\ \chi_\theta &= \frac{1}{r}\frac{dw}{dr} \end{aligned} \qquad \ldots(6.11)$$

6.4.2 Incremental Matrices

The incremental matrices for this case can be derived on the lines explained by Rajasekaran and Murray (1974), and come out to be

$$N^1 = \begin{bmatrix} 0 & 0 & C_{11}w_{,x} \\ 0 & 0 & C_{12}w_{,x} \\ C_{11}w_{,x} & C_{12}w_{,x} & C_{11}u_{,x} + C_{12}\frac{u}{r} \end{bmatrix} \qquad \ldots(6.12)$$

and

$$N^2 = \begin{bmatrix} 0 & 0 & 0 \\ 0 & 0 & 0 \\ 0 & 0 & 1.5C_{11}w_{,x}^2 \end{bmatrix} \qquad \ldots(6.13)$$

where

$$C_{11} = \frac{Eh}{(1-\nu^2)}\ ,\ C_{12} = \nu C_{11}$$

These incremental matrices are generic in nature and can be applied to different element formulations.

The case of a circular plate undergoing large deflection is now studied in detail using a 2-noded element with 3 degrees of freedom at each node (1 in-plane axial displacement, 1 transverse displacement and rotation).

6.4.3 Numerical Experiments and Discussion

The results from the above formulation for the case of a circular plate simply supported on the edges (radius = 10 in., E=1.0e7 psi, υ =0.3, and t=0.1 in. is subjected to a uniform load of 1 lb/in^2) are shown in Table 6.20. The approximate solution is from Timoshenko and Woinowsky-Krieger (1959). The ANSYS® (2008) solution is obtained from a discretisation of 1000 elements (of SHELL51 element), whereas the C^0 isoparametric solution is from a discretisation of 128 elements.

Deflection at centre of a circular simply supported plate - UDL			
Load	ANSYS	Isoparametric	Approximate Solution
0.1	0.048075	0.048077	0.044813
0.2	0.070373	0.070374	0.069054
0.3	0.085126	0.085125	0.085131
0.4	0.096427	0.096425	0.097462
0.5	0.105719	0.105716	0.107621
0.6	0.113684	0.113680	0.116350
0.7	0.120699	0.120693	0.124056
0.8	0.126996	0.126990	0.130989
0.9	0.132731	0.132724	0.137315
1	0.138012	0.138003	0.143150

Table 6.20 Deflection at the center of a shear-flexible simply supported circular plate (uniform load) – Isoparametric element, Large deflection analysis

The membrane forces for the simply supported circular plate are shown in Fig. 6.40, and the bending moments are shown in Fig. 6.41. Both of these plots show good comparison with results from ANSYS® (2008)

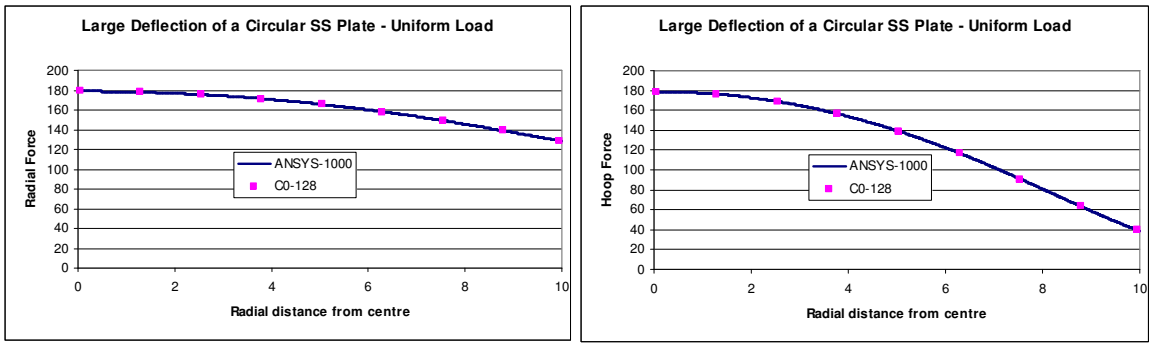

Fig. 6.40 Membrane forces in a simply supported shear-flexible circular plate (uniform load) – Isoparametric element, Large deflection analysis

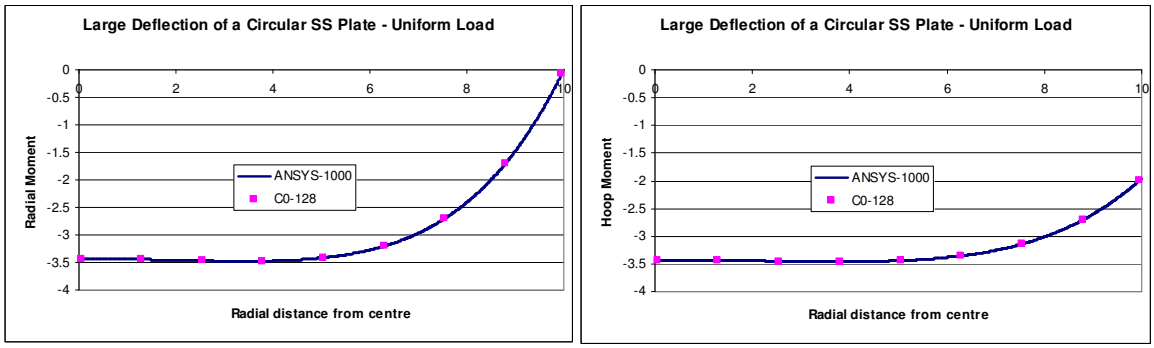

Fig. 6.41 Bending moments in a simply supported shear-flexible circular plate (uniform load) – Isoparametric element, Large deflection analysis

The deflection in a clamped circular plate is tabulated in Table 6.21 and found to match very closely with the ANSYS® (2008) results. The discretisation for the ANSYS® (2008) results is from 1000 elements (of SHELL51 element), and the C^0 isoparametric element uses 128 elements. The membrane forces and bending moments are shown in Fig. 6.42 and Fig. 6.43 and found to match closely with results from ANSYS® (2008).

Deflection at centre of a circular clamped plate - UDL			
Load	ANSYS	Isoparametric	Approximate Solution
0.1	0.016810	0.016811	0.016177
0.2	0.032283	0.032297	0.031917
0.3	0.045884	0.045902	0.045972
0.4	0.057679	0.057699	0.058311
0.5	0.067960	0.067982	0.069165
0.6	0.077024	0.077046	0.078801
0.7	0.085114	0.085136	0.087449
0.8	0.092416	0.092439	0.095292
0.9	0.099074	0.099098	0.102470
1	0.105198	0.105221	0.109093

Table 6.21 Deflection at the center of a shear-flexible clamped circular plate (uniform load) Isoparametric element, Large deflection analysis

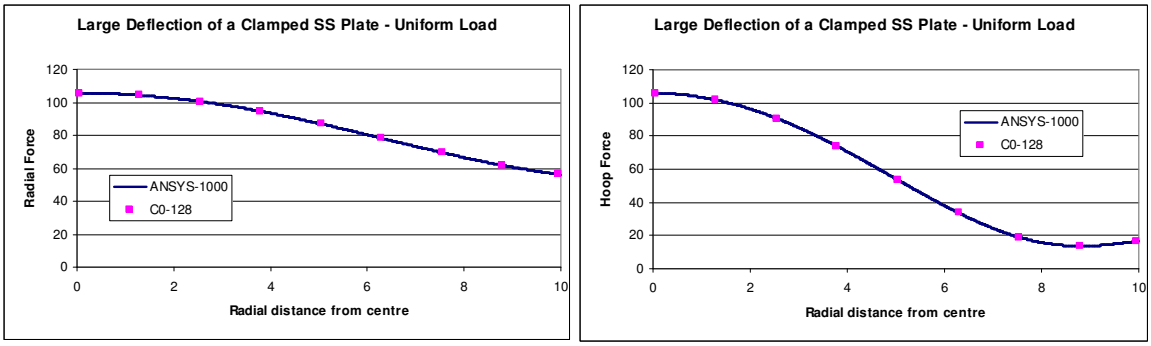

Fig. 6.42 Membrane forces in a clamped shear-flexible circular plate (uniform load) – Isoparametric element, Large deflection analysis

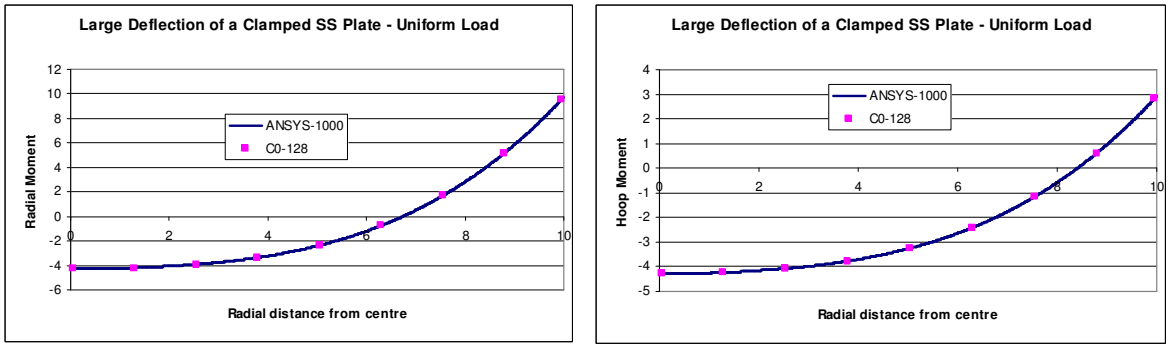

Fig. 6.43 Bending moments in a clamped shear-flexible circular plate (uniform load) – Isoparametric element, Large deflection analysis

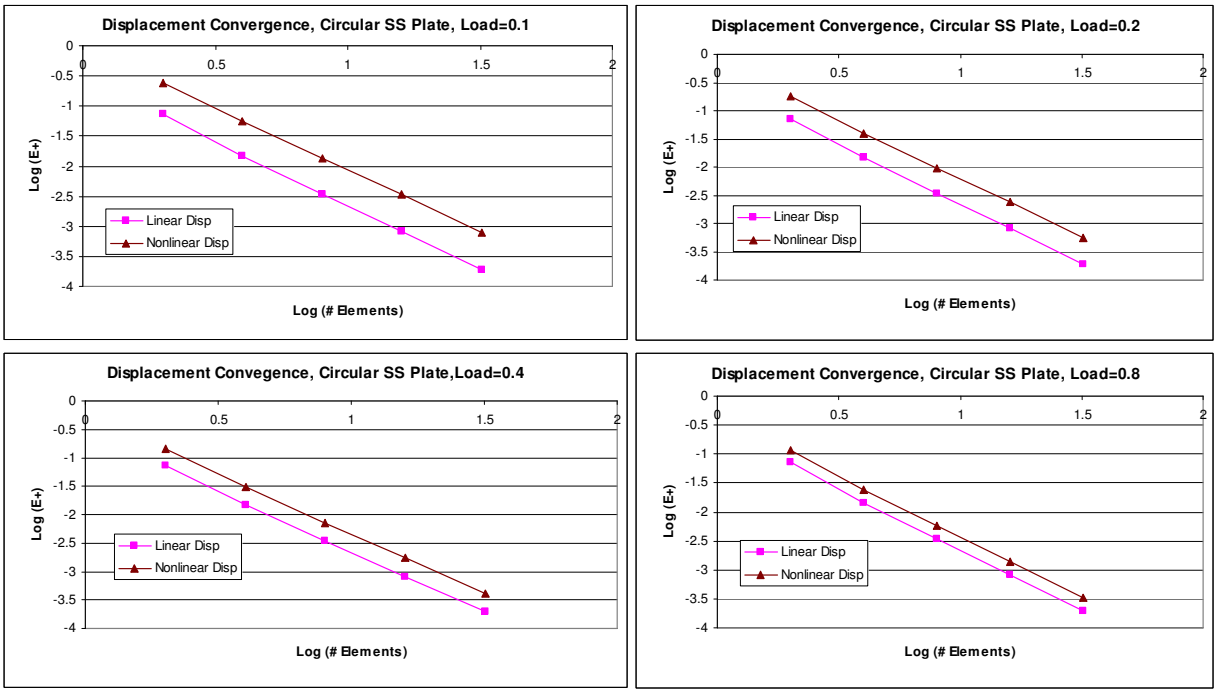

Fig. 6.44 Convergence of displacement in a simply supported shear-flexible circular plate (uniform load) – Isoparametric element, Large deflection analysis

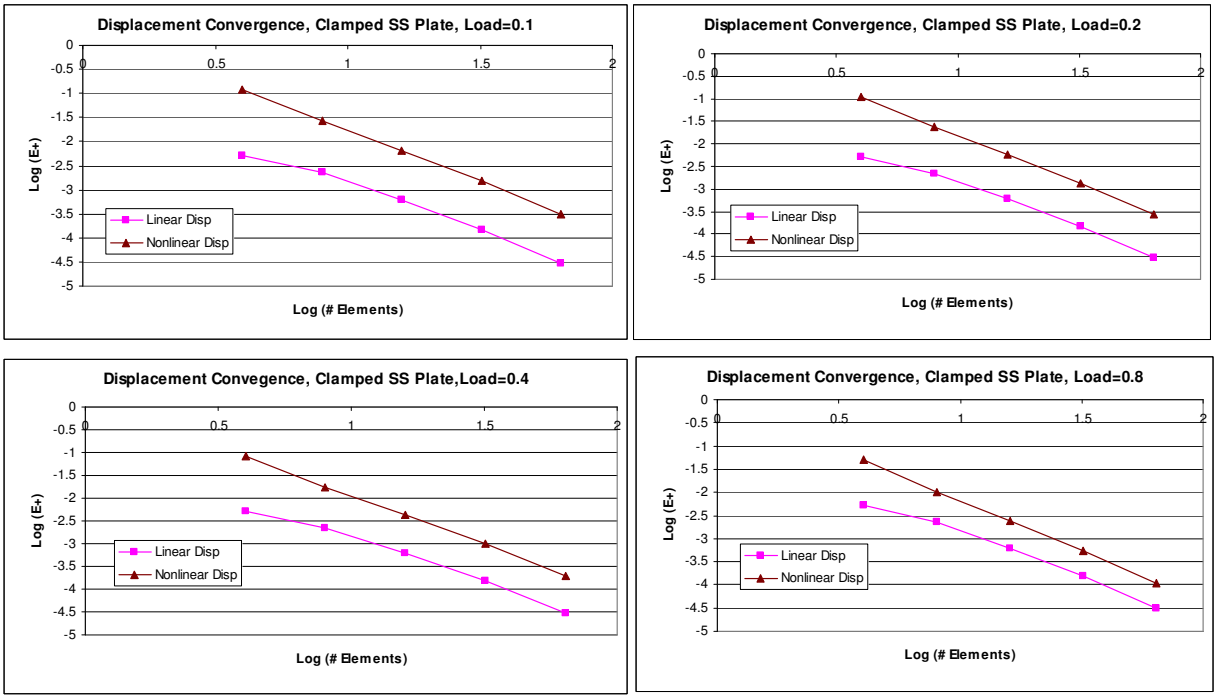

Fig. 6.45 Convergence of displacement in a clamped shear-flexible circular plate (uniform load) – Isoparametric element, Large deflection analysis

The convergence of displacements for the simply supported circular plate is shown in Fig. 6.44 for various load cases. For all the load cases, the convergence is $O(h^2)$, as expected. Similar results are seen for the case of a clamped circular plate as shown in Fig. 6.45.

The strain energy boundedness for the simply supported circular plate can be seen in Table 6.22. All the results shown in this table converge from below. For the case of a clamped circular plate, the boundedness is lost. It is to be noted that the shear strain terms here required the use of reduced integration and its effects are seen clearly.

Strain Energy in a Circular SS Plate - Uniform Load, Large Deflections, Isoparametric Formulation								
Load	2 Elements	4 Elements	8 Elements	16 Elements	32 Elements	64 Elements	128 Elements	ANSYS
0.1	0.282411	0.293486	0.2963887	0.29712146	0.297305	0.297351	0.297363	0.297347
0.2	0.764097	0.778919	0.7838158	0.78508903	0.785410	0.785491	0.785511	0.785476
0.3	1.315843	1.335238	1.3427289	1.3447031	1.345203	1.345328	1.345360	1.345320
0.4	1.916848	1.943083	1.9538734	1.95672569	1.957448	1.957629	1.957675	1.957630
0.5	2.558164	2.593485	2.6081853	2.61206665	2.613049	2.613296	2.613358	2.613260
0.6	3.234377	3.280826	3.2999533	3.30499109	3.306266	3.306585	3.306666	3.306590
0.7	3.941709	4.001119	4.0251193	4.03142277	4.033016	4.033416	4.033517	4.033410
0.8	4.677318	4.751339	4.7806021	4.78826657	4.790203	4.790689	4.790811	4.790710
0.9	5.438960	5.529090	5.5639595	5.5730695	5.575370	5.575947	5.576092	5.575990
1	6.224806	6.332410	6.3731958	6.38382735	6.386511	6.387184	6.387353	6.387250

Table 6.22 Strain energy boundedness in a shear-flexible simply supported circular plate (uniform load) – Isoparametric element, Large deflection analysis

Strain Energy in a Circular Clamped Plate - Uniform Load, Large Deflections, Isoparametric Formulation								
Load	2 Elements	4 Elements	8 Elements	16 Elements	32 Elements	64 Elements	128 Elements	ANSYS
0.1	0.085382	0.087180	0.087520	0.087614	0.087639	0.087645	0.087646	0.087646
0.2	0.332615	0.332657	0.332814	0.332904	0.332931	0.332938	0.332940	0.332710
0.3	0.719473	0.702109	0.699982	0.699613	0.699532	0.699514	0.699509	0.699050
0.4	1.219468	1.163397	1.156704	1.155390	1.155085	1.155012	1.154994	1.154260
0.5	1.808577	1.693683	1.680750	1.678148	1.677536	1.677387	1.677351	1.676290
0.6	2.467739	2.278069	2.257891	2.253800	2.252835	2.252599	2.252542	2.251120
0.7	3.182741	2.906848	2.878905	2.873229	2.871887	2.871559	2.871479	2.869660
0.8	3.943213	3.573479	3.537562	3.530267	3.528542	3.528120	3.528017	3.525760
0.9	4.741589	4.273361	4.229446	4.220536	4.218428	4.217913	4.217788	4.215040
1	5.572287	5.003119	4.951280	4.940780	4.938297	4.937690	4.937541	4.934290

Table 6.23 Strain energy boundedness in a shear-flexible clamped circular plate (uniform load) – Isoparametric element, Large deflection analysis

The results of the sweep-test for a simply supported circular plate are shown in Fig. 6.46. For higher loads, the curve crosses over the theoretical strain energy indicating the sensitivity of the position of the node. The results of the sweep-test on a clamped circular plate are shown in Fig. 6.47, where the boundedness is affected clearly

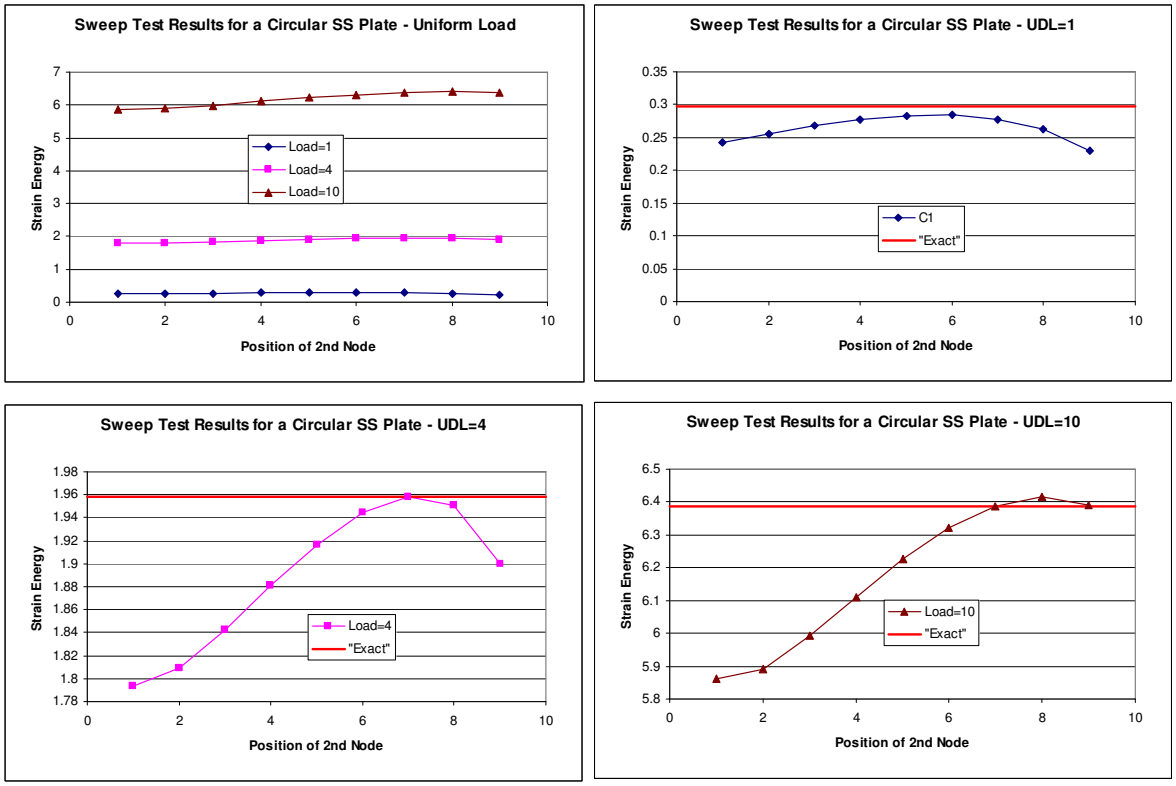

Fig. 6.46 Sweep-Test in a simply supported shear-flexible circular plate (uniform load) – Isoparametric element, Large deflection analysis

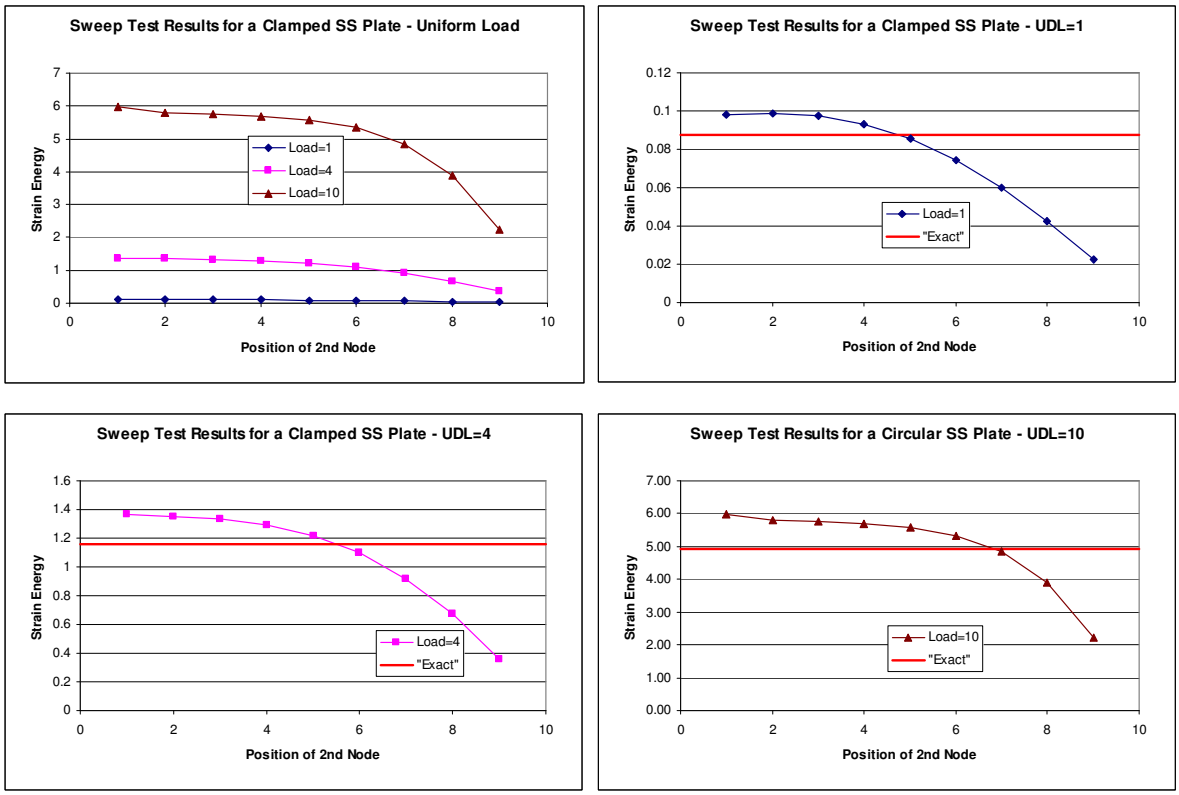

Fig. 6.47 Sweep-Test in a clamped shear-flexible circular plate (uniform load) – Isoparametric element, Large deflection analysis

6.5 Large Deformation of Circular Plates - Anisoparametric Formulation

The anisoparametric formulation is now exteneded to the study of large deflection of circular plates. In principle, the formulation applies to the study of any body of revolution (as was seen in section 4.3 for the linear elastostatics case).

6.5.1 Incremental Matrices

The incremental matrices are similar to the matrices shown in section 6.4.2. There is an additional degree of freedom here at each node which needs to be accounted in the formulation, as explained in section 4.3.3.

6.5.2 Numerical Experiments and Discussion

The test problems of a simply supported and clamped circular plates are taken again to study the response of the element. The deflection in the centre of a simply supported circular plate (radius = 10 in., E=1.0e7 psi, υ =0.3, and t=0.1 in. is subjected to a uniform load of 1 lb/in^2) is shown in Table 6.24 which show very good agreement with ANSYS® (2008) solution. The membrane forces and bending moments are shown in Fig. 6.48 and Fig. 6.49 respectively and match closely with ANSYS® (2008) solution (with SHELL63 element)

Deflection at centre of a circular simply supported plate - UDL			
Load	ANSYS	Anisoparametric	Approximate Solution
0.1	0.048075	0.048077	0.044813
0.2	0.070373	0.070373	0.069054
0.3	0.085126	0.085123	0.085131
0.4	0.096427	0.096423	0.097462
0.5	0.105719	0.105714	0.107621
0.6	0.113684	0.113678	0.116350
0.7	0.120699	0.120691	0.124056
0.8	0.126996	0.126988	0.130989
0.9	0.132731	0.132722	0.137315
1	0.138012	0.138001	0.143150

Table 6.24 Deflection at the center of a shear-flexible simply supported circular plate (uniform load) – Anisoparametric element, Large deflection analysis

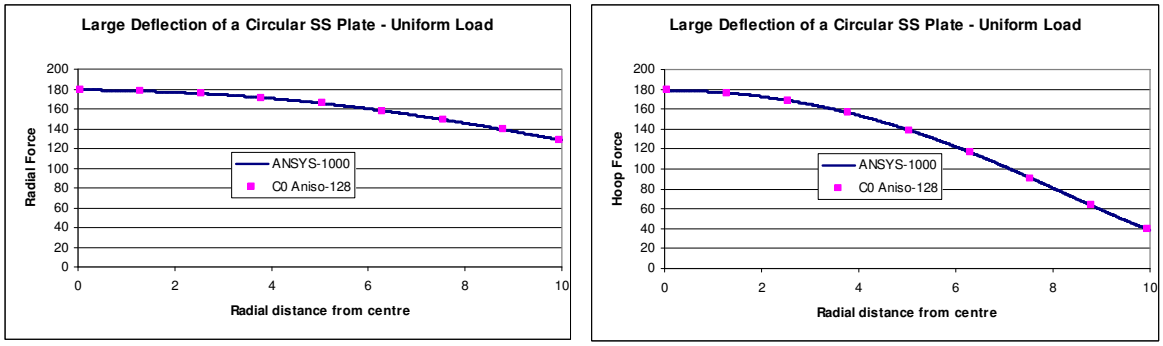

Fig. 6.48 Membrane forces in a simply supported shear-flexible circular plate (uniform load) – Anisoparametric element, Large deflection analysis

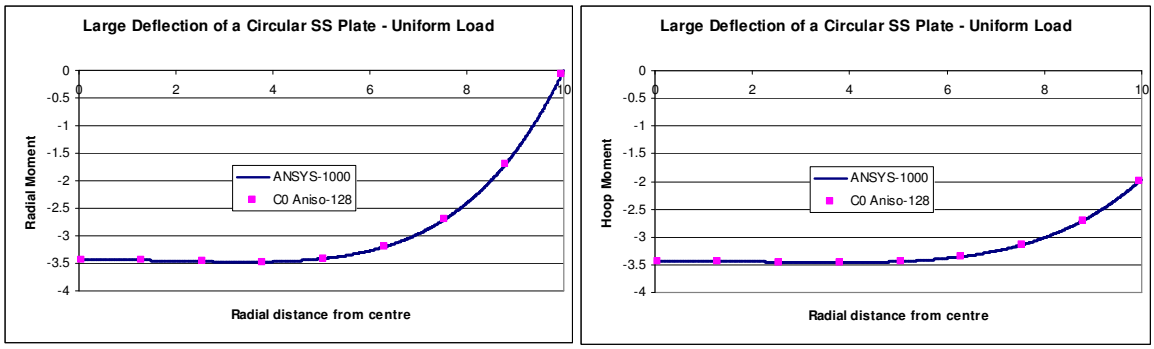

Fig. 6.49 Bending Moments in a simply supported shear-flexible circular plate (uniform load) – Anisoparametric element, Large deflection analysis

The deflection in a clamped circular plate is tabulated in Table 6.25 and the results from the anisoparametric element matches very well that of ANSYS® (2008). The membrane forces and bending moments are shown in Fig. 6.50 and Fig. 6.51, which confirm the confidence in the use of this element for further studies.

Deflection at centre of a clamped circular plate - UDL			
Load	ANSYS	Anisoparametric	Approximate Solution
0.1	0.016810	0.016810	0.016177
0.2	0.032283	0.032295	0.031917
0.3	0.045884	0.045899	0.045972
0.4	0.057679	0.057696	0.058311
0.5	0.067960	0.067977	0.069165
0.6	0.077024	0.077041	0.078801
0.7	0.085114	0.085131	0.087449
0.8	0.092416	0.092433	0.095292
0.9	0.099074	0.099091	0.102470
1	0.105198	0.105214	0.109093

Table 6.25 Deflection at the center of a shear-flexible clamped circular plate (uniform load) – Anisoparametric element, Large deflection analysis

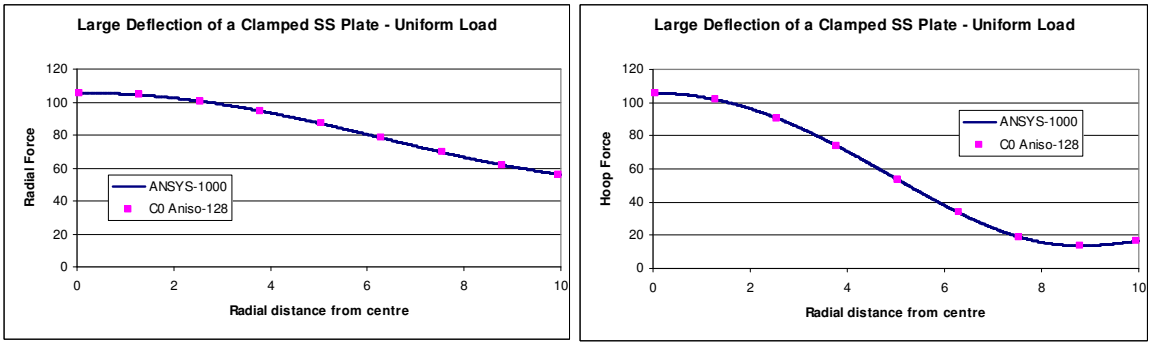

Fig. 6.50 Membrane forces in a clamped shear-flexible circular plate (uniform load) – Anisoparametric element, Large deflection analysis

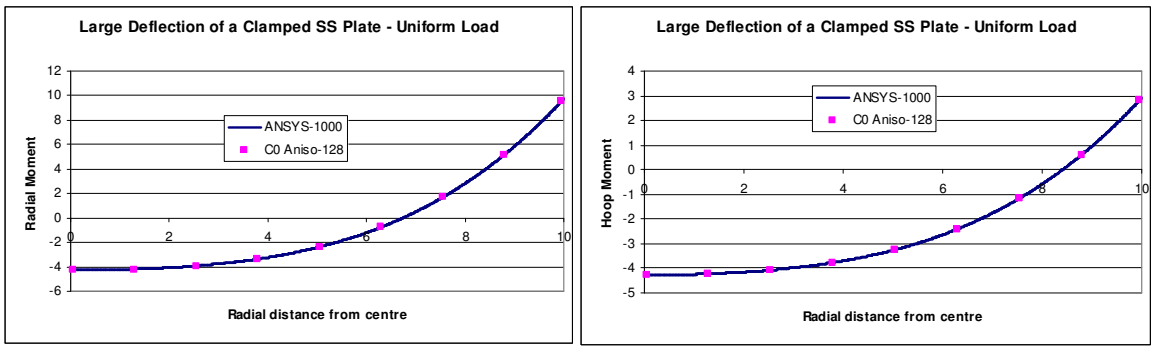

Fig. 6.51 Bending Moments in a clamped shear-flexible circular plate (uniform load) – Anisoparametric element, Large deflection analysis

The convergence of the displacements for simply supported circular plate is shown in Fig. 6.52. It converges at $O(h^2)$. The clamped circular plate also shows similar results as seen in Fig. 6.53.

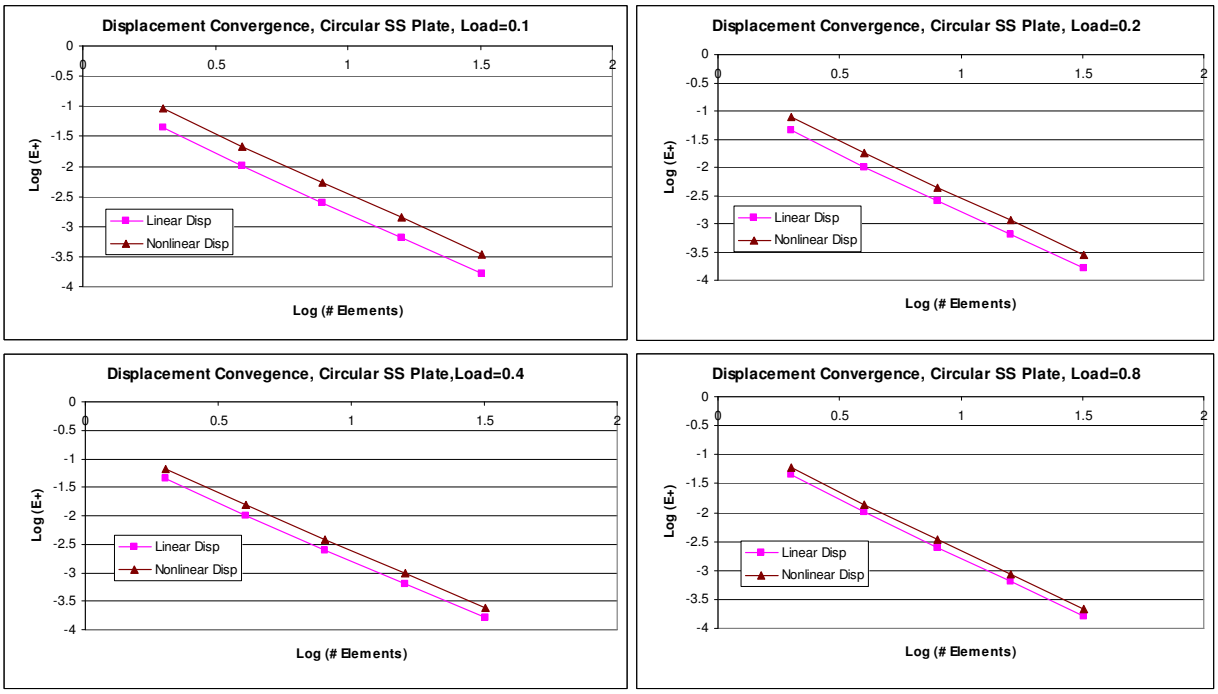

Fig. 6.52 Convergence of displacement in a simply supported shear-flexible circular plate (uniform load) – Anisoparametric element, Large deflection analysis

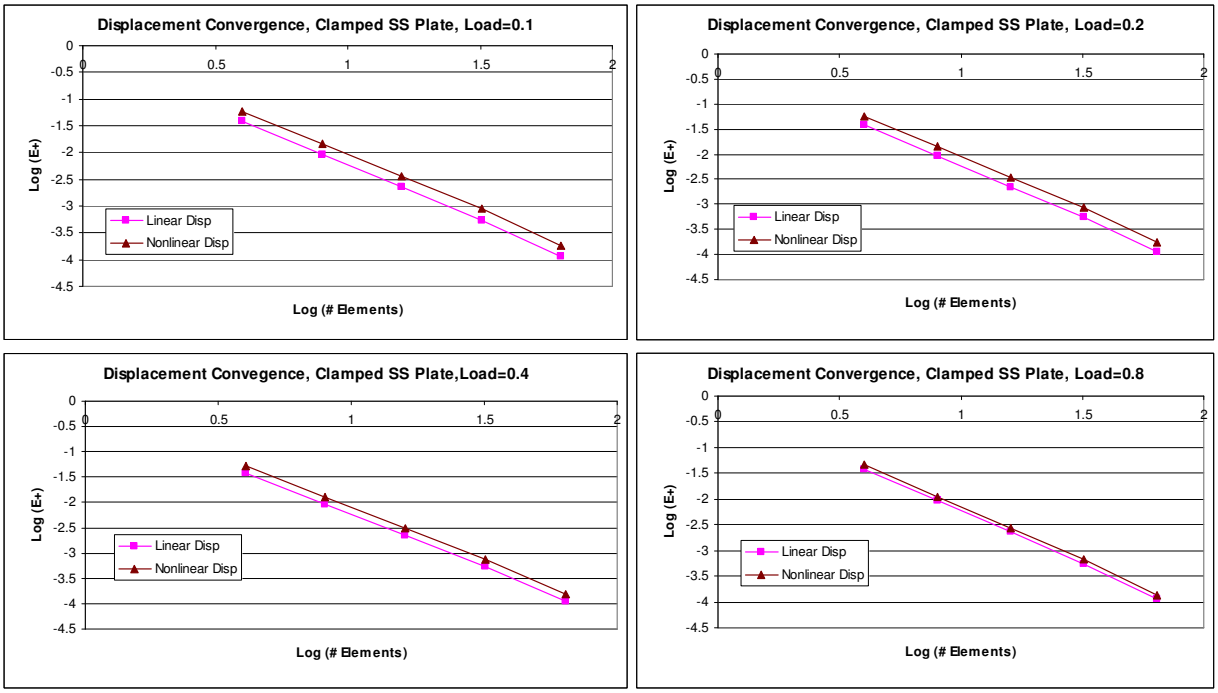

Fig. 6.53 Convergence of displacement in a clamped shear-flexible circular plate (uniform load) – Anisoparametric element, Large deflection analysis

The boundedness of strain energy for the case of a simply supported circular plate is seen in Table 6.26. The strain energy converges from below. For the clamped circular plate also, the strain energy is bounded, converging from below for all the load cases.

Strain Energy in a Circular SS Plate - Uniform Load, Large Deflections, Anisoparametric Formulation								
Load	2 Elements	4 Elements	8 Elements	16 Elements	32 Elements	64 Elements	128 Elements	ANSYS
0.1	0.287830	0.294619	0.296652	0.297186	0.297321	0.297355	0.297364	0.297347
0.2	0.762209	0.778417	0.783643	0.785043	0.785399	0.785488	0.785511	0.785476
0.3	1.304194	1.332496	1.341930	1.344497	1.345152	1.345316	1.345357	1.345320
0.4	1.895032	1.937789	1.952325	1.956324	1.957348	1.957605	1.957669	1.957630
0.5	2.526139	2.585355	2.605769	2.611435	2.612891	2.613257	2.613348	2.613260
0.6	3.192177	3.269571	3.296552	3.304097	3.306041	3.306530	3.306652	3.306590
0.7	3.889375	3.986452	4.020618	4.030232	4.032717	4.033342	4.033498	4.033410
0.8	4.614884	4.732975	4.774886	4.786747	4.789820	4.790594	4.790787	4.790710
0.9	5.366445	5.506747	5.556918	5.571189	5.574895	5.575829	5.576063	5.575990
1	6.142217	6.305815	6.364721	6.381554	6.385935	6.387041	6.387317	6.387250

Table 6.26 Strain energy boundedness in a shear-flexible simply supported circular plate (uniform load) – Anisoparametric element, Large deflection analysis

Strain Energy in a Clamped Circular Plate - UDL, Large Deflections, Anisoparametric Formulation								
Load	2 Elements	4 Elements	8 Elements	16 Elements	32 Elements	64 Elements	128 Elements	ANSYS
0.1	0.063161	0.081246	0.086020	0.087237	0.087544	0.087544	0.087640	0.087646
0.2	0.237830	0.308180	0.326660	0.331356	0.332541	0.332541	0.332915	0.332710
0.3	0.494019	0.645938	0.685955	0.696086	0.698646	0.698646	0.699453	0.699050
0.4	0.805883	1.063218	1.131844	1.149141	1.153515	1.153515	1.154894	1.154260
0.5	1.156518	1.538564	1.642462	1.668522	1.675118	1.675118	1.677197	1.676290
0.6	1.535655	2.058296	2.203877	2.240216	2.249421	2.249421	2.252324	2.251120
0.7	1.936985	2.613596	2.807083	2.855157	2.867344	2.867344	2.871190	2.869660
0.8	2.356474	3.198560	3.445997	3.507215	3.522744	3.522744	3.527647	3.525760
0.9	2.791410	3.809046	4.116306	4.192036	4.211257	4.211257	4.217329	4.215040
1	3.239888	4.442024	4.814805	4.906383	4.929638	4.929638	4.936988	4.934290

Table 6.27 Strain energy boundedness in a shear-flexible clamped circular plate (uniform load) – Anisoparametric element, Large deflection analysis

The results of the sweep-test for a simply supported circular plate are shown in Fig. 6.54, showing no cross-over of the curve. The clamped circular plate shows similar response, as seen in Fig. 6.55.

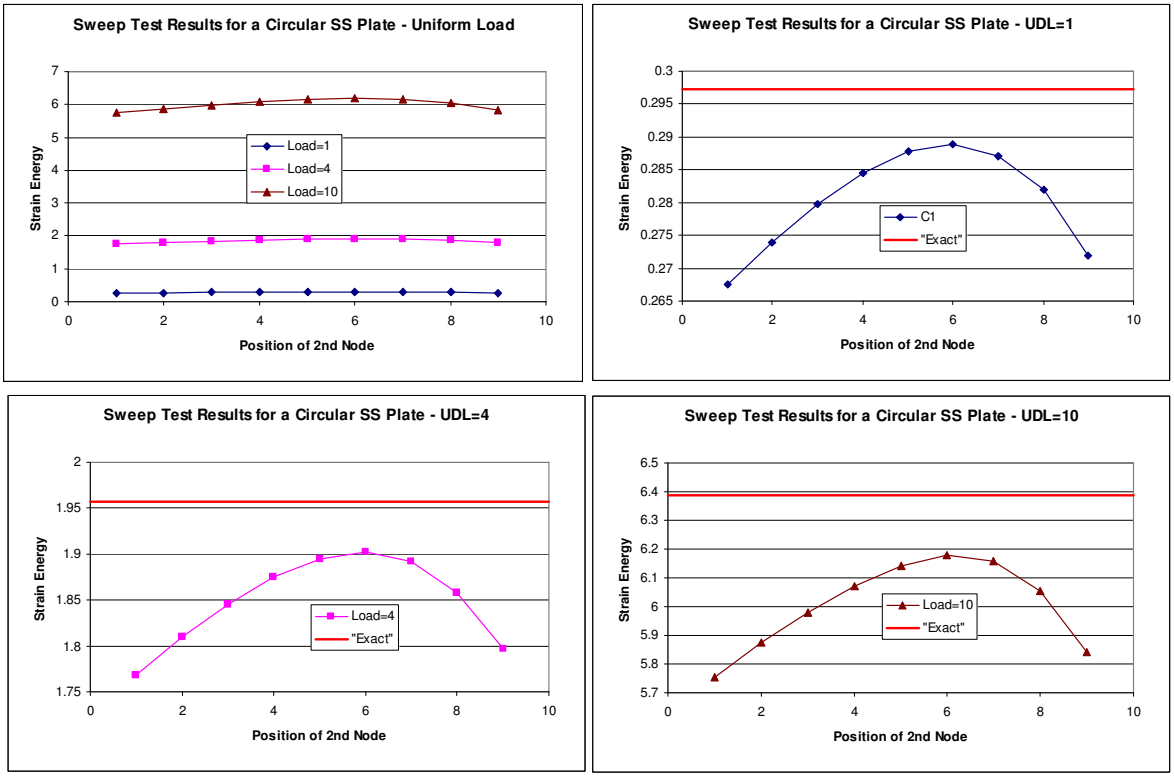

Fig. 6.54 Sweep-Test in a simply supported shear-flexible circular plate (uniform load) – Anisoparametric element, Large deflection analysis

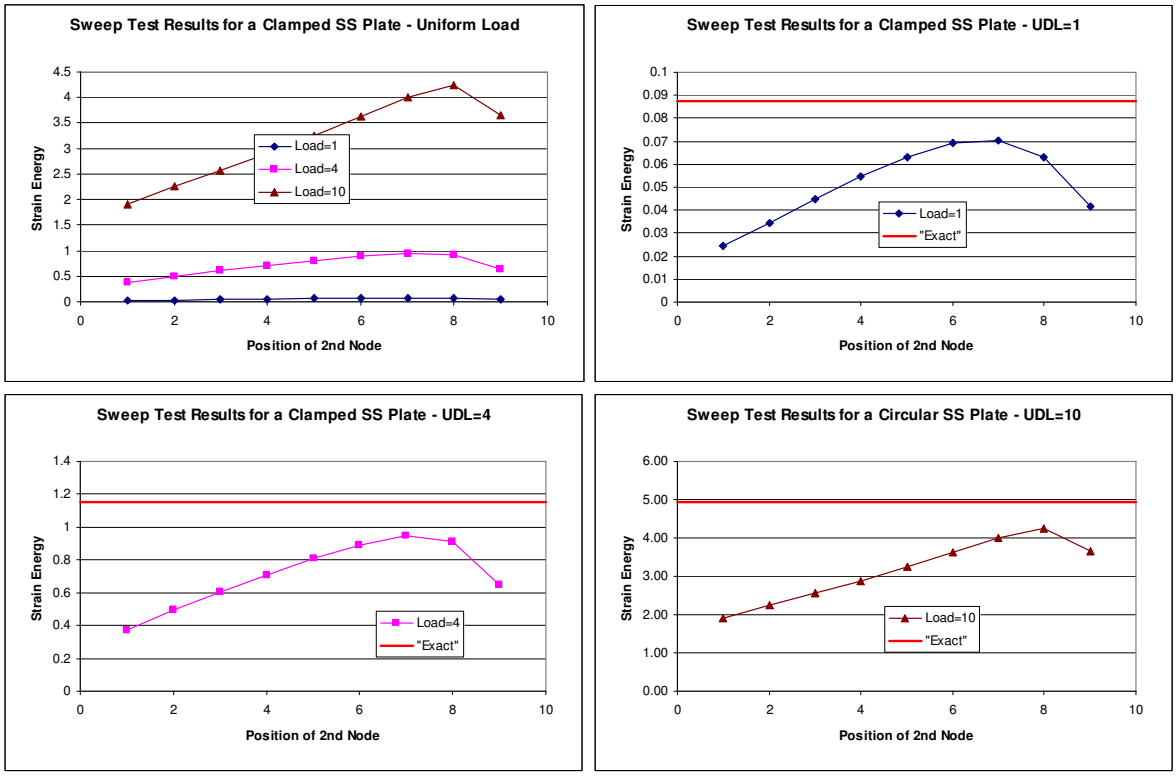

Fig. 6.55 Sweep-Test in a clamped shear-flexible circular plate (uniform load) – Anisoparametric element, Large deflection analysis

6.6 Large Deformation Analysis of Thin Plates – Isoparametric Formulation

The problem of large deflections of shear-flexible plates is discussed now. The element used here is similar to the one described in section 4.4.2 for the linear case, with additional complexities due to the nonlinear strains.

6.6.1 Strain Displacement Relations

The nonlinear strain displacement relations for the membrane strains are given by

$$\varepsilon_x = \frac{\partial u}{\partial x} + \frac{1}{2}\left[\frac{\partial w}{\partial x}\right]^2$$
$$\varepsilon_y = \frac{\partial v}{\partial y} + \frac{1}{2}\left[\frac{\partial w}{\partial y}\right]^2 \qquad \ldots(6.14)$$
$$\varepsilon_{xy} = \frac{\partial u}{\partial y} + \frac{\partial v}{\partial x} + \frac{\partial w}{\partial x}\frac{\partial w}{\partial y}$$

6.6.2 Incremental Matrices

The incremental matrices, in principle, remain similar to the incremental matrices of ACM element, described in section 5.4.3, with proper caution for the degrees of freedom that are different for the ACM and the QUAD-4 element.

6.6.3 Numerical Experiments and Discussion

The stiffness matrix now has both shear and membrane strains, and as explained in section 6.3.2, the use of selective integration for these strains are now studied independently. The results for a simply supported square plate (20x20 mm quarter plate, 0.4 mm thickness and Poisson's ratio of 0.3, Young's Modulus of 200000 N/mm^2) are tabulated in Table 6.28. It can be seen that there is no impact of full/reduced integration on membrane strain terms, whereas the shear strain has a big impact.

Large Deflection of a SS Plate - UDL (Mindlin Formulation-Selective Integration)					
Load	Shear-2, Membrane-3	Shear-2, Membrane-3	Shear-1, Membrane-3	Shear-1, Membrane-2	ANSYS Deflection
1	0.03770947	0.03770948	0.385668355	0.385684956	0.378168
2	0.07531037	0.07531040	0.517858799	0.517881586	0.506211
3	0.11269716	0.11269725	0.605648294	0.605674221	0.591338
4	0.14977017	0.14977036	0.673588001	0.673615885	0.657296
5	0.18643793	0.18643831	0.729968772	0.729998019	0.712085
6	0.22261903	0.22261966	0.778674251	0.778704522	0.759453
7	0.25824324	0.25824422	0.82186059	0.821891671	0.801477
8	0.29325207	0.29325346	0.860859167	0.860890916	0.839444
9	0.32759869	0.32760060	0.896554681	0.896587001	0.874208
10	0.36124752	0.36125003	0.929567557	0.929600375	0.906367

Table 6.28 Deflection at centre of a shear-flexible simply supported square plate (uniform load) - C^0 Selective integration formulation, Large deflection analysis

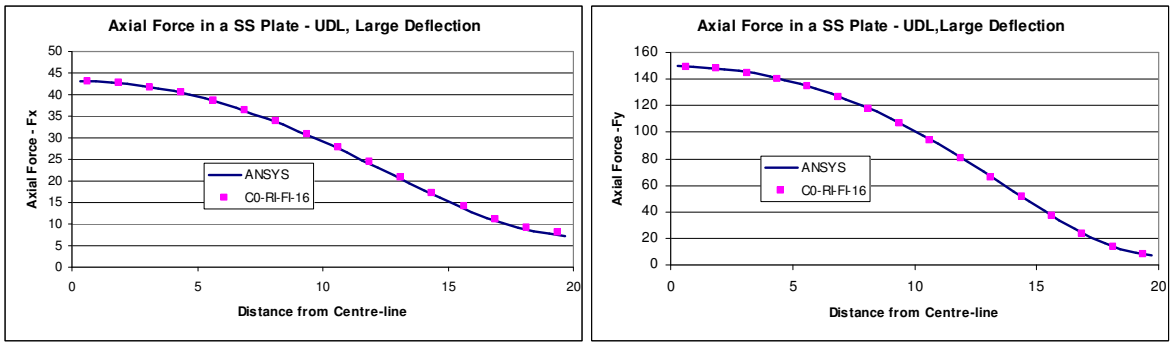

Fig. 6.56 Membrane forces in a simply supported shear-flexible square plate (uniform load) - C^0 Selective integration formulation, Large deflection analysis

The membrane forces and bending moments for the simply supported plate are shown in Fig. 6.56 and 6.57 respectively, and show close match with ANSYS® (2008) results (with SHELL63 element).

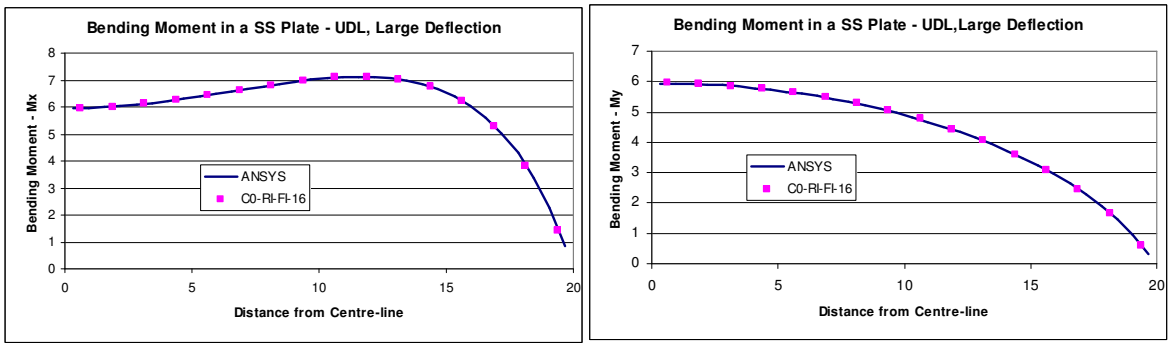

Fig. 6.57 Bending Moments in a simply supported shear-flexible square plate (uniform load) - C^0 Selective integration formulation, Large deflection analysis

Table 6.29 shows the deflection in a clamped square plate. When full integration is used for the shear strain terms, the element locks and produces very low deflections. The membrane strain is insensitive to use of full or reduced integration.

The axial forces and bending moment s for the clamped plate are shown in Fig. 6.58 and Fig. 6.59 and show good match with ANSYS® (2008) results.

Large Deflection of a Clamped Plate Plate - UDL (Mindlin Formulation-Selective Integration)					
Load	Shear-2, Membrane-3	Shear-2, Membrane-2	Shear-1, Membrane-3	Shear-1, Membrane-2	ANSYS Deflection
1	0.00801864	0.008018639	0.236373162	0.236378078	0.23399
2	0.01603703	0.016037028	0.383760284	0.383774054	0.37529
3	0.02405492	0.024054916	0.48512127	0.485142096	0.471923
4	0.03207205	0.032072054	0.562901028	0.562927408	0.546175
5	0.04008819	0.040088191	0.626571664	0.626602611	0.60713
6	0.04810308	0.048103079	0.680853661	0.680888503	0.659257
7	0.05611647	0.056116468	0.728424055	0.728462311	0.705075
8	0.06412811	0.064128109	0.770946536	0.770987847	0.746142
9	0.07213775	0.072137755	0.809526477	0.809570564	0.783492
10	0.08014515	0.080145158	0.844936416	0.844983056	0.817848

Table 6.29 Deflection at centre of a shear-flexible clamped square plate (uniform load) – C^0 Selective integration formulation, Large deflection analysis

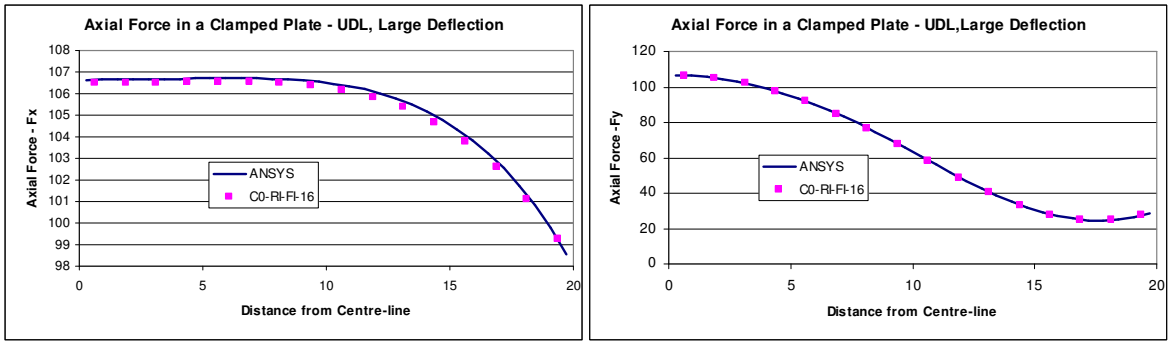

Fig. 6.58 Membrane forces in a clamped shear-flexible square plate (uniform load) – C^0 Selective integration formulation, Large deflection analysis

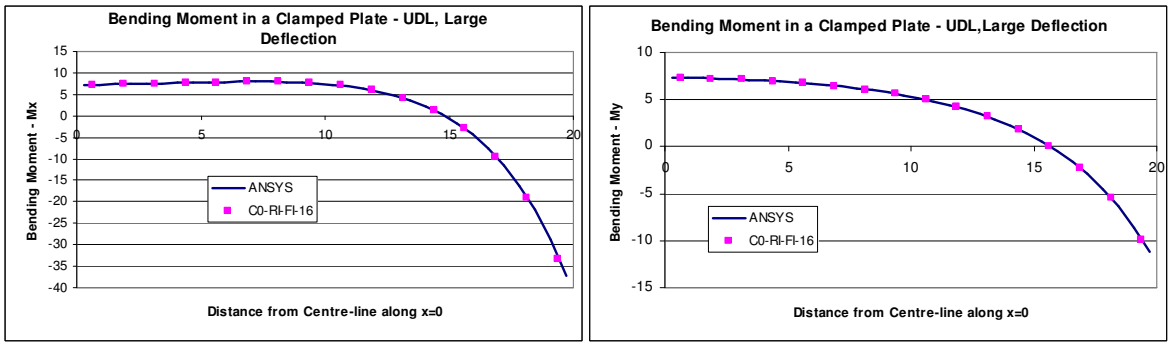

Fig. 6.59 Bending moments in a clamped shear-flexible square plate (uniform load) – C^0 Selective integration formulation, Large deflection analysis

The convergence of displacements is shown in Fig. 6.60 for the case of simply supported square plate, and in Fig. 6.61 for a clamped square plate. Both of them show a convergence of $O(h^2)$.

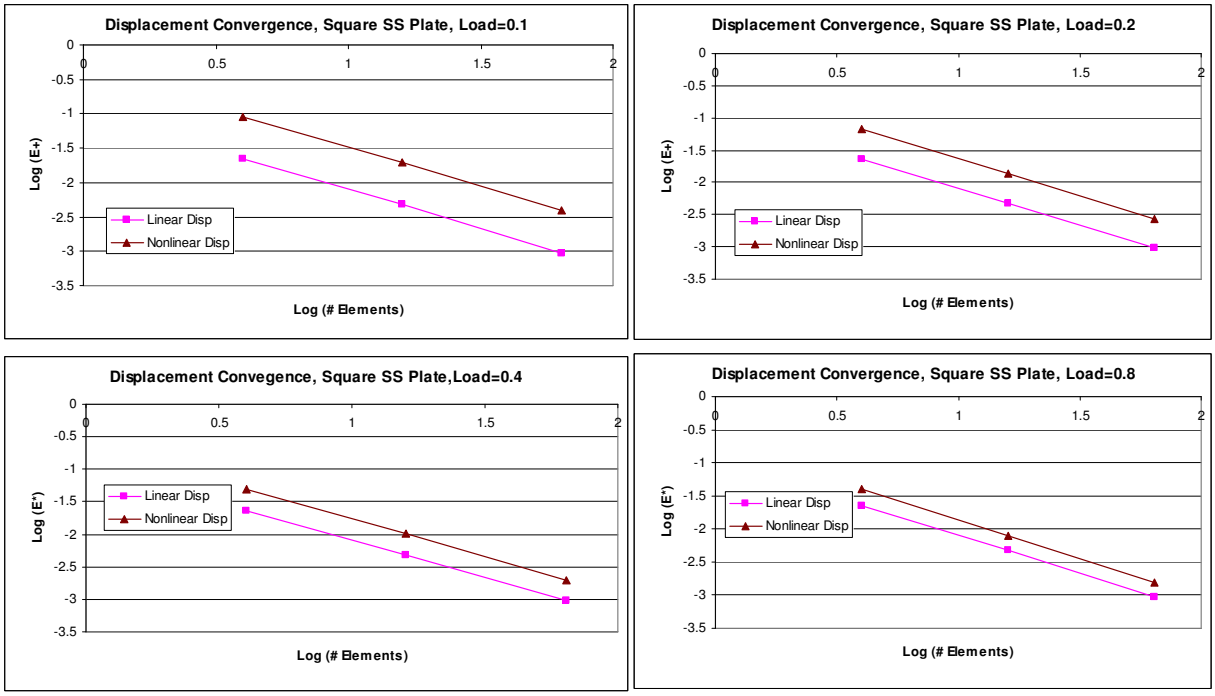

Fig. 6.60 Convergence of displacement in a simply supported shear-flexible square plate (uniform load) - C^0 Selective integration formulation, Large deflection analysis

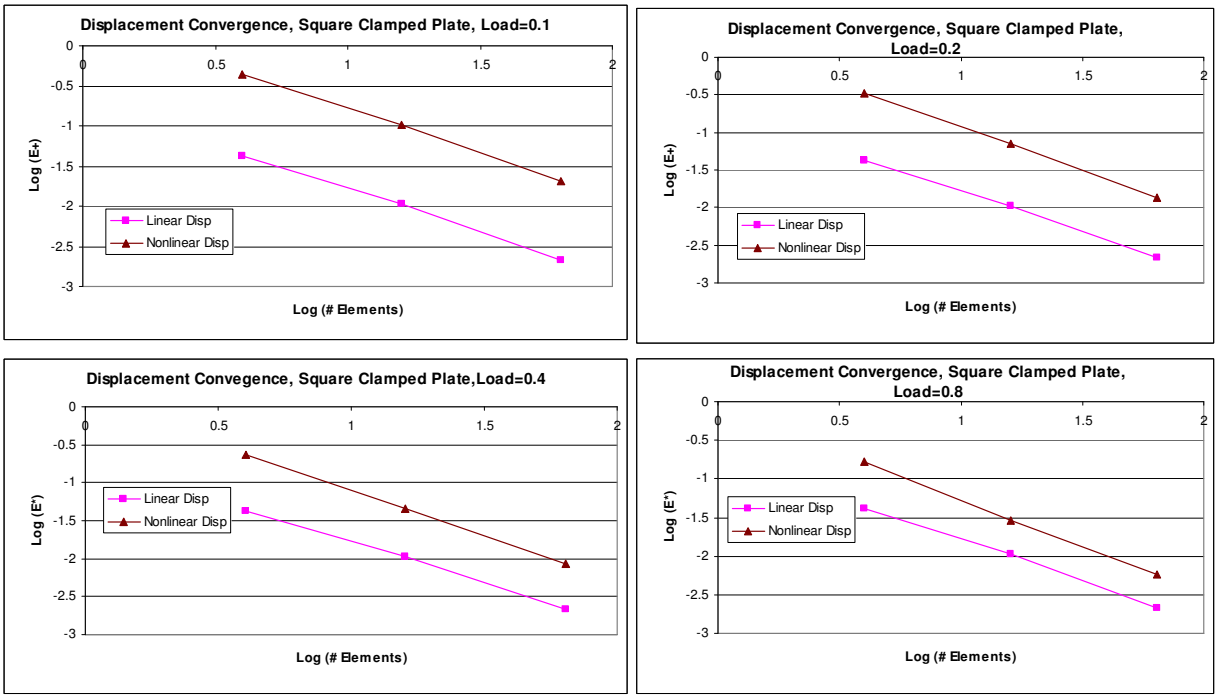

Fig. 6.61 Convergence of displacement in a clamped shear-flexible square plate (uniform load) - C^0 Selective integration formulation, Large deflection analysis

The strain energy boundedness is shown in Table 6.30 for the case of a simply supported square plate, and the strain energy converges from below. Similar behaviour is seen for a clamped square plate as well, as shown in Table 6.31.

Strain Energy in a SS Plate - UDL, Mindlin Formulation (Shear-RI, Memb-FI)					
Load	2x2	4x4	8x8	16x16	ANSYS
1	8.853526	9.356822	9.483089	9.514638	9.530380
2	21.849069	23.127766	23.444414	23.523429	23.566000
3	36.819848	39.060982	39.608123	39.744545	39.820800
4	53.311198	56.646164	57.452263	57.653230	57.769000
5	71.071039	75.601056	76.688832	76.960090	77.120800
6	89.932821	95.740629	97.129393	97.475849	97.686500
7	109.776260	116.932266	118.639041	119.065033	119.330000
8	130.509492	139.075345	141.115495	141.624943	141.949000
9	152.059577	162.090410	164.478024	165.074526	165.463000
10	174.366910	185.912830	188.660975	189.347868	189.804000

Table 6.30 Strain energy boundedness in a shear-flexible simply supported square plate (uniform load) - C^0 Selective integration formulation, Large deflection analysis

Strain Energy in a clamped plate - UDL, Mindlin Formulation (Shear-RI, Memb-FI)					
Load	2x2	4x4	8x8	16x16	ANSYS
1	4.643056	5.320888	5.488927	5.530809	5.522490
2	14.776828	16.474196	16.884242	16.985520	16.963600
3	27.190213	30.329981	31.031458	31.202507	31.162800
4	40.927318	46.058238	47.096108	47.346214	47.283800
5	55.642373	63.295293	64.702669	65.038745	64.948800
6	71.166248	81.823399	83.624565	84.051818	83.929800
7	87.397527	101.491715	103.705209	104.227745	104.069000
8	104.267031	122.187283	124.827981	125.449193	125.250000
9	121.723493	143.821372	146.901795	147.624606	147.381000
10	139.726759	166.321981	169.853110	170.680116	170.389000

Table 6.31 Strain energy boundedness in a shear-flexible clamped square plate (uniform load) - C^0 Selective integration formulation, Large deflection analysis

The results of the sweep-test for a simply supported square plate are shown in Fig. 6.62 and show the boundedness clearly for all the load cases. Fig. 6.63 shows the results of the sweep-test for a clamped plate, and here also the strain energy is bounded.

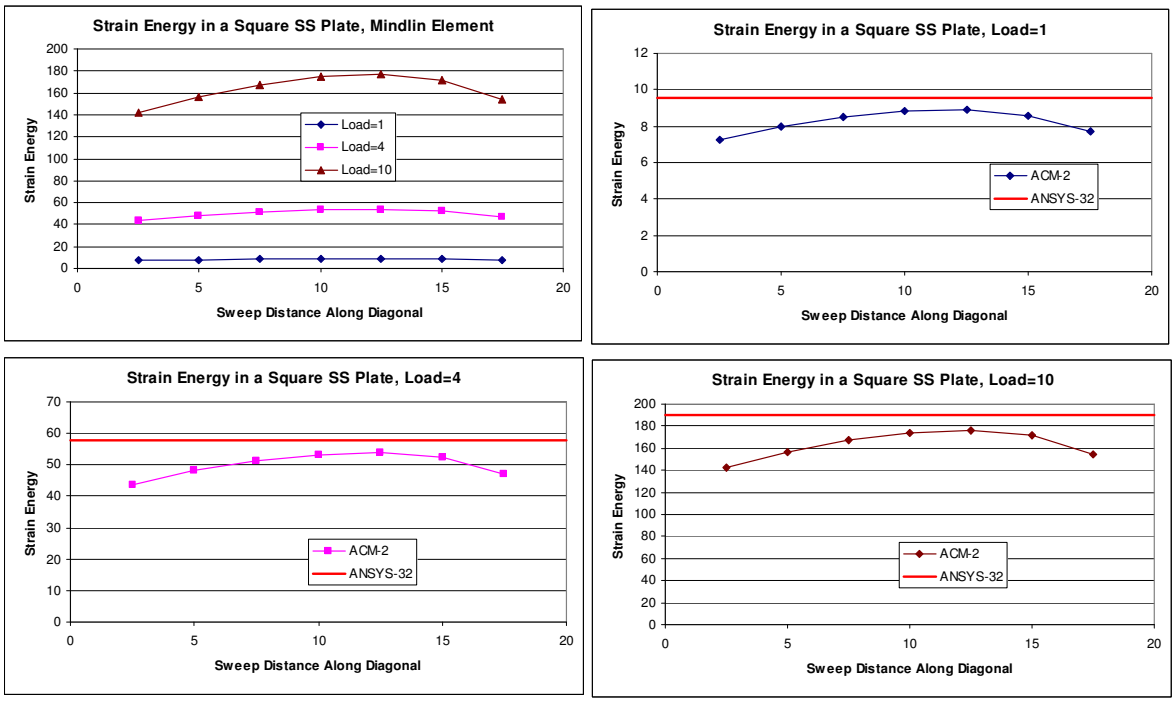

Fig. 6.62 Sweep-Test in a simply supported shear-flexible square plate (uniform load) – C^0 Selective integration formulation, Large deflection analysis

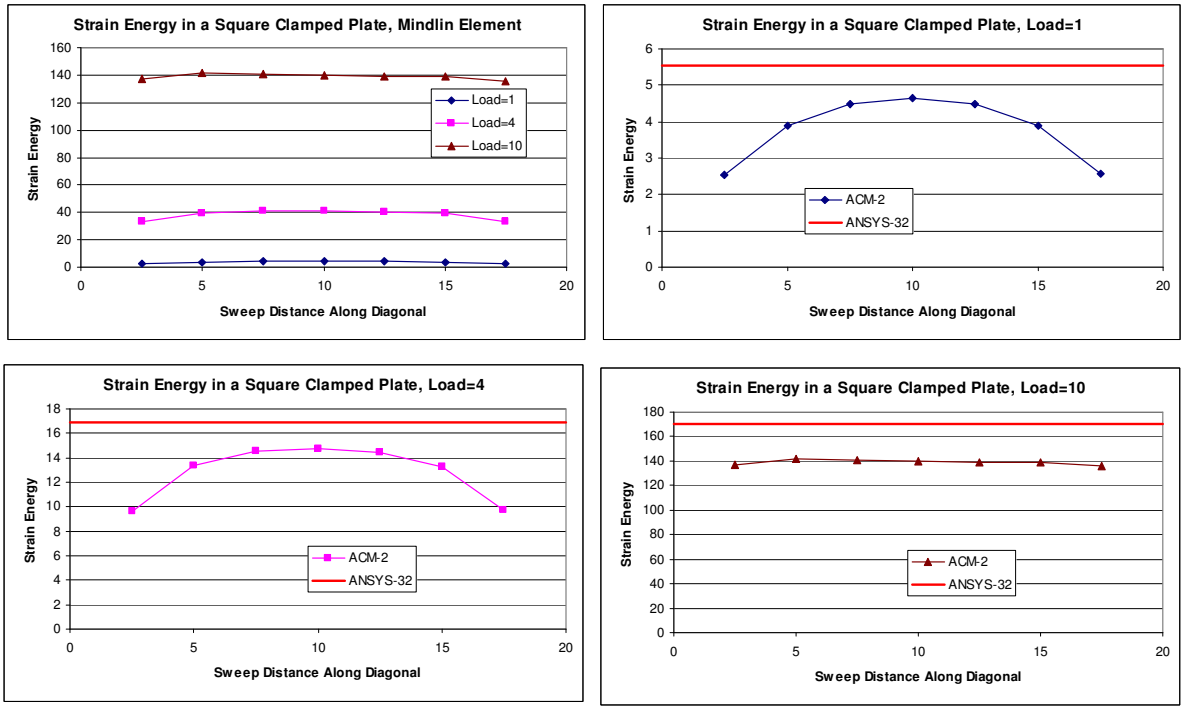

Fig. 6.63 Sweep-Test in a clamped shear-flexible square plate (uniform load) – C^0 Selective integration formulation, Large deflection analysis

6.7 Large Deformation Analysis of Thin Plates - Field-consistent Formulation

In section 4.4.3, the requirement of edge consistency for shear strains was explained clearly and the results of the element formulation with a reconstituted shear strain were shown. In this section, the results of this element (which is both field consistent and edge consistent) are shown for the case of large deflection problems. It is of interest to note that though this element has been used in the adaptive mesh refinement process by Mukherjee and Krishnamurthy (1996), here is assessed for large deflection purposes.

6.7.1 Element Matrices

The incremental matrices of Rajasekaran and Murray (1974) shown in section 5.4.1 are used for this element, and the same matrices are valid for the shear flexible plate element as well. The degrees of freedom corresponding to the slopes θx and θy do not directly participate in the nonlinear membrane strain terms and hence these matrices are valid.

6.7.2 Numerical Experiments and Discussion

For the case of a simply supported square plate (20x20 mm quarter plate, 0.4 mm thickness and Poisson's ratio of 0.3, Young's Modulus of 200000 N/mm^2) subjected to a uniformly distributed load, the deflection at the centre of the plate is shown in Table 6.32 for various load cases, and compared with results from ANSYS® (2008) (with SHELL63 element). Table 6.33 gives the deflection in a clamped plate for various loads, and the results are compared with ANSYS® (2008) results (with SHELL63 element). The membrane forces and bending moments for the simply supported plate are shown in Fig. 6.64 and Fig. 6.65 respectively, and show good match with the results from ANSYS® (2008) (with SHELL63 element). For a clamped square plate, the membrane forces and bending moments are shown in Fig. 6.66 and Fig. 6.67 respectively.

Large Deflection of a SS Plate - UDL (Mindlin Element, Field Consistent and Edge Consistent)		
Load	FC/EC Element	ANSYS Deflection
1	0.379510	0.378168
2	0.508263	0.506211
3	0.593823	0.591338
4	0.660088	0.657296
5	0.715114	0.712085
6	0.762674	0.759453
7	0.804860	0.801477
8	0.842966	0.839444
9	0.877853	0.874208
10	0.910122	0.906367

Table 6.32 Deflection at centre of a shear-flexible simply supported square plate (uniform load) – C^0 FC Formulation, Large deflection analysis

Large Deflection of a Clamped Plate - UDL (Mindlin Element, Field Consistent and Edge Consistent)		
Load	FC/EC Element	ANSYS Deflection
1	0.234520	0.233990
2	0.376980	0.375290
3	0.474476	0.471923
4	0.549351	0.546175
5	0.610773	0.607130
6	0.663263	0.659257
7	0.709369	0.705075
8	0.750671	0.746142
9	0.788217	0.783492
10	0.822736	0.817848

Table 6.33 Deflection at centre of a shear-flexible clamped square plate (uniform load) – C^0 FC Formulation, Large deflection analysis

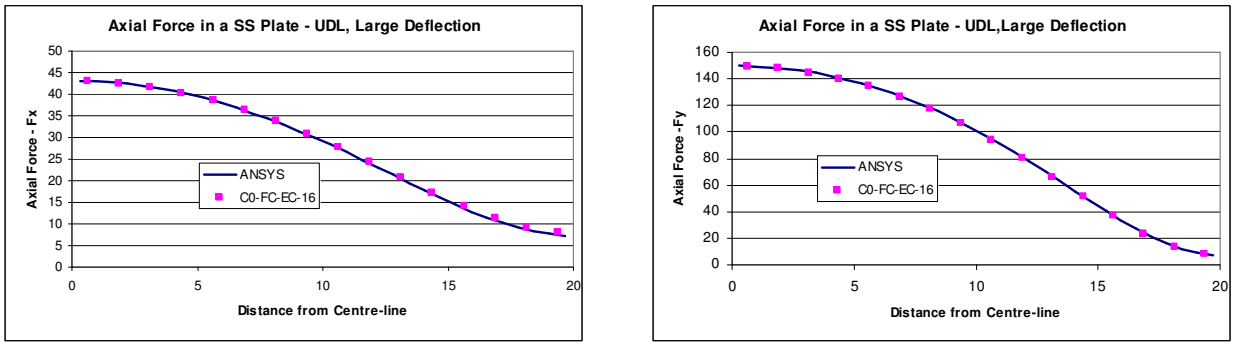

Fig. 6.64 Membrane forces in a simply supported shear-flexible square plate (uniform load) - C^0 Selective integration formulation, Large deflection analysis

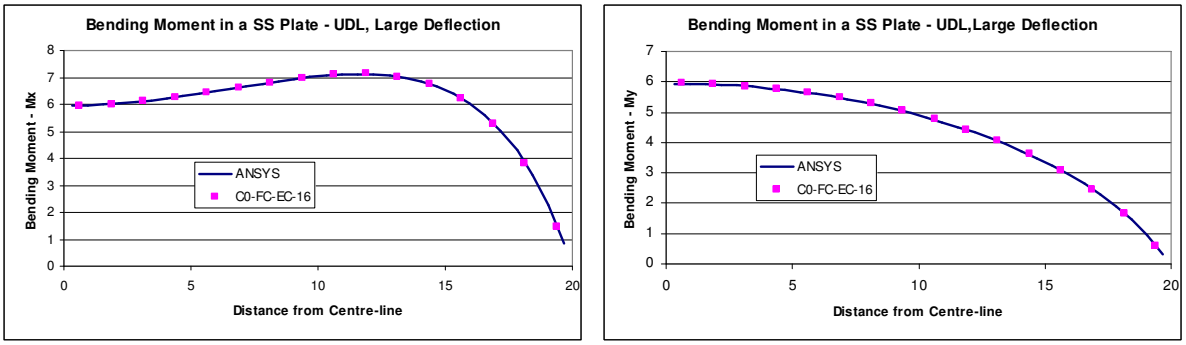

Fig. 6.65 Bending moments in a simply supported shear-flexible square plate (uniform load) - C^0 Selective integration formulation, Large deflection analysis

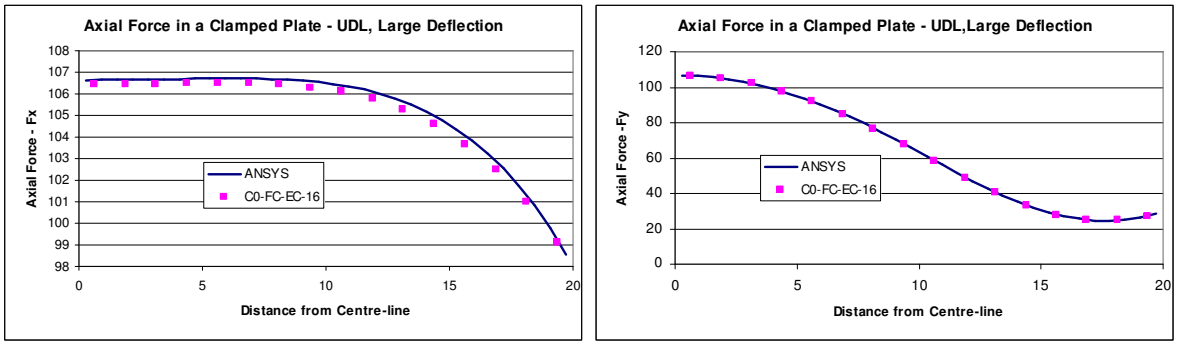

Fig. 6.66 Membrane forces in a clamped shear-flexible square plate (uniform load) – C^0 Selective integration formulation, Large deflection analysis

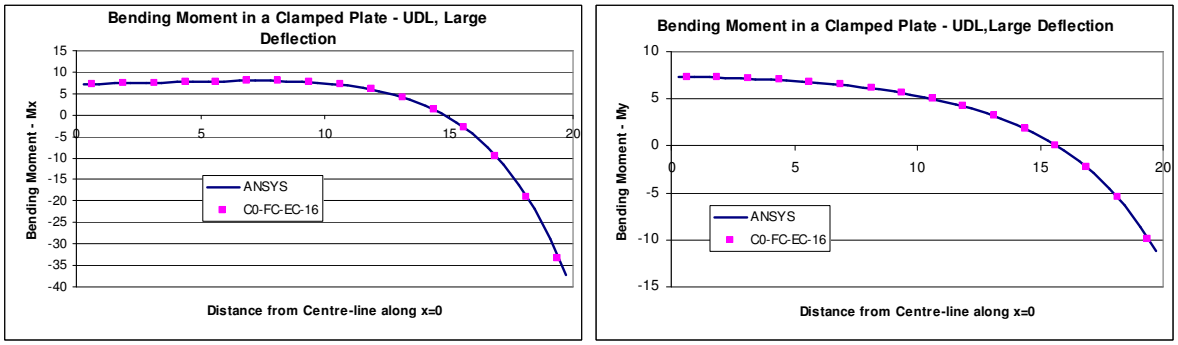

Fig. 6.67 Bending moments in a clamped shear-flexible square plate (uniform load) – C^0 Selective integration formulation, Large deflection analysis

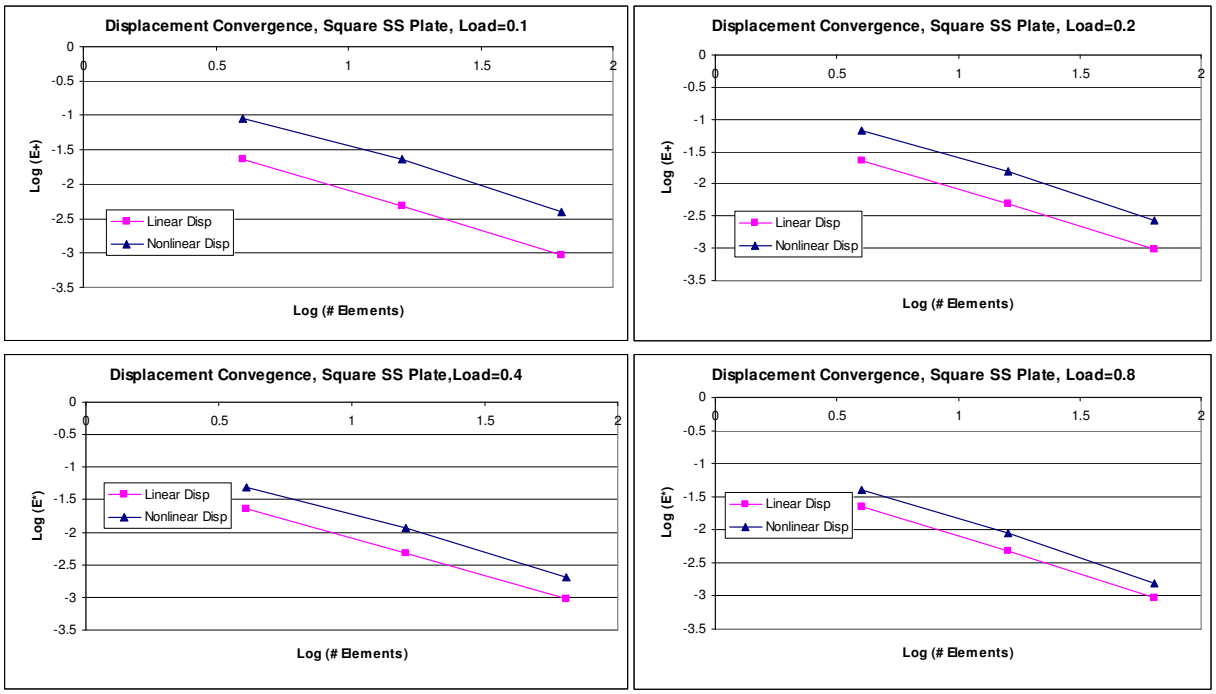

Fig. 6.68 Convergence of displacement in a simply supported shear-flexible square plate (uniform load) - C^0 Selective integration formulation, Large deflection analysis

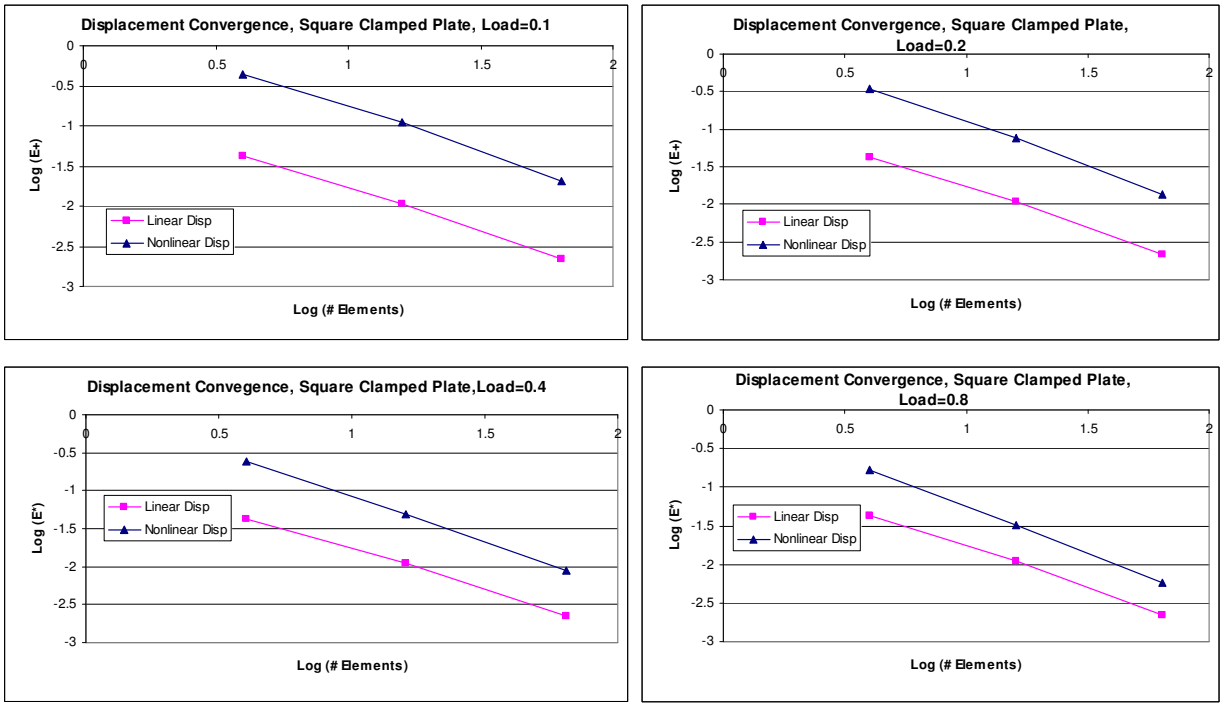

Fig. 6.69 Convergence of displacement in a clamped shear-flexible square plate (uniform load) - C^0 Selective integration formulation, Large deflection analysis

The convergence of displacements for a simply supported plate are shown in Fig. 6.68 and seen to be of $O(h^2)$. Similar results are seen for a clamped plate as shown in Fig. 6.69. The strain energy in a simply supported square plate is tabulated in Table 6.34 for various load cases, and for all the load cases, it is bounded and converging from below. The results for a clamped plate are on similar lines, as shown in Table 6.35.

Strain Energy in a SS Plate - UDL, Mindlin Formulation, FC EC Element					
Load	2x2	4x4	8x8	16x16	ANSYS
1	8.327700	9.325966	9.549603	9.612056	9.530380
2	20.259239	22.968570	23.592682	23.760604	23.566000
3	33.886208	38.715337	39.845014	40.141979	39.820800
4	48.833884	56.072538	57.783869	58.226795	57.769000
5	64.890971	74.766457	77.120579	77.723038	77.120800
6	81.916151	94.617398	97.666170	98.439691	97.686500
7	99.806480	115.496442	119.285315	120.240025	119.330000
8	118.482829	137.305703	141.875384	143.020380	141.949000
9	137.882061	159.967841	165.355359	166.698939	165.463000
10	157.952376	183.419921	189.659346	191.209168	189.804000

Table 6.34 Strain energy boundedness in a shear-flexible simply supported square plate (uniform load)- C^0 FC Formulation, Large deflection analysis

Strain Energy in a clamped plate - UDL, Mindlin Formulation, FC EC Element					
Load	2x2	4x4	8x8	16x16	ANSYS
1	4.317712	5.278874	5.512561	5.573793	5.522490
2	13.565560	16.335085	16.952810	17.119606	16.963600
3	24.660214	30.047189	31.147497	31.446629	31.162800
4	36.733924	45.592974	47.259100	47.711717	47.283800
5	49.498254	62.614945	64.911627	65.534056	64.948800
6	62.823085	80.899488	83.878425	84.683759	83.929800
7	76.635058	100.298568	104.002892	105.002073	104.069000
8	90.886146	120.701237	125.168400	126.370893	125.250000
9	105.541631	142.020273	147.283857	148.698065	147.381000
10	120.574696	164.184863	170.275713	171.909248	170.389000

Table 6.35 Strain energy boundedness in a shear-flexible clamped square plate (uniform load)- C^0 FC Formulation, Large deflection analysis

The results of the sweep-test for a simply supported plate are shown in Fig. 6.70 and the strain energy is bounded for all the load cases. The clamped plate also shows a similar result, as seen in Fig. 6.71.

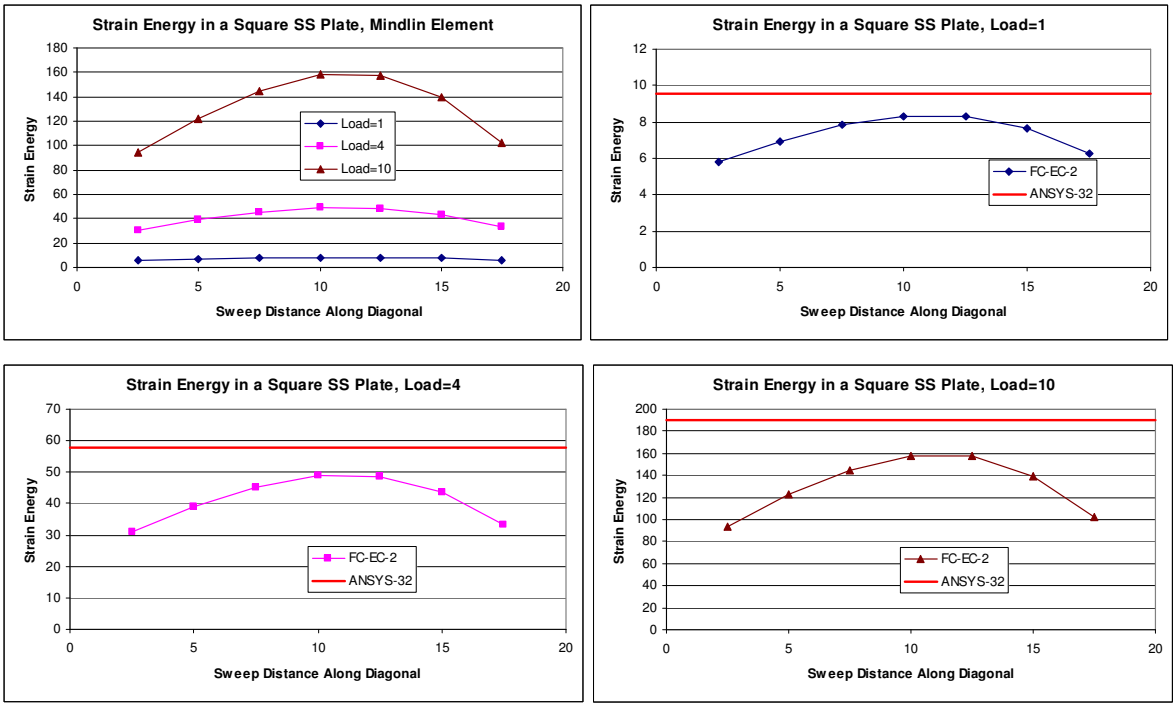

Fig. 6.70 Sweep-Test in a simply supported shear-flexible square plate (uniform load) – C^0 Selective integration formulation, Large deflection analysis

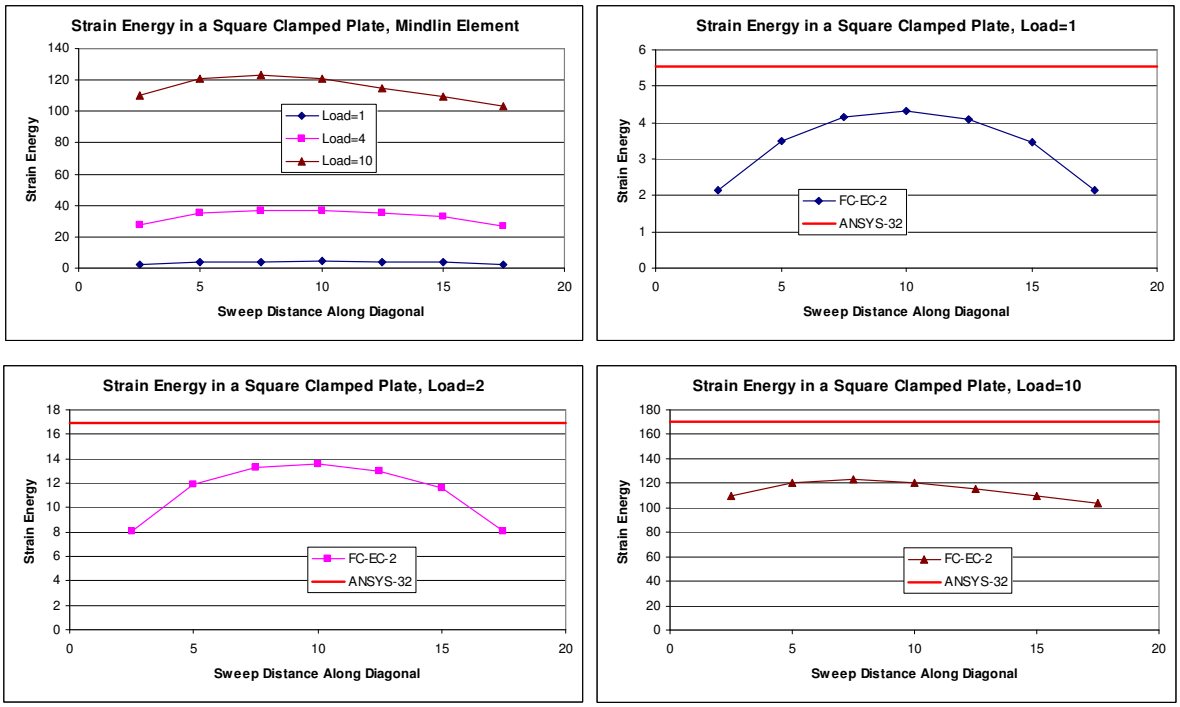

Fig. 6.71 Sweep-Test in a clamped shear-flexible square plate (uniform load) – C^0 Selective integration formulation, Large deflection analysis

6.8 Large Deformation Analysis of Thin Plates - Anisoparametric Formulation

6.8.1 Incremental Matrices

The incremental matrices remain in the same form as used in section 6.6.2. In fact the incremental matrices for the anisoparametric element leverage the incrementral matrices of the BFS element discussed in section 5.4.2. There are now 8 degrees of freedom at each of the 4 nodes, u, v, w, $w_{,x}$, θ_x,$w_{,y}$,θ_y and $w_{,xy}$. The reason for chosing the BFS element over the ACM element for the anisoparametric formulation here is the simplicity of the interpolation functions for $w_{,x}$,$w_{,y}$ and $w_{,xy}$ which have Hermite cubic polynomials. The interpolation functions for u, v, θ_x and θ_y are bilinear polynomials. This element has already been discussed for linear elastostatics applications in section 4.5.

6.8.2 Numerical Experiments and Discussion

The results for a simply supported plate (20x20 mm quarter plate, 0.4 mm thickness and Poisson's ratio of 0.3, Young's Modulus of 200000 N/mm^2) are discussed in Table 6.36. The anisoparametric formulation for shar-flexible plates does not produce any shear locking and there is no necessity of using selective integration. For plate bending problems, it has already been demonstrated in section 5.4 that the membrane locking is not significant, and hence there is no need for selective integration for the membrane strains either. This is clearly seen in Table 6.36, and the results are compared with ANSYS® (2008) (with SHELL63 element) and are seen to match closely.The results for the clamped square plate are tabulated in Table 6.37, and show a similar trend as that of the simply supported case. The membrane forces and bending moments for the simply supported plate are compared with ANSYS® (2008) (SHELL 63 element) in Fig. 6.72 and Fig. 6.73 and match very well. The anisoparametric element that

was used here had a discretisaion of 16 x 16 elements in one quadrant of the plate. The ANSYS® (2008) mesh had 32 x 32 elements in each quadrant.

Large Deflection of a shear-flexible simply supported plate - UDL			
Load	Integration (5x5)	Integration (2x2)	ANSYS Deflection
1	0.377644	0.377646	0.378168
2	0.505898	0.505900	0.506211
3	0.591216	0.591217	0.591338
4	0.657338	0.657339	0.657296
5	0.712272	0.712273	0.712085
6	0.759767	0.759767	0.759453
7	0.801906	0.801905	0.801477
8	0.839976	0.839975	0.839444
9	0.874834	0.874833	0.874208
10	0.907081	0.907079	0.906367

Table 6.36 Deflection at centre of a shear-flexible simply supported square plate (uniform load), C^0 Anisoparametric formulation, Large deflection analysis

Large Deflection of a shear flexible clamped plate - UDL			
Load	Integration (5x5)	Integration (2x2)	ANSYS Deflection
1	0.229365	0.229374	0.233990
2	0.369089	0.369116	0.375290
3	0.464803	0.464847	0.471923
4	0.538336	0.538394	0.546175
5	0.598663	0.598735	0.607130
6	0.650215	0.650299	0.659257
7	0.695492	0.695587	0.705075
8	0.736042	0.736148	0.746142
9	0.772894	0.773009	0.783492
10	0.806766	0.806889	0.817848

Table 6.37 Deflection at centre of a shear-flexible clamped square plate (uniform load), C^0 Anisoparametric formulation, Large deflection analysis

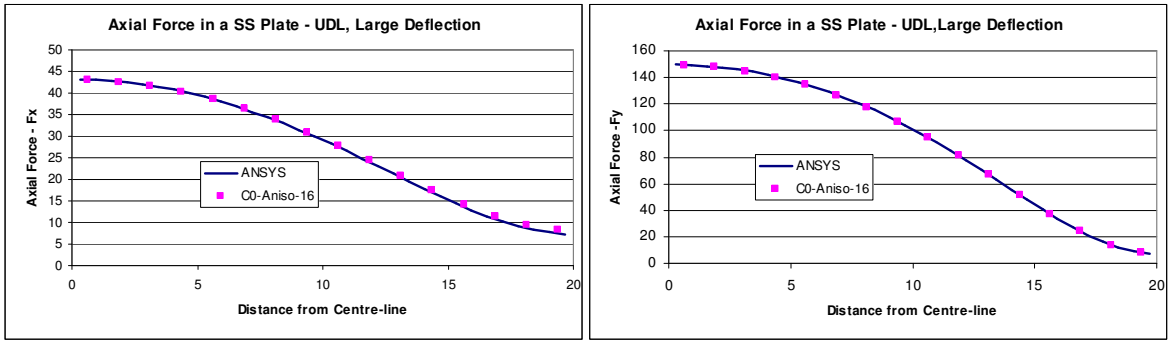

Fig. 6.72 Membrane forces in a simply supported shear-flexible square plate (uniform load), C^0 Anisoparametric formulation, Large deflection analysis

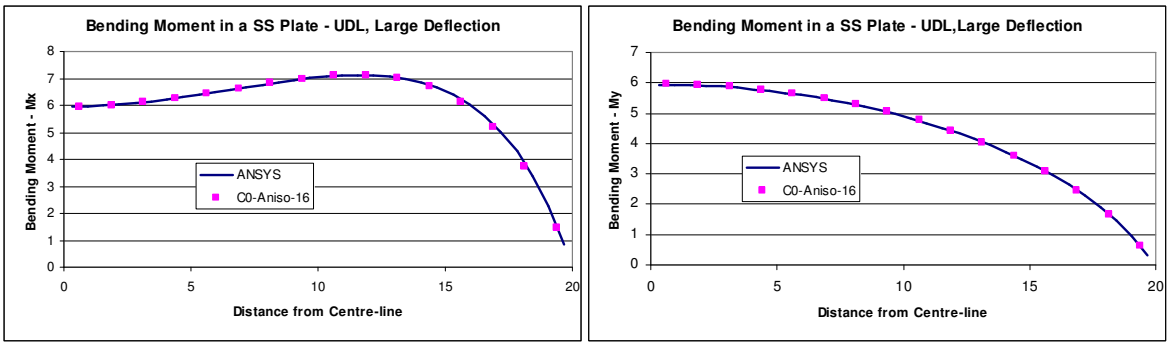

Fig. 6.73 Bending moments in a simply supported shear-flexible square plate (uniform load), C^0 Anisoparametric formulation, Large deflection analysis

The membrane forces and bending moments for the clamped plate are shown in Fig. 6.74 and Fig. 6.75 respectively and show a good match with ANSYS® (2008). The mesh discretisation is the same as used earlier for the simply supported plate.

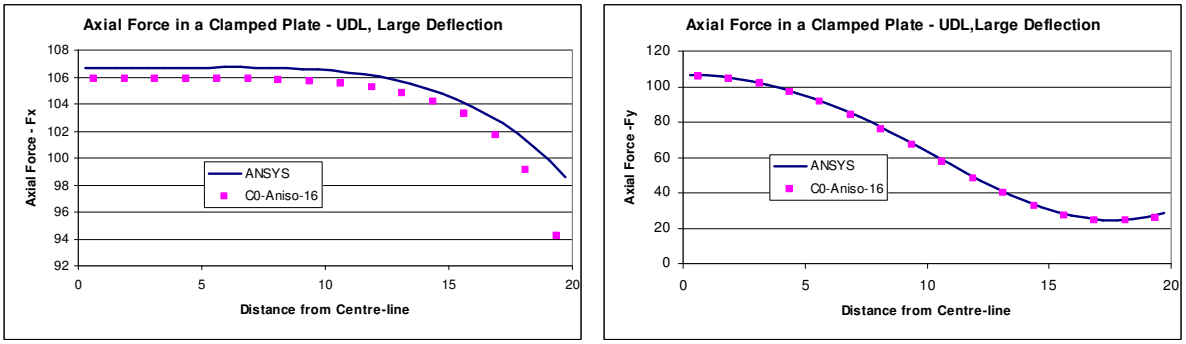

Fig. 6.74 Membrane forces in a clamped shear- square plate (uniform load), C^0 Anisoparametric formulation, Large deflection analysis

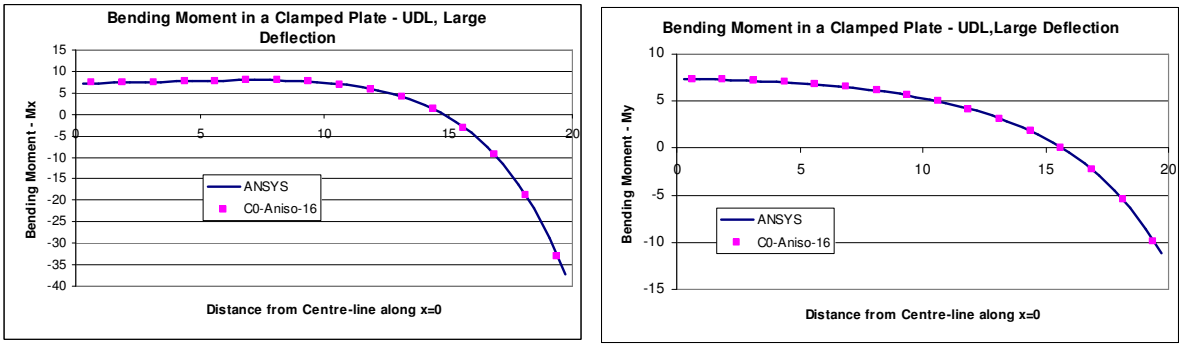

Fig. 6.75 Bending moments in a clamped shear-flexible square plate (uniform load), C^0 Anisoparametric formulation, Large deflection analysis

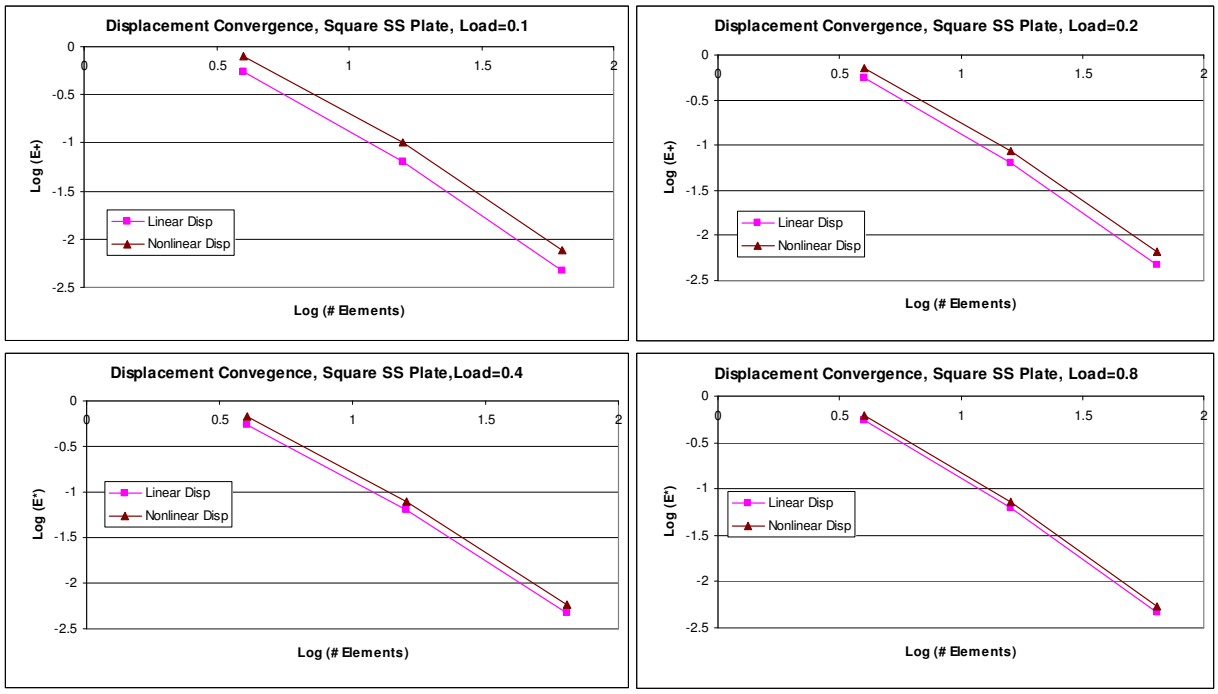

Fig. 6.76 Convergence of displacement in a simply supported shear-flexible square plate (uniform load), C^0 Anisoparametric formulation, Large deflection analysis

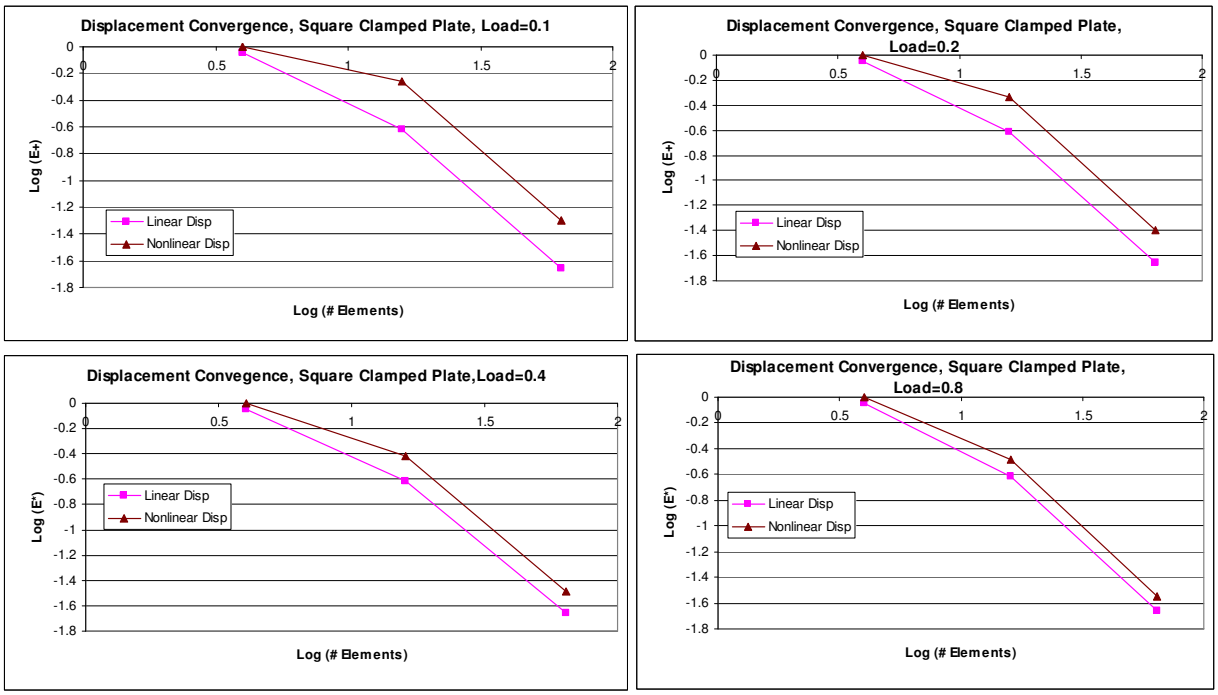

Fig. 6.77 Convergence of displacement in a clamped shear-flexible square plate (uniform load), C^0 Anisoparametric formulation, Large deflection analysis

The convergence of displacements in a simply supported plate is shown in Fig. 6.76. It can be seen that the order of convergence is less than $O(h^2)$, and the reason that is attributed is due to the complex interpolation functions that were used in the element formulation. Similar trend is seen in the displacement convergence of the clamped plate which is shown in Fig. 6.77.

The boundedness of strain energy for simply supported plate is seen in Table 6.38 for all the load cases. The clamped plate also shows similar results as seen in Table 6.39.

Strain Energy in a SS Plate - UDL, Mindlin Anisoparametric Formulation				
Load	4x4	8x8	16x16	ANSYS
1	9.408245	9.495917	9.517486	9.530380
2	23.267190	23.465179	23.527272	23.566000
3	39.266875	39.629988	39.747448	39.820800
4	56.901555	57.469316	57.653485	57.769000
5	75.893027	76.696017	76.956194	77.120800
6	96.059148	97.122324	97.466461	97.686500
7	117.269366	118.613851	119.048940	119.330000
8	139.424580	141.068725	141.601034	141.949000
9	162.446478	164.406546	165.041771	165.463000
10	186.271313	188.561930	189.305309	189.804000

Table 6.38 Strain energy boundedness in a shear-flexible simply supported square plate (uniform load), C^0 Anisoparametric element, Large deflection analysis

Strain Energy in a clamped plate - UDL, Anisoparametric Formulation				
Load	4x4	8x8	16x16	ANSYS
1	4.165290	5.340577	5.492589	5.522490
2	13.535636	16.407941	16.855445	16.963600
3	25.383898	30.091113	30.938756	31.162800
4	38.803545	45.564026	46.910672	47.283800
5	53.412571	62.457817	64.395863	64.948800
6	68.999604	80.551746	83.168105	83.929800
7	85.427656	99.694299	103.071415	104.069000
8	102.599355	119.773269	123.989895	125.250000
9	120.441296	140.701450	145.833212	147.381000
10	138.895853	162.408748	168.528557	170.389000

Table 6.39 Strain energy boundedness in a shear-flexible clamped square plate (uniform load), C^0 Anisoparametric element, Large deflection analysis ,

The results of the sweep-test for a simply supported plate are shown in Fig. 6.78 and for smaller loads, the strain energy curve does not cross the theroretical line. However, for larger loads, as the membrane forces start developing, the total strain energy appears to show a cross-over. This is attributed to the relative higher stiffness of the elements at larger loads, as seen in Table 6.37 as well. The boundary conditions for the clamped plate for performing the sweep-test are not good enough for mesh used in the study, and hence are not reported.

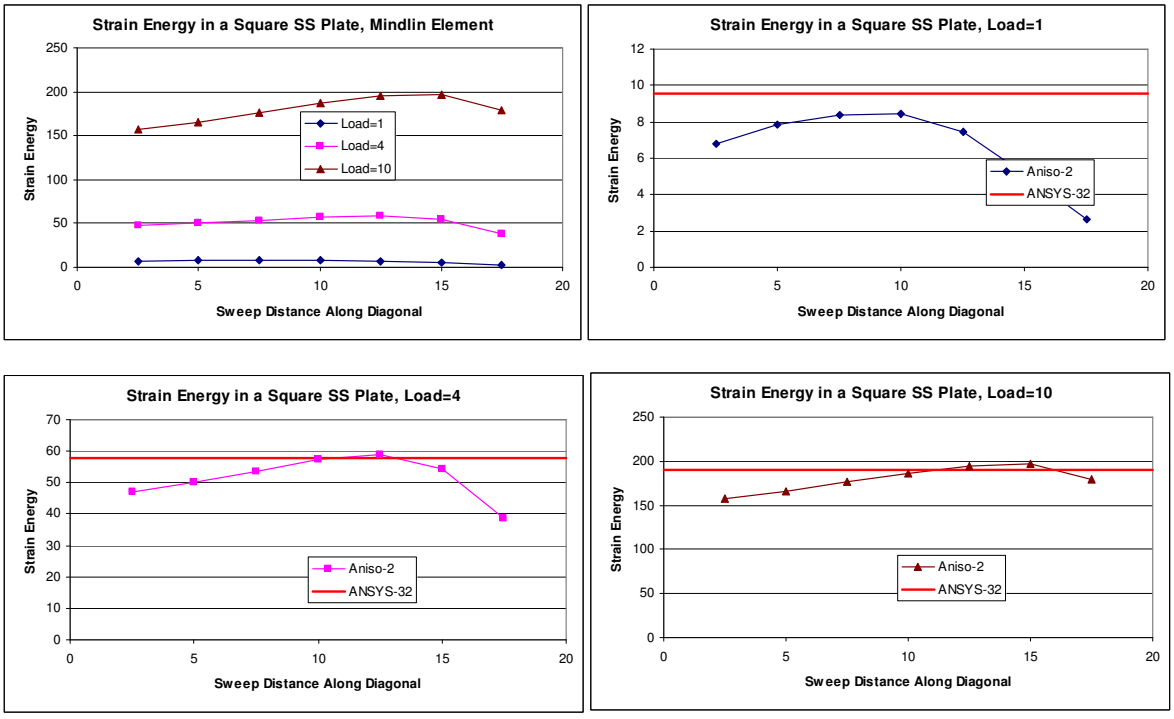

Fig. 6.78 Sweep-Test in a simply supported shear-flexible square plate (uniform load), C^0 Anisoparametric element, Large deflection analysis

6.9 Closure

In this chapter, the use of field-consistent formulation for the large deformation analyses of shear-flexible beams, shells and plates were presented. This formulation overcomes both the shear and membrane locking that is normally associated with this class of problems. Alternate mechanisms of overcoming the locking phenomena were examined, and compared with the field-consistent formulation. Since the field-consistent formulation is derived from first-principles, it is variationally correct, and the results clearly bring this out.

Summary of Results for Nonlinear Elastostatics for Shear-flexible problems					
Element Formulation	**C-Concept Deviation**	**Example Problem**	**Strain Energy Boundedness**	**Rate of Convergence**	**Sweep-Test**
C^0 Beam - RI	Correctness	Pinned-Pinned Beam	×	✓	✓
		Hinged-Hinged Beam	✓	✓	✓
		Clamped-Clamped Beam	×	✓	✓
Aniso Beam - RI	Correctness	Pinned-Pinned Beam	×	↓	×
		Hinged-Hinged Beam	✓	↓	✓
		Clamped-Clamped Beam	✓	✓	✓
Aniso Beam - FC	None	Pined-Pined Beam	×	✓	×
		Hinged-Hinged Beam	✓	✓	✓
		Clamped-Clamped Beam	×	✓	✓
C^0 Shell – RI	Correctness	SS Circular Plate	✓	✓	×
		Clamped Circular Plate	×	✓	×
Aniso Shell - FI	Consistency	SS Circular Plate	✓	✓	✓
		Clamped Circular Plate	✓	✓	✓
Aniso Shell - RI	Correctness	SS Circular Plate	✓	✓	✓
		Clamped Circular Plate	✓	✓	✓
C^0 Plate – RI	Correctness	SS Plate	✓	✓	✓
		Clamped Plate	✓	✓	✓
C^0 Plate – FC	None	SS Plate	✓	✓	✓
		Clamped Plate	✓	✓	✓
Aniso Plate	Correctness	SS Plate	✓	✓	×

Table 6.40 3C concepts and performance of various shear-flexible element formulations (large deflection analysis)

Note: ✓ implies that the performance is good/satisfies the respective attribute

× implies that it is a violation of the respective attribute

↓ implies that the performance of the respective attribute is degraded

Chapter-7
Linear Elastodynamics

7.1 Introduction

Finite element analysis of structures subjected to transient loads quite often requires the natural frequencies of the structure to be determined. Though the analysis required may vary depending on the nature of applied loads, *e.g*. spectrum analysis, random vibration analysis, time-history analysis, impact analysis *etc*., one important feature common to all these types of analysis is the accurate determination of the natural frequencies of the structure. In a finite element analysis, this involves the formulation of the stiffness and mass matrices of the structure. Once these matrices are established, the mathematical treatment of the generalized eigenvalue problem is used to determine the natural frequencies and the mode shapes. It is the input that goes to these algorithms, *viz*., the stiffness and mass matrices of the discretised structure that determines the accuracy of the natural frequencies as compared to the exact frequencies of the actual structures. For example, the natural frequencies of the simplest problem such as the simply supported beam when obtained from the finite element model of the beam still contain an error, when compared to the exact frequencies. In this work, the source of this error is interpreted due to the discretisation of the structure and the manner in which the mass matrices were obtained to the 3C concepts paradigm.

A deeper study of the rates of convergence and behaviour of the elements (bar element, beam element, plate element *etc*.) is required for better understanding of the errors in the natural frequencies. In this chapter the natural frequencies of the beams and plates using different elements are studied. The C^1 plate bending element based on classical Kirchhoff theory, and the C^0 plate bending element based on Mindlin's theory are used in this study. The effect of using consistent

and lumped mass matrices on the natural frequencies are studied using the above elements. The various types of lumping schemes are briefly discussed. The effect of using reduced integration in the stiffness matrices for determining the natural frequencies is also addressed.

The modeling of dynamic behaviour of structural elements requires correct modeling of strain energy and kinetic energy. Any errors in either or both of these terms can cause errors in the natural frequencies, and the respective mode shapes. The source of the errors in the kinetic energy terms is the mass matrix, and various formulations of mass matrix were studied by many researchers.

Leckie and Lindberg (1963) proposed a dynamic stiffness matrix whose error in the frequency varies inversely as the fourth power of the number of elements. Lindberg and Olson (1970) showed that the conforming plate bending element converges from above, and is far superior to the non-conforming element. Fried (1971) estimated *a priori* the accuracy in eigenvalues as a function of order of element and geometrical characteristics of the element.

Hinton *et al.* (1976) used a scaling factor to scale all the diagonal elements of a mass matrix. This scaling factor is based on the ratio of the total mass to the sum of the diagonal coefficients of the mass matrix associated with the translational degree of freedom that are in the same direction. Cook (1991) proposed the use of a linear combination of lumped (6%) and consistent (94%) mass matrices to estimate the errors in the natural frequencies. There is no rationale for the basis for this specific combination of the lumped and mass matrices. Rajendran and Prathap (1999) showed that the lumped mass approach conserves mass but not necessarily the momentum or kinetic energy of the consistent mass matrix.

Archer and Whalen (2005) proposed a new formulation of the mass matrix for plate and beam elements, and study the errors in the natural frequencies. In this

approach, there is a possibility of generation of negative mass terms in certain cases, and a work-around is suggested.

Error measures of the natural frequencies were studied by Ladeveze and Pelle (1989, 2003), Cook and Avrashi (1992), Stephen and Steven (1997a, 1997b, 1997c), Zhao and Steven(1996a, 1996b). Fuenmayor *et al.* (2001) dealt with the problem by taking the contributions of the individual errors in stiffness and mass matrices, and also address the errors due to the choice of consistent or lumped mass matrices in the formulation. A combination of errors in the kinetic and strain energy was used by Hager and Wiberg (2000). Cheung *et al.* (2000) used a 4-noded refined non-conforming plate bending element to form the stiffness matrix and a modified mass matrix based on a combination of the conventional displacement interpolation function (of cubic order) and linear displacement interpolation function with an adjustable factor α to improve the accuracy of the vibration analysis. The rationale for the choice of α is however not explained. Singh and Venkateswara Rao (2000a) used a four-node shear flexible rectangular element with six degrees of freedom per node. The interpolation functions are derived from the equilibrium conditions and the element does not exhibit shear locking. Jafarali *et al.* (2004) used a hybrid beam element that has the stiffness matrix based on Timoshenko beam theory and the mass matrix from classical beam theory and show that it is the cancellation of errors that results in the apparent accurate performance of the element. Jafarali *et al.* (2007) showed that use of reduced integration violates virtual work principle which in turn causes the loss of boundedness of the finite element eigenvalues.

In this chapter, the error analyses is based on the projection theorem of Prathap and Mukherjee (2003a). The projection theorem for the elastodynamics problem was outlined in chapter-2, and these results are used to assess the performance measures, rate of convergence and boundedness for beam and plate problems. What is important is that the error is still governed by the error in the strain energy, and therefore, as long as no variational crimes are committed, the orders

of convergence for the elastostatics case should apply. These concepts are now applied to study the accuracy of the natural frequencies of beams and plates, and the accompanying errors due to use of extra-variational concepts. For this, it is important that the measure of error to be used is clearly defined. For elastodynamics, where, a variationally correct formulation would have produced higher frequencies, one can define error as

$$\text{Error} = (\omega^h)^2/\omega^2 - 1 \qquad \ldots(7.1)$$

It was already seen even in the elastostatics cases earlier that, if the problem is not formulated in a variationally correct way, boundedness is lost. In an elastodynamics case, it will therefore be possible that frequencies are lower than the analytical ones. In such cases it may be necessary to use $|Error|$ in the logarithmic plots.

7.2 Natural Frequencies of Classical Beams and Plates

7.2.1 Formulation of Element Matrices

The derivation of the stiffness matrix and mass matrix for a finite element follows standard finite element textbook, Cook *et al.* (1989). Here, the final forms of these matrices are reproduced. The stiffness matrix is represented as

$$[K] = \int [B]^T[D][B]\, dV \qquad \ldots(7.2)$$

and the mass matrix M as

$$[M] = \int \rho\, [N]^T[N]\, dV \qquad \ldots(7.3)$$

where

ρ is the density of the material

N is the interpolation function

Depending on the element being used, interpolation functions N can be defined. For a C^1 plate bending element, the ACM and BFS elements described in Chapter-3 are used. For the C^0 plate bending element, the field consistent and edge consistent formulation of Prathap and Somasekhar (1988) is used. The mass matrix formulated as above is termed consistent mass matrix. The other formulation of the mass matrix, lumped mass matrix, is implemented using the HRZ lumping scheme of Hinton *et al.* (1976) lumping scheme, which is discussed in section 7.2

The stiffness matrices and mass matrices are formed using the above interpolation functions and respective strain displacement relations. Numerical integration is used, and the order of integration used is for exact integration. For the specific case of reduced integration for the C^0 formulation of Mindlin element, the stiffness matrix is obtained as

$$[K] = [K_b] + [K_s] \qquad \ldots(7.4)$$

$$[K] = \int [B_b]^T [D_b][B_b]\, dA + \int [B_s]^T [D_s][B_s]\, dA \qquad \ldots(7.5)$$

where $[B_b]$ represents the strain displacement relations between the bending strains and the displacements, and $[B_s]$ represents the strain displacement relations between the shear strains and the displacements. The stiffness matrix $[K_b]$ is integrated using the routine 2X2 Gaussian Quadrature, and $[K_s]$ is integrated using 1X1 rule.

7.2.2 Numerical Experiments

A simply supported beam of length 1000 mm, width 10 mm and depth 10 mm is considered first. The Young's modulus of the material of the beam is 200000 N/mm^2, and the density is 7850 kg/m^3. The theoretical fundamental frequency for this beam is

$$\omega = (\pi)^2 \, sqrt(EI/ml^4) \qquad \ldots(7.6)$$

where EI is the flexural rigidity of the beam, and m is the mass per unit length of the beam, and l is the length of the beam.

The results obtained using BFS, ACM and Mindlin elements are shown in Fig. 7.1. The beam is discretised into 40 elements. The variation of error is shown with respect to the mode number as explained in Prathap and Pavankumar (2001). We observe that the rate of convergence for the BFS/ACM is $O(h^4)$.

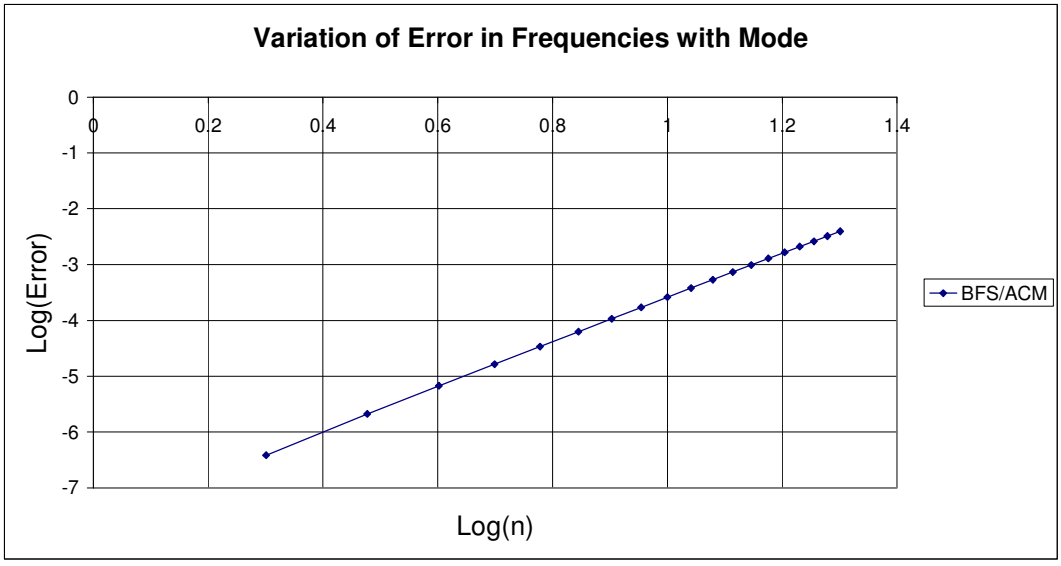

Fig. 7.1 Variation of error with mode number for a simply supported beam

7.2.3 Effect of Conformance and Non-conformance

A second example, of a simply supported plate is taken with the following properties – Square plate of 40 mm side, Thickness as 0.4 mm, Young's Modulus as 200000 N/mm^2, Poisson's ratio as 0.3 and density as 7850 kg/m^3. Due to the symmetry of the plate, we use only one quadrant of the plate. The theoretical frequency is given in Shames and Dym (1987), as

$$\omega = \pi^2 \{p^2/a^2 + n^2/b^2\}\sqrt{\frac{D}{m}} \qquad \ldots(7.7)$$

where D is the flexural rigidity of the plate, and m is the mass per unit area of the plate, a and b are the dimensions of the rectangular plate, and n and p are the mode numbers.

The results obtained using BFS and ACM elements for this plate are shown in Fig. 7.2. The error is now reported as varying with respect to the mesh refinement.

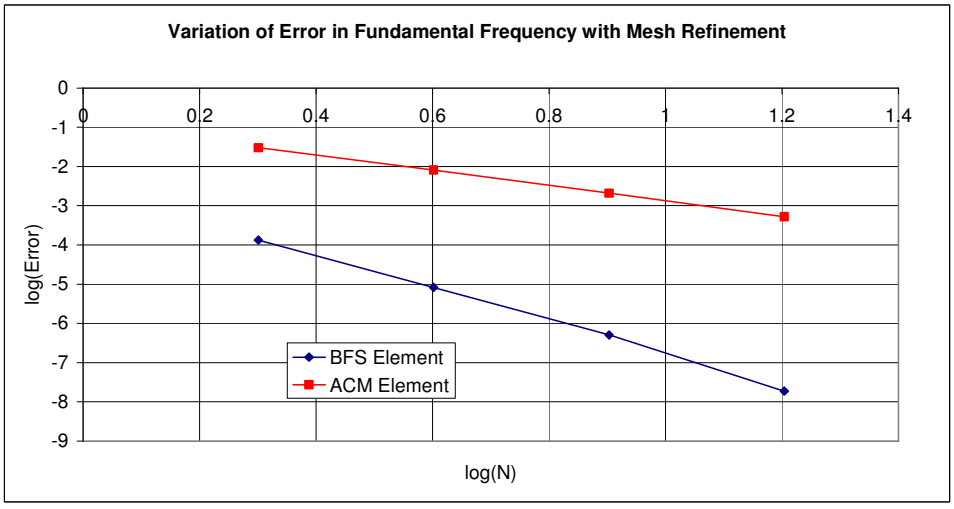

Fig. 7.2 Comparison of convergence of frequencies of a simply supported plate

Note that the BFS element gives very low errors even for a mesh of 2x2. This can be attributed to the fact the BFS is a conforming element while ACM is a non-conforming element. Also, it can be observed that the results for the BFS

element converge from the top, whereas for the ACM element converge from the bottom.

7.2.4 Effect of Consistent and Lumped Mass Modeling

The effects of consistent and lumped formulation of the mass matrices are discussed now. The same two examples of simply supported beam and simply supported square plate are considered. Formulation of the consistent mass matrix was explained in section 7.1. For BFS element, numerical integration of order 4x4 is used for formulating the mass matrix. For ACM element also, 4x4 order is used. For the lumped formulation the HRZ lumping scheme of Hinton *et al.* (1976) is used. This process is summarized in the following steps:

1. Compute the diagonal terms of consistent mass matrix.
2. Compute total mass of element, *m*
3. Compute *s* by adding diagonal coefficients associated with translational D-O-F that are in same direction.
4. Scale all diagonal coefficients by multiplying by *m/s*

The results for the case of a simply supported beam in which the beam is discretised into two elements, for both consistent and lumped mass matrices are shown in Fig. 7.3

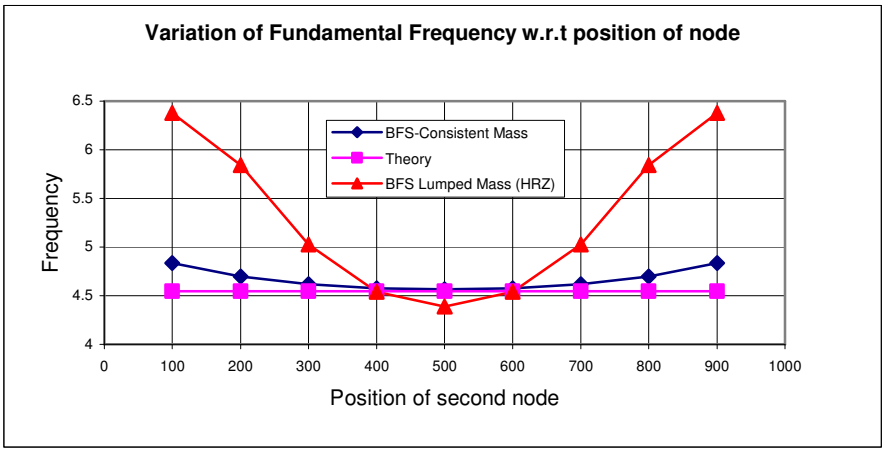

Fig. 7.3 Sweep-Test in a simply supported beam

The results for the case of the fundamental frequency of the plate using BFS element are shown in Fig. 7.4

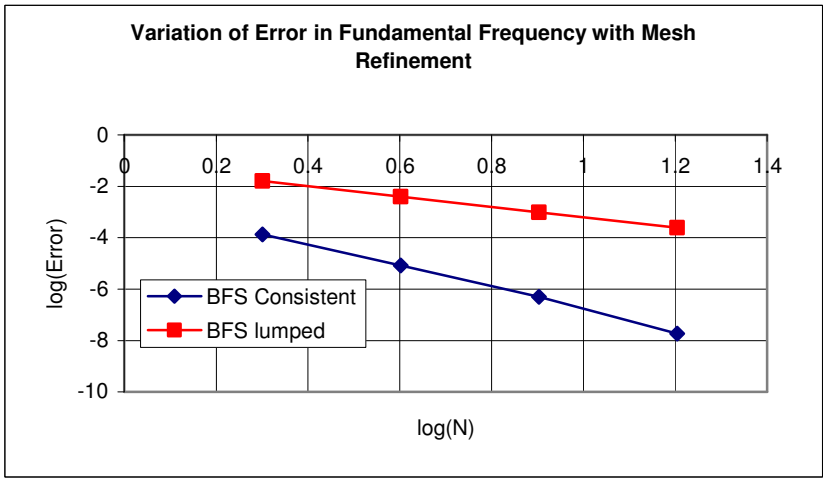

Fig. 7.4 Comparison of frequencies in a simply supported plate – BFS Element

Here it can be observed that the results for the consistent mass matrix converge from the top, whereas for the lumped mass matrix converge from the bottom. Also, the rate of convergence of lumped mass is lower than the consistent mass.

For the ACM element, the results are shown in Fig. 7.5

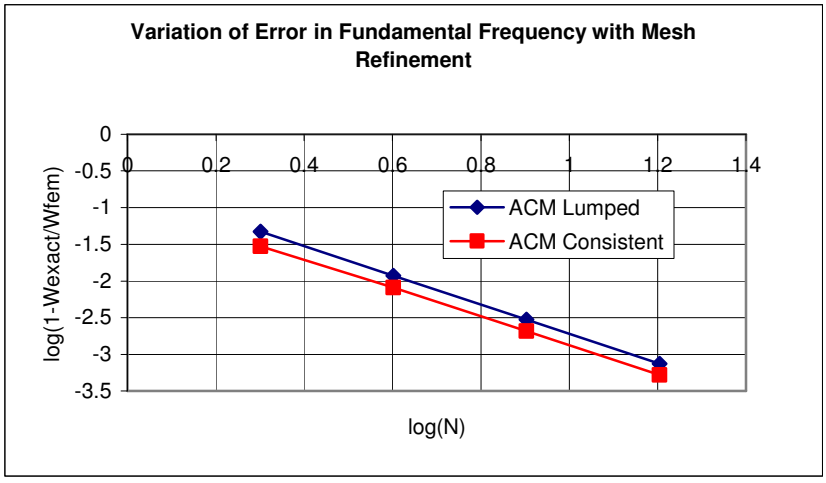

Fig. 7.5 Comparison of frequencies in a simply supported plate – ACM Element

In this case, the results for both consistent and lumped mass matrices converge from the bottom. Also when Fig. 7.4 and Fig. 7.5, are compared the rate of convergence of the BFS lumped mass case is almost the same as the rate of convergence of ACM consistent and lumped mass case.

7.2.4 Discussion of Results

The problem of determining the position of the nodes in a given mesh that makes the error between the computed natural frequency and the exact frequency, a minimum is considered. This position can be considered as the optimal mesh. The simple case of a simply supported beam is considered. When the beam is discretised into two elements, and the natural frequency is computed by varying position of the middle node, it can be observed from the variation of the error from the consistent case, that the error is the least when the mid node is positioned exactly at the center of the beam. The results are shown in Fig. 7.3

Based on the same argument if the position of the mid node is to be ascertained in the case of lumped mass which makes the error in the fundamental frequency the least, it is found that it is not at the center but at two locations of 400 mm and 600 mm from one end. This is a result, which does not give any physical meaning as the consistent case. This is explained by the fact that the lumping process has introduced additional errors in the representation of the the kinetic energy and in the process has lost variational correctness that is maintained in the consistent mass approach.

One half of the beam can be considered, (due to symmetry of the beam and the symmetry of the fundamental mode), and this is discretised into two elements. The position of the middle node which makes the error minimum, is determined from the following results, as shown in Fig. 7.6.

Note that due to symmetry only one half is taken, and the same variation of the curve is expected for the other half.

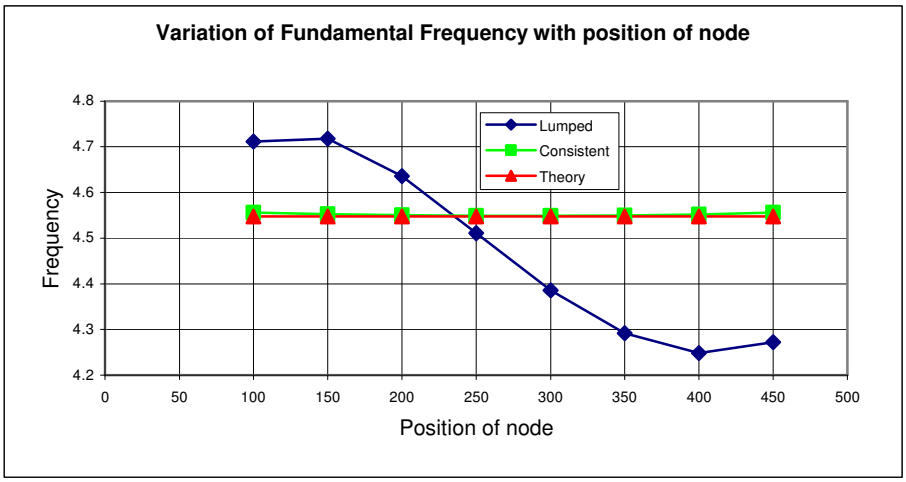

Fig. 7.6 Sweep-Test in a simply supported beam (4 elements)

For the lumped mass matrix case, it can be deduced from the curve that the error is minimum, once again, at two locations, thus corroborating the finding that lumped mass matrix does not give a unique position of nodes leading to an optimum mesh. Thus it can be seen that the variational violations due to lumping of mass matrices may produce results which could mislead.

To study the rate of convergence of the errors, the approach introduced by Prathap and Pavankumar (2001) is followed. An accurate high density mesh of uniformly sized elements (*NxN* mesh) is used and then the error in the frequencies is computed with increasing mode number (for a plate, *m* or *n*, varying one and keeping the other fixed). Consider a simply supported plate, where the exact solution involves simple trigonometric waves; for example, the (*m,n*) mode will be the eigenfunction $sin(m\pi x/a)sin(n\pi y/b)$. The ratio of the element length, $h = a/N$ to the wave-length of the mth wave $\lambda = a/m$, is now $r = h/\lambda = m/N$, when the other mode number (say *n*) is kept fixed. The errors will now be a function of *r*, and this will mean that the order of convergence with one of the mode numbers of the frequency (say *m*) will follow the exact trend as with *h*, if *N* and *n* are fixed for the problem. Thus, with one single eigenvalue computation, the errors can be swept for varying mode number *m*. Fig. 7.7 shows the error trends in this fashion, for the BFS model of the free vibration of a simply

supported plate. It is seen that the convergence is consistent with the prediction that the eigenfrequencies will have a convergence of $O(h^4)$. Fig. 7.8 shows the errors in the natural frequencies, when ACM model is used. It is clear that there is no definite order of convergence for any general mode (m,n). However, it is interesting to note that for m=n modes, it follows $O(h^2)$.

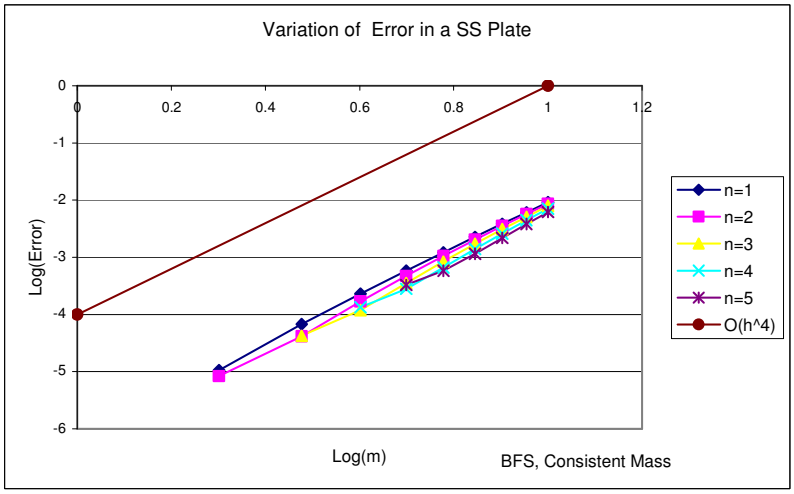

Fig. 7.7 Errors in natural frequencies of a simply supported plate - BFS element

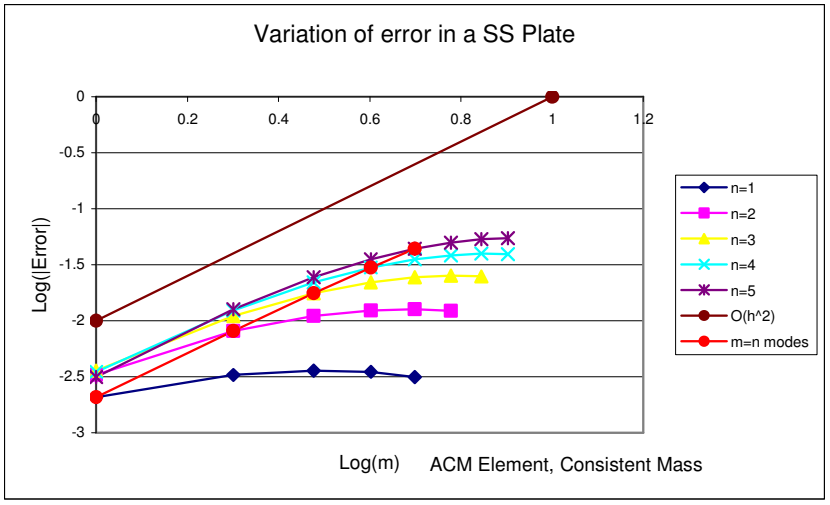

Fig. 7.8 Errors in natural frequencies of a simply supported plate - ACM element

The question of boundedness of the eigenvalue predictions is now considered, when conformity is not assured. For this, the simply supported plate is chosen, and a 2x2 mesh is used. The central nodal point of the mesh of the plate is swept

so that have a highly asymmetrical mesh is obtained. Fig. 7.9 shows the eigenvalues obtained when the node is swept over the plate for the BFS element model.

Fig. 7.9 shows that the frequencies are very neatly bounded, and the perfectly symmetrical mesh, which is also the mesh which is uniform, has the most accurate frequency. Fig. 7.11 shows what happens when the central node is swept along the diagonal ($x = y$). The boundedness aspect is seen very clearly.

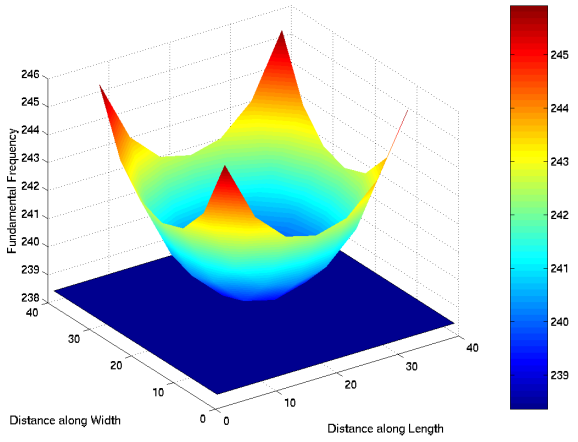

Fig. 7.9 Sweep-Test in a simply supported plate – Surface plot (BFS element)

.

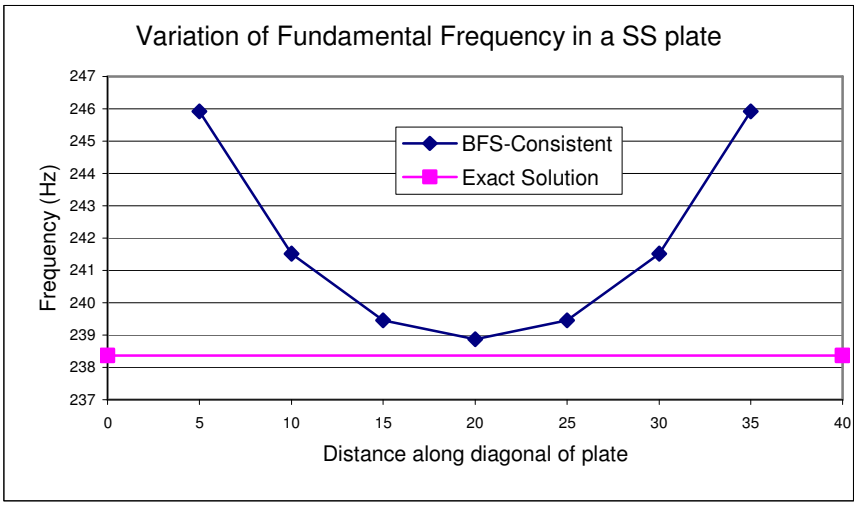

Fig. 7.10 Sweep-Test in a simply supported plate – Line plot (BFS element)

Fig. 7.11 and 7.12 show this exercise repeated with the ACM elements. Boundedness is now lost, and in fact, there are points where the mesh, if sufficiently non-symmetrical, gives the exact frequency. This can be interpreted to mean that the extra-variational errors introduced due to loss of conformity have exactly compensated for the errors due to the discretisation process described by eqn. (7.2) and (7.3). It is easy to see that this has important implications where error estimates are used to achieve automatic mesh refinement.

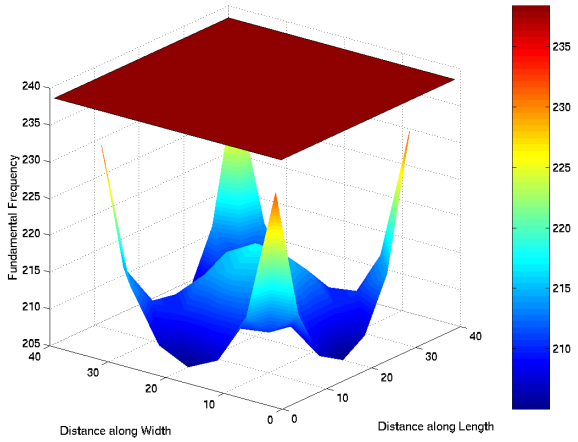

Fig. 7.11 Sweep-Test in a simply supported plate – Surface plot (ACM element)

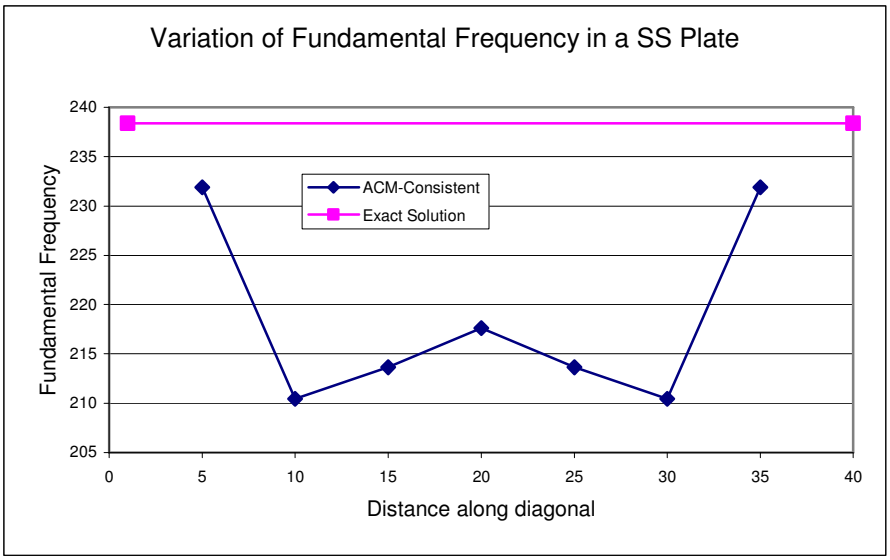

Fig. 7.12 Sweep-Test in a simply supported plate – Line plot (ACM element)

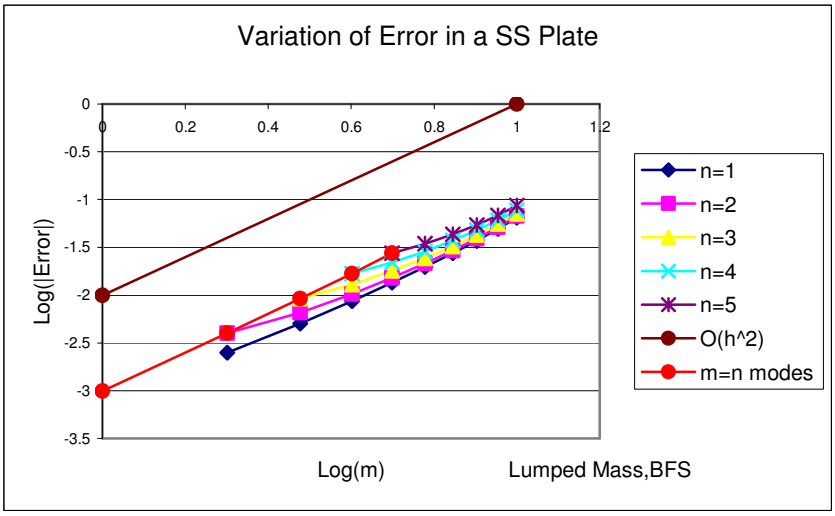

Fig. 7.13 Errors in natural frequencies of a simply supported plate due to lumping (BFS Element)

In Fig. 7.13, it can be noted that the rates of convergence have dropped to $O(h^2)$ as compared to the $O(h^4)$ achieved for the consistent mass case for the BFS element.

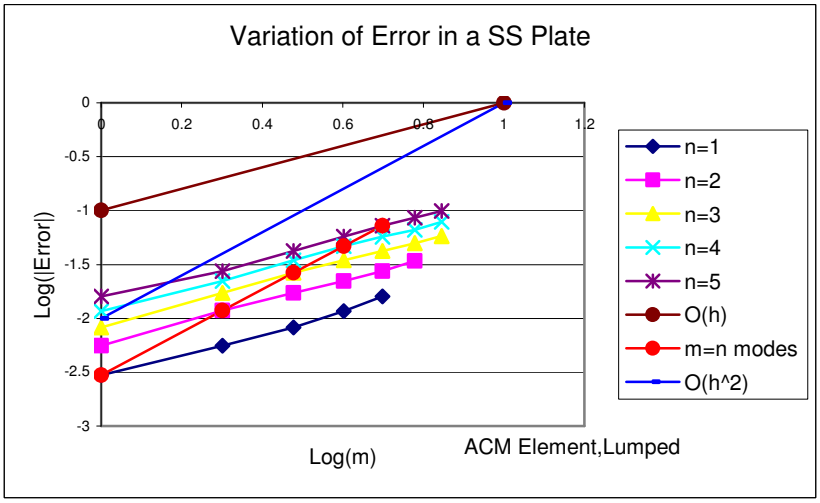

Fig. 7.14 Errors in natural frequencies of a simply supported plate due to lumping (ACM Element)

In Fig. 7.14, the effect of lumping on the natural frequencies of the plate is shown for the ACM formulation. Here again, the loss of rate of convergence can be

observed. Fig. 7.15 emphasizes the boundedness aspect further from the lumping point of view. A 2x2 element mesh is used, with the central node swept to cover the whole plate. Lumping causes the boundedness to be lost. The perfectly symmetrical mesh yields a frequency that is lower than the exact frequency. For a non-symmetrical mesh, the frequencies increase at first, and at some fortuitous configurations, the exact frequencies are obtained. At highly non-symmetrical situations, the trend changes and the frequencies begin to fall.

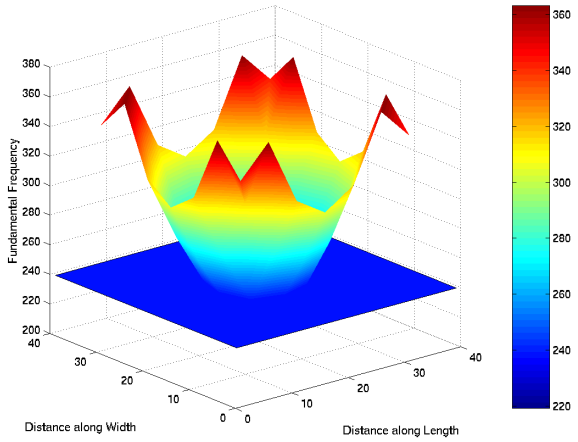

Fig. 7.15 Sweep-Test in a simply supported plate – Surface plot (BFS element Lumped Mass)

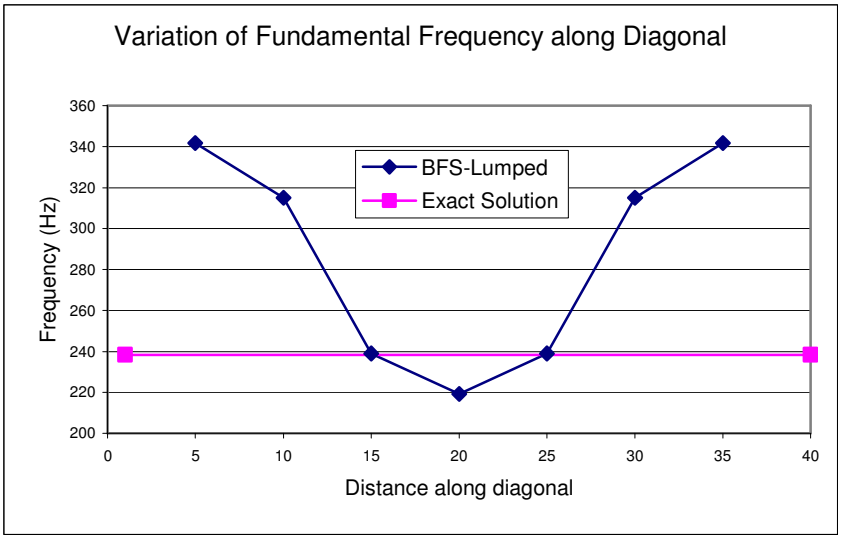

Fig. 7.16 Sweep-Test in a simply supported plate – Line plot (BFS element Lumped Mass)

The main conclusion from this is that it is unreliable to use lumped mass approaches in an automatic adaptive mesh refining approach, as the errors of lumping may actually be compensating for the errors of discretisation. Fig. 7.16 shows what happens when the central node is swept along the diagonal of the plate.

Fig. 7.17 and 7.18 show the results obtained when the same exercise is repeated with lumped ACM elements. More information on these investigations is reported in Muralikrishna and Prathap (2003).

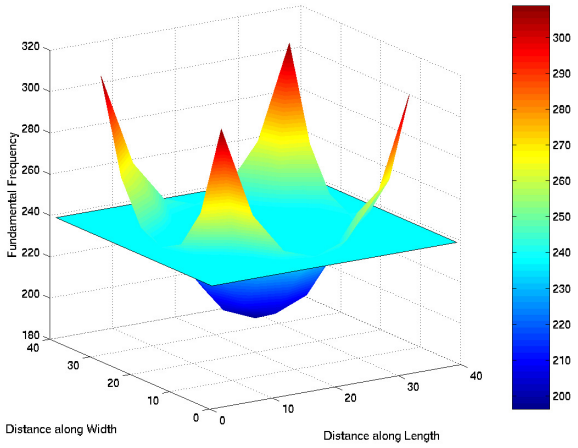

Fig. 7.17 Sweep-Test in a simply supported plate – Surface plot (ACM element Lumped Mass)

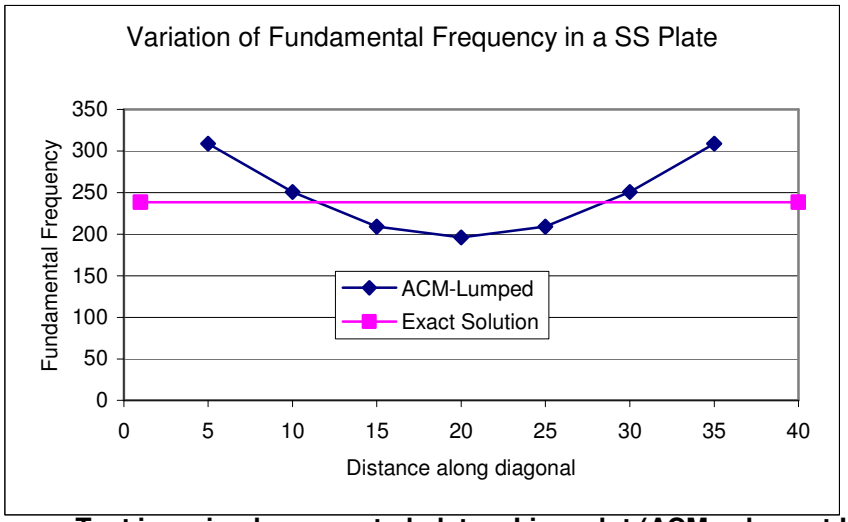

Fig. 7.18 Sweep-Test in a simply supported plate – Line plot (ACM element Lumped Mass)

7.3 Natural Frequencies of Shear-Flexible Beams and Plates – Isoparametric Formulation

7.3.1 Formulation of Element Matrices

The effect of C^0 elements on the natural frequencies of a simply supported beam is discussed now. Here, the locking phenomenon that is observed in the C^0 elements for certain problems is not discussed in depth. Rather, the focus is on the effect of the C^0 element per se, on the natural frequencies, when the most often suggested remedy of reduced integration is used. Fig. 7.19 compares the errors in frequencies between the C^1 and C^0 elements. It is to be noted that a plate element can be used for computing the frequencies of a beam as well, and in all these studies the plate elements are used for beams as well.

7.3.2 Numerical Experiments

The element formulations are now tested on beams and plates for which theoretical frequencies are available. The impact of integration on the natural frequencies is assessed for both full integration and reduced integration. This is followed by assessing the impact of consistent and lumped matrices.

7.3.3 Effect of Full Integration/Selective Integration

The results of the standard C^0 element formulated using Mindlin theory are compared with the field and edge consistent C^0 element of Prathap and Somasekhar (1988) in Fig. 7.20. It can be observed that the erratic behaviour of the error at higher modes, is due to the use reduced integration for formulating the stiffness matrices. This indicates that the reduced integration strategy has introduced spurious zero energy modes which act up at higher modes.

7.3.4 Effect of Consistent and Lumped Mass Modeling

Fig. 7.21 shows the effect of lumping on the C^0 element. There is no loss of convergence due to lumping. The results of the sweep-test for a simply supported beam (length 1000 mm, width 10 mm, depth 10 mm, Young's modulus of the material of the beam is 200000 N/mm^2, and the density is 7850 kg/m^3) and a simply supported plate (square plate of 40 mm side, thickness as 0.4 mm, Young's Modulus as 200000 N/mm^2, Poisson's ratio as 0.3 and density as 7850 kg/m^3) for different lumping schemes, HRZ (Hinton *et al.* 1976) and Archer (Archer and Whalen 2005) are shown in Fig. 7.22 and Fig. 7.23.

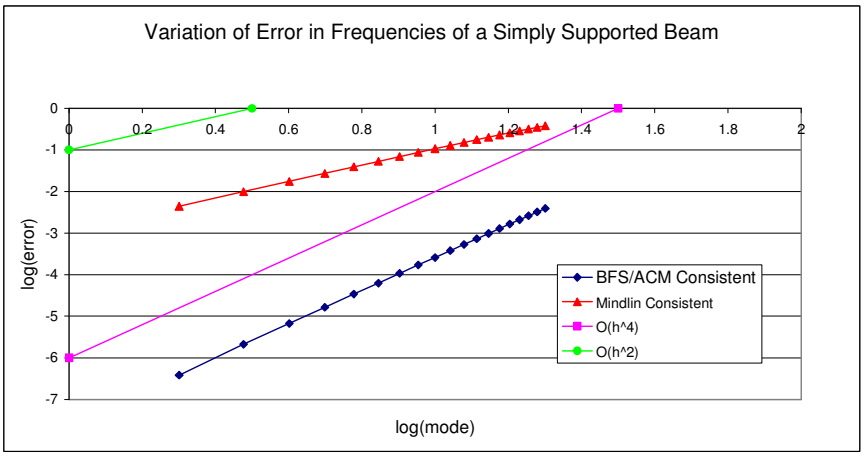

Fig. 7.19 Comparison of errors in natural frequencies of a simply supported beam

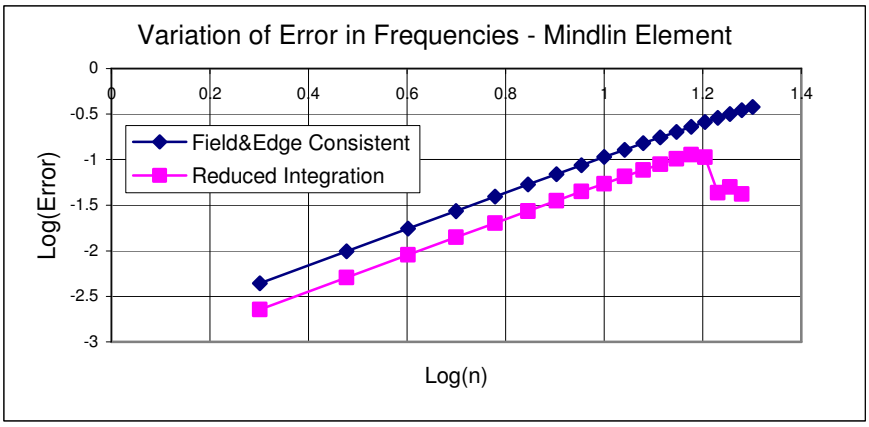

Fig. 7.20 Comparison of errors in natural frequencies of a simply supported plate

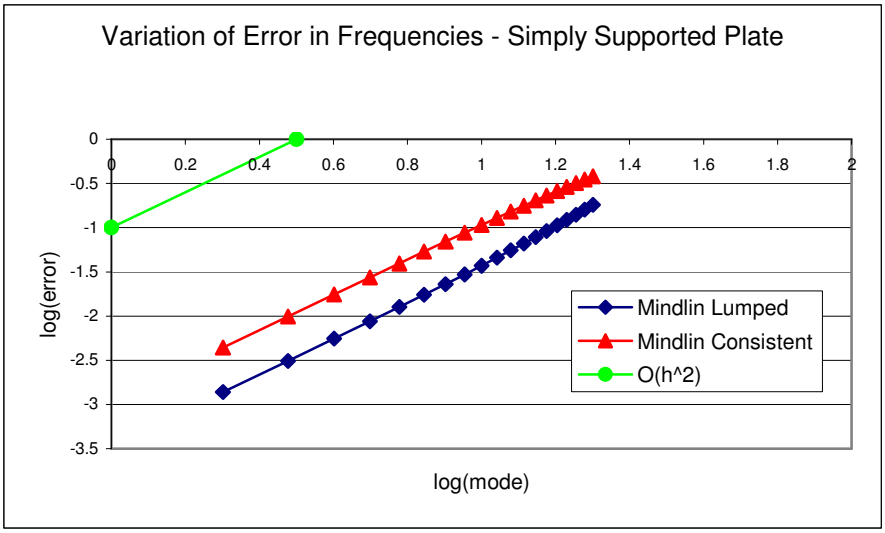

Fig. 7.21 Effect of lumping on natural frequencies of a simply supported shear-flexible beam

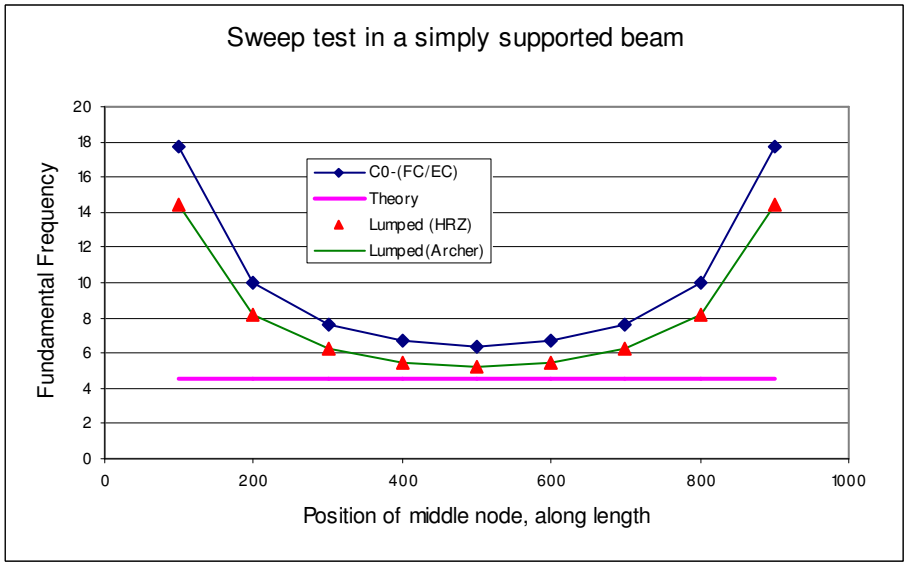

Fig. 7.22 Effect of different lumping schemes on natural frequencies of a simply supported shear-flexible beam

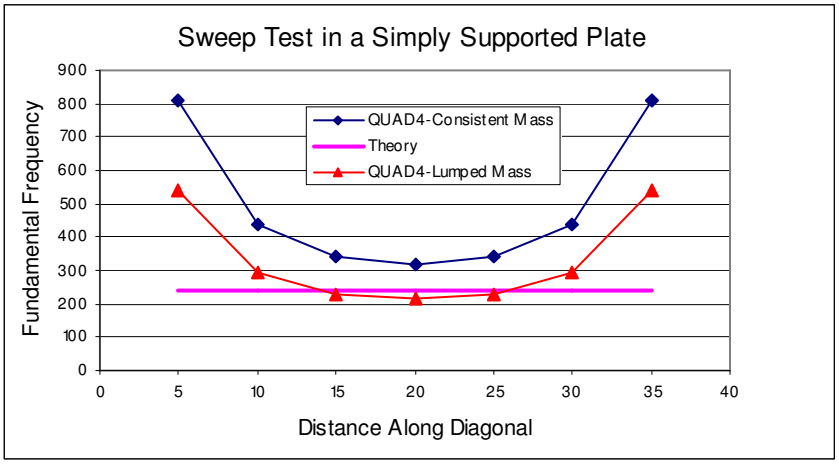

Fig. 7.23 Effect of lumping on natural frequencies of a simply supported shear-flexible plate

7.3.5 Discussion of Results

In the plots shown in Fig.7.22 and Fig. 7.23, the effects of lumping can be clearly seen. Fig. 7.23 shows that lumping causes a cross-over of the frequency curve with the exact frequency, thus indicating a loss of boundedness. Table 7.1 shows the impact of the two lumping schemes considered here. The lumping scheme of Archer and Whalen (2005) gives consistently higher frequencies for all the modes.

Effect of different lumping schemes on Natural Frequencies in a SS Plate				
n	m	Theory	HRZ	Archer
1	1	238.3629	237.7701	239.3208
1	2	595.9072	595.1089	605.0952
2	1	595.9072	595.1089	605.0952
2	2	953.4515	944.0367	969.8232
1	3	1191.8143	1197.9182	1240.4106
3	1	1191.8143	1197.9182	1240.4106
2	3	1549.3586	1532.8187	1604.1254
3	2	1549.3586	1532.8187	1604.1254
1	4	2026.0843	2058.1581	2193.1484
4	1	2026.0843	2058.1581	2193.1484
3	3	2145.2658	2098.1910	2238.1027
2	4	2383.6286	2373.4010	2557.3227
4	2	2383.6286	2373.4010	2557.3227
3	4	2979.5358	2905.9519	3194.3793
4	3	2979.5358	2905.9519	3194.3793
1	5	3098.7172	3194.9855	3555.9475
5	1	3098.7172	3194.9855	3555.9475
2	5	3456.2615	3484.9001	3925.0454
5	2	3456.2615	3484.9001	3925.0454
4	4	3813.8058	3667.6617	4160.9731

Table 7.1 Effect of different lumping schemes on natural frequencies of a simply supported square plate

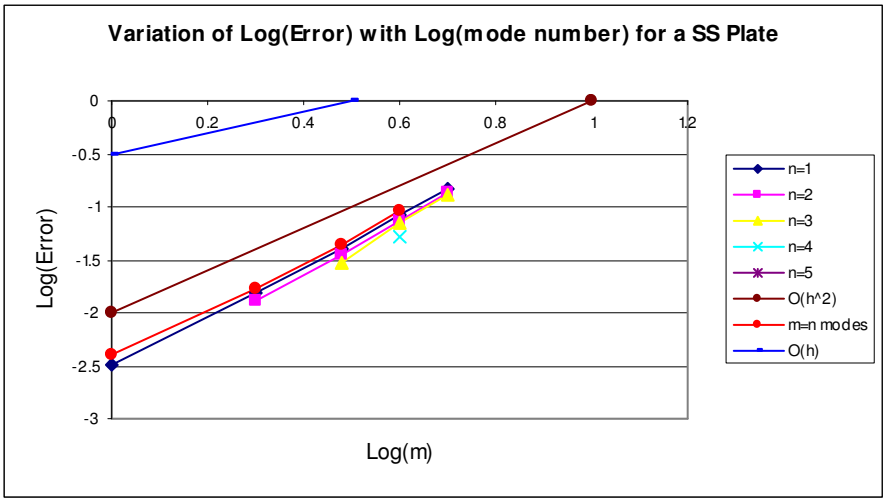

Fig. 7.24 Errors in natural frequencies of a simply supported shear-flexible plate due to lumping

7.4 Natural Frequencies of Shear-Flexible Beams– Anisoparametric Formulation

7.4.1 Formulation of Element Matrices

The anisoparametric elements developed in chapter-4 are now studied for their dynamic behaviour. The 2-node anisoparametric beam described in section 4.2 is now used for studying the natural frequencies of beams.

The error in the fundamental frequency of a simply supported beam (length 1000 mm, width 10 mm, depth 10 mm, Young's modulus of the material of the beam is 200000 N/mm^2, and the density is 7850 kg/m^3) for various combinations of stiffness matrix and mass matrix is shown in Fig. 7.23. As already discussed in chapter-4, the use of full integration and reduced integration for an anisoparametric beam does not make any impact (anisoparametric beam does not cause shear locking, and hence there is no need for a reduced integration).

The use of lumped mass does not degrade the rate of convergence as can be seen in Fig. 7.23.

7.4.2 Numerical Experiments

Fig. 7.25 shows the convergence of the fundamental frequency of a simply supported beam, for the various combinations of full/reduced integration and consistent/lumped mass.

7.4.3 Effect of Full Integration/Selective Integration

As already demonstrated for the linear elastostatics case, the use of full/reduced integration for the anisoparametric formulation of a straight beam does not have any impact on the stiffness of the beam. The same is seen in Fig. 7.25.

7.4.4 Effect of Consistent and Lumped Mass Modeling

Further, the anisoparametric formulation has shown that the use of consistent or lumped mass matrix does not degrade the performance of the element from a convergence perspective.

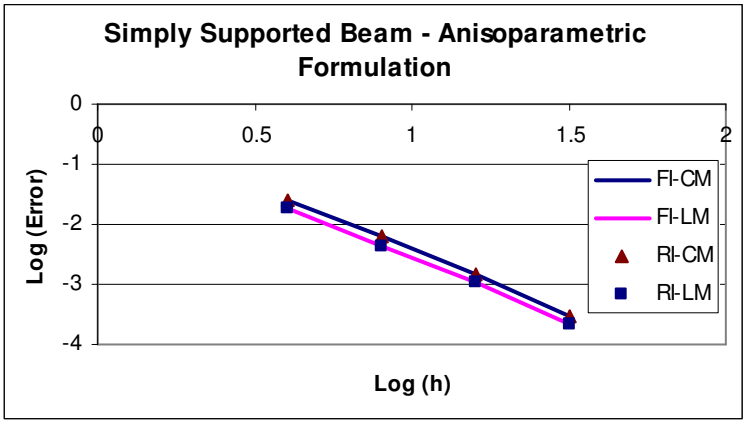

Fig. 7.25 Comparison of errors in fundamental frequency – shear-flexible beam, Anisoparametric formulation

7.4.5 Discussion of Results

Table 7.2 compares the fundamental frequency of the beam for the various formulations for a beam that was discretised in to n elements.

Anisoparametric - SS Beam Frundamental Frequency				
# Elements	FI-Full	RI-Full	FI-Lump	RI-Lump
2	4.656956	4.656927	4.633446	4.633437
4	4.567484	4.567484	4.567809	4.567807
8	4.545493	4.545492	4.552340	4.552339
16	4.540018	4.540018	4.548529	4.548529
32	4.538651	4.538651	4.547580	4.547580

Table 7.2 Comparison of fundamental frequency of shear-flexible simply supported beam - Anisoparametric formulation

The results of the sweep test are shown in Fig. 7.26 for various combinations of stiffness and mass matrices. It can be seen clearly that use of lumped mass matrices clearly cuts the theoretical frequency line and is no more bounded, whereas the use of reduced integration preserves the boundedness (as reduced integration for an anisoparametric formulation has very little impact on the stiffness of the beam).

For a simply supported plate (square plate of 40 mm side, thickness as 0.4 mm, Young's Modulus as 200000 N/mm^2, Poisson's ratio as 0.3 and density as 7850 kg/m^3), the results of the sweep test are shown in Fig. 7.27 for the case of a consistent mass matrix, and the boundedness of results can be seen clearly.

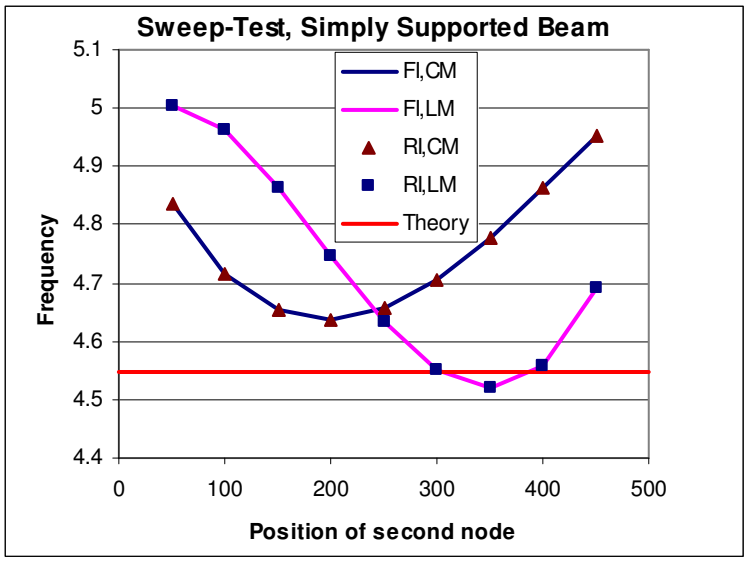

Fig. 7.26 Sweep-Test in a simply supported shear-flexible beam - Anisoparametric formulation

When lumped mass matrix is used, the fundamental frequency is compared with the results obtained using consistent mass matrix in Fig. 7.28 and there is no degradation of the results.

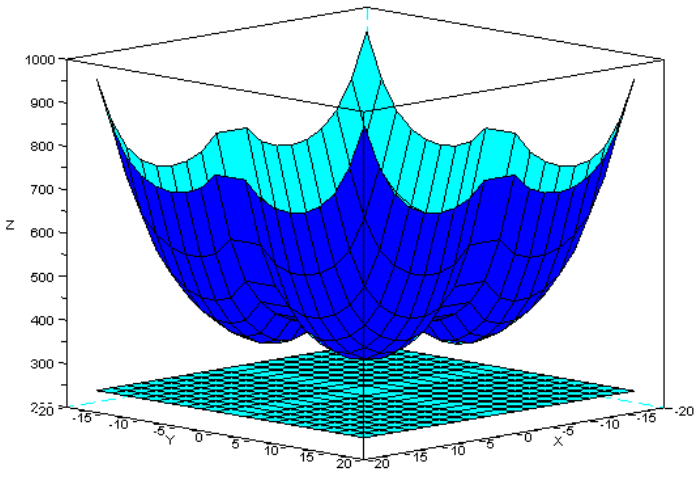

Fig. 7.27 Sweep-Test in a simply supported shear-flexible plate- Anisoparametric formulation

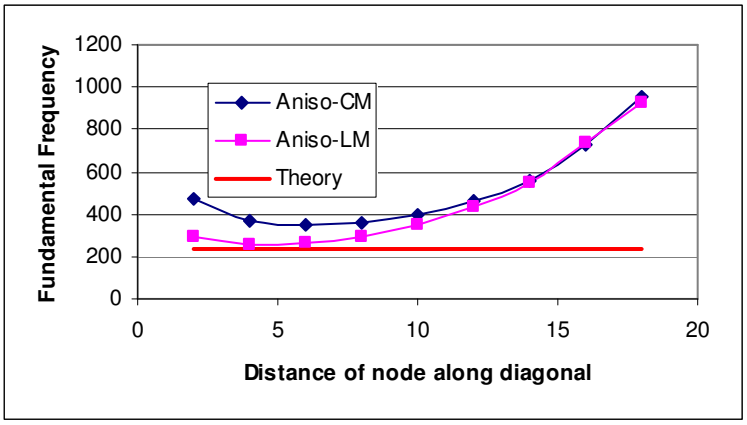

Fig. 7.28 Effect of lumped mass on a shear-flexible plate with anisoparametric formulation

7.5 Closure

It can be seen from the above detailed study of the errors produced due to the use of extra-variational processes in beam and plate bending problems, that whenever the variational principles are not adhered to, there is no guaranteed boundedness of the results. Use of non-conforming elements, and lumped mass matrix for both conforming and non-conforming elements brings down the order of convergence. Similarly, the use of reduced integration introduces errors that show for higher frequencies. The anisoparametric element has been found to relatively more stable with respect to use of full/reduced integration or consistent/lumped mass matrix. Table 7.3 summarizes the results of the studies carried out on linear elastodynamics in this chapter.

Summary of Results for Linear Elastodynamics					
Element Formulation	**C-Concept Deviation**	**Example Problem**	**Frequency Boundedness**	**Rate of Convergence**	**Sweep-Test**
BFS Element	None	SS Beam	✓	✓	✓
		SS Plate	✓	✓	✓
		Clamped Plate	✓	✓	✓
BFS Element	Lumping	SS Beam	×	↓	×
		SS Plate	×	↓	×
		Clamped Plate	×	↓	×
ACM Element	Conformance only	SS Beam	✓	✓	✓
		SS Plate	✓	↓	✓
		Clamped Plate	✓	↓	✓
ACM Element	Conformance + Lumping	SS Beam	✓	↓	×
		SS Plate	✓	↔	×
		Clamped Plate	✓	↔	×
Quad-4 RI	Correctness only	SS Beam	✓	✓	✓
		SS Plate	✓	↓	×
Quad-4 RI	Correctness + Lumping	SS Beam	↔	↔	✓
		SS Plate	↔	↔	×
Quad-4 FC	Lumping	SS Beam	↔	↔	✓
		SS Plate	↔	↔	×
Quad-4 FC	None	SS Beam	✓	✓	✓
		SS Plate	✓	✓	✓
		Clamped Plate	✓	✓	✓
Aniso	None	SS Beam	×	✓	✓
		SS Plate	×	✓	✓
		Clamped Plate	×	✓	✓
Aniso	Lumping	SS Beam	×	↔	×
		SS Plate	×	↔	✓
		Clamped Plate	×	↔	✓

Table 7.3 3C concepts and performance of various element formulations – Linear elastodynamics

Note: ✓ implies that the performance is good/satisfies the respective attribute

× implies that it is a violation of the respective attribute

↓ implies that the performance of the respective attribute is degraded

↔ implies that there is no degradation of the performance

Chapter-8

Conclusions

This thesis has made an attempt to lay a framework for element formulations based on novel 3C concepts of consistency, correspondence and correctness. Towards this end, a total of 67 element formulations were studied in detail covering beams, axisymmetric shells and plates (*i.e.* 1D and 2D problems) for their applications to linear and nonlinear elastostatics and linear elastodynamics problems. Isoparametric elements are the most widely used elements and this thesis has attempted to assess the robustness of these elements using 3C concepts. By robustness is meant the ability of elements to produce accurate results even with coarse meshes. In the course of this study, it was also seen that some of the historical plate bending elements that were formulated in 1960s, did not adhere to the canonical principles and hence were worthwhile re-examining now using the 3C concepts. It was further seen that anisoparametric elements have been sporadically used for studying the shear-flexible structures, and have not really been studied in detail for their use in wider applications like axisymmetric shells and large deflections, and hence offered a lot of ground for further study. In fact, out of the 67 element formulations studied in this thesis, 24 are anisoparametric formulations, and 16 of these element formulations are new.

As a part of this thesis, a systematic study of the conforming and non-conforming plate bending elements has also been undertaken. Through the examples of a rectangular plate with both simply supported and clamped boundary conditions, it has been demonstrated that the non-conforming elements do not follow the best-fit rule (correspondence concept). It has also been shown that the non-conforming elements do not guarantee the boundedness of strain energy. The conforming element follows the best-fit rule and guarantee the boundedness of

strain energy. For the case of axisymmetric shell problems, an element that is formulated using the canonical principles, adheres to the best-fit rule and the strain energy is bounded.

This thesis included a detailed study of shear-flexible structures, which are investigated using isoparametric and anisoparametric elements. The consequence of use of procedures like reduced integration (used for overcoming shear locking) results in violation of best-fit rule and once again does not necessarily guarantee the strain energy boundedness. Anisoparametric elements were thought to overcome shear locking, without the requirement of any additional techniques like reduced integration. It has been shown in this thesis for a general curved axisymmetric structure, even anisoparametric elements cause locking, and it is field-consistent formulation that overcomes locking by virtue of its element formulation. A novel 4-noded anisoparametric element that does not require specifically field or edge consistency modifications has been formulated for the analysis of plates, and has been shown to behave well.

Through consistency concepts, the phenomenon of membrane locking has been explained for large deformation problems. A detailed study of errors due to the linear and nonlinear deflections has been carried out. The incremental matrices that are used during the solution of large deformation problems are explicitly derived for axisymmetric shell elements. An innovative sweep test has been devised for assessing the comparative behaviour of element formulations, reduced integration, partial field-consistency and full field-consistency. For all the cases of the beam problems that were studied, it has been shown that the fully field-consistent formulation produces the best results. The field-consistency concept is used to explain that for the case of an axisymmetric shell problem or a plate bending problem, the problem of membrane locking in large deflection problems is very mild, and there is no requirement of techniques like reduced integration.

For large deformation of shear-flexible structures, the coupling of shear and membrane locking has been investigated in detail, using both isoparametric and anisoparametric elements. The 4-noded field and edge consistent element has been shown to be a reliable element for large deformation problems as well. This thesis contains the first known study on anisoparametric elements for large deformation problems for beam, axisymmetric shells and plates. Since, exact solutions exist for very limited problems, all the results of the isoparametric and anisoparametric elements for the problems studies are compared with those obtained from a commercial finite element software ANSYS ®, and the results from the elements that are formulated in this thesis are in excellent agreement. It has been shown that use of few elements based on the 3C concepts perform as accurately as a mesh of much larger number of conventional elements, indicating the robustness of elements formulated based on 3C concepts.

The correspondence and correctness concepts for linear elastodynamics were studied in detail. Use of lumped mass matrices is a direct violation of the variational correctness of the formulation, and through sweep tests, it has been shown that use of lumped mass does not necessarily guarantee the boundedness of the natural frequencies. The results of non-conforming plate bending elements, as shown in this thesis also prove this fact. The new 4-noded anisoparametric beam/plate bending element formulated earlier for the linear and nonlinear elastostatics applications has been found to behave well for linear elastodynamics applications as well.

A summary of the above paragraphs is captured below.

1. Non-conforming elements do not follow the best-fit rule (correspondence concept), and do not guarantee the boundedness of strain energy. The conforming elements follow the best-fit rule and guarantee the boundedness of strain energy.

2. Reduced integration results in violation of best-fit rule and once again does not necessarily guarantee the strain energy boundedness.
3. For a general curved axisymmetric structure, anisoparametric elements cause locking, and it is field-consistent formulation that overcomes locking by virtue of its element formulation.
4. Anisoparametric element with reduced integration and the anisoparametric formulation with field-consistent formulation give identical results for beams and flat shells.
5. A novel 4-noded anisoparametric element that does not require field or edge consistency has been formulated for the analysis of plates.
6. For large deflections of beams, strong membrane locking occurs for conventional element formulations. Field consistent formulation overcomes the membrane locking. Minimal membrane locking for large-deflections of plates and axisymmetric shells.
7. Anisoparametric element formulations behave extremely well for large deflection problems as well.
8. Use of non-conforming element/lumped mass matrices shows loss of boundedness during sweep-test for fundamental frequency.
9. The anisoparametric element is relatively stable with respect to errors and order of convergence, when full/reduced integration and consistent/lumped mass matrices are used.
10. Elements based on 3C concepts are robust – a mesh of a few of these elements performs as well as a mesh of a much large number of conventional elements.

Chapter-9

Specific Contributions

In this thesis a total of 67 element formulations were studied in detail. Fig. 9.1 captures the summary of the element formulations. The body of knowledge on anisoparametric elements has been expanded through a thorough study of 24 different formulations out of which 16 are new. The field-consistent and edge – consistent formulation for Mindlin plates has been extended to large deflection problems.

This thesis has explored the anisoparametric finite element formulations for beam, shell and plate problems in detail for linear and nonlinear elastostatics problems. The significance of the novel 3C concepts of correspondence, consistency and correctness in element formulations is examined in depth, by taking classical and shear-flexible beams, shells and plates. The work presented in this thesis on use of anisoparametric formulations to the study of large deformation of shear-flexible structures has expanded the applications of anisoparametric elements. The ansioparametric formulations for the 2-noded axisymmetric shell element and 4-noded plate element are new additions to the anisoparametric element family. The current understanding that the use of ansioparamertic elements does not cause shear locking has been shown to be true only for limited cases. Using the consistency concept, it is shown clearly that for curved axisymmetric problems anisoparametric formulation causes both shear and membrane locking.

Shear-flexible formulations with isoparametric elements that use reduced integration have been shown to deviate from the correspondence concept. It is

also shown that there is no guaranteed boundedness of the strain energy when such elements are used.

For large deformation problems, the errors due to linear and nonlinear terms have been studied in detail, and it has been shown that the rates of convergence need to be analysed for each of them separately. The stress oscillations for a large deformation problem are explained from a consistency concept in this thesis.

The correspondence concept for non-conforming classical plate bending finite element formulation has been critically analysed and the results presented in this thesis clearly show that the non-conformance is a clear violation of the correspondence concept.

This thesis briefly reports the study on the correctness concept for elastodynamics of both classical and shear-flexible beams and plates. The boundedness of the frequencies has been examined by conducting a sweep-test, and it has been demonstrated that this boundedness is lost in cases where lumped mass matrices are used.

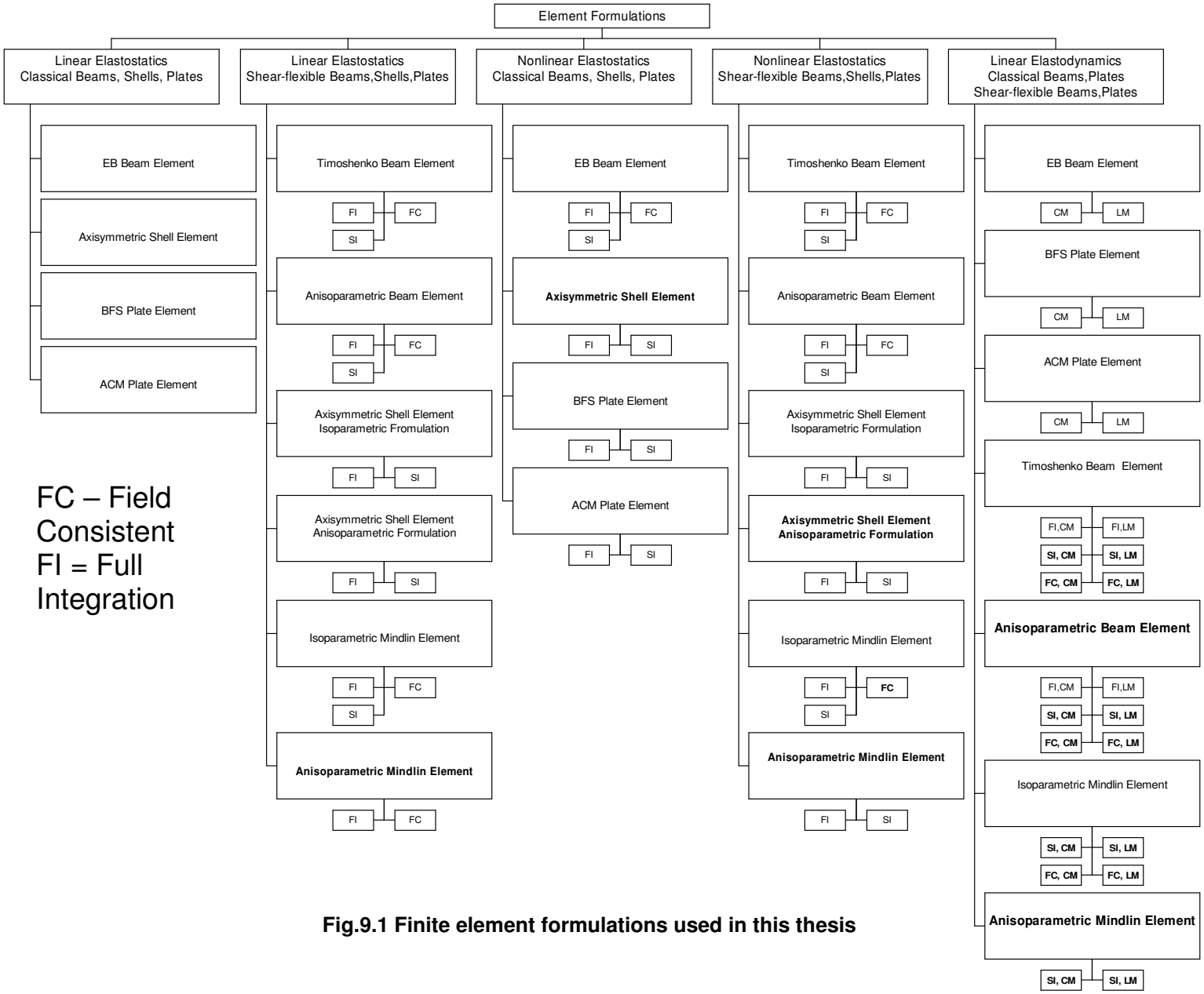

Fig.9.1 Finite element formulations used in this thesis

Chapter-10

Further Scope of Work

The consistency concept was examined in detail in this thesis for the cases of shear locking and membrane locking. Another type of locking called volumetric locking occurs in the finite element analysis of incompressible materials. This is an area where not much of work has been carried out from the perspective of 3C concepts and has potential for detailed study. Constitutive modeling in finite element analysis is a challenging field and current practices in this field have not been studied in detail from the perspective of 3C concepts. The application of 3C concepts to nonlinear material problems (*e.g.* hyperelastic materials, elasto-plastic materials) definitely has a bigger scope. Detailed studies on higher order shear deformation theories can be undertaken with the help of 3C concepts.

For nonlinear dynamics the problem becomes more challenging due to coupling of large deformations, material nonlinearity and dynamics. A detailed examination of the 3C concepts for this class of problems can be undertaken, based on the framework laid out in this thesis.

For buckling problems, the boundedness of the buckling loads predicted from the finite element solutions is a good further scope of work.

Some of the current practices in element technology, viz., use of bubble functions, condensation, recovery of stresses/eigen frequencies, *etc.* have not yet been fully tested from these 3C concepts and hence provide a great scope for further study.

The 3C concepts are derived from fundamental principles and in this thesis their applications to displacement based finite element formulations were highlighted.

Presently the territory of some of the recent advancements in the field of computational mechanics like meshless methods, boundary element method remains quite open and invites the study of 3C concepts in their domain. The 3C concepts can also be extended to coupled field problems like fluid-structure interactions.

References

Agarwal S, Chakraborty A, Gopalakrishnan S (2006), Large deformation analysis for anisotropic and inhomogeneous beams using exact linear static solutions, Composite Structures, 72, 91–104.

Ahmed S, Irons B.M, Zienkiewicz O.C (1968), Curved thick shell and membrane elements with particular reference to axisymmetric problems, in Conf. on matrix methods in structural mechanics, Wright Patterson Air Force Base, Ohio.

ANSYS® (2008), Version 11.0, ANSYS, Inc., Pennsylvania, USA.

Archer G.C, Whalen T.M (2005), Development of rotationally consistent diagonal mass matrices for plate and beam elements, Comput. Methods Appl. Mech. Engrg., 194, 675-689.

Asta A.D, Zona A (2002), Non-linear analysis of composite beams by a displacement approach, Computers & Structures, 80, 2217–2228.

Auricchio F, Taylor R.L (1994), A shear deformable plate element with an exact thin limit, Comput. Methods Appl. Mech. Engrg., 118, 393-412.

Averill R.C, Reddy J.N (1990), Behaviour of plate elements based on the first-order shear deformation theory, Engineering Computations, 7, 57-74.

Barlow J (1976), Optimal stress locations in finite element models, Int. J. Numer. Methods Engrg., 10, 243-251.

Barlow J (1989), More on optimal stress points – reduced integration, element distortions and error estimation, Int. J. Numer. Methods Engrg., 28, 1487-1504.

Bathe K.J, Dvorkin E.N (1985), A four-node plate bending element based on Mindlin/Reissner plate theory and a mixed interpolation, Int. J. Numer. Methods Engrg., 21, 367–383.

Bathe K.J, Dvorkin E.N (1986), A formulation of general shell elements–the use of mixed interpolation of tensorial components, Int. J. Numer. Methods Engrg., 22, 697–722.

Bathe K.J (2002), Finite element procedures, Prentice-Hall of India, New Delhi.

Belytschko T, Liu W.K, Moran B (2000), Nonlinear finite elements for continua and structures, John Wiley & Sons Ltd., Chichester.

Bletzinger K.U, Bischoff M, Ramm E (2000), A unified approach for shear-locking-free triangular and rectangular shell finite elements, Computers & Structures, 75, 321-334.

Bogner F.K, Fox R.L, Schmidt L.A (1965), The Generation of inter-element compatible stiffness and mass matrices by the use of interpolation formulas, in Conf. on matrix methods in structural mechanics, Wright Patterson Air Force Base, Ohio.

Boroomand B, Zienkiewicz O.C (1997), Recovery by equilibrium in patches (REP), Int. J. Numer. Methods Engrg., 40, 137-164.

Brebbia C.A, Connor J.J (1969), Geometrically nonlinear finite element analysis, Journal of the Engineering Mechanics Division, Proc. of ASCE, 95, 463-483.

Brebbia C. A, Connor J.J (1973), Fundamentals of finite element techniques for structural engineers, Butterworth Press, London

Briassoulis D (1989a), On the basics of the shear locking problem of C^0 isoparametric plate elements, Computers & Structures, 33, 169-185.

Briassoulis D (1989b), The C^0 shell plate and beam elements freed from their deficiencies, Comput. Methods Appl. Mech. Engrg, 72, 243-266.

Cen S, Long Y.Q, Yao Z.H, Chiew S.P (2006), Application of the quadrilateral area coordinate method: A new element for Mindlin-Reissner plate, Int. J. Numer. Methods Engrg., 66, 1-45.

Cheung Y.K, Zhang Y.X, Wanji C (2000), The application of a refined non-conforming quadrilateral plate bending element in thin plate vibration and stability analysis, Finite Elements in Analysis and Design, 34, 175-191.

Choi C.K, Lee T.Y (2003), Efficient remedy for membrane locking of 4-node flat shell elements by non-conforming modes, Comput. Methods Appl. Mech. Engrg., 192, 1961–197.

Cook R.D, Malkus D.S, Plesha,M.E (1989), Concepts and applications of finite element analysis, 2nd edition, John Wiley & Sons, New York.

Cook R.D. (1991), Error estimators for eigen values computed from discretized models of vibrating structures, AIAA Journal, 29,1527-1529.

Cook R.D, Avrashi J (1992), Error estimation and adaptive meshing for vibration problems, Computers & Structures, 44, 619-626.

Courant R (1943), Variational methods for the solution of problems of equilibrium and vibrations, Bulletin of Amer. Math. Soc., 49, 1 –23.

Crisfield M.A (1991), Non-Linear Finite element analysis of solids and structures, Volume 1: Essentials. John Wiley, New York.

de Veubeke B.F (1965), Displacement and equilibrium models in the finite element method, in: O. Zienkiewicz, G. Holister (Eds.), Stress Analysis, Wiley.

Desai C.S, Abel J.G (1987), Introduction to finite element method, CBS Publihshers & Distributors, New Delhi.

Donea J, Lamain L.G (1987), A Modified representation of transverse shear in C^0 quadrilateral plate elements, Comput. Methods Appl. Mech. Engrg., 63,183-207.

Dvorkin E.N, Bathe K.J (1984), A continuum mechanics based four-node shell element for general nonlinear analysis, Eng. Comput., 1, 77-88.

Dvorkin E.N, Onate E, Oliver J (1988), On the nonlinear formulation for curved Timoshenko beam elements considering large displacement/rotation increments, Int. J. Numer. Methods Engrg., 26, 1597- 1613.

Felippa C.A (2002), Fitting strains and displacements by minimizing dislocation energy, CU-CAS-02-25, Centre for Aerospace Structures, Colorado University, Boulder.

Felippa C.A (2005), Centre for Aerospace Structures, Colorado University, http://www.colorado.edu/engineering/Aerospace/CAS/courses.d/NFEM.d/NFEM.Ch09.d/NFEM.Ch09.pdf.

Felippa C.A (2006), Supernatural QUAD4: A template formulation, Comput. Methods Appl. Mech. Engrg. 195, 5316–5342.

Fried I (1971), Accuracy of finite element eigenproblems, J. Sound Vib., 18, 289-295.

Fried I, Malkus D.S (1975), Finite element mass matrix lumping by numerical integration with no convergence rate loss, Int. J. Solids Structures, 11, 461-466.

Fuenmayor F.J, Restrepo J.L, Taranco J.E, Baeza L (2001), Error estimation and h -adaptive refinement in the analysis of natural frequencies, Finite Elements in Analysis and Design, 38, 137-153.

Fung Y.C (1968), Foundations of solid mechanics, Prentice-Hall India, New Delhi.

Ganapathi M, Patel B.P, Saravanan J, Touratier M (1999), Shear flexible curved spline beam element for static analysis, Finite Elements in Analysis and Design, 32, 181-202.

Ganapathi M, Gupta S.S, Patel B.P (2003), Nonlinear axisymmetric dynamic buckling of laminated angle-ply composite spherical caps, Composite Structures, 59, 89–97.

Ganapathi M, Patel B.P, Patel H.G (2004), Free flexural vibration behavior of laminated angle-ply elliptical cylindrical shells, Computers & Structures, 82, 509 – 518.

Gilewski W, Radwanska M (1991), A survey of finite element models for the analysis of moderately thick shells, Finite Elements in Analysis and Design, 9, 1-21.

Grafton P.E, Strome D.R (1963), Analysis of axisymmetrical shells by the direct stiffness method, AIAA Journal, 1, 2342-2347.

Gratsch T, Bathe K.J (2005), A posteriori error estimation techniques in practical finite element analysis, Computers & Structures, 83, 235–265.

Haefner L, Willam K.J (1984), Large deflection formulations of a simple beam element including shear deformations, Eng. Comput., 1, 359-368.

Hager P, Wiberg N.E (2000), Error estimation and h-adaptivity for eigen-frequency analysis of plates in bending: numerical results, Computers & Structures, 78, 1-10.

Hernandez A, Albizuri J, Aviles R, Amezua E (1999), An adaptive procedure for the finite element computation of nonlinear structural problems, Eng. Comp., 16, 443-466.

Hernandez A, Pinto Ch, Amezua E, Fernandes H (2003), Analysis of the components of discretization error in nonlinear structural problems, Finite Elements in Analysis and Design, 39, 835–864.

Hermann L.R (1972), Interpretation of finite element procedure as stress error minimization procedure, Journal of Engineering Mechanics, Proc. of ASCE, 98, 1330 – 1336.

Hiller J.F, Bathe K.J (2001), On higher-order-accuracy points in isoparametric finite element analysis and an application to error assessment, Computers & Structures, 79, 1275-1285.

Hinton E, Campbell J.J (1974), Local and global smoothing of discontinuous finite element functions using a least squares method, Int. J. Numer. Methods Engrg., 8, 461-480.

Hinton E, Huang H.C (1986), A family of quadrilateral Mindlin plate elements with substitute shear strain fields, Computer & Structures, 23, 409-431.

Hinton E, Rock T, Zienkiewicz O.C (1976), A note on mass lumping and related processes in the finite element method, Earthquake Engrg. Struct. Dynamics, 4, 245–249.

Hrabok M.M, Hrudey T.M (1984), A review and catalogue of plate bending elements, Computers & Structures, 19, 479-495.

Ibrahimbegovic A (1995), On finite element implementation of geometrically nonlinear Reissner's beam theory: Three-dimensional curved beam elements, Comput. Methods Appl. Mech. Engrg., 122, 11-26.

Iyer N.R, Appa Rao T.V.S.R (1992a), A Review of error analysis and adaptive refinement methodologies in finite element applications, Part I: Error analysis, J. Struct. Eng. (Madras), 19, 77-94.

Iyer N.R, Appa Rao T.V.S.R (1992b), A Review of error analysis and adaptive refinement methodologies in finite element applications Part II: Adaptive refinements, J. Struct. Eng. (Madras), 19, 125-137.

Izzuddin B.A, Chew A, Lloyd S.D (2004), Error estimation for geometrically non-linear analysis of framed structures, Int. J. Numer. Methods Engrg., 61, 532-558.

Jafarali P, Chattopadhyay L, Prathap G, Rajendran S (2004), Error analysis of a hybrid beam element with Timoshenko stiffness and classical mass, Int. J. Comput. Engrg. Sci., 5, 495-508.

Jafarali P, Mohammed A, Mukherjee S, Prathap G (2007), Variational correctness and Timoshenko beam finite element elastodynamics, J. Sound Vib., 299, 196-211.

Jones R.E, Strome D.R (1965), A survey of analysis of shells by the displacement method, in Conf. on matrix methods in structural mechanics, Wright Patterson Air Force Base, Ohio.

Kasper E.P, Taylor R.L (2000a), A mixed-enhanced strain method, Part I: Geometrically linear problems, Computers & Structures, 78, 237-250.

Kasper E.P, Taylor R.L (2000b), A mixed-enhanced strain method, Part II: Geometrically nonlinear problems, Computers & Structures, 75, 251-260.

Kikuchi F, Aizawa T (1982), Locking phenomena in finite element analysis of large deflection problems, Proc. 32nd Japan Congress of Applied Mechanics. University of Tokyo Press, Tokyo.

Koschnick F, Bischoff M, Camprubı N, Bletzinger K.U (2005), The discrete strain gap method and membrane locking, Comput. Methods Appl. Mech. Engrg., 194, 2444–2463.

Kreja I, Cywinski Z (1988), Is reduced integration just a numerical trick, Computers & Structures, 29, 491-496.

Ladeveze P, Pelle J.P (1989), Accuracy in finite element computation for eigenfrequencies, Int. J. Numer. Methods Engrg., 28, 1929-1949.

Ladeveze P, Pelle J.P (2003), Estimation of discretization error in dynamics, Computers & Structures, 81, 1133-1148.

Laulusa A, Reddy J.N (2004), On shear and extensional locking in nonlinear composite beams, Engineering Structures, 26, 151–170.

Leckie F.A, Lindberg G.M (1963), The effect of lumped parameters on beam frequencies, The Aeronautical Quarterly, 14, 224-240.

Lee N.S, Bathe K.J (1994), Error indicators and adaptive remeshing in large deformation finite element analysis, Finite Elements in Analysis and Design, 16, 99-139.

Li X.K, Liu G.Q, Owen D. R. J. (1984), Geometrically non-linear analysis of thin plates and shells using a generalized displacement method, Eng. Comput., 1, 318-323.

Li L.Y, Bettess P (1997), Adaptive finite element methods: A review, Applied Mechanics Review, 50, 581-591.

Li M. (1997), The finite deformation theory for beam, plate and shell Part I. The two-dimensional beam theory, Comput. Methods Appl. Mech. Engrg., 146, 53-63.

Li M. (1998), The finite deformation theory for beam, plate and shell Part III. The three-dimensional beam theory and the FE formulation, Comput. Methods Appl. Mech. Engrg., 162, 287-300.

Liew K. M, Rajendran S (2002), New superconvergent points of the 8-node serendipity plane element for patch recovery, Int. J. Numer. Methods Engrg., 54,1103–1130.

Liu J. H, Surana K.S (1993), p-version axisymmetric shell element for geometrically nonlinear analysis, Computers & Structures, 49, 1017-1026.

Liu J. H, Surana K.S (1995), Piecewise hierarchical p-version axisymmetric shell element for geometrically nonlinear behaviour of laminated composites, Computers & Structures, 55, 67-84.

Lindberg G.M, Olson M.D (1970), Convergence studies of eigenvalue solutions using two finite plate bending elements, Int. J. Numer. Methods Engrg., 2, 99-116.

Little G.H (1999), Efficient large deflection analysis of rectangular plates with general transverse form of displacement, Computers & Structures, 71, 333-352.

Liu J, Riggs H.R, Tessler A (2000), A four-node, shear-deformable shell element developed via explicit Kirchhoff constraints, Int. J. Numer. Methods Engrg., 49, 1065-1086.

Lo S.H, Lee C.K (1998), On constructing accurate recovered stress fields for the finite element solution of Reissner-Mindlin plate bending problems, Comput. Methods Appl. Mech. Engrg., 160, 175-191.

Mackerle J (2001), Error estimates and adaptive finite element methods – A bibliography (1990-2000), Engineering Computations, 18, 802-914.

MacNeal R.H (1993), Finite elements: Their design and performance, Marcel Dekker, New York.

MacNeal R.H (1998), Perspective on finite elements for shell analysis, Finite Elements in Analysis and Design, 30, 175-186.

Mallett R.H, Marcal P.V (1968), Finite element analysis of nonlinear structures, Journal of the Structural Division, Proc. of ASCE, 94, 2081-2105.

Mao S, Chen S (2006), Accuracy analysis of Adini's non-conforming plate element on anisotropic meshes, Commun. Numer. Meth. Engng., 22, 433-440.

Marur S. R, Prathap G (2000), Consistency and correctness evaluation of shear deformable anisoparametric formulations, Int. J. Solids Structures, 37, 701-713.

Martin H.C (1965), On the derivation of stiffness matrices for the analysis of large deflection and stability problems, in Conf. on matrix methods in structural mechanics, Wright Patterson Air Force Base, Ohio.

Mattiasson K (1981), Numerical results from large deflection beam and frame problems analyzed by means of elliptic integrals, Int. J. Numer. Methods Engrg., 17,145-153.

Melosh R.J (1963), Basis for derivation of matrices for the direct stiffness method, AIAA J, 1, 1631-1637.

Militello C, Felippa C. A (1990a), A variational justification of the assumed natural strain formulation of finite elements—I. Variational principles, Computers & Structures, 34, 431-438.

Militello C, Felippa C. A (1990b), A variational justification of the assumed natural strain formulation of finite elements- The C^0 four-node plate element, Computers & Structures, 34, 439-444.

Miranda S, Ubertini F (2002), Recovery of consistent stresses for compatible finite elements, Comput. Methods Appl. Mech. Engrg., 191, 1595-1609.

Miranda S, Ubertini F (2003), Consistency and recovery in electroelasticity Part-1: Standard finite elements, Comput. Methods Appl. Mech. Engrg., 192, 831-850.

Moan T (1973), On the local distribution of errors by finite element approximations, Theory and practice in finite element structural analysis, Proceedings of the 1973 Tokyo Seminar on Finite Element Analysis, University of Tokyo Press, 43-60.

Mohite P.M, Upadhyay C.S (2002), Local quality of smoothening based a posteriori error estimators for laminated plates under transverse loading, Computers & Structures, 80, 1477-1488.

Mohr G.A (1982), Application of penalty functions to a curved isoparametric axisymmetric thick shell element, Computers & Structures, 15, 685-690.

Mukherjee S, Krishnamoorthy C.S (1996), Adaptive FE analysis of plates by shear-flexible quadrilateral Reissner-Mindlin elements, Finite Elements in Analysis and Design, 22, 329-366.

Mukherjee S, Prathap G (2001), Analysis of shear locking in Timoshenko beam elements using the function space approach, Commun. Numer. Meth. Engng.,17, 385-393.

Mukherjee S, Reddy J.N, Krishnamoorthy C.S (2001), Convergence properties and derivative extraction of the superconvergent Timoshenko beam finite element, Comput. Methods Appl. Mech. Engrg., 190, 3475-3500.

Mukherjee S, Prathap G (2002a), Analysis of delayed convergence in the three-noded Timoshenko beam element using the function space approach, Sadhana, 27, 507–526.

Mukherjee S, Prathap G (2002b), Variational correctness in finite element solutions through reduced integration, Research Report CM 0204, CSIR Centre for Mathematical Modelling and Computer Simulation, Bangalore, India.

Mukherjee S, Jafarali P, Prathap G (2005), A variational basis for error analysis in finite element elastodynamic problems, J. Sound Vib., 285, 615-635.

Mukherjee S, Jafarali P (2008), Prathap's best-fit paradigm and optimal strain recovery points in indeterminate tapered bar analysis using linear elements, Commun. Numer. Meth. Engng, DOI:10.1002/cnm:1197.

Muralikrishna R, Prathap G (2003), Studies on variational correctness of finite element elastodynamics of some plate elements, Research Report CM 0306, CSIR Centre for Mathematical Modelling and Computer Simulation, Bangalore, India.

Muralikrishna R, Prathap G (2006), Field-consistency aspects of locking in a geometrically non-linear beam formulation, Research Report CM 0601, CSIR Centre for Mathematical Modelling and Computer Simulation, Bangalore, India.

Nanakorn P, Wu L.N (2006), A 2D field-consistent beam element for large displacement analysis using the total Lagrangian formulation, Finite Elements in Analysis and Design, 42, 1240-1247.

Narayanan G, Krishnamoorthy C.S (1989), A simplified formulation of a plate/shell element for geometrically nonlinear analysis of moderately large deflections with small rotations, Finite Elements in Analysis and Design, 4 333-350.

Narayanan G, Krishnamoorthy C.S (1990), An investigation of geometric non-linear formulations for 3D beam elements, International Journal of Non-Linear Mechanics, 25, 643-662.

Oden J.T, Belytschko T, Babuska I, Hughes T.J.R (2003), Research directions in computational mechanics, Comput. Methods Appl. Mech. Engrg., 192, 913–922.

Olesen J.F (1983), Field redistribution in finite elements- a mathematical alternative to reduced integration, Computers & Strucutres, 17, 157-159.

Oh H.S, Batra R.C (1999), Locations of optimal stress points in higher-order elements, Commun. Numer. Meth. Engng., 15, 127-136.

Oliver J, Onate E (1984), A total Lagrangian formulation for the geometrically nonlinear analysis of structures using finite elements. Part I:Two-dimensional problems: shell and plate structures, Int. J. Numer. Methods Engrg, 20, 2253-2281.

Oliver J, Onate E (1986), A total Lagrangian formulation for the geometrically nonlinear analysis of structures using finite elements. Part II: Arches, frames and axisymmetric shells, Int. J. Numer. Methods Engrg, 23, 253-274.

Olovsson L, Simonsson K, Unosson M (2006), Shear locking reduction in eight-noded tri-linear solid finite elements, Computers & Structures, 84, 476–484.

Ozkul T.A, Ture U (2004), The transition from thin plates to moderately thick plates by using finite element analysis and the shear locking problem, Thin-Walled Structures, 42, 1405–1430.

Pai P.F, Anderson T.J, Wheate E.A (2000), Large-deformation tests and total-Lagrangian finite element analyses of flexible beams, Int.J.Solids Structures, 37, 2951-2980.

Palazotto A.N, Dennis S.T (1992), Nonlinear analysis of shell structures, AIAA education series, AIAA, Washington DC.

Paramasivam V, Thulasi Ramachandra Gowda S.P, Raj Muthiah D (1992), Timoshenko beam finite element with four dof and convergence of $O(h^4)$ Computers & Structures, 43, 1187-I 189.

Paramasivam V, Raj Muthiah D (1994), Shear-deformable axisymmetric conical shell element with 6-DOF and convergence of $O(h^4)$, Comput. Methods Appl. Mech. Engrg., 113, 47-54.

Perego U (2000), A variationally consistent generalized variable formulation for enhanced strain finite elements, Commun. Numer. Meth. Engng., 16, 151-163.

Pica A, Wood R.D, Hinton E (1980), Finite element analysis of geometrically nonlinear plate behaviour using a Mindlin formulation, Computers & Structures, 11, 203 - 215.

Pinto D.S (2008), Studies on Barlow points, Gauss points and Superconvergent points in 1D with Lagrangian and Hermitian finite element basis, Comput. Appl. Math., 27, 275-303.

Pitkaranta J. (2000), The first locking-free plane-elastic finite element: Historia mathematica, Comput. Methods Appl. Mech. Engrg.,190, 1323-1366.

Prathap G, Bhashyam G.R (1982), Reduced integration and the shear-flexible beam element, Int. J. Numer. Methods Engrg., 18, 195-210.

Prathap G (1984), Field consistent finite element formulations, DVFLR IB 131-84/33, Institute of Structural Mechanics, Braunschweig, Germany.

Prathap G (1985), The curved beam/deep arch/finite ring element revisited, Int. J. Numer. Methods Engrg., 21, 389-407.

Prathap G, Ramesh Babu C (1986), A field consistent three-noded quadratic curved axisymmetric shell element, Int. J. Numer. Methods Engrg., 23, 711-723.

Prathap G, Ramesh Babu C (1987a), Field-consistency and violent stress oscillations in the finite element method, Int. J. Numer. Methods Engrg., 24, 2017-2033.

Prathap G, Ramesh Babu C (1987b), Accurate force evaluation with a simple, bi-linear, plate bending element, Computers & Structures, 25, 259-270.

Prathap G, Somashekar B.R (1988), Field- and Edge-Consistency synthesis of a 4-noded quadrilateral plate bending element, Int. J. Numer. Methods Engrg., 26, 1693-1708.

Prathap G, Nirmala K (1990), Finite element formulations for constrained media elasticity - A bibliography, Finite Elements in Analysis and Design, 7, 253-270.

Prathap G, Naganarayana B.P (1992), Stress oscillations and spurious load mechanisms in variationally inconsistent assumed strain formulations, Int. J. Numer. Methods Engrg., 33, 2181-2197.

Prathap G (1993), Variational basis for the Barlow points, Computers & Structures, 49, 381-383.

Prathap G (1996a), Barlow points and Gauss points and the aliasing and best-fit paradigms, Computers & Structures, 58, 321-325.

Prathap G (1996b), Finite element analysis and the stress correspondence paradigm, Sadhana, Academy Proceedings in Engineering Sciences, 21,525-546.

Prathap G (1999), A Priori error estimation of finite element models from first principles, Sadhana, Academy Proceedings in Engineering Sciences, 24,199-214.

Prathap G, Pavan Kumar D.V.T.G (2001), Error analysis of Timoshenko beam finite element dynamic models, Int.J.of Computational Engineering Science, 2, 1-10.

Prathap G, Mukherjee S (2003a), The engineer grapples with Theorem 1.1 and Lemma 6.3 of Strang and Fix, Current Science, 85, 989-994.

Prathap G, Mukherjee S, Muralikrishna R (2003b), A priori error estimation for FEA of elastodynamic problems, Proceedings of the Workshop on FEADS'03, Structural Engineering Research Centre, CSIR, Chennai, 19-27.

Prathap G, Mukherjee S (2004), Management-by-stress model of finite element computation. Research Report CM 0405, CSIR Centre for Mathematical Modelling and Computer Simulation, Bangalore, India.

Prigogine I (1997), Non-linear science and the laws of nature, J. Franklin Inst., 334B, 745-758.

Proceedings of Conference on matrix methods in structural mechanics (1965), AFFDL-TR-66-80, Wright-Patterson Air force Base, Dayton.

Proceedings of Conference on matrix methods in structural mechanics (1968), AFFDL-TR-68-150, Wright-Patterson Air force Base, Dayton.

Rajasekaran S, Murray D.W (1974), Incremental finite element matrices, Journal of the Structural Division, Proc. of ASCE, 99, 2423-2438.

Rajendran S, Prathap G (1999), Convergence of eigenvalues of a cantilever beam with 8- and 20-node hexahedral elements, J. Sound Vib., 227, 667-681.

Rajendran S, Liew K.M (2003a), Optimal stress sampling points of plane triangular elements for patch recovery of nodal stresses, Int. J. Numer. Methods Engrg., 58, 579–607.

Rajendran S, Liew K.M (2003b), A novel unsymmetric 8-node plane element immune to mesh distortion under a quadratic displacement field, Int. J. Numer. Methods Engrg., 58, 1713–1748.

Rajendran S (2008), Optimal stress recovery points for higher-order bar elements by Prathap's best-fit method, Commun. Numer. Meth. Engng.,25, 864-881.

Ramesh Babu C, Somashekar B.R, Prathap G (1985), Development of field-consistent finite elements, Journal of Aero. Soc. of India, 37, 327-335.

Ramesh Babu C, Prathap G (1986), A field consistent two-noded quadratic curved axisymmetric shell element, Int. J. Numer. Methods Engrg., 23, 1245-1261.

Raveendranath P, Singh Gajbir, Pradhan B (1999a), A two-noded locking-free shear flexible curved beam element, Int. J. Numer. Methods Engrg., 44, 265-280.

.

Raveendranath P, Singh Gajbir, Pradhan B (1999b), A two-node curved axisymmetric shell element based on coupled displacement field, Int. J. Numer. Methods Engrg., 45, 921-935 .

Reddy J.N (1986), Applied Functional Analysis and Variational Methods in Engineering, Mc Graw-Hill, Singapore.

Reddy J.N (1997), On locking-free shear deformable beam finite elements, Comput. Methods Appl. Mech. Engrg.,190, 3475-3500.

Reddy J.N, Wang C.M, Lee K.H (1997), Relationships between bending solutions of classical and shear deformation beam theories, Int. J. Solids Structures, 34, 3373-3384.

Reddy J.N (2004), An introduction to nonlinear finite element analysis, Oxford University Press Inc, New York.

Reese S, Wriggers P, Reddy B.D (2000), A new locking-free brick element technique for large deformation problems in finite elasticity, Computers & Structures, 75, 291-304.

Riggs H.R, Tessler A, Chu H (1997), C^1-Continuous stress recovery in finite element analysis, Comput. Methods Appl. Mech. Engrg., 143, 299-316.

Rong T.Y, Lu A.Q (2003), Generalized mixed variational principles and solutions of ill-conditioned problems in computational mechanics. Part II: Shear locking, Comput. Methods Appl. Mech. Engrg., 192, 4981-5000.

Satyamoorthy M (1997), Nonlinear analysis of structures, CRC Press, Boca Raton.

Shames I.H, Dym C.M (1987), Energy and finite element methods in structural mechanics, Affiliated east west press, New Delhi.

Shi G, Voyiadjis G.Z (1991a), Efficient and accurate four-node quadrilateral C^0 plate bending element based on assumed strain fields, Int. J. Numer. Methods Engrg., 32, 1041-1055.

Shi G, Voyiadjis G.Z (1991b), Simple and efficient shear flexible two-node arch/beam and four-node cylindrical shell/plate finite elements, Int. J. Numer. Methods Engrg., 31, 759-776

Shi G, Voyiadjis G.Z (1991c), Geometrically nonlinear analysis of plates by assumed strain element with explicit tangent stiffness matrix Computers & Structures, 41, 757-763.

Simo J.C, Rifai M.S (1990), A class of mixed assumed strain methods and the method of incompatible modes, Int. J. Numer. Methods Engrg., 29, 1595-1638.

Singh Gajbir, Venkateswara Rao G, Iyengar N G R (1993), Large deflection behaviour of shear deformable composite plates using a simple higher order theory, Compos. Eng. 3: 507 – 525.

Singh Gajbir, Raju K.K, Venkateswara Rao G (1998), A new lock-free, material finite element for flexure of moderately thick rectangular composite plates, Computers & Structures, 69, 609-623.

Singh Gajbir, Venkateswara Rao G (2000a), Nonlinear oscillations of laminated plates using an accurate four-node rectangular shear flexible material finite element, Sadhana, 25, 367 - 380.

Singh Gajbir, Raveendranath P, Venkateswara Rao G (2000b), An accurate four-node shear flexible composite plate element, Int. J. Numer. Methods Engrg., 47, 1605-1620.

Singh Gajbir, Venkateswara Rao G (2000c), Shear flexible finite elements: Retrospect and prospects, Inst. Eng. (I) J., 81, 12-19.

Singh Gajbir, Venkateswara Rao G (2003), Error estimates in 2-node shear-flexible beam elements, Commun. Numer. Meth. Engng., 19, 491-501.

Sita Thankam V, Singh Gajbir, Venkateswara Rao G, Rath A.K (2003), Shear flexible element based on coupled displacement field for large deflection analysis of laminated plates, Computers & Structures, 81, 309–320.

Stephen D.B, Steven G.P (1997a), Error estimation for natural frequency analysis using plate elements, Engineering Computations, 14,119-134.

Stephen D.B, Steven G.P (1997b), Natural frequency error estimation using a patch recovery technique, J. Sound Vib., 200,151-165.

Stephen D.B, Steven G.P (1997c), Error Estimation for natural frequency finite element analysis, Finite Elements in Analysis and Design, 26, 21-40.

Stolarski H, Belytschko T, (1983), Shear and membrane locking in curved C^0 elements, Comput. Methods Appl. Mech. Engrg., 41, 279-296.

Strang G (1973), Piecewise polynomials and the finite element method, Bull. Amer. Math. Soc., 79, 1128-1137.

Strang G, Fix G.J (1973), An analysis of the finite element method, Prentice–Hall series in automatic computation, Prentice-Hall, New Jersey

Surana K.S (1982), Geometrically nonlinear formulation for the axisymmetric shell elements, Int. J. Numer. Methods Engrg, 18,477–502

Tessler A (1981), On a conforming, Mindlin-type plate element, MAFELAP, J.R.Whiteman (Ed), 119-126.

Tessler A (1986), Shear-deformable bending element with penalty relaxation, in Finite element methods for plate and shell structures, Vol.1, Element Technology, Pineridge Press International, Swansea.

Tessler A, Spiridigliozzi L (1986), Curved beam elements with penalty relaxation, Int. J. Numer. Methods Engrg., 23 2245 – 2262.

Tessler A, Spiridigliozzi L (1988), Resolving membrane and shear locking phenomena in curved shear-deformable axisymmetric shell elements, Int. J. Numer. Methods Engrg., 26, 1071–1086.

Tessler A (1991), A two-node beam element including transverse shear and transverse normal deformations, Int. J. Numer. Methods Engrg., 32, 1027–1039.

Tessler A, Riggs H.R, Macy S.C (1994), A variational method for finite element stress recovery and error estimation, Comput. Methods Appl. Mech. Engrg., 111, 369-382.

Tessler A, Riggs H.R, Freece C.E, Cook G.M (1998a), An improved variational method for finite element stress recovery and a posteriori error estimation, Comput. Methods Appl. Mech. Engrg., 155, 15-30.

Tessler A, Riggs H.R, Dambach M (1998b), A novel four-node quadrilateral smoothing element for stress enhancement and error estimation, AIAA-98-1713, 1-12.

Timoshenko S.P, Woinowsky-Krieger S (1959), Theory of Plates and Shells (2nd edition), Mc Graw Hill, New York.

Turner M.J, Clough R.W, Martin H.C, Topp L.J (1956), Stiffness and deflection analysis of complex structures, J. Aero. Sci., 23, 805-823.

Urthaeler Y, Reddy J.N (2005), A corotational finite element formulation for the analysis of planar beams, Commun. Numer. Meth. Engng., 21, 553-570.

Venkataramana J, Venkateswara Rao G (1975), Finite element analysis of moderately thick shells, Nuclear Engineering and Design, 33, 398-402.

Von Karman T (1939), The engineer grapples with nonlinear problems, Fifteenth Josiah Willard Gibbs Lecture, American Mathematical Society, Columbus, Ohio.

Voyiadjis G.Z, Woelke P (2006), General non-linear finite element analysis of thick plates and shells, Int. J. Solids Structures, 43, 2209–2242.

Walz J.E, Fulton R.E, Cyrus N.J (1968), Accuracy and convergence of finite element approximations, Proc. Conf. Matrix Meth. Struct. Mech., AFFDL-TR-68-150, 995-1027.

Wang C.M, Reddy J.N, Lee K.H (2000), Shear deformable beams and plates: Relationships with classical solutions, Elsevier Science.

Wang C.M, Wang Y.C, Reddy J.N (2002), Problems and remedy for the Ritz method in determining stress resultants of corner supported rectangular plates, Computers & Structures, 80, 145-154.

Wanji C, Cheung Y.K (1997), Refined non-conforming quadrilateral thin plate bending element, Int. J. Numer. Methods Engrg., 40, 3937-3953.

Wood R.D, Zienkiewicz O.C (1977), Geometrically nonlinear finite element analysis of beams, frames, arches and axisymmetric shells, Computers & Structures, 7, 725-735.

Yang H.T.Y, Saigal S, Masud A, Kapania R. K (2000), A survey of recent shell finite elements, Int. J. Numer. Methods Engrg., 47, 101-127.

Yong-woo K, Oak-key M (1996), Optimal strain locations of two-dimensional continuum elements in terms of field-consistency, Computers & Structures, 59, 1121-1138.

Yuan K.Y, Liang C.C (1989), Nonlinear analysis of an axisymmetric shell using three nodded degenerated isoparametric shell elements, Computers & Structures, 32, 1225-1239.

Yunhua L (1998), Explanation and elimination of shear locking and membrane locking with field consistence approach, Comput. Methods Appl. Mech. Engrg., 162, 249-269.

Yunhua L, Eriksson A (1999), Extension of field consistence approach in to developing plane stress elements, Comput. Methods Appl. Mech. Engrg., 173, 111-134.

Zhang X (2008), Why do Barlow points not coincide with the reduced Gauss quadrature points for higher order finite elements?, Commun. Numer. Meth. Engng., 24, 1251-1256.

Zhang Y.X, Cheung Y.K (2003), A refined non-linear non-conforming triangular plate/shell element, Int. J. Numer. Methods Engrg., 56, 2387–2408.

Zhang Y.X, Kim K.S (2006), Geometrically nonlinear analysis of laminated composite plates by two new displacement-based quadrilateral plate elements Composite Structures, 72, 301-310.

Zhao C, Steven G.P (1996a), Predicted natural frequencies of two-dimensional elastodynamic problems: A practical error estimator, Engineering Computations, 13, 19-37.

Zhao C, Steven G.P (1996b), A-posteriori error estimator/corrector for natural frequencies of thin plate vibration problems, Computers & Structures, 59, 949-963.

Zhu J, Chen W (1997), Geometric nonlinear analysis by using triangular thin plate element and free from membrane locking, Computers & Structures, 63, 999-1005.

Zienkiewicz O.C, Cheung Y.K (1964), The finite element method for analysis of elastic isotropic and orthotropic slabs, Proc. Inst. Civil Engineers, 28, 471-488.

Zienkiewicz O.C, Taylor R.L, Too J.M (1971), Reduced integration technique in general analysis of plates and shells, Int. J. Numer. Methods Engrg., 3, 275–290.

Zienkiewicz O.C, Hinton E (1976), Reduced integration, function smoothing and non-conformity in finite element analysis (with special reference to thick plates), Journal of Franklin Institute, 302, 443-461.

Zienkiewicz O.C, Bauer J, Morgan K, Onate E (1977), A simple and efficient element for axisymmetric shells, Int. J. Numer. Methods Engrg.,11,1545–1558.

Zienkiewicz O.C, Zhu J.Z (1992), Superconvergent patch recovery and a posteriori error estimation in the finite element method, Part I: A general superconvergent recovery technique, Int. J. Numer. Methods Engrg., 33, 1331-1364.

Zienkiewicz O.C (2006), The background of error estimation and adaptivity in finite element computations, Comput. Methods Appl. Mech. Engrg., 195, 207-213.

Publications out of this work

International Conferences

Muralikrishna R, Mukherjee S, Prathap G, Verification, validation and variational crimes in finite element computations, ICCMS, 2004

Muralikrishna R, Mukherjee S, Prathap G, Variational Crimes and Finite Element Elastodynamics, ICCES, 2005

Reports

Muralikrishna R, Prathap G (2003), Studies on variational correctness of finite element elastodynamics of some plate elements, Research Report CM 0306, CSIR Centre for Mathematical Modelling and Computer Simulation, Bangalore, India

Muralikrishna R, Prathap G (2006), Field-consistency aspects of locking in a geometrically non-linear beam formulation, Research Report CM 0601, CSIR Centre for Mathematical Modelling and Computer Simulation, Bangalore, India.

International Journals

Muralikrishna R, Prathap G, Field-consistency aspects of locking in a geometrically non-linear beam formulation, communicated to Sadhana

Muralikrishna R, Prathap G, Geometric Nonlinear Finite Element Analysis of Shear-Flexible Beams – A Field Consistent Formulation, To be communicated

Muralikrishna R, Marur S, Prathap G, Correspondence, Consistency and Correctness of Shear-Flexible Isoparametric & Anisoparametric Curved Axisymmetric Finite Elements – Part:1 Theoretical Considerations & Element Formulations, To be communicated

Muralikrishna R, Marur S, Prathap G, Correspondence, Consistency and Correctness of Shear-Flexible Isoparametric & Anisoparametric Curved Axisymmetric Finite Elements – Part:2 Applications to Linear & Nonlinear Elastostatics, To be communicated

Jafarali P, Muralikrishna R, Mukherjee S, Prathap G, Analysis of conforming and non-conforming elements in computational elastodynamics using the function space approach, To be communicated

Biography of the candidate

R. Muralikrishna completed his B.E (Hons) in Civil Engineering from BITS, Pilani in 1991, and M.E in Civil Engineering, with specialization in structural engineering, from the same institute in 1993. After a brief academic stint for 2 years as BITS, Pilani and IIT, Delhi, he was with the Department of Atomic Energy from 1995 – 1999, at the Indira Gandhi Centre for Atomic Research, Kalpakkam. From October 1999 till date he has been working with the General Electric Company for its Aviation Business. Currently, he is the manager for the Commercial High Pressure Turbine Team at the Product Engineering Centre, GE Aviation and is located at the GE India Technology Centre, Bangalore. He is married to Srividya, and has 2 sons, Sanjay and Sai Sanjeeth.

He has presented papers in several international conferences, both within and outside the country. His research interests include finite element formulations, structural dynamics, and error estimation.

Biography of the supervisor

Dr. Gangan Prathap graduated from IIT, Madras, winning the President of India Prize for 1st rank in B.Tech. Degree Course for 1969-174. He completed his Ph.D in 1977. He was with the National Aerospace Laboratories from 1978 – 2000. He was the Scientist-in-Charge, CSIR Centre for Mathematical Modelling and Computer Simulation from Apr. 2000 – Jan. 2008. He was the Vice-Chancellor, Cochin University of Science and Technology from Feb. 2008 – Feb. 2009. He was the Vice-Chancellor-in-Charge, Kerala University, Aug. 2008 – Dec. 2008. Presently, he is the Director, NISCAIR, New Delhi from Feb. 2009.

His research areas include, non-linear structural mechanics, constrained multi-strain field problems, and non-linear vibrations. He has won the SS Bhatnagar Prize for Engineering in 1990 (the highest award for scientific research in the country). He has published over 90 publications in International Journals. He has written a book titled Finite Element Method in Structural Mechanics, Kluwer Academic Publishers, Dodrecht, Holland, 1993. He has over 300 short papers, reports, technical memoranda, papers/lectures at Symposia and Conferences etc. He has 1 paper with over 100 citations, another 10 papers with over 20 cumulative citations and another 17 papers with 10-19 cumulative citations. He has delivered over 60 key-note lectures in various national/international conferences. He serves on the editorial board of many international journal

Annexure

Flow chart for solution of large deflection problems